Université Paris-Saclay

MÉMOIRE D'HABILITATION À DIRIGER DES RECHERCHES

(spécialité Informatique)

From permutahedra to associahedra, a walk through geometric and algebraic combinatorics

Vincent PILAUD

Soutenue publiquement le 10 juillet 2020 en visio-conférence devant le jury composé de :

Frédéric CHAPOTON	DR CNRS	Université de Strasbourg	(rapporteur)
Florent HIVERT	Professeur	Université Paris-Saclay	
Bernard LECLERC	Professeur	Université de Caen	
Lionel POURNIN	Professeur	Université Paris Nord	
Nathan READING	Professeur	North Carolina State University	(rapporteur)
Maria RONCO	Professeur	Universidad de Talca	
Sibylle SCHROLL	Professeur	University of Leicester	
Hugh THOMAS	Professeur	Université du Québec à Montréal	(rapporteur)

CONTENTS

Introduction 1

I Lattice congruences, polytopes and Hopf algebras 11

1 Permutahedra, associahedra, cubes 15
- 1.1 Lattices . . . 15
  - 1.1.1 Lattices and their congruences . . . 15
  - 1.1.2 Three classical lattices . . . 16
- 1.2 Polytopes . . . 17
  - 1.2.1 Fans and polytopes . . . 17
  - 1.2.2 Three classical polytopes . . . 18
- 1.3 Hopf algebras . . . 20
  - 1.3.1 Combinatorial Hopf algebras . . . 20
  - 1.3.2 Three classical Hopf algebras . . . 20

2 Brick polytopes 23
- 2.1 Acyclic twist lattices . . . 23
  - 2.1.1 Pipe dreams, (k, n)-twists and k-triangulations of the n-gon . . . 23
  - 2.1.2 k-twist correspondence . . . 24
  - 2.1.3 k-twist congruence . . . 25
  - 2.1.4 Flips and acyclic k-twist lattices . . . 25
  - 2.1.5 k-recoils and k-canopy schemes . . . 26
- 2.2 Brick polytopes . . . 27
  - 2.2.1 Permutahedra, brick polytopes, zonotopes . . . 27
  - 2.2.2 The geometry of the surjections $\mathbf{twi}^k$, $\mathbf{can}^k$, $\mathbf{rec}^k$ . . . 27
- 2.3 The twist Hopf algebra . . . 30
  - 2.3.1 Hopf subalgebra . . . 30
  - 2.3.2 Quotient Hopf algebra . . . 31

3 Permutreehedra 33
- 3.1 Permutree lattices . . . 33
  - 3.1.1 Permutrees . . . 33
  - 3.1.2 Permutree correspondence . . . 34
  - 3.1.3 Permutree congruences . . . 35
  - 3.1.4 Rotations and permutree lattices . . . 35
  - 3.1.5 Decoration refinements . . . 36
- 3.2 Permutreehedra . . . 37
  - 3.2.1 Permutree fans . . . 37
  - 3.2.2 Permutreehedra . . . 37
- 3.3 The permutree Hopf algebra . . . 38
  - 3.3.1 The Hopf algebra on decorated permutations . . . 39
  - 3.3.2 Hopf subalgebra . . . 40
  - 3.3.3 Quotient Hopf algebra . . . 41

4 Quotientopes **43**
4.1 Lattice quotients and arc diagrams . . . 43
4.1.1 Canonical representations and non-crossing arc diagrams . . . 43
4.1.2 Lattice quotients of the weak order and arc ideals . . . 44
4.2 Quotientopes . . . 45
4.2.1 Quotient fans . . . 45
4.2.2 Quotientopes . . . 46
4.2.3 Minkowski sums of associahedra or shard polytopes . . . 47
4.3 Hopf algebra structures . . . 49
4.3.1 Decorated permutations . . . 49
4.3.2 Decorated non-crossing arc diagrams . . . 50
4.3.3 Three applications . . . 51

II Beyond the weak order **53**

5 Facial weak order **57**
5.1 Ordered partitions and pseudopermutahedron . . . 57
5.1.1 Permutahedron faces . . . 57
5.1.2 Pseudopermutahedron and its quotients . . . 58
5.1.3 Hopf algebras . . . 59
5.2 Facial weak order on finite Coxeter groups . . . 61
5.2.1 Finite Coxeter groups . . . 61
5.2.2 Root and weight sets of a face . . . 64
5.2.3 Three equivalent definitions of the facial weak order . . . 65
5.2.4 The facial weak order is a lattice . . . 66
5.2.5 Lattice quotients of the facial weak order . . . 67
5.2.6 Two relevant lattice congruences . . . 68
5.3 Facial weak order on arrangements . . . 71
5.3.1 Poset of regions of a hyperplane arrangement . . . 71
5.3.2 Facial weak order of a hyperplane arrangement . . . 71

6 Weak order on integer posets **73**
6.1 Weak order on integer posets . . . 73
6.1.1 Weak order on integer binary relations and integer posets . . . 73
6.1.2 Weak order on relevant families of integer posets . . . 75
6.2 Hopf algebra on integer posets . . . 78
6.2.1 Hopf algebras on binary relations and integer posets . . . 78
6.2.2 Hopf algebras on relevant families of integer posets . . . 79
6.3 Weak order on Coxeter posets . . . 81
6.3.1 Φ-posets . . . 81
6.3.2 Weak order on Φ-posets . . . 82
6.3.3 Weak order on relevant families of Φ-posets . . . 84

III Cluster algebras and generalized associahedra 85

7 Polytopal realizations of finite type g-vector fans 89
7.1 Cluster algebras and $\boldsymbol{g}$-vector fans . . . 89
7.1.1 Cluster algebras . . . 89
7.1.2 Finite type . . . 90
7.1.3 Principal coefficients, $\boldsymbol{g}$- and $\boldsymbol{c}$-vectors . . . 91
7.1.4 The $\boldsymbol{g}$-vector fan . . . 92
7.1.5 Coefficient specialization and universal cluster algebra . . . 93
7.2 Generalized associahedra for $\boldsymbol{g}$-vector fans . . . 94
7.2.1 Polytopal realizations of $\boldsymbol{g}$-vector fans . . . 94
7.2.2 Universal associahedron . . . 95
7.2.3 Further properties of $\mathbb{A}\mathrm{sso}(B_\circ)$ . . . 96
7.3 Type cones of $\boldsymbol{g}$-vector fans . . . 97
7.3.1 Type cone of a simplicial fan . . . 97
7.3.2 Type cones of $\boldsymbol{g}$-vector fans . . . 99

8 Brick polytopes of subword complexes 101
8.1 Combinatorics of subword complexes . . . 101
8.1.1 Subword complex . . . 101
8.1.2 Root function and flips . . . 103
8.2 Brick polytopes of subword complexes . . . 104
8.2.1 Weight function and brick polytope . . . 104
8.2.2 Properties of brick polytopes . . . 105
8.2.3 Duplicated words . . . 106
8.3 Generalized associahedra revisited . . . 107
8.3.1 Generalized associahedra from brick polytopes . . . 107
8.3.2 Word operations and vertex barycenter . . . 108

IV Non-kissing and non-crossing complexes 109

9 Non-kissing versus non-crossing 113
9.1 Non-kissing complex . . . 113
9.1.1 Locally gentle quivers and their blossoming quivers . . . 113
9.1.2 Strings and walks . . . 114
9.1.3 Non-kissing complex . . . 115
9.2 Accordion complex, slalom complex, and non-crossing complex . . . 116
9.2.1 Dual dissections of a surface . . . 116
9.2.2 Accordion complex and slalom complex . . . 117
9.2.3 Accordions versus slaloms and the non-crossing complex . . . 119
9.3 Non-kissing versus non-crossing . . . 119
9.3.1 The quiver of a dissection . . . 119
9.3.2 The surface of a locally gentle quiver . . . 121
9.3.3 Non-crossing and non-kissing complexes coincide . . . 123

10 Non-kissing lattices and non-kissing associahedra **125**
10.1 Flips in non-kissing complexes . . . 125
10.1.1 Distinguished walks, arrows and strings . . . 126
10.1.2 Flips . . . 127
10.2 Non-kissing lattices . . . 128
10.2.1 Biclosed sets of strings . . . 128
10.2.2 Non-kissing congruence . . . 129
10.2.3 Non-kissing lattice . . . 130
10.2.4 Canonical join complex . . . 131
10.3 Non-kissing associahedra . . . 132
10.3.1 $\boldsymbol{g}$- and $\boldsymbol{c}$-vectors . . . 132
10.3.2 Non-kissing fans . . . 134
10.3.3 Non-kissing associahedra . . . 135
10.3.4 Type cones of non-kissing fans . . . 136
10.3.5 Coordinate sections and projections . . . 138

Open problems and perspectives **142**

A Permutreehedra and quotientopes . . . 142
A.1 Permutreehedra, quotientopes and removahedra . . . 142
A.2 Permutreehedra for finite Coxeter groups . . . 143
A.3 Quotientopes for hyperplane arrangements . . . 144
A.4 Type cones of quotient fans . . . 145
A.5 Schröderization for quotientopes . . . 146
B Pipe dreams and subword complexes . . . 147
B.1 Lattices of acyclic pipe dreams . . . 147
B.2 Compatibility degrees for subword complexes . . . 148
B.3 Algebraic connections of pipe dreams . . . 150
C Non-kissing associahedra . . . 150
C.1 Sections of scattering diagrams . . . 150
C.2 Rays of the type cones of non-kissing fans . . . 151
C.3 Graph properties of non-kissing associahedra . . . 151

Bibliography **153**

REMERCIEMENTS

Je souhaite tout d'abord remercier chaleureusement Frédéric Chapoton, Nathan Reading et Hugh Thomas d'avoir accepté de rapporter ce manuscrit. Certains de leurs résultats ont largement inspiré et étayé mes travaux, c'est donc un grand honneur de recevoir ainsi en quelque sorte leur bénédiction. J'en profite aussi pour les remercier des discussions et éclaircissements qu'ils sont toujours prêts à me donner sur le sujet. Un merci tout particulier à Florent Hivert pour avoir parrainé cette habilitation en me guidant à chaque étape et en me donnant de très justes conseils sur le manuscrit. Je suis très heureux que Bernard Leclerc, Lionel Pournin, Maria Ronco et Sibylle Schroll aient également accepté de faire partie du jury. Je remercie aussi Bernard Leclerc, Maria Ronco et Francisco Santos d'avoir écrit une lettre soutenant mon inscription, et Nicole Bidoit-Tollu et Stéphanie Druetta pour leur soutien administratif dans ce processus.

Puisqu'une habilitation est destinée à diriger des recherches, je veux remercier mes étudiants de doctorat et leurs coencadrants pour notre travail passé, présent et futur. Merci donc à Thibault Manneville et Gilles Schaeffer, Joël Gay et Florent Hivert, Aram Dermenjian et Christophe Hohlweg, Mathias Lepoutre et Marie Albenque, Julian Ritter, Doriann Albertin et Jean-Christophe Novelli, Daniel Tamayo Jiménez et Viviane Pons, Noémie Cartier et Florent Hivert, et Germain Pouillot et Arnau Padrol. J'espère que cette habilitation me permettra d'en encadrer bien d'autres, mais ne m'empêchera pas de poursuivre ces coencadrements que je trouve si enrichissants.

Je veux aussi remercier mes coauteurs pour les travaux que nous avons effectués ensemble et pour tout ce qu'ils m'ont appris. Un merci particulier à ceux qui ont travaillé sur le contenu de ce mémoire : Doriann Albertin, Cesar Ceballos, Grégory Chatel, Aram Dermenjian, Joël Gay, Florent Hivert, Christophe Hohlweg, Carsten Lange, Thibault Manneville, Thomas McConville, Arnau Padrol, Yann Palu, Pierre-Guy Plamondon, Michel Pocchiola, Viviane Pons, Julian Ritter, Francisco Santos, Salvatore Stella et Christian Stump.

Je remercie chaleureusement mes collègues du Laboratoire et du Département d'Informatique de l'Équipe Polytechnique pour nos échanges en recherche et en enseignement. Merci en particulier aux membres de l'équipe combinatoire. Je salue aussi les communautés de combinatoire et de géométrie discrète d'Ile de France pour nos échanges fréquents dans des séminaires ou groupes de travail, en particulier les équipes de combinatoire de Marne-la-Vallée, de Paris 7, et de Villetaneuse.

Enfin, je veux remercier ma famille et mes amis pour leur présence et leur soutien. Je sais qu'ils partagent mon goût pour la recherche et les mathématiques, mais surtout ils m'apportent une joie et un équilibre inestimable. Merci à Claude et Bernard pour avoir partagé leur goût des mathématiques, et à Christophe et Thomas pour notre complicité. Enfin, merci à Arnau pour nous réveiller tous les matins en nous montrant les oiseaux, et à Marga pour le bonheur de partager ces moments.

RÉSUMÉ

Ce document présente un tour d'horizon de mes recherches qui gravitent autour de deux polytopes classiques appelés permutaèdre et associaèdre et illustrés à la figure 1.

Le *permutaèdre* est un polytope dont la structure faciale est décrite par le groupe symétrique $\mathfrak{S}_n$: ses sommets correspondent aux permutations de $[n] := \{1, \dots, n\}$; ses arêtes correspondent aux paires de permutations reliées par une transposition simple ; et ses faces correspondent aux partitions ordonnées de $[n]$ (ou de manière équivalente aux classes à gauches des sous-groupes paraboliques de $\mathfrak{S}_n$). De nombreuses propriétés du groupe symétrique $\mathfrak{S}_n$ se lisent géométriquement sur le permutaèdre : le diagramme de Hasse de l'ordre faible sur $\mathfrak{S}_n$ (où les permutations sont ordonnées par inclusion de leurs ensembles d'inversions) est donné par une orientation linéaire du graphe du permutaèdre, les expressions réduites des permutations en produits de transpositions simples correspondent aux chemins dans ce graphe orienté ; les relations de tresses entre ces expressions réduites correspondent au balayage de faces de dimension 2 du permutaèdre ; etc.

L'*associaèdre* est un polytope "mythique" [Hai84] dont la structure faciale peut se décrite par différentes structures de Catalan : ses sommes correspondent aux parenthésages d'un produit non-associatif, aux triangulations d'un polygone convexe, ou aux arbres binaires ; ses arêtes correspondent aux applications de la règle associativité dans les produits, aux flips de diagonales dans les triangulations, ou aux rotations dans les arbres binaires ; et ses faces correspondent aux parenthésages partiels, aux dissections du polygone, ou aux arbres de Schröder. De plus, une orientation bien choisie du graphe de l'associaèdre donne le diagramme de Hasse du classique treillis de Tamari [Tam51]. L'associaèdre est une structure fondamentale dans diverses branches des mathématiques, en particulier pour les espaces modulaires et la topologie [Sta63, Kel01], les operades et la théorie de la réécriture [Str12, MTTV19], les algèbres de Hopf combinatoires [LR98, CP17, Pil18], les algèbres amassées [FZ02, FZ03a], la théorie des harmoniques diagonaux [BPR12, PRV17], la physique mathematique [AHBHY18], etc. La structure combinatoire et topologique de l'associaèdre a été introduite dans les travaux originaux de D. Tamari [Tam51] et J. Stasheff [Sta63], et un premier modèle polytopal 3-dimensionnel a été réalisé par J. Milnor pour la soutenance de doctorat de J. Stasheff. Les premières réalisations polytopales systématiques ont été construites par M. Haiman [Hai84] et C. Lee [Lee89]. Depuis, l'associaèdre a été largement "démystifié" avec de nombreuses constructions polytopales, basées sur la théorie des polytopes secondaires [GKZ08, BFS90], les éventails de $\boldsymbol{d}$-vecteurs [CFZ02, CSZ15, MP17], les éventails de $\boldsymbol{g}$-vecteurs [Lod04, HL07, LP18, HLT11, HPS18], les polytopes de briques [PS12, PS15a], etc.

Ces polytopes peuvent être étudiés sous différentes perspectives : par la combinatoire avec leur structure de treillis, par la géométrie discrète avec leur structure polytopale, ou par l'algèbre avec leurs connexions aux algèbres de Hopf combinatoires et aux algèbres amassées. De plus, ces structures sur les permutaèdres et les associaèdres sont fortement liées. Ces connexions prototypiques ainsi que les prérequis nécessaires à la lecture de ce document sont présentés au chapitre 1.

Le but de ce document est de présenter diverses généralisations du permutaèdre et de l'associaèdre naturellement motivées par différentes perspectives. Le document traite quatre directions spécifiques, résumées ci-dessous :

- Partie I : Congruences de treillis, polytopes et algèbres de Hopf.
- Partie II : Au delà de l'ordre faible.
- Partie III : Algèbres amassées et associaèdres généralisés.
- Partie IV : Complexes platoniques des carquois aimables.

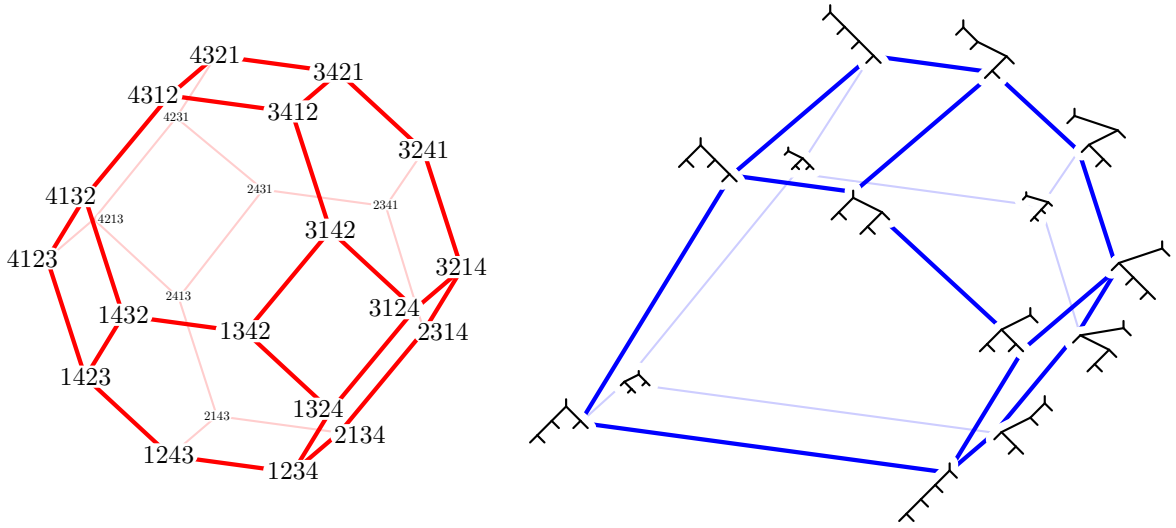

FIGURE 1 : Le permutaèdre (à gauche) et l'associaèdre (à droite) de dimension 3.

Partie I : Congruences de treillis, polytopes et algèbres de Hopf. Cette première partie est motivée par les interactions entre les structures combinatoire, géométrique et algébrique provenant des congruences de treillis de l'ordre faible. Le prototype est la congruence sylvestre [HNT05], qui peut être définie par une règle de réécriture sur les permutations ou comme les fibres de l'insertion des permutations dans des arbres binaires de recherche. Cette congruence donne une perspective éclairante sur le treillis de Tamari [Tam51], sur l'éventail normal de l'associaèdre de J.-L. Loday [Lod04], et sur l'algèbre de J.-L. Loday et M. Ronco sur les arbres binaires [LR98]. Cette perspective a été largement étendue par N. Reading dans [Rea05] : le message général est que les congruences de treillis de l'ordre faible permettent de construire des treillis, des éventails et (parfois) des algèbres de Hopf. Dans la première partie de ce document, nous étudions cette direction pour trois généralisations de la congruence sylvestre :

Chapitre 2. Polytopes de briques. Nous considérons une famille des congruences de treillis motivée par certaines multitriangulations [PS09] et leurs connexions [PP12] avec certaines familles d'arrangements de tuyaux [BB93, KM05]. Ces congruences correspondent à la géométrie des éventails normaux de certains polytopes de briques [PS12] et permettent de construire l'algèbre de briques [Pil18]. Elle fournissent un exemple intéressant de la théorie de N. Reading [Rea05].

Chapitre 3. Permutarbrèdres. Nous étudions les permutarbres [PP18], objets combinatoires qui généralisent et interpolent entre les permutations, les arbres binaires, et les séquences binaires. Nous construisons des structures de treillis sur les permutarbres, des réalisations géométriques appelées permutarbrèdres, et définissons l'algèbre de Hopf des permutarbres. Il s'agit d'un premier pas au delà de la théorie de N. Reading puisque nous considérons simultanément 4^n congruences de l'ordre faible sur $\mathfrak{S}_n$ pour tout $n \in \mathbb{N}$ et notre algèbre de Hopf permet de calculer des produits et des coproduits entre les permutarbres de toutes ces congruences.

Chapitre 4. Quotientopes. Finalement, nous traitons simultanément toutes les congruences de treillis de l'ordre faible. Nous construisons des réalisations géométriques appelées quotientopes [PS19] et nous construisons des structures d'algèbres de Hopf contenant toutes les congruences de treillis simultanément [Pil19].

Partie II : Au delà de l'ordre faible. L'objectif de cette deuxième partie est d'étendre les structures étudiées dans la partie I au delà de l'ordre faible dans deux directions différentes : remplacer d'une part l'arrangement de tresses par l'arrangement de Coxeter d'un groupe de Coxeter fini quelconque, ou même par un arrangement d'hyperplans arbitraire ; et remplacer d'autre part l'ordre faible sur les permutations par des ordres similaires sur toutes les faces du permutaèdre, sur tous les intervals de l'ordre faible, ou même sur tous les ordres partiels sur des entiers. Ces généralisations sont organisées en deux étapes :

Chapitre 5. Ordre faible facial. Nous considérons d'abord une structure de treillis naturelle sur toutes les faces du permutaèdre, appelée pseudopermutaèdre dans [KLN+01], qui étend l'ordre faible sur les permutations. Nous étudions la généralisation de cet ordre à tout groupe de Coxeter fini W : suivant les traces de [PR06], nous définissons un ordre sur toutes les faces du W-permutaèdre qui étend l'ordre faible sur W, et que nous appelons donc ordre faible facial [DHP18]. En outre, nous définissons et étudions l'ordre faible facial d'un arrangement d'hyperplans arbitraire [DHMP19], étendant ainsi l'ordre des régions de l'arrangement [BEZ90]. Dans ces deux situations, nous fournissons plusieurs interprétations de l'ordre faible facial, qui sont fondamentales pour montrer que l'ordre faible facial est un treillis dès que l'ordre des régions est un treillis. Finalement, nous observons que toute congruence de l'ordre faible s'étend en une congruence de treillis de l'ordre faible facial, ce qui permet de définir une structure de treillis sur les faces de l'éventail quotient correspondant.

Chapitre 6. Ordre faible sur les ordres partiels entiers. Suivant la direction donnée par le chapitre 5, nous définissons l'ordre faible sur les relations binaires entières (*i.e.* les relations binaires sur $[n] := \{1, \dots, n\}$), et ses restrictions aux ordres partiels entiers [CPP19]. Cet ordre définit encore une structure de treillis qui nous permet de réinterpréter les structures de treillis sur les sommets, les intervalles et les faces du permutaèdre et de l'associaèdre (et plus généralement des permutarbrèdres) comme des sous-ordres (et parfois des sous-treillis) de l'ordre faible sur les ordres partiels entiers. En suivant le même modèle, nous définissons également une algèbre de Hopf sur les ordres partiels entiers [PP20] qui nous permet de réinterpréter certaines (ou définir de nouvelles) algèbres de Hopf sur les sommets, les intervalles ou les faces du permutaèdre et de l'associaèdre (et plus généralement des permutarbrèdres). Finalement, nous discutons l'extension de cet ordre faible sur les ordres partiels entiers aux sous-ensembles antisymétriques et clos d'un système de racines d'un groupe de Coxeter fini arbitraire [GP18]. Pour un groupe de Weyl W, nous obtenons à nouveau une structure de treillis qui contient comme sous-ordre l'ordre faible sur les éléments, les intervalles et les faces du W-permutaèdre (présenté au chapitre 5) et des W-associaèdres. En revanche, cette construction échoue étonnamment à définir une structure de treillis au delà des systèmes de racines crystallographiques.

Partie III : Algèbres amassées et associaèdres généralisés. Cette troisième partie est centrée sur les algèbres amassées et les associaèdres généralisés. Les algèbrees amassées ont été introduites par S. Fomin et A. Zelevinsky dans [FZ02] avec des motivations provenant de la positivité totale et des bases canoniques, et se sont rapidement révélées comme une structure fondamentale dans de nombreux domaines des mathématiques (théorie des représentations de carquois, géométrie de Poisson, systèmes intégrables, etc). Les algèbres amassées de type fini ont été rapidement classifiées dans [FZ03a], et des réalisations polytopales des complexes d'amas de type fini, appelées associaèdres généralisés, ont été construites dans [CFZ02, HLT11, Ste13]. Les complexes d'amas de type fini ont aussi été réinterprétés plus tard dans [CLS14] en termes de complexes de sous-mots sur des groupes

de Coxeter finis définis par A. Knutson et E. Miller dans [KM04]. Cette partie du document étudie les réalisations polytopales des complexes d'amas et des complexes de sous-mots :

Chapitre 7. Réalisations polytopales des éventails de g-vecteurs de type fini. Nous présentons d'abord une réponse définitive à la question de la polytopalité de l'éventail des g-vecteurs d'une algèbre amassée de type fini par rapport à une graine initiale (cyclique ou acyclique). En fait, nous rapportons deux approches différentes : la première utilise l'associaèdre universel de [HPS18] qui contient simultanément tous les éventails de g-vecteurs, la deuxième utilise le cône de type de [PPPP19] qui décrit toutes les réalisations polytopales d'un éventail de g-vecteurs donné.

Chapitre 8. Polytopes de briques des complexes de sous-mots. Nous présentons ensuite la construction et les propriétés des polytopes de briques des complexes de sous-mots [PS15a]. En utilisant la connexion entre les complexes d'amas et les complexes de sous-mots [CLS14], nous obtenons une construction alternative des associaèdres généralisés de [HLT11], qui fournit en particulier une description explicite de leurs sommets et permet de prouver une propriété intrigante de leurs barycentres [PS15b]. Contrairement aux méthodes développées au chapitre 7, l'approche par polytopes de briques ne réalise que les éventails de g-vecteurs des algèbres amassées de type fini par rapport à une graine initiale acyclique, mais couvre aussi des complexes de sous-mots au delà des complexes d'amas.

Partie IV : Complexes platoniques des carquois aimables. Cette quatrième partie étudie une généralisation très riche de l'associaèdre, appelée associaèdre aimable. La motivation initiale provient de deux generalisations récentes de l'associaèdre : les associaèdres de grilles [PPS10, SSW17, McC17, GM17a] et les accordéoèdres [Bar01, Cha16, GM18, MP19]. Il s'agit de réalisations géométriques des complexes platoniques (sans bisous) de sous-ensembles de la grille et des complexes parallèles (sans croisements) de dissections de polygones convexes. Nous avons observé dans [PPP17] que ces complexes simpliciaux sont des cas particuliers des complexes platoniques de carquois aimables. Ces derniers fournissent des modèles combinatoires pour les complexes support τ-basculants [AIR14] des algèbres aimables [BR87], une notion algébrique définie par la théorie des représentations des carquois et essentiellement omise dans ce document. Cette famille de complexes simpliciaux partage de nombreuses propriétés avec les associaèdres classiques, en particulier ils ont de riches structures de treillis et peuvent être réalisés par des polytopes convexes. Nous avons seulement réalisé plus tard dans [PPP19] que les complexes platoniques des algèbres aimables peuvent aussi s'interpréter comme des complexes parallèles de dissections sur des surfaces. Dans ce document, nous inversons la chronologie et présentons ces complexes dans l'ordre logique :

Chapitre 9. Platonique contre parallèle. Nous définissons d'abord le complexe platonique (sans bisous) d'un carquois localement aimable et le complexe parallèle (sans croisements) d'une surface orientée à bords munie d'une paire de dissections cellulaires duales. Nous montrons ensuite une bijection entre les carquois localement aimables et les surfaces orientées à bords munies de paires de dissections cellulaires duales, qui envoie naturellement les complexes platoniques de carquois localement aimables sur les complexes parallèles des surfaces orientés munies de dissections.

Chapitre 10. Treillis platoniques et associaèdres platoniques. Nous nous concentrons ensuite sur les complexes platoniques et montrons certaines de leurs propriétés structurelles développées dans [PPP17] qui généralisent les propriétés classiques de l'associaèdre. Nous décrivons d'abord l'opération d'échange sur les facettes platoniques, qui montre que le complexe platonique est

une pseudo-variété. Suivant l'approche de [McC17], nous construisons ensuite une structure de treillis sur le graphe d'échange platonique comme quotient de treillis d'un treillis de sous-ensembles biclos de cordes, généralisant ainsi la connexion entre l'ordre faible sur les permutations et le treillis de Tamari sur les arbres binaires. Finalement, nous construisons les associaèdres platoniques réalisant les complexes platoniques et généralisant les associaèdres classiques.

Nous concluons par quelques directions de recherche et problèmes ouverts motivés par le matériel présenté dans ce document et qui offrent de bons points d'entrée sur le sujet et des projets de recherches adaptés à des étudiants de master ou de doctorat. Ces problèmes sont organisés autour de trois sujets : les permutarbreèdres et les quotientopes (section A), les arrangements de tuyaux et les complexes de sous-mots (section B), et les algèbres aimables (section C).

INTRODUCTION

This document proposes an overview of my recent work gravitating around two famous and ubiquitous polytopes, called permutahedron and associahedron.

The *permutahedron* is a polytope whose face structure is described by the symmetric group $\mathfrak{S}_n$: its vertices correspond to permutations of $[n] := \{1, \dots, n\}$; its edges correspond to pairs of permutations related by a simple transposition; and its faces correspond to ordered partitions of $[n]$ (or equivalently to parabolic cosets of $\mathfrak{S}_n$). Many algebraic properties of the symmetric group $\mathfrak{S}_n$ can be read geometrically on the permutahedron: the Hasse diagram of the weak order on $\mathfrak{S}_n$ (where permutations are ordered by inclusion of their inversion sets) is given by a linear orientation of the graph of the permutahedron; reduced expressions of permutations as product of simple transpositions correspond to paths in this oriented graph; braid relations among reduced expressions correspond to sweeping 2-dimensional faces of the permutahedron; etc.

The *associahedron* is a "mythical polytope" [Hai84] whose face structure can be described by different Catalan families: its vertices correspond to parenthesizations of a non-associative product, triangulations of a convex polygon, or binary trees; its edges correspond to applications of the associativity rule, diagonal flips, or edge rotations; and its faces correspond to partial parenthesizations, diagonal dissections, or Schröder trees. Moreover, a suitable orientation of the graph of the associahedron gives the Hasse diagram of the famous Tamari lattice [Tam51]. The associahedron appears as a fundamental structure in several mathematical theories, in particular moduli spaces and topology [Sta63, Kel01], operads and rewriting theory [Str12, MTTV19], combinatorial Hopf algebras [LR98, CP17, Pil18], cluster algebras [FZ02, FZ03a], diagonal harmonics [BPR12, PRV17], mathematical physics [AHBHY18], etc. The combinatorial and topological structure of the associahedron was introduced in early works of D. Tamari [Tam51] and J. Stasheff [Sta63], and a first 3-dimensional polytopal model was realized by J. Milnor for the PhD defense of J. Stasheff. The first systematic polytopal realizations were constructed by M. Haiman [Hai84] and C. Lee [Lee89]. Since then, the associahedron has been largely "demystified" with several polytopal constructions, based on secondary polytopes [GKZ08, BFS90], $\boldsymbol{d}$-vector fans [CFZ02, CSZ15, MP17], $\boldsymbol{g}$-vectors fans [Lod04, HL07, LP18, HLT11, HPS18], brick polytopes [PS12, PS15a], etc.

These polytopes can be considered from different perspectives: from combinatorics with their lattice structure, from discrete geometry with their polytopal structure, and from algebra with their connections to combinatorial Hopf algebras and cluster algebras. Moreover, these structures on the permutahedra and associahedra are strongly related. These prototypical connections together with the minimal background needed to read this document are presented in Chapter 1.

The aim of this document is to present various generalizations of the permutahedron and associahedron that naturally arise from these different perspectives. We explore four specific directions that we briefly summarize below:

- Part I: Lattice congruences, polytopes and Hopf algebras.
- Part II: Beyond the weak order.
- Part III: Cluster algebras and generalized associahedra.
- Part IV: Non-kissing and non-crossing complexes.

Part I: Lattice congruences, polytopes and Hopf algebras. This first part is motivated by the interplay between the combinatorial, geometric and algebraic structures arising from lattice congruences of the weak order. The prototype is the sylvester congruence [HNT05], which can be defined by a rewriting rule on permutations or by the fibers of the binary search tree insertion of permutations. This congruence provides an enlighting perspective on the Tamari lattice [Tam51], on the normal fan of J.-L. Loday's associahedron [Lod04], and on J.-L. Loday and M. Ronco's Hopf algebra on binary trees [LR98]. This perspective has been widely extended by N. Reading in [Rea05]: the general message is that lattice congruences of the weak order enable to construct relevant lattices, fans, and (sometimes) Hopf algebras. In the first part of this document, we investigate this direction for three generalizations of the sylvester congruence:

Chapter 2. Brick polytopes. We consider a family of lattice congruences motivated by certain multitriangulations [PS09] and their connection [PP12] to certain families of pipe dreams [BB93, KM05]. These congruences correspond to the geometry of the normal fans of certain brick polytopes [PS12] and enable to construct the brick algebra of [Pil18]. They provide a relevant example of N. Reading's setting [Rea05].

Chapter 3. Permutreehedra. We investigate permutrees [PP18], some combinatorial objects that generalize and interpolate between permutations, binary trees, and binary sequences. We construct lattice structures on permutrees, geometric realizations called permutreehedra, and define the permutree Hopf algebra. This is our first step beyond N. Reading's setting as we consider simultaneously 4^n lattice congruences of the weak order on $\mathfrak{S}_n$ for each $n \in \mathbb{N}$ and our Hopf algebra performs product and coproducts between all permutrees for all these congruences.

Chapter 4. Quotientopes. We finally deal simultaneously with all lattice congruences of the weak order. We construct geometric realizations called quotientopes [PS19] and construct Hopf algebra structures containing all lattice congruences simultaneously [Pil19].

Part I is mainly based on the following contributions:

- Vincent Pilaud. *Brick polytopes, lattice quotients, and Hopf algebras*. Journal of Combinatorial Theory, Series A, vol. 155, pp. 418 – 457, 2018.
- Vincent Pilaud & Viviane Pons. *Permutrees*. Algebraic Combinatorics, vol. 1(2), pp. 173 – 224, 2018.
- Vincent Pilaud & Francisco Santos. *Quotientopes*. Bulletin of the London Mathematical Society, vol. 51(3), pp. 406 – 420, 2019.
- Vincent Pilaud. *Hopf algebras on decorated noncrossing arc diagrams*. Journal of Combinatorial Theory, Series A, vol. 161, pp. 486 – 507, 2019.

The following contributions are also closely connected to this part:

- Vincent Pilaud & Francisco Santos. *Multitriangulations as complexes of star-polygons*. Discrete & Computational Geometry, vol. 41(2), pp. 284 – 317, 2009.
- Vincent Pilaud & Michel Pocchiola. *Multitriangulations, pseudotriangulations and primitive sorting networks*. Discrete & Computational Geometry, vol. 48(1), pp. 142 – 191, 2012.
- Vincent Pilaud & Francisco Santos. *The brick polytope of a sorting network*. European Journal of Combinatorics, vol. 33(4), pp. 632 – 662, 2012.
- Carsten Lange & Vincent Pilaud. *Associahedra via spines*. Combinatorica, vol. 38(2), pp. 443 – 486, 2018.
- Grégory Chatel & Vincent Pilaud. *Cambrian Hopf Algebras*. Advances in Mathematics, vol. 311, pp. 598 – 633, 2017.
- Florent Hivert & Vincent Pilaud. *Signaletic operads*. Preprint, 97 pp., arXiv:1906.02228, 2019.

Part II: Beyond the weak order. The objective of this second part is to extend the structures studied in Part I beyond the weak order in two different directions: replacing on the one hand the braid arrangement by Coxeter arrangements of arbitrary finite Coxeter groups, or even by arbitrary hyperplane arrangements; and replacing on the other hand the weak order on permutations by similar orders on all faces of the permutahedron, on all intervals of the weak order, or even on all integer posets. These generalizations are organized in two steps:

Chapter 5. Facial weak order. We first consider a natural lattice structure on all faces of the permutahedron, called pseudopermutahedron in [KLN+01], that extends the weak order on permutations. We investigate the generalization of this order to any finite Coxeter group W: following [PR06], we define an order on all faces of the W-permutahedron that extends the weak order on W, and which we therefore call the facial weal order [DHP18]. We also define and study the facial weak order of arbitrary hyperplane arrangements [DHMP19], extending the poset of regions of the arrangement [BEZ90]. In both settings, we provide various interpretations of the facial weak order, which are instrumental to prove that the facial weak order is a lattice when the poset of regions is a lattice. Finally, we observe that any lattice congruence of the weak order extends to a lattice congruence of the facial weak order, thus defining a lattice structure on all faces of the corresponding quotient fan.

Chapter 6. Weak order on integer posets. Following the guiding line of Chapter 5, we then define the weak order on integer binary relations (*i.e.* binary relations on $[n] := \{1, \dots, n\}$), and its restriction to integer posets [CPP19]. This order again defines a lattice structure which enables to reinterpret the lattice structures on the vertices, the intervals and the faces of the permutahedron and associahedron (and more generally permutreehedra) as subposets (and sometimes sublattices) of the weak order on integer posets. Following the same template, we also define a Hopf algebra on integer posets [PP20] that enables to reinterpret classical (or define new) Hopf algebra structures on the vertices, the intervals and the faces of the permutahedron and associahedron (and more generally permutreehedra). Finally, we discuss the extension of the weak order on integer posets to antisymmetric closed subsets of roots of the root system of an arbitrary finite Coxeter group [GP18]. For a Weyl group W, we obtain again a lattice structure, which contains as subposets the weak order on elements, intervals and faces of the W-permutahedron (presented in Chapter 5) and W-associahedra. In contrast, it surprisingly fails to define a lattice structure beyond crystallographic root systems.

Part II is based on the following contributions:

- Aram Dermenjian, Christophe Hohlweg & Vincent Pilaud. *The facial weak order and its lattice quotients*. Transactions of the American Mathematical Society, vol. 370(2), pp. 1469 – 1507, 2018.
- Aram Dermenjian, Christophe Hohlweg, Thomas McConville & Vincent Pilaud. *The facial weak order on hyperplane arrangements*. Preprint, 34 pp., arXiv:1910.03511, 2019.
- Grégory Chatel, Vincent Pilaud & Viviane Pons. *The weak order on integer posets*. Algebraic Combinatorics, vol. 2(1), pp. 1 – 48, 2019.
- Vincent Pilaud & Viviane Pons. *The Hopf algebra of integer binary relations*. IRMA Lectures in Mathematics and Theoretical Physics (Algebraic Combinatorics, Resurgence, Moulds and Applications, CARMA), vol. 31, pp. 299 – 344, 2020.
- Joël Gay & Vincent Pilaud. *The weak order on Weyl posets*. Canadian Journal of Mathematics, online first, 2019.

Part III: Cluster algebras and generalized associahedra. This third part focusses on cluster algebras and generalized associahedra. Cluster algebras were introduced by S. Fomin and A. Zelevinsky in [FZ02] with motivations from total positivity and canonical bases, and quickly appeared to be a fundamental structure in many areas of mathematics (representation theory of quivers, Poisson geometry, integrable systems, etc). The finite type cluster algebras were soon classified in [FZ03a], and polytopal realizations of finite cluster complexes, called generalized associahedra, were constructed in [CFZ02, HLT11, Ste13]. Finite type cluster complexes were also reinterpreted later in [CLS14] using subword complexes on finite Coxeter groups defined by A. Knutson and E. Miller in [KM04]. In this part of the document, we investigate further polytopal realizations of finite cluster complexes and subword complexes:

Chapter 7. Polytopal realizations of finite type $\boldsymbol{g}$-vector fans. We first provide a definitive answer to the question of the polytopality of the $\boldsymbol{g}$-vector fan of a finite type cluster algebra with respect to any initial seed (acyclic or not). We actually report two approaches with different advantages: first using the universal associahedron of [HPS18] which contains simultaneously all $\boldsymbol{g}$-vector fans and then with the type cone approach of [PPPP19] which provides all polytopal realizations of a given $\boldsymbol{g}$-vector fan.

Chapter 8. Brick polytopes of subword complexes. We then present the construction and properties of brick polytopes of subword complexes [PS15a]. Using the connection between cluster complexes and subword complexes [CLS14], we obtain an alternative interpretation of the generalized associahedra of [HLT11], which provides in particular their explicit vertex description and yields the first proof of an intriguing property of their barycenter [PS15b]. In contrast to the methods developed in Chapter 7, the brick polytope approach only realizes acyclic $\boldsymbol{g}$-vector fans of finite type cluster algebras, but also covers subword complexes beyond cluster complexes.

Part III is mainly based on the following contributions:

- Christophe Hohlweg, Vincent Pilaud & Salvatore Stella. *Polytopal realizations of finite type* g*-vector fans*. Advances in Mathematics, vol. 328, pp. 713 – 749, 2018.
- Arnau Padrol, Yann Palu, Vincent Pilaud & Pierre-Guy Plamondon. *Associahedra for finite type cluster algebras and minimal relations between* g*-vectors*. Preprint, 64 pp., arXiv:1906.06861, 2019.
- Vincent Pilaud & Christian Stump. *Brick polytopes of spherical subword complexes and generalized associahedra*. Advances in Mathematics, vol. 276, pp. 1 – 61, 2015.
- Vincent Pilaud & Christian Stump. *Vertex barycenter of generalized associahedra*. Proceedings of the American Mathematical Society, vol. 143(6), pp. 2623 – 2636, 2015.

The following contributions are also closely connected to this part:

- Vincent Pilaud & Christian Stump. *EL-labelings and canonical spanning trees for subword complexes*. Discrete Geometry and Optimization, Fields Institute Communications Series, Springer, pp. 213 – 248, 2013.
- Cesar Ceballos & Vincent Pilaud. *Denominator vectors and compatibility degrees in cluster algebras of finite type*. Transactions of the American Mathematical Society, vol. 367, pp. 1421 – 1439, 2015.
- Thibault Manneville & Vincent Pilaud. *Compatibility fans for graphical nested complexes*. Journal of Combinatorial Theory, Series A, vol. 150C, pp. 36 – 107, 2017.

Part IV: Non-kissing and non-crossing complexes. This fourth part investigates a rich generalization of the associahedron, called gentle associahedron. The initial motivation arises from two recent generalizations of the associahedron: grid associahedra [PPS10, SSW17, McC17, GM17a] and accordiohedra [Bar01, Cha16, GM18, MP19]. These are geometric realizations of the non-kissing complexes of subsets of the grid and of the non-crossing complexes of dissections of convex polygons. We observed in [PPP17] that these simplicial complexes are special cases of non-kissing complexes of gentle quivers. The latter provide combinatorial models for support τ-tilting complexes [AIR14] of gentle algebras [BR87], an algebraic notion defined from representation theory of quivers and essentially omitted in this document. This family of simplicial complexes shares many properties with the classical associahedra, in particular they have rich lattice structures and can all be realized as convex polytopes. Only later we realized in [PPP19] that non-kissing complexes of gentle quivers can also be interpreted as non-crossing complexes of dissection of surfaces. Here, we revert the chronology to present these complexes in a logical order:

Chapter 9. Non-kissing versus non-crossing. We first define the non-kissing complex of a locally gentle quiver and the non-crossing complex of an oriented surface with boundary endowed with a pair of dual cellular dissections. We then show a bijection between locally gentle bound quivers and oriented surfaces with boundary endowed with a pair of dual cellular dissections, which naturally sends non-kissing complexes on locally gentle quivers to non-crossing complexes of oriented surfaces with dissections.

Chapter 10. Non-kissing lattices and non-kissing associahedra. We then focus on non-kissing complexes and show some of their structural properties developed in [PPP17] that generalize properties of the classical associahedron. First, we describe the flip operation on non-kissing facets, which shows that the non-kissing complex is a pseudomanifold. Following the approach of [McC17], we then construct a lattice structure on the non-kissing flip graph obtained as a lattice quotient of a lattice of biclosed sets of strings, generalizing the connection between the weak order on permutations and the Tamari lattice on binary trees. Finally, we construct the non-kissing associahedra realizing the non-kissing complexes and generalizing the classical associahedra.

Part IV is mainly based on the following contributions:

- Yann Palu, Vincent Pilaud & Pierre-Guy Plamondon. *Non-kissing and non-crossing complexes for locally gentle algebras*. Journal of Combinatorial Algebra, vol. 3(4), pp. 401 – 438, 2019.
- Yann Palu, Vincent Pilaud & Pierre-Guy Plamondon. *Non-kissing complexes and τ-tilting for gentle algebras*. To appear in Memoirs of the American Mathematical Society, 2018.
- Arnau Padrol, Yann Palu, Vincent Pilaud & Pierre-Guy Plamondon. *Associahedra for finite type cluster algebras and minimal relations between* g*-vectors*. Preprint, 64 pp., `arXiv:1906.06861`, 2019.

The following contributions are also closely connected to this part:

- Thibault Manneville & Vincent Pilaud. *Geometric realizations of the accordion complex of a dissection*. Discrete & Computational Geometry, vol. 61(3), pp. 507 – 540, 2019.
- Vincent Pilaud, Pierre-Guy Plamondon & Salvatore Stella. *A τ-tilting approach to dissections of polygons*. Symmetry, Integrability & Geometry: Methods & Applications, vol. 14, Paper 045, 8 pp., 2018.

We conclude with some research directions and open problems motivated by the material presented in this document that provide good entry points to the topic and research projects suitable for Master and PhD students. These problems are organized in three topics: permutreehedra and quotientopes (Section A), pipe dreams and subword complexes (Section B), and gentle algebras (Section C).

To conclude this brief introduction, three disclaimers about this document:

- First, besides the organization and the articulation of the text, nothing is new in this document: all results appeared in publications or preprints that I have (co-)authored. In fact, this document is a compilation of these works and thus reproduces or paraphrases large passages from these papers (either from their journal version or from their extended abstract version for conferences), and borrows many of their figures. To avoid surcharging the text, definitions and statements that appeared in my works are not systematically referenced one by one. However, both the summaries presented above and the introduction of each chapter clearly indicate the origin of the results. In contrast, definitions and statements due to other authors should all be attributed individually.
- Second, to focus on the general philosophy of my research and avoid pedestrian details, all proofs are omitted and only the statements appear in the document. The reader interested in the proofs will find all necessary details in the corresponding long version papers.
- Finally, this document does not present all my research so far. I have in particular decided to completely omit my works on polytopality of Cartesian products of graphs [MPP11, PPS12], geometric configurations and oriented matroids [FPP11, BP14, BP15, BP16], graph associahedra [MP15, MP17, Pil17], and combinatorics of type D cluster algebras [CP15a, CP16]. A complete list of my publications is available in the next page.

COMPLETE PUBLICATION LIST

Journals

[J1] Vincent Pilaud & Francisco Santos. *Multitriangulations as complexes of star-polygons*. Discrete & Computational Geometry, vol. 41(2), pp. 284 – 317, 2009.

[J2] Julien Ferté, Vincent Pilaud & Michel Pocchiola. *On the number of simple arrangements of five double pseudolines*. Discrete & Computational Geometry, vol. 45(2), pp. 279 – 302, 2011.

[J3] Benjamin Matschke, Julian Pfeifle & Vincent Pilaud. *Prodsimplicial neighborly polytopes*. Discrete & Computational Geometry, vol. 46(1), pp. 100 – 131, 2011.

[J4] Julian Pfeifle, Vincent Pilaud & Francisco Santos. *Polytopality and Cartesian products of graphs*. Israel Journal of Mathematics, vol. 192(1), pp. 121 – 141, 2012.

[J5] Vincent Pilaud & Michel Pocchiola. *Multitriangulations, pseudotriangulations and primitive sorting networks*. Discrete & Computational Geometry, vol. 48(1), pp. 142 – 191, 2012.

[J6] Vincent Pilaud & Francisco Santos. *The brick polytope of a sorting network*. European Journal of Combinatorics, vol. 33(4), pp. 632 – 662, 2012.

[J7] Minghui Jiang, Vincent Pilaud & Pedro Tejada. *On a dispersion problem in grid labeling*. SIAM Journal on Discrete Mathematics, vol. 26(1), pp. 39 – 51, 2012.

[J8] Vincent Pilaud & Christian Stump. *EL-labelings and canonical spanning trees for subword complexes*. Discrete Geometry and Optimization, Fields Institute Communications Series, Springer, pp. 213 – 248, 2013.

[J9] Nicolai Hähnle, Steven Klee & Vincent Pilaud. *Obstructions to weak decomposability for simplicial polytopes*. Proceedings of the American Mathematical Society, vol. 142(9), pp. 3249 – 3257, 2014.

[J10] Jürgen Bokowski & Vincent Pilaud. *Enumerating topological (n_k)-configurations*. Computational Geometry: Theory and Applications, vol. 47(2), pp. 175 – 186, 2014.

[J11] Vincent Pilaud & Juanjo Rué. *Analytic combinatorics of chord and hyperchord diagrams with k crossings*. Advances in Applied Mathematics, vol. 57, pp. 60 – 100, 2014.

[J12] Vincent Pilaud & Christian Stump. *Vertex barycenter of generalized associahedra*. Proceedings of the American Mathematical Society, vol. 143(6), pp. 2623 – 2636, 2015.

[J13] Cesar Ceballos & Vincent Pilaud. *Denominator vectors and compatibility degrees in cluster algebras of finite type*. Transactions of the American Mathematical Society, vol. 367, pp. 1421 – 1439, 2015.

[J14] Vincent Pilaud & Christian Stump. *Brick polytopes of spherical subword complexes and generalized associahedra*. Advances in Mathematics, vol. 276, pp. 1 – 61, 2015.

[J15] Jürgen Bokowski & Vincent Pilaud. *On topological and geometric (19_4) configurations*. European Journal of Combinatorics, vol. 50, pp. 4 – 17, 2015.

[J16] Thibault Manneville & Vincent Pilaud. *Graph properties of graph associahedra*. Séminaire Lotharingien de Combinatoire, B73d, 31 pp., 2015.

[J17] Cesar Ceballos & Vincent Pilaud. *Cluster algebras of type D pseudotriangulations approach*. Electronic Journal of Combinatorics, vol. 22(4), #P4.44, 27 pp., 2015.

[J18] Cesar Ceballos & Vincent Pilaud. *The diameter of type D associahedra and the non-leaving-face property*. European Journal of Combinatorics, vol. 51, pp. 109 – 124, 2016.

[J19] Jürgen Bokowski & Vincent Pilaud. *Quasi-configurations building blocks for point-line configurations*. ARS Mathematica Contemporanea, vol. 10(1), pp. 99 – 112, 2016.

[J20] Thibault Manneville & Vincent Pilaud. *Compatibility fans for graphical nested complexes*. Journal of Combinatorial Theory, Series A, vol. 150C, pp. 36 – 107, 2017.

[J21] Grégory Chatel & Vincent Pilaud. *Cambrian Hopf Algebras*. Advances in Mathematics, vol. 311, pp. 598 – 633, 2017.
[J22] Vincent Pilaud. *Which nestohedra are removahedra?* Revista Colombiana de Matemáticas, vol. 51, pp. 21 – 42, 2017.
[J23] Aram Dermenjian, Christophe Hohlweg & Vincent Pilaud. *The facial weak order and its lattice quotients*. Transactions of the American Mathematical Society, vol. 370(2), pp. 1469 – 1507, 2018.
[J24] Vincent Pilaud. *Brick polytopes, lattice quotients, and Hopf algebras*. Journal of Combinatorial Theory, Series A, vol. 155, pp. 418 – 457, 2018.
[J25] Christophe Hohlweg, Vincent Pilaud & Salvatore Stella. *Polytopal realizations of finite type* g*-vector fans*. Advances in Mathematics, vol. 328, pp. 713 – 749, 2018.
[J26] Vincent Pilaud & Viviane Pons. *Permutrees*. Algebraic Combinatorics, vol. 1(2), pp. 173 – 224, 2018.
[J27] Vincent Pilaud, Pierre-Guy Plamondon & Salvatore Stella. *A τ-tilting approach to dissections of polygons*. Symmetry, Integrability & Geometry: Methods & Applications, vol. 14, Paper 045, 8 pp., 2018.
[J28] Carsten Lange & Vincent Pilaud. *Associahedra via spines*. Combinatorica, vol. 38(2), pp. 443 – 486, 2018.
[J29] Vincent Pilaud. *Hopf algebras on decorated noncrossing arc diagrams*. Journal of Combinatorial Theory, Series A, vol. 161, pp. 486 – 507, 2019.
[J30] Thibault Manneville & Vincent Pilaud. *Geometric realizations of the accordion complex of a dissection*. Discrete & Computational Geometry, vol. 61(3), pp. 507 – 540, 2019.
[J31] Grégory Chatel, Vincent Pilaud & Viviane Pons. *The weak order on integer posets*. Algebraic Combinatorics, vol. 2(1), pp. 1 – 48, 2019.
[J32] Vincent Pilaud & Francisco Santos. *Quotientopes*. Bulletin of the London Mathematical Society, vol. 51(3), pp. 406 – 420, 2019.
[J33] Joël Gay & Vincent Pilaud. *The weak order on Weyl posets*. Canadian Journal of Mathematics, online first, 2019.
[J34] V. Pilaud. *Cambrian triangulations and their tropical realizations*. European Journal of Combinatorics, vol. 83, 19 pp., 2020.
[J35] Vincent Pilaud & Viviane Pons. *The Hopf algebra of integer binary relations*. IRMA Lectures in Mathematics and Theoretical Physics (Algebraic Combinatorics, Resurgence, Moulds and Applications, CARMA), vol. 31, pp. 299 – 344, 2020.
[J36] Yann Palu, Vincent Pilaud & Pierre-Guy Plamondon. *Non-kissing and non-crossing complexes for locally gentle algebras*. Journal of Combinatorial Algebra, vol. 3(4), pp. 401 – 438, 2019.
[J37] Yann Palu, Vincent Pilaud & Pierre-Guy Plamondon. *Non-kissing complexes and τ-tilting for gentle algebras*. To appear in Memoirs of the American Mathematical Society, 2018.

Preprints

[P1] Vincent Pilaud. *Signed tree associahedra*. Preprint, 50 pp., arXiv:1309.5222, 2013.
[P2] Nantel Bergeron, Cesar Ceballos & Vincent Pilaud. *Hopf dreams*. Preprint, 40 pp., arXiv:1807.03044, 2018.
[P3] Florent Hivert & Vincent Pilaud. *Signaletic operads*. Preprint, 97 pp., arXiv:1906.02228, 2019.
[P4] Arnau Padrol, Yann Palu, Vincent Pilaud & Pierre-Guy Plamondon. *Associahedra for finite type cluster algebras and minimal relations between* g*-vectors*. Preprint, 64 pp., arXiv:1906.06861, 2019.
[P5] Aram Dermenjian, Christophe Hohlweg, Thomas McConville & Vincent Pilaud. *The facial weak order on hyperplane arrangements*. Preprint, 34 pp., arXiv:1910.03511, 2019.

International conferences

Almost all my conference contributions are extended abstracts of articles that have appeared latter as journal contributions. I mainly contribute to the following conferences:

- FPSAC = International Conference on Formal Power Series and Algebraic Combinatorics
- EuroComb = European Conference on Combinatorics, Graph Theory and Applications
- AofA = International Conference on Probabilistic, Combinatorial and Asymptotic Methods for the Analysis of Algorithms
- CCCG = Canadian Conference on Computational Geometry
- EuroCG = European Workshop on Computational Geometry

[Ci1] Vincent Pilaud & Francisco Santos. *Multitriangulations as complexes of star-polygons*. FPSAC'08 (poster), DMTCS Proc., pp. 319 – 330, 2008.

[Ci2] Vincent Pilaud & Michel Pocchiola. *Multipseudotriangulations*. EuroCG'09, pp. 227 – 230, 2009.

[Ci3] Jürgen Bokowski & Vincent Pilaud. *On symmetric realizations of the simplicial complex of 3-crossing-free sets of diagonals of the octagon*. CCCG'09, 4 pp., 2009.

[Ci4] Minghui Jiang, Vincent Pilaud & Pedro Tejada. *On a dispersion problem in grid labeling*. CCCG'10, 8 pp., 2010.

[Ci5] Jürgen Bokowski & Vincent Pilaud. *Enumerating topological (n_k)-configurations*. CCCG'11, 6 pp., 2011.

[Ci6] Vincent Pilaud & Francisco Santos. *The brick polytope of a sorting network*. FPSAC'11 (talk), DMTCS Proc., pp. 777 – 788, 2011.

[Ci7] Vincent Pilaud. *The greedy flip tree of a subword complex*. 8ème Conf. de Génération Aléatoire de Structures Combinatoires, 11 pp., 2012.

[Ci8] Vincent Pilaud & Christian Stump. *Generalized associahedra via brick polytopes*. FPSAC'12 (talk), DMTCS Proc., pp. 73 – 84, 2012.

[Ci9] Cesar Ceballos & Vincent Pilaud. *Denominator vectors and compatibility degrees in cluster algebras of finite type*. FPSAC'13 (talk), DMTCS Proc., pp. 85 – 96, 2013.

[Ci10] Vincent Pilaud & Christian Stump. *EL-labelings and canonical spanning trees for subword complexes*. FPSAC'13 (poster), DMTCS Proc., pp. 611 – 622, 2013.

[Ci11] Vincent Pilaud. *Signed tree associahedra*. FPSAC'14 (poster), DMTCS Proc., pp. 309 – 320, 2014.

[Ci12] Vincent Pilaud & Juanjo Rué. *Analytic combinatorics of chord and hyperchord diagrams with k crossings*. AofA'14, DMTCS Proc., 339 – 350, 2014.

[Ci13] Grégory Chatel, Carsten Lange & Vincent Pilaud. *Cambrian trees*. Oberwolfach report, pp. 43 – 44, 2015.

[Ci14] Grégory Chatel & Vincent Pilaud. *The Cambrian Hopf Algebra*. FPSAC'15 (talk), DMTCS Proc., pp. 61 – 72, 2015.

[Ci15] Cesar Ceballos, Thibault Manneville, Vincent Pilaud & Lionel Pournin. *Diameters and geodesic properties of generalizations of the associahedron*. FPSAC'15 (poster), DMTCS Proc., pp. 345 – 356, 2015.

[Ci16] Vincent Pilaud & Michel Pocchiola. *Multitriangulations, pseudotriangulations and friezes*. Oberwolfach report, 3 pp., 2015.

[Ci17] Aram Dermenjian, Christophe Hohlweg & Vincent Pilaud. *The facial weak order in finite Coxeter groups*. FPSAC'16 (talk), DMTCS Proc., pp. 359 – 370, 2016.

[Ci18] Thibault Manneville & Vincent Pilaud. *Compatibility fans realizing graphical nested complexes*. FPSAC'16 (talk), DMTCS Proc., pp. 827 – 838, 2016.

[Ci19] Vincent Pilaud. *Brick polytopes, lattices and Hopf algebras*. FPSAC'16 (poster), DMTCS Proc., pp. 1003 – 1014, 2016.

[Ci20] Amir-Hossein Bateni, Thibault Manneville & Vincent Pilaud. *On quadrangulations and Stokes complexes*. EuroComb'17, ENDM, Vol. 61, pp. 107 – 113, 2017.

[Ci21] Vincent Pilaud & Viviane Pons. *Permutrees*. EuroComb'17, ENDM, Vol. 61, pp. 987 – 993, 2017.

[Ci22] Christophe Hohlweg, Vincent Pilaud & Salvatore Stella. *Universal associahedra*. FPSAC'18 (talk), SLC Proc. 80B #15, 12 pp., 2018.

[Ci23] Yann Palu, Vincent Pilaud & Pierre-Guy Plamondon. *Non-kissing complexes for gentle algebras*. FPSAC'18 (talk), SLC Proc. 80B #39, 12 pp., 2018.

[Ci24] Vincent Pilaud & Viviane Pons. *Algebraic structures on integer posets*. FPSAC'18 (poster), SLC Proc. 80B #61, 12 pp., 2018.

[Ci25] Vincent Pilaud. *Polytopal realizations and Hopf algebra structures for lattice quotients of the weak order*. FPSAC'19 (poster), SLC Proc., 82B #3, 12 pp., 2019.

[Ci26] Yann Palu, Vincent Pilaud & Pierre-Guy Plamondon. *Non-kissing versus non-crossing*. FPSAC'19 (poster), SLC Proc., 82B #12, 12 pp., 2019.

[Ci27] Nantel Bergeron, Cesar Ceballos & Vincent Pilaud. *Hopf dreams (extended abstract)*. FPSAC'19 (exposé), SLC Proc., 82B #19, 12 pp., 2019.

[Ci28] Vincent Pilaud & Florent Hivert. *Signaletic operads*. FPSAC'20 (poster), SLC Proc., 12 pp., 2020.

[Ci29] Arnau Padrol, Yann Palu, Vincent Pilaud & P.-G. Plamondon. *On type cones of* g*-vector fans*. FPSAC'20 (exposé), SLC Proc., 12 pp., 2020.

[Ci30] Aram Dermenjian, Christophe Hohlweg, Thomas McConville & Vincent Pilaud. *The facial weak order on hyperplane arrangements*. FPSAC'20 (poster), SLC Proc., 11 pp., 2020.

I

Part One

LATTICE CONGRUENCES, POLYTOPES AND HOPF ALGEBRAS

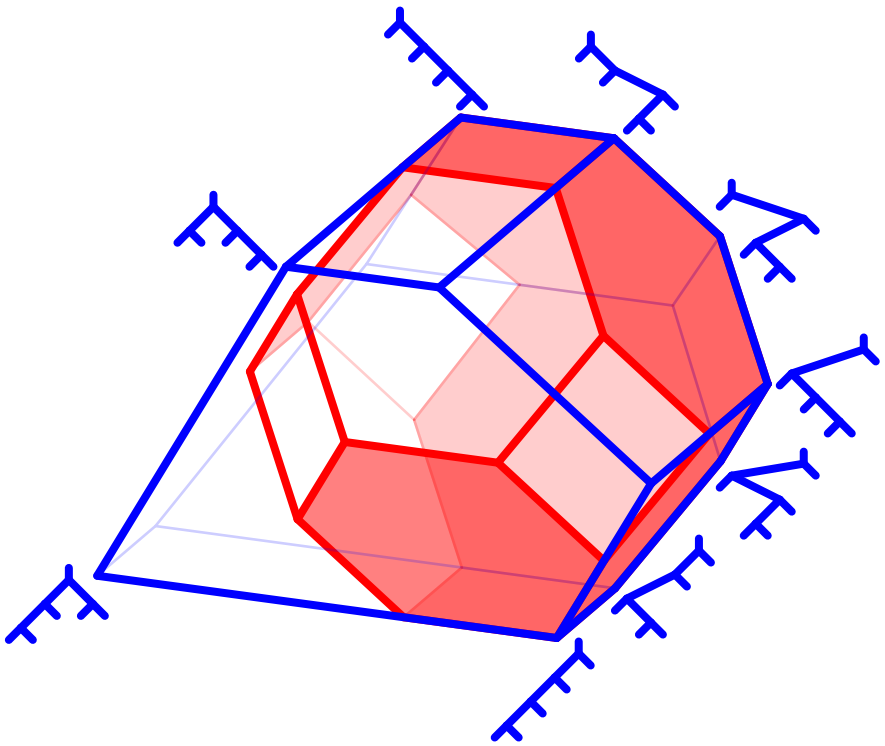

Permutahedra, associahedra, cubes. The motivation of this part is the fascinating interplay between the combinatorial, geometric and algebraic structures of permutations, binary trees and binary sequences (see Chapter 1 for a brief survey on these connections):

⋆ **Combinatorics:** The recoil map from permutations to binary sequences factors via binary trees through the binary search tree insertion and the canopy map. These maps define lattice morphisms from the weak order via the Tamari lattice to the boolean lattice.

⋆ **Geometry:** The permutahedron is contained in J.-L. Loday's associahedron [Lod04] which is in turn contained in the parallelepiped generated by the simple roots $\boldsymbol{e}_{i+1}-\boldsymbol{e}_i$. These polytopes are just obtained by deleting inequalities from the facet description of the permutahedron. See Figure 1.4.

⋆ **Algebra:** These maps translate to Hopf algebra inclusions from C. Malvenuto and C. Reutenauer's Hopf algebra on permutations [MR95] via J.-L. Loday and M. Ronco's Hopf algebra on binary trees [LR98] to the recoil Hopf algebra of [GKL+95].

Lattice quotients of the weak order. These connections were widely extended by N. Reading in his work on "Lattice congruences, fans and Hopf algebras" [Rea05]. He starts from the combinatorics of lattice congruences and lattice quotients of the weak order (see Section 1.1.1 for proper definitions). The prototypical instance is the Tamari lattice seen as the quotient of the weak order by the sylvester congruence [HNT05]. There are two important ways to see this congruence:

- its classes are the fibers of the binary search tree insertion algorithm (or equivalently the sets of linear extensions of the standard binary search trees),
- it is the transitive closure of the rewriting rule $UacVbW \equiv^{\text{sylv}} UcaVbW$ where $a < b < c$ are letters and U, V, W are words on $[n]$.

It turns out that the combinatorial, geometric and algebraic properties of the permutations, binary trees, and binary sequences mentioned above partially extend to all lattice quotients of the weak order:

⋆ **Combinatorics:** This setting provides a plethora of lattice quotients in each dimension (like the Tamari lattice for the sylvester congruence), coming with natural lattice morphisms between them.

⋆ **Geometry:** N. Reading proves in [Rea05] that any lattice congruence $\equiv$ of the weak order on the permutations of $\mathfrak{S}_n$ defines a complete simplicial fan $\mathcal{F}(\equiv)$ refined by the braid arrangement. This raises the question to construct polytopes whose normal fans are $\mathcal{F}(\equiv)$ (like the associahedron for the sylvester congruence).

⋆ **Algebra:** N. Reading characterizes in [Rea05] in terms of simple rewriting rules the families $(\equiv_n)_{n\in\mathbb{N}}$ of lattice congruences of the weak orders on $(\mathfrak{S}_n)_{n\in\mathbb{N}}$ which yield Hopf subalgebras of C. Malvenuto and C. Reutenauer's Hopf algebra on permutations. This construction produces a combinatorial Hopf algebra whose basis is indexed by the congruence classes of $(\equiv_n)_{n\in\mathbb{N}}$. It opens two natural questions:

- First, the product and coproduct in this Hopf algebra are performed extrinsically: the algebra is embedded in C. Malvenuto and C. Reutenauer's algebra on permutations and the computations are performed at that level. The remaining challenge is to realize the resulting Hopf algebra intrinsically by attaching a combinatorial object to each congruence class of $(\equiv_n)_{n\in\mathbb{N}}$ and working out the rules for the product and coproduct directly on these combinatorial objects.
- Second, the conditions on the family $(\equiv_n)_{n\in\mathbb{N}}$ are quite strong. Although they provide very relevant combinatorial families of congruences, it is somewhat frustrating that this conditions disallow to multiply for instance a binary tree by a permutation. It is tempting to look for Hopf algebra structures that would allow to manipulate simultaneously all lattice congruences of the weak order.

This part of the document proposes some answers to these questions through three chapters that we briefly present now.

Brick polytopes. Chapter 2 provides a relevant example of N. Reading's setting, studied in [Pil18]. Our motivation comes from k-triangulations of a convex polygon [PS09], that can be interpreted by duality [PP12] as certain pipe dreams (pseudoline arrangements in a triangular shape) that we call k-twists. These k-twists form the facets of a simplicial sphere, and it remains a challenging open problem to realize this sphere as the boundary complex of a polytope. Motivated by this question, we defined in [PS12] the brick polytope of a sorting network, whose vertices correspond to certain acyclic k-twists. When $k = 1$, the brick polytope coincides with J.-L. Loday's associahedron [Lod04], and the 1-twists are all acyclic and correspond to all triangulations of the $(n + 2)$-gon, or equivalently to the equivalence classes of the sylvester congruence. The above-mentioned properties of binary trees extend to acyclic k-twists for $k \geq 1$ as follows:

- ⋆ **Combinatorics:** In Section 2.1, we show that the acyclic k-twists correspond to the equivalence classes of the k-twist congruence $\equiv^k$ of the weak order. This congruence can be defined either as the congruence whose classes are the fibers of the k-twist insertion, or as the transitive closure of the rewriting rule $UacV_1b_1V_2b_2 \cdots V_kb_kW \equiv^k UcaV_1b_1V_2b_2 \cdots V_kb_kW$ where $a, b_1, \ldots, b_k, c \in [n]$ are such that $a < b_i < c$ for all $i \in [k]$ and $U, V_1, \ldots, V_k, W$ are words on $[n]$. The corresponding lattice quotient of the weak order $\mathfrak{S}_n/\equiv^k$ is the increasing flip order on the acyclic k-twists, generalizing the Tamari lattice. Moreover, this k-twist congruence $\equiv^k$ refines the k-recoil congruence already considered by N. Reading [Rea05] and by J.-C. Novelli, C. Reutenauer and J.-Y. Thibon [NRT11].
- ⋆ **Geometry:** In Section 2.2, we briefly survey the geometry of acyclic k-twists and k-recoil schemes. The acyclic k-twists correspond to the vertices of some brick polytope, and the k-recoil schemes correspond to the vertices of some graphical zonotope. Moreover, the normal fan of the permutahedron refines that of the brick polytope, which refines that of the graphical zonotope. A more general treatment on brick polytopes is presented in Chapter 8.
- ⋆ **Algebra:** It turns out that the k-twist congruence satisfies the compatibility conditions of [Rea05] to define a Hopf subalgebra of C. Malvenuto and C. Reutenauer's Hopf algebra on permutations [MR95]. Our approach with k-twists provides a combinatorial interpretation for this Hopf subalgebra, and we describe in Section 2.3 the product and the coproduct directly on acyclic k-twists. Moreover, our Hopf algebra on acyclic k-twists contains as a Hopf subalgebra the k-recoil Hopf algebra of J.-C. Novelli, C. Reutenauer and J.-Y. Thibon [NRT11].

Permutreehedra. Chapter 3 is our first step beyond N. Reading's approach. It defines new combinatorial objects, called permutrees, introduced in a joint work with V. Pons [PP18]. They are labeled and oriented trees where each vertex can have one or two parents and one or two children, and with local rules around each vertex similar to the classical rule for binary trees (see Definition 3.1 for a precise statement). These trees generalize permutations, binary trees, and binary sequences, and actually allow for interpolations between them: we obtain combinatorial objects that are structurally "half" binary trees and "half" permutations. We explore the following properties of permutrees:

- ⋆ **Combinatorics:** In Section 3.1, we describe a natural insertion map from decorated permutations to permutrees similar to the binary tree insertion. The fibers of this map define a lattice congruence of the weak order, which can also be described as the transitive closure of a rewriting rule that depends on the decorations of the permutations. Therefore, there is a morphism from the weak order on permutations to the rotation lattice on permutrees. This rotation lattice specializes to the weak order on permutations, the Tamari order on binary trees, and the boolean lattice on binary sequences.

⋆ **Geometry:** In Section 3.2, we provide vertex and facet descriptions of the permutreehedron, a polytope whose graph is the Hasse diagram of the rotation lattice on permutrees. The permutreehedron is obtained by deleting facets from the classical permutahedron. The permutreehedron specializes to the classical permutahedron, to J.-L. Loday's associahedron [Lod04], and to the parallelepiped generated by the simple roots $\boldsymbol{e}_{i+1} - \boldsymbol{e}_i$.

⋆ **Algebra:** In Section 3.3, we construct a Hopf algebra on all permutrees as a Hopf subalgebra of a decorated version of C. Malvenuto and C. Reutenauer Hopf algebra on permutations. We describe the product and coproduct in this algebra and its dual in terms of cut and paste operations on permutrees. It contains as Hopf subalgebras C. Malvenuto and C. Reutenauer's Hopf algebra on permutations [MR95], J.-L. Loday and M. Ronco's Hopf algebra on binary trees [LR98], and the recoil Hopf algebra on binary sequences of [GKL+95].

Quotientopes. In Chapter 4, we finally deal simultaneously with all lattice congruences of the weak order. To manipulate these lattice congruences, we use the powerful combinatorial model of non-crossing arc diagrams [Rea15], briefly reviewed in Section 4.1. We present progress in two directions:

⋆ **Geometry:** In Section 4.2, we show that the quotient fan $\mathcal{F}(\equiv)$ of any lattice congruence $\equiv$ of the weak order is the normal fan of a polytope $\mathbb{QT}(\equiv)$, that we call quotientope. The graph of this polytope $\mathbb{QT}(\equiv)$, oriented in the appropriate direction, is the Hasse diagram of the lattice quotient $\mathfrak{S}_n/\equiv$. This result of [PS19] closes the long-standing open question of N. Reading [Rea05]. We also report on a recent alternative construction [PPR20] based on Minkowski sums of associahedra or of simpler pieces called shard polytopes.

⋆ **Algebra:** In Section 4.3, we present the construction of [Pil19] for Hopf algebra structures on the congruence classes of all lattice quotients of the weak order. Starting from a convenient notion of decorated sets, we construct decorated versions of C. Malvenuto and C. Reutenauer Hopf algebra on permutations [MR95]. We then study conditions on insertion algorithms such that the fibers of this algorithm define a Hopf subalgebra of the decorated permutation Hopf algebra. Tuning the choices of decoration sets and insertion algorithm, we obtain three relevant examples of Hopf algebra structures on lattice quotients of the weak order:
  - First, our conditions enable to recover the translational and insertional conditions of N. Reading [Rea05] that characterize which families of lattice congruences $(\equiv_n)_{n\in\mathbb{N}}$ define a Hopf subalgebra of C. Malvenuto and C. Reutenauer's Hopf algebra on permutations.
  - Then, we obtain a Hopf algebra on certain lattice congruences of the weak order defined by arcs that cross certain walls at most a certain number of times. It contains as Hopf subalgebras many Hopf algebras, in particular the k-twist Hopf algebra of [Pil18] (see Chapter 2) and the permutree Hopf algebra of [PP18] (see Chapter 3).
  - Finally, we construct a Hopf algebra that contains simultaneously the congruence classes of all lattice congruences of the weak order, and which contains as a Hopf subalgebra the permutree Hopf algebra of [PP18] (see Chapter 3).

Chapter One

1 PERMUTAHEDRA, ASSOCIAHEDRA, CUBES

This chapter proposes a brief introduction to the combinatorial, geometric, and algebraic connections between the permutahedra, associahedra and cubes presented in Table 1.1. These connections will be extended in several directions in this document. All the material presented in this chapter is classical and elementary, our main purpose here is to introduce classical notions on lattices, polytopes and Hopf algebras, and to fix conventions and notations.

Combinatorics	Weak order on permutations	Tamari lattice on binary trees	Boolean lattice on binary sequences
Geometry	Permutahedron $\mathbb{P}\mathrm{erm}(n)$	Loday's associahedron $\mathbb{A}\mathrm{sso}(n)$ [Lod04]	Parallelepiped $\mathbb{P}\mathrm{ara}(n)$ generated by $\boldsymbol{e}_{i+1} - \boldsymbol{e}_i$
Algebra	Malvenuto–Reutenauer Hopf algebra [MR95]	Loday–Ronco Hopf algebra [LR98]	Recoil Hopf algebra [GKL+95]

Table 1.1: Related combinatorial, geometric and algebraic structures on permutations, binary trees, and binary sequences.

1.1 LATTICES

1.1.1 Lattices and their congruences

Recall that a *poset* is a reflexive ($a \leq a$), antisymmetric ($a \leq b$ and $b \leq a \Rightarrow a = b$) and transitive ($a \leq b$ and $b \leq c \Rightarrow a \leq c$) binary relation. A *lattice* is a poset where any subset admits a *meet* $\wedge$ (greatest lower bound) and a *join* $\vee$ (least upper bound). For instance, the inclusion poset of subsets of a given set is the *boolean lattice* where the meet is the intersection and the join is the union.

A *lattice congruence* of a lattice $(L, \leq, \wedge, \vee)$ is an equivalence relation on L that respects the meet and the join, *i.e.* such that $x \equiv x'$ and $y \equiv y'$ implies $x \wedge y \equiv x' \wedge y'$ and $x \vee y \equiv x' \vee y'$. Equivalently, it is an equivalence relation on L such that:

(i) each equivalence class under $\equiv$ is an interval of L,
(ii) the projection maps $\pi_{\downarrow}$ and $\pi^{\uparrow}$, which send an element of L to the minimal and maximal elements of its equivalence class respectively, are both order preserving.

A lattice congruence $\equiv$ automatically defines a *lattice quotient* $L/\equiv$ on the congruence classes of $\equiv$ where the order relation is given by $X \leq Y$ if and only if there exists $x \in X$ and $y \in Y$ such that $x \leq y$. The meet $X \wedge Y$ (resp. the join $X \vee Y$) of two congruence classes X and Y is the congruence class of $x \wedge y$ (resp. of $x \vee y$) for arbitrary representatives $x \in X$ and $y \in Y$.

Further lattice theoretic notions will be introduced along this document when needed, in particular canonical join representations (Section 4.1.1) and congruence uniform lattices (Section 10.2).

1.1.2 Three classical lattices

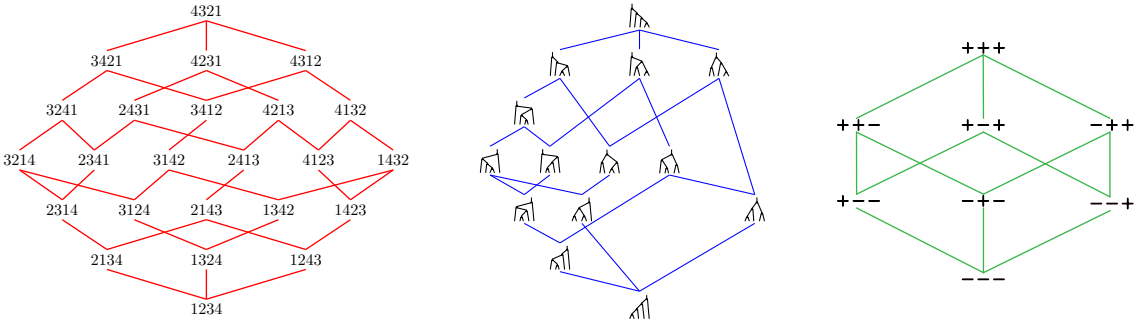

Figure 1.1: Weak order on $\mathfrak{S}_4$ (left), Tamari lattice on $\mathfrak{T}_4$ (middle), boolean lattice on $\mathfrak{B}_4$ (right).

Weak order on permutations. We denote by $\mathfrak{S}_n$ the set of permutations of $[n] := \{1, \dots, n\}$. Besides its classical group structure, we focus on a fundamental lattice structure on $\mathfrak{S}_n$. A (left) *inversion* in a permutation $\sigma \in \mathfrak{S}_n$ is a pair of values $1 \leq i < j \leq n$ such that $\sigma^{-1}(i) > \sigma^{-1}(j)$, *i.e.* i appears after j in σ. The (left) *inversion set* of σ is the set $\mathrm{inv}(\sigma)$ of inversions of σ. For instance, the inversion set of the permutation $\sigma = 31542$ is $\mathrm{inv}(\sigma) = \{(1,3),(2,3),(2,4),(2,5),(4,5)\}$. The (right) *weak order* is the partial order $\leq_{\mathsf{W}}$ on $\mathfrak{S}_n$ defined by inclusion of inversion sets: $\sigma \leq_{\mathsf{W}} \tau$ if and only if $\mathrm{inv}(\sigma) \subseteq \mathrm{inv}(\tau)$. Its cover relations are given by transpositions of two consecutive letters (*i.e.* right multiplications by simple transpositions). It is a lattice on $\mathfrak{S}_n$. See Figure 1.1 (left).

Tamari lattice on binary trees. We denote by $\mathfrak{T}_n$ be the set of *rooted binary trees* with n nodes. A tree $T \in \mathfrak{T}_n$ is always labeled in inorder: all vertices in the left (resp. right) subtree of a vertex v of T receive a label smaller (resp. larger) than the label of v. See Figure 1.2 (right). The *Tamari lattice* on $\mathfrak{T}_n$ is the lattice $\leq_{\mathsf{T}}$ whose cover relations are given by *right rotations* on binary trees, *i.e.* the application of the local transformation illustrated above at any node. See Figure 1.1 (middle). It was defined by D. Tamari [Tam51] and it is known to be a lattice. By classical bijections between Catalan families (*i.e.* combinatorial objects counted by the Catalan numbers), it can also be seen as applications of an associativity rule on all possible parenthesizations of a non-associative product, as diagonal flips on all triangulations of a convex polygon, or as elementary moves on all Dyck paths, see [Sta99, Exm. 6.19].

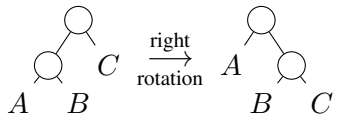

The Tamari lattice was reinterpreted in [BW91, Rea06] as a lattice quotient of the weak order as follows. Consider the surjection $\mathbf{bt}$ which sends a permutation $\sigma := \sigma_1 \dots \sigma_n \in \mathfrak{S}_n$ to the binary tree $\mathbf{bt}(\sigma) \in \mathfrak{T}_n$ obtained by successive insertions of $\sigma_n, \dots, \sigma_1$ in a binary search tree (rather than a formal definition, we prefer to recall this classical insertion procedure by the illustration of Figure 1.2).

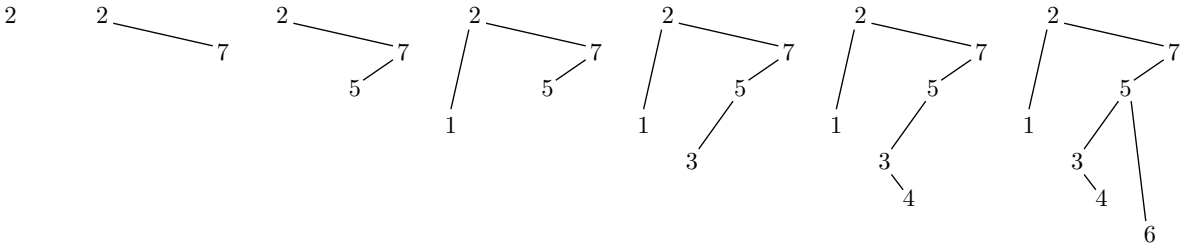

Figure 1.2: Inserting the permutation 6431572 in a binary search tree.

The $\mathbf{bt}$ fiber of a tree T is precisely the set of linear extensions of T, *i.e.* all permutations σ such that for any $i, j \in [n]$, if i is a descendant of j in T, then i appears before j in σ. Each fiber is an interval of the weak order whose minimal and maximal elements respectively avoid the patterns 312 and 132. The equivalence relation $\equiv^{\text{sylv}}$ whose classes are these fibers is a lattice congruence of the weak order, called *sylvester congruence* [HNT05]. It can be defined equivalently as the transitive closure of the rewriting rule $UacVbW \equiv^{\text{sylv}} UcaVbW$ where $a < b < c$ are letters and U, V, W are words on $[n]$. The Tamari lattice $\leq_{\mathsf{T}}$ is the quotient $\leq_{\mathsf{W}} / \equiv^{\text{sylv}}$ of the weak order by this sylvester congruence. In other words, for any $T, T' \in \mathfrak{T}_n$, we have $T \leq_{\mathsf{T}} T'$ if and only if there exist $\sigma, \sigma' \in \mathfrak{S}_n$ such that $\mathbf{bt}(\sigma) = T$, $\mathbf{bt}(\sigma') = T'$ and $\sigma \leq_{\mathsf{W}} \sigma'$.

Boolean lattice on binary sequences. We denote by $\mathfrak{B}_n$ the set of binary sequences of $n-1$ signs $+$ or $-$. The *boolean lattice* on $\mathfrak{B}_n$ is the lattice $\leq_{\mathsf{B}}$ defined by $\chi \leq_{\mathsf{B}} \zeta$ if and only if $\chi_i \leq \zeta_i$ for all $i \in [n-1]$ for the natural order $- \leq +$. See Figure 1.1 (right).

Again, this lattice can be understood via lattice congruences. We need two definitions:

- A *recoil* of a permutation σ is a value $i \in [n-1]$ such that $\sigma^{-1}(i) > \sigma^{-1}(i+1)$, *i.e.* i appears after $i+1$ in σ. Let $\mathbf{rec}(\sigma)$ be the binary sequence with $+$ for each recoil of σ and $-$ otherwise.
- The *canopy* of a binary tree T is the sequence $\mathbf{can}(T)$ with a $-$ if i appears below $i+1$ and a $+$ if i appears above $i+1$ in the tree T labeled in inorder. This map was already used by J.-L. Loday in [LR98, Lod04], but the name "canopy" was coined by X. Viennot [Vie07].

The recoil and canopy maps define the following commutative diagram of lattice morphisms:

$$\begin{array}{ccc} \mathfrak{S}_n & \xrightarrow{\quad\mathbf{rec}\quad} & \mathfrak{B}_n \\ & {\scriptstyle\mathbf{bt}}\searrow \quad \nearrow{\scriptstyle\mathbf{can}} & \\ & \mathfrak{T}_n & \end{array}$$

In other words, the fibers of these maps define lattice congruences of the weak order and of the Tamari lattice, and the boolean lattice is a lattice quotient of both.

1.2 POLYTOPES

1.2.1 Fans and polytopes

Let $(V, \langle \cdot \mid \cdot \rangle)$ be a real Euclidean vector space[1]. We denote by $\mathbb{R}_{\geq 0}\boldsymbol{R} := \left\{ \sum_{\boldsymbol{r} \in \boldsymbol{R}} \lambda_{\boldsymbol{r}}\, \boldsymbol{r} \;\middle|\; \lambda_{\boldsymbol{r}} \in \mathbb{R}_{\geq 0} \right\}$ the *positive span* of a set $\boldsymbol{R}$ of vectors of V. A *polyhedral cone* is a subset of V defined equivalently as the positive span of finitely many vectors or as the intersection of finitely many closed linear half-spaces. The *faces* of a cone C are the intersections of C with the supporting hyperplanes of C. The 1-dimensional (resp. codimension 1) faces of C are called *rays* (resp. *facets*) of C. A cone is *simplicial* if it is generated by a set of independent vectors.

A *polyhedral fan* is a collection $\mathcal{F}$ of polyhedral cones such that:

- if $C \in \mathcal{F}$ and F is a face of C, then $F \in \mathcal{F}$,
- the intersection of any two cones of $\mathcal{F}$ is a face of both.

The *face lattice* of a fan is the inclusion lattice of its cones (including the origin and adding the complete space). See Figure 1.3 (top) for an example. A fan is *simplicial* if all its cones are, *complete* if the union of its cones covers the ambient space V, and *essential* if the intersection of all its cones is reduced to the origin. For two fans $\mathcal{F}, \mathcal{G}$ in V, we say that $\mathcal{F}$ *refines* $\mathcal{G}$ (and that $\mathcal{G}$ *coarsens* $\mathcal{F}$) if every cone of $\mathcal{F}$ is contained in a cone of $\mathcal{G}$.

A *polytope* is a subset $\mathbb{P}$ of V defined equivalently as the convex hull of finitely many points or as a bounded intersection of finitely many closed affine halfspaces. The *dimension* $\dim(\mathbb{P})$ is

[1] As we work in finite dimension, we always implicitly identify the Euclidean vector space V with its dual V^*. In particular, we consider that a polytope and its normal fan live in the same space.

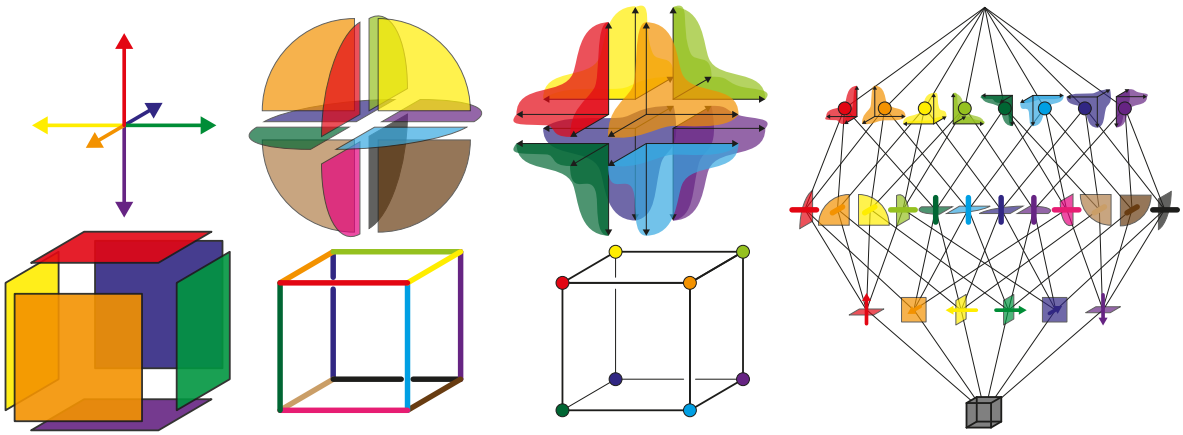

Figure 1.3: A complete simplicial fan (top), a simple polytope (bottom), and their face lattice (right). The fan is the normal fan of the polytope.

the dimension of the affine hull of $\mathbb{P}$. The *faces* of $\mathbb{P}$ are the intersections of $\mathbb{P}$ with its supporting hyperplanes. The dimension 0 (resp. dimension 1, resp. codimension 1) faces are called *vertices* (resp. *edges*, resp. *facets*) of $\mathbb{P}$. The *face lattice* of a polytope is the inclusion lattice of its faces (including the empty face and the polytope itself). See Figure 1.3 (bottom) for an example. A polytope is *simple* if its supporting hyperplanes are in general position, meaning that each vertex is incident to $\dim(\mathbb{P})$ facets (or equivalently to $\dim(\mathbb{P})$ edges).

The (inner) *primal cone* of a face F of $\mathbb{P}$ is the cone $\boldsymbol{C}(F)$ generated by $\{u - v \,|\, u \in \mathbb{P}, v \in F\}$. The (outer) *normal cone* of a face F of $\mathbb{P}$ is the cone $\boldsymbol{C}^\diamond(F)$ generated by the outer normal vectors of the facets of $\mathbb{P}$ containing F. In other words, it is the cone of vectors $\boldsymbol{c}$ such that the linear form $\boldsymbol{x} \mapsto \langle \boldsymbol{c} \,|\, \boldsymbol{x} \rangle$ on $\mathbb{P}$ is maximized by all points of the face F. Note that these two cones are polar to each other: $\boldsymbol{C}^\diamond(F) = \{\boldsymbol{x} \in V \,|\, \langle \boldsymbol{x} \,|\, \boldsymbol{y} \rangle \leq 0 \text{ for all } \boldsymbol{y} \in \boldsymbol{C}(F)\}$. The (outer) *normal fan* of $\mathbb{P}$ is the collection of the (outer) normal cones of all its faces. We say that a complete polyhedral fan in V is *polytopal* when it is the normal fan of a polytope of V. See Proposition 7.28 for a characterization of the realizations of a simplicial fan.

1.2.2 Three classical polytopes

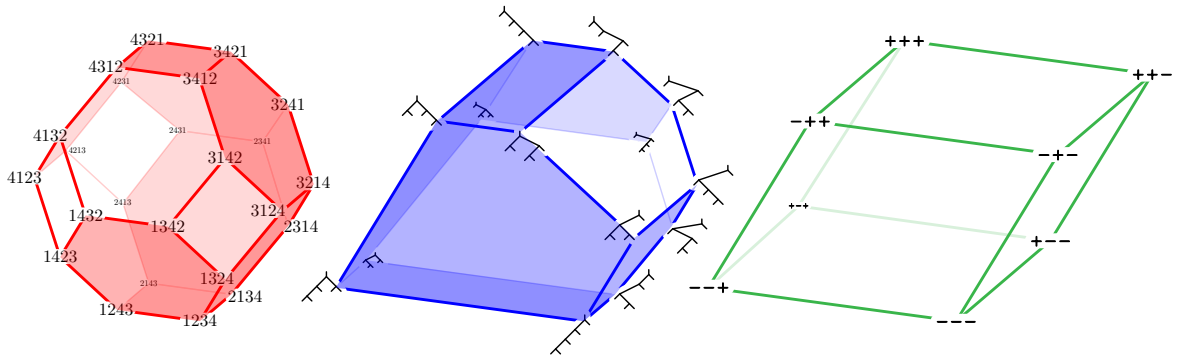

Figure 1.4: Permutahedron $\mathbb{P}\mathrm{erm}(4)$ (left), J.-L. Loday's associahedron $\mathbb{A}\mathrm{sso}(4)$ (middle), parallelepiped $\mathbb{P}\mathrm{ara}(4)$ (right). Shaded facets are preserved to get the next polytope.

We denote by $(\boldsymbol{e}_i)_{i\in[n]}$ the canonical basis of $\mathbb{R}^n$ and $\mathbb{1} := \sum_{i\in[n]} \boldsymbol{e}_i$. All our polytopal constructions will lie in the affine subspace $\mathbb{H} := \{\boldsymbol{x} \in \mathbb{R}^n \mid \langle \mathbb{1} \,|\, \boldsymbol{x}\rangle = \sum_{i\in[n]} x_i = \binom{n+1}{2}\}$, and their normal fans will lie in the vector subspace $\mathbb{1}^\perp := \{\boldsymbol{x} \in \mathbb{R}^n \,|\, \langle \mathbb{1} \,|\, \boldsymbol{x}\rangle = 0\}$. In particular, all our polytopes and fans are $(n-1)$-dimensional, even if they live in the ambient space $\mathbb{R}^n$.

Permutahedron. The *permutahedron* $\mathbb{P}\mathrm{erm}(n)$ is the polytope of $\mathbb{R}^n$ obtained equivalently as:

- the convex hull of the points $\sum_{i\in[n]} i\, \boldsymbol{e}_{\sigma(i)}$ for all permutations $\sigma \in \mathfrak{S}_n$,
- or the intersection of the hyperplane $\mathbb{H}$ with the halfspaces $\{\boldsymbol{x} \in \mathbb{R}^n \mid \sum_{i\in I} x_i \geq \binom{|I|+1}{2}\}$ for all $\varnothing \neq I \subsetneq [n]$,
- or (a translate of) the Minkowski sum of all segments $[\boldsymbol{e}_i, \boldsymbol{e}_j]$ for all $(i,j) \in \binom{[n]}{2}$ (where the Minkowski sum of two polytopes $\mathbb{P}, \mathbb{Q} \subseteq \mathbb{R}^n$ is the polytope $\mathbb{P}+\mathbb{Q} := \{p+q \,|\, p \in \mathbb{P}, q \in \mathbb{Q}\}$).

See Figure 1.4 (left). Oriented in the direction $\boldsymbol{\omega} := (n, \dots, 1) - (1, \dots, n) = \sum_{i\in[n]} (n+1-2i)\, \boldsymbol{e}_i$, the graph of the permutahedron $\mathbb{P}\mathrm{erm}(n)$ is the Hasse diagram of the weak order on $\mathfrak{S}_n$.

The normal fan of the permutahedron $\mathbb{P}\mathrm{erm}(n)$ is the *braid fan* $\mathcal{F}(n)$ defined by the (type A) Coxeter arrangement formed by the hyperplanes $\{\boldsymbol{x} \in \mathbb{1}^\perp \,\big|\, x_i = x_j\}$ for all $1 \leq i < j \leq n$. Namely, each permutation $\sigma \in \mathfrak{S}_n$ corresponds to a maximal cone $\boldsymbol{C}^\diamond(\sigma) := \{\boldsymbol{x} \in \mathbb{1}^\perp \,\big|\, x_{\sigma(1)} \leq \cdots \leq x_{\sigma(n)}\}$ of the braid fan $\mathcal{F}(n)$, formed by all points whose coordinates are ordered by the permutation σ.

The braid fan $\mathcal{F}(n)$ provides geometric interpretations for many combinatorial objects. In particular, posets on $[n]$ are nothing else than convex cones in the braid arrangement $\mathcal{F}(n)$. Namely, the *incidence cone* $\boldsymbol{C}(\lhd)$ and the *braid cone* $\boldsymbol{C}^\diamond(\lhd)$ of a poset $\lhd$ on $[n]$ are the polyhedral cones defined by $\boldsymbol{C}(\lhd) := \mathbb{R}_{\geq 0}\{\boldsymbol{e}_i - \boldsymbol{e}_j \,|\, \text{for all } i \lhd j\}$ and $\boldsymbol{C}^\diamond(\lhd) := \{\boldsymbol{x} \in \mathbb{1}^\perp \,\big|\, x_i \leq x_j \text{ for all } i \lhd j\}$. These two cones lie in the space $\mathbb{1}^\perp := \{\boldsymbol{x} \in \mathbb{R}^n \,|\, \langle \boldsymbol{x} \,|\, \mathbb{1}\rangle = 0\}$ and are polar to each other. Note that the braid cone $\boldsymbol{C}^\diamond(\lhd)$ is the union of the cones $\boldsymbol{C}^\diamond(\sigma)$ over all linear extensions σ of $\lhd$ and therefore $\boldsymbol{C}(\lhd)$ is the intersection of the cones $\boldsymbol{C}(\sigma)$ over all linear extensions σ of $\lhd$. All along this document, we denote by $\mathcal{L}(\lhd)$ the set of linear extensions of $\lhd$.

Associahedron. The *associahedron* $\mathbb{A}\mathrm{sso}(n)$ is the polytope of $\mathbb{R}^n$ obtained equivalently as:

- the convex hull of the points $\sum_{i\in[n]} \ell(T,i)\, r(T,i)\, \boldsymbol{e}_i$ for all binary trees $T \in \mathfrak{T}_n$, where $\ell(T,i)$ and $r(T,i)$ respectively denote the numbers of leaves in the left and right subtrees of the ith node of T in infix labeling, see [Lod04],
- or the intersection of the hyperplane $\mathbb{H}$ with the halfspaces $\{\boldsymbol{x} \in \mathbb{R}^n \mid \sum_{i\leq\ell\leq j} x_\ell \geq \binom{j-i+2}{2}\}$ for all $1 \leq i \leq j \leq n$, see [SS93],
- or (a translate of) the Minkowski sum of the faces $\triangle_{[i,j]}$ of the standard simplex $\triangle_{[n]}$ for all $1 \leq i \leq j \leq n$, where $\triangle_X := \mathrm{conv}\{\boldsymbol{e}_x \,|\, x \in X\}$ for $X \subseteq [n]$, see [Pos09].

See Figure 1.4 (middle). Observe that the facet description of $\mathbb{A}\mathrm{sso}(n)$ is a subset of inequalities of the facet description of $\mathbb{P}\mathrm{erm}(n)$. Oriented in the direction $\boldsymbol{\omega}$, the graph of the associahedron $\mathbb{A}\mathrm{sso}(n)$ is the Hasse diagram of the Tamari lattice on $\mathfrak{T}_n$.

The normal fan of the associahedron $\mathbb{A}\mathrm{sso}(n)$ is a coarsening of the braid fan $\mathcal{F}(n)$. Each binary tree $T \in \mathfrak{T}_n$ corresponds to a normal cone $\boldsymbol{C}^\diamond(T) := \{\boldsymbol{x} \in \mathbb{1}^\perp \,\big|\, x_i \leq x_j \text{ for } i \text{ descendant of } j \text{ in } T\}$, which is the union of the cones $\boldsymbol{C}^\diamond(\sigma)$ over all permutations σ such that $\mathbf{bt}(\sigma) = T$.

Parallelepiped. Finally, we consider the *parallelepiped* $\mathbb{P}\mathrm{ara}(n)$ of $\mathbb{R}^n$ obtained equivalently as:

- the convex hull of the points $\frac{n+1}{2}\mathbb{1} + \frac{n-1}{2}\sum_{i\in[n-1]} \chi_i(\boldsymbol{e}_i - \boldsymbol{e}_{i+1})$ for all binary sequences $\chi \in \mathfrak{B}_n$,
- or the intersection of the hyperplane $\mathbb{H}$ with the halfspaces $\{\boldsymbol{x} \in \mathbb{R}^n \mid \sum_{1\leq\ell\leq i} x_\ell \geq \binom{i+1}{2}\}$ and $\{\boldsymbol{x} \in \mathbb{R}^n \mid \sum_{i<\ell\leq n} x_\ell \geq \binom{n-i+1}{2}\}$ for all $i \in [n-1]$,
- or (a translate of) the Minkowski sum of the segments $(n-1)\cdot[\boldsymbol{e}_i, \boldsymbol{e}_{i+1}]$ for $i \in [n-1]$.

See Figure 1.4 (right). Observe that the facet description of $\mathbb{P}\mathrm{ara}(n)$ is a subset of inequalities of the facet description of $\mathbb{A}\mathrm{sso}(n)$, and therefore also of $\mathbb{P}\mathrm{erm}(n)$. Oriented in the direction $\boldsymbol{\omega}$, the graph of the parallelepiped $\mathbb{P}\mathrm{ara}(n)$ is the Hasse diagram of the boolean lattice on $\mathfrak{B}_n$. In other words, $\mathbb{P}\mathrm{ara}(n)$ is combinatorially a $(n-1)$-dimensional cube.

The normal fan of the parallalepiped $\mathbb{P}\mathrm{ara}(n)$ is a coarsening of that of the associahedron $\mathbb{A}\mathrm{sso}(n)$, and therefore also of that of the permutahedron $\mathbb{P}\mathrm{erm}(n)$. Each binary sequence $\chi \in \mathfrak{B}_n$ corresponds to a normal cone $\boldsymbol{C}^\diamond(\chi) := \{\boldsymbol{x} \in \mathbb{1}^\perp \mid \chi_i(x_i - x_{i+1}) \geq 0 \text{ for all } i \in [n-1]\}$, which is the union of the cones $\boldsymbol{C}^\diamond(T)$ over all binary trees T such that $\mathbf{can}(T) = \chi$, and thus also the union of the cones $\boldsymbol{C}^\diamond(\sigma)$ over all permutations σ such that $\mathbf{rec}(\sigma) = \chi$.

1.3 Hopf algebras

1.3.1 Combinatorial Hopf algebras

A *combinatorial vector space* is a graded vector space $V := \bigoplus_{n\in\mathbb{N}} V_n$ where the dimension of V_n is finite for any $n \in \mathbb{N}$. Such combinatorial vector spaces are typically constructed as vector spaces with a basis indexed by a combinatorial family.

A *product* on a vector space $\mathfrak{A}$ is a linear operation $\cdot : \mathfrak{A} \otimes \mathfrak{A} \to \mathfrak{A}$ and a *coproduct* on $\mathfrak{A}$ is a linear operation $\triangle : \mathfrak{A} \to \mathfrak{A} \otimes \mathfrak{A}$. We often use the notation $x \cdot y$ instead of $\cdot(x, y)$ to manipulate products, and the notation $\triangle(x) = \sum x_1 \otimes x_2$ to manipulate coproducts. When $\mathfrak{A}$ is graded, we furthermore require the products and coproducts to be graded, *i.e.* such that $\mathfrak{A}_m \cdot \mathfrak{A}_n \subseteq \mathfrak{A}_{m+n}$ for any $m, n \in \mathbb{N}$ and $\triangle\mathfrak{A}_p \subseteq \bigoplus_{m+n=p} \mathfrak{A}_m \otimes \mathfrak{A}_n$ for any $p \in \mathbb{N}$.

A *combinatorial Hopf algebra* is a combinatorial vector space $\mathfrak{A}$ endowed with an associative product $\cdot : \mathfrak{A} \otimes \mathfrak{A} \to \mathfrak{A}$ and a coassociative coproduct $\triangle : \mathfrak{A} \to \mathfrak{A} \otimes \mathfrak{A}$, subject to the compatibility relation $\triangle(a \cdot b) = \triangle(a) \cdot \triangle(b)$, where the right hand side product has to be understood componentwise. More precisely, we require that the following commutative diagram commutes:

$$\begin{array}{ccccc}
\mathfrak{A} \otimes \mathfrak{A} & \xrightarrow{\cdot} & \mathfrak{A} & \xrightarrow{\triangle} & \mathfrak{A} \otimes \mathfrak{A} \\
{\scriptstyle \triangle \otimes \triangle}\downarrow & & & & \uparrow{\scriptstyle \cdot \otimes \cdot} \\
\mathfrak{A} \otimes \mathfrak{A} \otimes \mathfrak{A} \otimes \mathfrak{A} & & \xrightarrow[I \otimes \mathrm{swap} \otimes I]{} & & \mathfrak{A} \otimes \mathfrak{A} \otimes \mathfrak{A} \otimes \mathfrak{A}
\end{array}$$

where $\mathrm{swap}(x \otimes y) = y \otimes x$ is just a swap. Note that the existence of the antipode is automatical for combinatorial Hopf algebras. While its properties are interesting to study in general, we ignore the antipode in this document.

For a combinatorial Hopf algebra $(\mathfrak{A}, \cdot, \triangle)$, the *dual Hopf algebra* $(\mathfrak{A}^*, \triangle^*, \cdot^*)$ is the Hopf algebra on the dual vector space $\mathfrak{A}^*$ of linear forms on $\mathfrak{A}$, endowed with the product $\triangle^* : \mathfrak{A}^* \otimes \mathfrak{A}^* \to \mathfrak{A}^*$ defined by $(f \triangle^* g)(x) = \sum f(x_1) \otimes f(x_2)$ for any $x \in \mathfrak{A}$ such that $\triangle(x) = \sum x_1 \otimes x_2$, and the coproduct $\cdot^* = \mathfrak{A}^* \to \mathfrak{A}^* \otimes \mathfrak{A}^*$ defined by $\cdot^*(f)(x \otimes y) = f(x \cdot y)$ for any $x, y \in \mathfrak{A}$.

A *Hopf subalgebra* of a Hopf algebra $(\mathfrak{A}, \cdot, \triangle)$ is a vector subspace $\mathfrak{B}$ of $\mathfrak{A}$ which is stable by the product $\cdot$ and the coproduct $\triangle$, *i.e.* such that $\mathfrak{B} \cdot \mathfrak{B} \subseteq \mathfrak{B}$ and $\triangle\mathfrak{B} \subseteq \mathfrak{B} \otimes \mathfrak{B}$.

1.3.2 Three classical Hopf algebras

Malvenuto–Reutenauer Hopf algebra on permutations. We recall a fundamental combinatorial Hopf algebra on permutations introduced by C. Malvenuto and C. Reutenauer [MR95]. There are several ways to present it, we choose one that fits the rest of this document.

The *standardization* of a word $w \in \mathbb{N}^q$ with distinct entries is the permutation $\mathbf{std}(w)$ of $[q]$ whose entries are in the same relative order as the entries of w. For a permutation $\tau \in \mathfrak{S}_p$ and a sub-

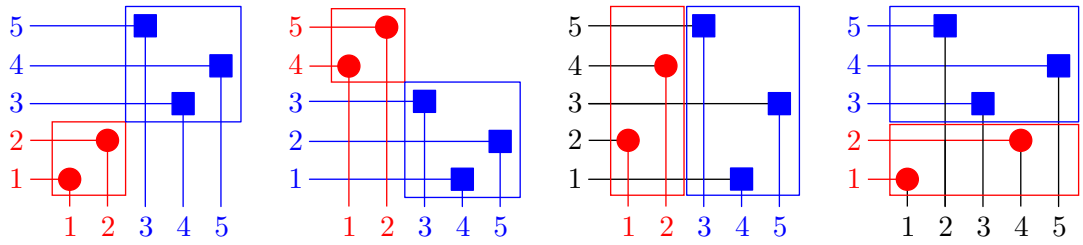

Figure 1.5: The tables of the products $\rho\backslash\sigma$ (left) and ρ/σ (middle left) have two blocks containing the tables of $\rho = 12$ and $\sigma = 231$. Elements of the shifted shuffle product $\rho \,⧢\, \sigma$ (middle right) and the convolution product $\rho \star \sigma$ (right) are obtained by shuffling the rows and columns of the table of $\rho\backslash\sigma$.

set $R \subseteq [p]$, we define $\mathbf{stdp}(\tau, R)$ (resp. $\mathbf{stdv}(\tau, R)$) as the standardization of the word obtained by deleting from τ the entries whose positions (resp. values) are not in R. For two permutations $\rho \in \mathfrak{S}_m$ and $\sigma \in \mathfrak{S}_n$, define the *shifted shuffle* $\rho \,⧢\, \sigma$ and the *convolution* $\rho \star \sigma$ by:

$$\rho \,⧢\, \sigma := \{\tau \in \mathfrak{S}_{m+n} \,|\, \mathbf{stdv}(\tau, [m]) = \rho \text{ and } \mathbf{stdv}(\tau, [m+n] \setminus [m]) = \sigma\},$$
$$\text{and} \qquad \rho \star \sigma := \{\tau \in \mathfrak{S}_{m+n} \,|\, \mathbf{stdp}(\tau, [m]) = \rho \text{ and } \mathbf{stdp}(\tau, [m+n] \setminus [m]) = \sigma\}.$$

E.g., $12 \,⧢\, 231 = \{12453, 14253, 14523, 14532, 41253, 41523, 41532, 45123, 45132, 45312\}$,
$12 \star 231 = \{12453, 13452, 14352, 15342, 23451, 24351, 25341, 34251, 35241, 45231\}$.

These operations are illustrated in Figure 1.5 on the tables of the permutations. Note that to fit the constructions of [LR98, HNT05, CP17], we use an unconventional orientation for the table of a permutation: rows are labeled by positions from bottom to top and columns are labeled by values from left to right. In other words, the table contains a dot at coordinates (σ_i, i) for all $i \in [n]$.

Let $\mathfrak{S} := \bigsqcup_{n\in\mathbb{N}} \mathfrak{S}_n$ be the set of all permutations (any size) and $\boldsymbol{k}\mathfrak{S}$ denote its $\boldsymbol{k}$-vector span. C. Malvenuto and C. Reutenauer's Hopf algebra on permutations is defined as follows.

Theorem 1.1 ([MR95]). *The combinatorial vector space $\boldsymbol{k}\mathfrak{S}$ with basis $(\mathbb{F}_\tau)_{\tau\in\mathfrak{S}}$ endowed with the product $\mathbb{F}_\rho \cdot \mathbb{F}_\sigma = \sum_{\tau\in\rho \,⧢\, \sigma} \mathbb{F}_\tau$ and the coproduct $\triangle\mathbb{F}_\tau = \sum_{\tau\in\rho\star\sigma} \mathbb{F}_\rho \otimes \mathbb{F}_\sigma$ is a Hopf algebra.*

The product in $\boldsymbol{k}\mathfrak{S}$ behaves nicely with the weak order $\leq_{\mathsf{W}}$ on $\mathfrak{S}_n$. For two permutations $\rho \in \mathfrak{S}_m$ and $\sigma \in \mathfrak{S}_n$, consider the permutations $\rho\backslash\sigma$ and ρ/σ of $\mathfrak{S}_{m+n}$ defined by:

$$\rho\backslash\sigma(i) = \begin{cases} \rho(i) & \text{if } i \in [m] \\ m + \sigma(i-m) & \text{otherwise} \end{cases} \qquad \text{and} \qquad \rho/\sigma(i) = \begin{cases} m + \sigma(i) & \text{if } i \in [n] \\ \rho(i-n) & \text{otherwise.} \end{cases}$$

These notations should be clear on the permutation tables of $\rho\backslash\sigma$ and ρ/σ, illustrated in Figure 1.5 (remember our unconventional orientation!). The shifted shuffle $\rho \,⧢\, \sigma$ is then the interval between $\rho\backslash\sigma$ and ρ/σ in the weak order $\leq_{\mathsf{W}}$ on $\mathfrak{S}_{m+n}$. This extends to a product of weak order intervals as follows.

Proposition 1.2. *A product of weak order intervals in $\boldsymbol{k}\mathfrak{S}$ is a weak order interval: for two weak order intervals $[\underline{\rho}, \overline{\rho}]_{\mathsf{W}} \subseteq \mathfrak{S}_m$ and $[\underline{\sigma}, \overline{\sigma}]_{\mathsf{W}} \subseteq \mathfrak{S}_n$, we have $\sum_{\underline{\rho}\leq_{\mathsf{W}}\rho\leq_{\mathsf{W}}\overline{\rho}} \mathbb{F}_\rho \cdot \sum_{\underline{\sigma}\leq_{\mathsf{W}}\sigma\leq_{\mathsf{W}}\overline{\sigma}} \mathbb{F}_\sigma = \sum_{\underline{\rho}\backslash\underline{\sigma}\leq_{\mathsf{W}}\tau\leq_{\mathsf{W}}\overline{\rho}/\overline{\sigma}} \mathbb{F}_\tau$.*

We refer to [MR95, AS05] for more properties of C. Malvenuto and C. Reutenauer's Hopf algebra $\boldsymbol{k}\mathfrak{S}$ on permutations. We also consider its dual Hopf algebra.

Definition 1.3. *The dual Hopf algebra of $\boldsymbol{k}\mathfrak{S}$ is the Hopf algebra $\boldsymbol{k}\mathfrak{S}^*$ with basis $(\mathbb{G}_\tau)_{\tau\in\mathfrak{S}}$ endowed with the product $\mathbb{G}_\rho \cdot \mathbb{G}_\sigma = \sum_{\tau\in\rho\star\sigma} \mathbb{G}_\tau$ and the coproduct $\triangle\mathbb{G}_\tau = \sum_{\tau\in\rho \,⧢\, \sigma} \mathbb{G}_\rho \otimes \mathbb{G}_\sigma$.*

Loday–Ronco Hopf algebra on binary trees. We denote by $\boldsymbol{k}\mathfrak{T}$ the vector subspace of $\boldsymbol{k}\mathfrak{S}$ generated by the elements $\mathbb{P}_T := \sum_{\substack{\tau\in\mathfrak{S}\\ \mathbf{bt}(\tau)=T}} \mathbb{F}_\tau = \sum_{\tau\in\mathcal{L}(T)} \mathbb{F}_\tau$, for all binary trees $T \in \mathfrak{T}$ of any size.

Theorem 1.4 ([LR98]). *The vector subspace $\boldsymbol{k}\mathfrak{T}$ is a Hopf subalgebra of $\boldsymbol{k}\mathfrak{S}$.*

Again, the product in $\boldsymbol{k}\mathfrak{T}$ behaves nicely with the Tamari lattice $\leq_\mathsf{T}$ on $\mathfrak{T}_n$. For two binary trees $R \in \mathfrak{T}_m$ and $S \in \mathfrak{T}_n$, consider the binary trees $R\backslash S$ and R/S of $\mathfrak{T}_{m+n}$ obtained as follows:

- $R\backslash S$ is obtained by grafting R to the leftmost leaf of S,
- R/S is obtained by grafting S to the rightmost leaf of R.

See Figure 1.6.

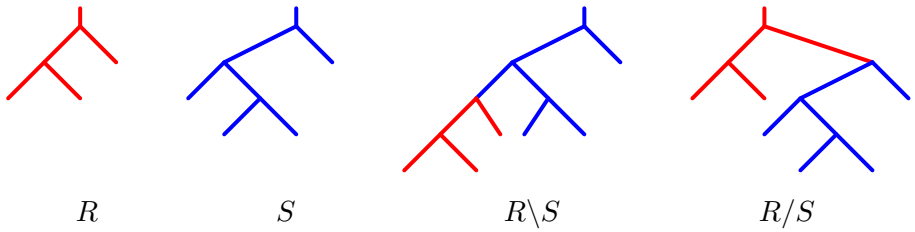

Figure 1.6: Two binary trees $R \in \mathfrak{T}_2$ and $S \in \mathfrak{T}_3$ and the graftings $R\backslash S$ and R/S of $\mathfrak{T}_5$.

The product $R \cdot S$ is then the interval between $R\backslash S$ and R/S in the Tamari lattice $\leq_\mathsf{T}$ on $\mathfrak{T}_{m+n}$. This extends to a product of Tamari intervals as follows.

Proposition 1.5. *A product of Tamari intervals in $\boldsymbol{k}\mathfrak{T}$ is a Tamari interval: for two Tamari intervals $[\underline{R}, \overline{R}]_\mathsf{T} \subseteq \mathfrak{T}_m$ and $[\underline{S}, \overline{S}]_\mathsf{T} \subseteq \mathfrak{T}_n$, we have* $\sum_{\underline{R}\leq_\mathsf{T} R\leq_\mathsf{T}\overline{R}} \mathbb{F}_R \cdot \sum_{\underline{S}\leq_\mathsf{T} S\leq_\mathsf{T}\overline{S}} \mathbb{F}_S = \sum_{\underline{R}\backslash\underline{S}\leq_\mathsf{T} T\leq_\mathsf{T}\overline{R}/\overline{S}} \mathbb{F}_T.$

One can also describe the coproduct in $\boldsymbol{k}\mathfrak{T}$ and both the product and the coproduct in the dual Hopf algebra $\boldsymbol{k}\mathfrak{T}^*$ in terms of cut and past operations in binary trees. We skip these descriptions here as they will appear as special cases of those described for permutrees in Section 3.3. We refer to [LR98, AS06, HNT05] for more properties of J.-L. Loday's and M. Ronco's Hopf algebra $\boldsymbol{k}\mathfrak{T}$ on binary trees.

Recoil Hopf algebra on binary sequences. We denote by $\boldsymbol{k}\mathfrak{B}$ the vector subspace of $\boldsymbol{k}\mathfrak{S}$ generated by the elements $\mathbb{X}_\chi := \sum_{\substack{\tau\in\mathfrak{S}\\ \mathbf{rec}(\tau)=\chi}} \mathbb{F}_\tau = \sum_{\substack{T\in\mathfrak{T}\\ \mathbf{can}(T)=\chi}} \mathbb{P}_T$, for all binary sequences $\chi \in \mathfrak{B}$ of any size.

Theorem 1.6 ([GKL+95]). *The vector subspace $\boldsymbol{k}\mathfrak{B}$ is a Hopf subalgebra of $\boldsymbol{k}\mathfrak{S}$ and of $\boldsymbol{k}\mathfrak{T}$.*

Again, the product in $\boldsymbol{k}\mathfrak{B}$ behaves nicely with the boolean lattice $\leq_\mathsf{B}$ on $\mathfrak{B}_n$. For two binary sequences $\chi \in \mathfrak{B}_m$ and $\zeta \in \mathfrak{B}_n$, consider the binary sequences $\chi\backslash\zeta := \chi-\zeta$ and $\chi/\zeta := \chi+\zeta$ of $\mathfrak{B}_{m+n}$ (where we just concatenate the sequences). The product $\chi\cdot\zeta$ is then the interval between $\chi\backslash\zeta$ and χ/ζ in the boolean lattice $\leq_\mathsf{B}$ on $\mathfrak{B}_{m+n}$. This extends to a product of boolean intervals as follows.

Proposition 1.7. *A product of boolean intervals in $\boldsymbol{k}\mathfrak{B}$ is a boolean interval: for two boolean intervals $[\underline{\chi}, \overline{\chi}]_\mathsf{B} \subseteq \mathfrak{B}_m$ and $[\underline{\zeta}, \overline{\zeta}]_\mathsf{B} \subseteq \mathfrak{B}_n$, we have* $\sum_{\underline{\chi}\leq_\mathsf{B}\chi\leq_\mathsf{B}\overline{\chi}} \mathbb{F}_\chi \cdot \sum_{\underline{\zeta}\leq_\mathsf{B}\zeta\leq_\mathsf{B}\overline{\zeta}} \mathbb{F}_\zeta = \sum_{\underline{\chi}\backslash\underline{\zeta}\leq_\mathsf{B}\omega\leq_\mathsf{B}\overline{\chi}/\overline{\zeta}} \mathbb{F}_\omega.$

Again, the descriptions of the products and coproducts in the permutree Hopf algebra and its dual provide classical descriptions of the coproduct in $\boldsymbol{k}\mathfrak{B}$ and the product and coproduct in the dual $\boldsymbol{k}\mathfrak{B}^*$.

Chapter Two

BRICK POLYTOPES

This chapter presents combinatorial, geometric and algebraic properties of certain pipe dreams, called acyclic k-twists and studied in [Pil18]. They generalize binary trees and the Tamari lattice and were motivated by the brick polytope construction of [PS12] for k-triangulations (a general version of the brick polytope construction is reported in Chapter 8). They provide a relevant example of the setting described by N. Reading in [Rea05]: the acyclic k-twists are endowed with a lattice structure arising from a lattice congruence of the weak order generalizing the sylvester congruence (Section 2.1), correspond to the vertices of a brick polytope (Section 2.2), and index the basis of a Hopf subalgebra of C. Malvenuto and C. Reutenauer's Hopf algebra on permutations (Section 2.3).

2.1 ACYCLIC TWIST LATTICES

2.1.1 Pipe dreams, (k, n)-twists and k-triangulations of the n-gon

A *pipe dream* is a filling of a triangular shape with crosses $+$ and elbows $\curvearrowright$ so that all pipes entering on the left side exit on the top side. These objects were studied in the literature, under different names including "pipe dreams" [KM05], "RC-graphs" [BB93], or as specific "pseudoline arrangements on sorting networks" [PS12]. Here, we consider the following specific family of pipe dreams.

Definition 2.1. *For $k, n \in \mathbb{N}$, a (k, n)-twist is a pipe dream with $n + 2k$ pipes such that:*

- *no two pipes cross twice (the pipe dream is reduced),*
- *the pipe which enters in row i exits in column i if $k + 1 \leq i \leq k + n$, and $n + 2k + 1 - i$ otherwise. Note that rows are indexed from bottom to top and columns are indexed from left to right.*

Besides the first k and last k trivial pipes, a (k, n)-twist has n relevant pipes, labeled by $[n]$ from bottom to top, or equivalently from left to right (see Figure 2.1, where only relevant pipes are shown).

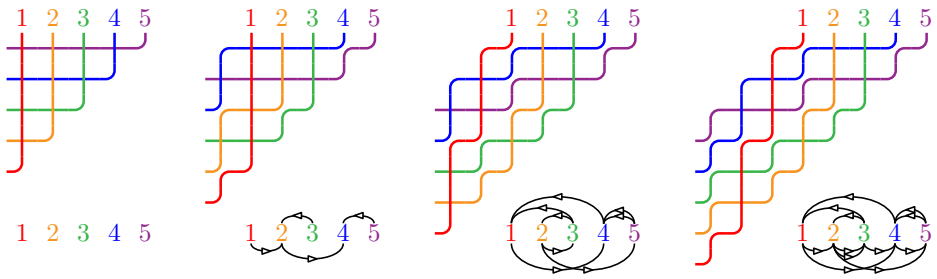

Figure 2.1: Some $(k, 5)$-twists (top) and their contact graphs (bottom) for $k = 0, 1, 2, 3$.

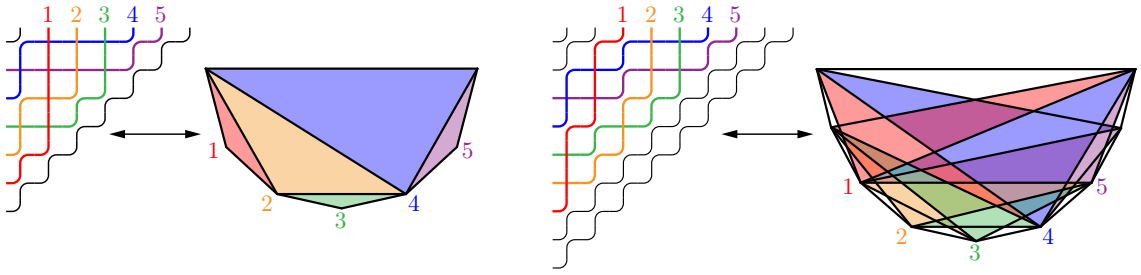

Figure 2.2: Duality between (k, n)-twists and k-triangulations of the $(n + 2k)$-gon.

Definition 2.2. *The contact graph of a (k, n)-twist T is the directed multigraph $T^\#$ with vertex set $[n]$ and with an arc from the* SE*-pipe to the* WN*-pipe of each elbow in T involving two relevant pipes (see Figure 2.1). We say that a twist T is acyclic if its contact graph $T^\#$ is (no oriented cycle), and we then denote by $\lhd_T$ the transitive closure of $T^\#$. We denote by $\mathfrak{AT}_n^k$ the set of acyclic (k, n)-twists.*

Remark 2.3. A *k-triangulation* of a convex $(n + 2k)$-gon is a maximal set of diagonals such that no $k + 1$ of them are pairwise crossing. Multitriangulations appeared in the context of extremal theory for geometric graphs and were studied for their rich combinatorial structure, see references in [PS09]. Based on k-stars in k-triangulations [PS09], it is shown in [PP12] sending an elbow in row i and column j of the $(n + 2k) \times (n + 2k)$ triangular shape to the diagonal $[i, j]$ of a $(n + 2k)$-gon gives a bijection between the (k, n)-twists and the k-triangulations of the $(n + 2k)$-gon (see Figure 2.2).

Example 2.4. When $k = 1$, a $(1, n)$-twist T corresponds to a triangulation $T^\star$ of an $(n+2)$-gon, and the contact graph of T coincides with the dual binary tree of $T^\star$.

2.1.2 k-twist correspondence

We now define a bijective correspondence between permutations of $\mathfrak{S}_n$ and leveled (k, n)-twists. It relies on an insertion operation in k-twists similar to the insertion operation in binary search trees (see Figure 1.2). Given a permutation $\sigma := \sigma_1 \dots \sigma_n$, we start from the empty triangular shape and insert the pipes $\sigma_n, \dots, \sigma_1$ such that each new pipe is as northwest as possible in the space left by the pipes already inserted (see Figure 2.3). The result $\mathbf{ltwi}^k(\sigma)$ of this procedure is a *leveled (k, n)-twist*, *i.e.* an acyclic (k, n)-twist endowed with a linear extension of its contact graph.

Proposition 2.5. *The map $\mathbf{ltwi}^k$ is a bijection from permutations to leveled k-twists.*

Example 2.6. For $k = 1$, the contact graph of the 1-twist $\mathbf{ltwi}^1(\sigma)$ is the binary search tree obtained by successive insertions of the entries of σ from right to left (see Figure 1.2). The 1-twist correspondence is thus the sylvester correspondence [HNT05] between permutations and leveled binary trees.

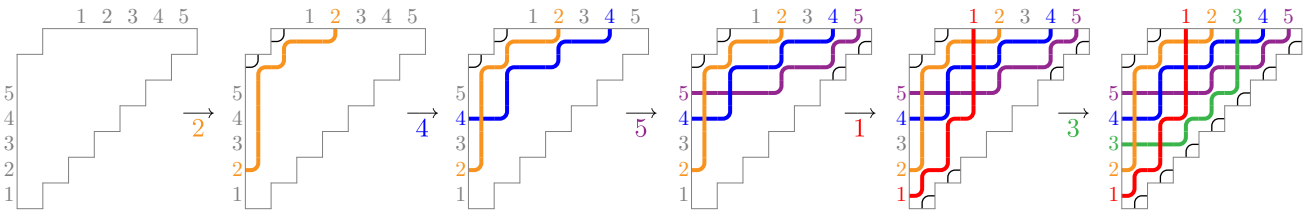

Figure 2.3: Insertion of the permutation 31542 in a 2-twist.

2.1.3 k-twist congruence

In the rest of the chapter, we forget the order of the leveled (k, n)-twist $\mathbf{ltwi}^k(\sigma)$ and we denote the resulting (k, n)-twist by $\mathbf{twi}^k(\sigma)$. We are interested in the fibers of this map.

Proposition 2.7. *The permutations σ such that $\mathbf{twi}^k(\sigma) = T$ are precisely the linear extensions of (the transitive closure of) the contact graph $T^\#$. In particular, $\mathbf{twi}^k$ is surjective from $\mathfrak{S}_n$ to $\mathfrak{AT}_n^k$.*

We then characterize the permutations in the same fiber in terms of a congruence relation defined by a rewriting rule, generalizing the sylvester congruence [HNT05] obtained for $k = 1$.

Definition 2.8. *The k-twist congruence $\equiv^k$ on $\mathfrak{S}_n$ is obtained as the transitive closure of the rewriting rule $UacV_1b_1V_2b_2\cdots V_kb_kW \equiv^k UcaV_1b_1V_2b_2\cdots V_kb_kW$, where $a, b_1, \dots, b_k, c$ are elements of $[n]$ such that $a < b_i < c$ for all $i \in [k]$, while $U, V_1, \dots, V_k, W$ are (possibly empty) words on $[n]$.*

Proposition 2.9. *The classes of $\equiv^k$ are the fibers of $\mathbf{twi}^k$, i.e. $\sigma \equiv^k \tau \iff \mathbf{twi}^k(\sigma) = \mathbf{twi}^k(\tau)$.*

Proposition 2.10. *The k-twist congruence $\equiv^k$ is a lattice congruence of the weak order.*

2.1.4 Flips and acyclic k-twist lattices

Definition 2.11. *A flip in a k-twist is the exchange of an elbow $\lrcorner$ between two relevant pipes with the unique crossing $+$ between them. The flip is increasing if the initial elbow is located (largely) south-west of the final elbow. See Figure 2.4.*

Proposition 2.12. *The transitive closure of the increasing flip graph on acyclic (k, n)-twists is a lattice, called acyclic k-twist lattice. It isomorphic to the quotient of the weak order by the k-twist congruence $\equiv^k$. The map $\mathbf{twi}^k$ is thus a morphism from the weak order to the acyclic k-twist lattice.*

Example 2.13. When $k = 1$, the 1-twist lattice is isomorphic to the Tamari lattice on binary trees.

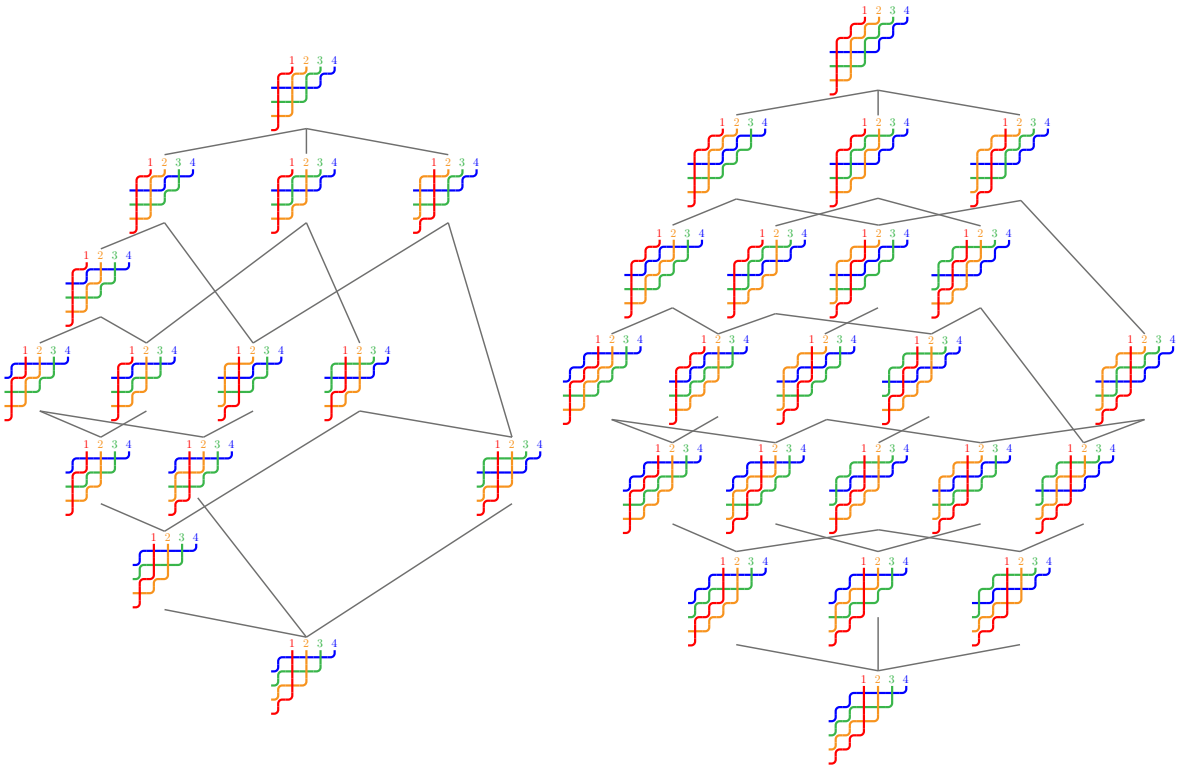

Figure 2.4: The increasing flip lattices on $(k, 4)$-twists for $k = 1$ (left) and $k = 2$ (right).

2.1.5 k-recoils and k-canopy schemes

To prepare the definition of the canopy of acyclic k-twists, we first recall the notion of k-recoil schemes of permutations already considered in [Rea05, NRT11]. We use a description in terms of acyclic orientations as it is closer to the description of the vertices of the zonotope that we will use later in Section 2.2. We consider the graph G_n^k with vertex set $[n]$ and edge set $\big\{\{i,j\} \in [n]^2 \,\big|\, i < j \le i+k\big\}$. See for instance the graphs G_5^k for $k = 0, 1, 2, 3$ on the right. We let $\mathfrak{AO}_n^k$ be the set of acyclic orientations of G_n^k (no oriented cycle).

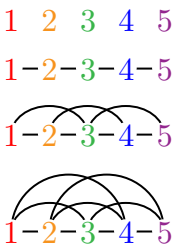

Definition 2.14. *The k-recoil scheme of a permutation $\sigma \in \mathfrak{S}_n$ is the orientation $\mathbf{rec}^k(\sigma) \in \mathfrak{AO}_n^k$ with an edge $i \to j$ for all $i, j \in [n]$ such that $|i-j| \le k$ and $\sigma^{-1}(i) < \sigma^{-1}(j)$. The map $\mathbf{rec}^k : \mathfrak{S}_n \to \mathfrak{AO}_n^k$ is called k-recoil map.*

Example 2.15. When $k = 1$, the graph G_n^1 is just the n-path. The 1-recoil scheme of $\sigma \in \mathfrak{S}_n$ thus stores the *recoils* of σ, *i.e.* the values $i \in [n-1]$ such that $\sigma^{-1}(i) > \sigma^{-1}(i+1)$.

Definition 2.16. *The k-recoil congruence $\approx^k$ on $\mathfrak{S}_n$ is the transitive closure of the rewriting rule $UijV \approx^k UjiV$, where $i, j \in [n]$ are such that $i+k < j$ while U, V are (possibly empty) words on $[n]$.*

Proposition 2.17. *The classes of $\approx^k$ are the fibers of $\mathbf{rec}^k$, i.e. $\sigma \approx^k \tau \iff \mathbf{rec}^k(\sigma) = \mathbf{rec}^k(\tau)$.*

Proposition 2.18. *The k-recoil congruence $\approx^k$ is a lattice congruence of the weak order.*

Definition 2.19. *A flip in an acyclic orientation of G_n^k is the switch of the direction of an edge of G_n^k. The flip is increasing if the initial direction was increasing (i.e. $i \to j$ with $i < j$).*

Theorem 2.20. *The transitive closure of the increasing flip graph on acyclic orientations of G_n^k is a lattice, called k-recoil lattice. It isomorphic to the quotient of the weak order by the k-recoil congruence $\approx^k$. The map $\mathbf{rec}^k$ is thus a morphism from the weak order to the k-recoil lattice.*

We can now extend the notion of canopy of binary trees to acyclic k-twists. To ensure that Definition 2.22 is valid, we need the following observation on comparisons of closed pipes in a k-twist.

Lemma 2.21. *If $|i-j| \le k$, the ith and jth pipes in an acyclic k-twist T are comparable for $\lhd_T$.*

Definition 2.22. *The k-canopy scheme of a (k,n)-twist T is the orientation $\mathbf{can}^k(T) \in \mathfrak{AO}_n^k$ with an edge $i \to j$ for all $i, j \in [n]$ such that $|i-j| \le k$ and $i \lhd_T j$. It indeed defines an acyclic orientation of G_n^k by Lemma 2.21. We call k-canopy the map $\mathbf{can}^k : \mathfrak{AT}_n^k \to \mathfrak{AO}_n^k$.*

Example 2.23. When $k = 1$, the 1-canopy scheme of a $(1,n)$-twist T is the classical canopy of $T^\#$.

Finally, it is immediate from Definitions 2.8 and 2.16 that for $k > \ell$, the k-twist congruence $\equiv^k$ refines the ℓ-twist congruence $\equiv^\ell$ and the k-recoil congruence $\approx^k$ refines the ℓ-recoil congruence $\approx^\ell$. This defines surjective restrictions $\mathbf{res}^{k\to\ell} : \mathfrak{AT}_n^k(n) \to \mathfrak{AT}_n^\ell(n)$ and $\mathbf{res}^{k\to\ell} : \mathfrak{AO}_n^k(n) \to \mathfrak{AO}_n^\ell(n)$. The following statement concludes our lattice theoretic study of acyclic k-twists.

Proposition 2.24. *We have the following commutative diagram of lattice morphisms:*

$$\begin{array}{ccc}
\mathfrak{AT}_n^k(n) & \xrightarrow{\mathbf{res}^{k\to\ell}} & \mathfrak{AT}_n^\ell(n) \\
{\scriptstyle \mathbf{can}^k}\downarrow & \overset{\mathbf{twi}^k}{\nwarrow}\ \ \overset{\mathbf{twi}^\ell}{\nearrow} & \downarrow{\scriptstyle \mathbf{can}^\ell} \\
\mathfrak{AO}_n^k(n) & \xrightarrow[\mathbf{res}^{k\to\ell}]{} & \mathfrak{AO}_n^\ell(n)
\end{array} \qquad \mathfrak{S}_n \quad \begin{array}{l} \swarrow \mathbf{rec}^k \\ \searrow \mathbf{rec}^\ell \end{array}$$

2.2 BRICK POLYTOPES

This section is devoted to the polyhedral geometry of permutations of $\mathfrak{S}_n$, acyclic twists of $\mathfrak{AT}_n^k$, and acyclic orientations of $\mathfrak{AO}_n^k$. It is mainly based on properties of brick polytopes of sorting networks, defined and studied in [PS12]. A more general treatment on brick polytopes is presented in Chapter 8.

2.2.1 Permutahedra, brick polytopes, zonotopes

We still denote by $(\boldsymbol{e}_i)_{i\in[n]}$ the canonical basis of $\mathbb{R}^n$. We recall the definition of three families of polytopes, which are illustrated in Figure 2.5:

Permutahedron. The *permutahedron* $\mathbb{P}\mathrm{erm}(n)$ is the convex hull of $\sum_{i\in[n]} i\boldsymbol{e}_{\sigma(i)}$ for all $\sigma \in \mathfrak{S}_n$.

Brick polytope. We call *bricks* the squares $[i, i+1] \times [j, j+1]$ of the triangular shape. The *brick area* of a pipe p is the number of bricks located below p but inside the axis-parallel rectangle defined by the two endpoints of p. The *brick vector* of a k-twist T is the vector of $\mathbb{R}^n$ whose ith coordinate is the brick area of the ith relevant pipe of T. The *brick polytope* $\mathbb{B}\mathrm{rick}^k(n)$ is the convex hull of the brick vectors of all (k, n)-twists. Its vertices correspond to the acyclic (k, n)-twists of $\mathfrak{AT}_n^k$.

Zonotope. The *graphical zonotope* $\mathbb{Z}\mathrm{ono}(G)$ of a graph G is the Minkowski sum of the segments $[\boldsymbol{e}_i, \boldsymbol{e}_j]$ for all edges $\{i, j\}$ of G. We consider the zonotope $\mathbb{Z}\mathrm{ono}^k(n) := \mathbb{Z}\mathrm{ono}(G_n^k)$. Its vertices correspond to the acyclic orientations of $\mathfrak{AO}_n^k$.

Example 2.25. When $k = 1$, the brick polytope $\mathbb{B}\mathrm{rick}^1(n)$ coincides (up to a translation) with J.-L. Loday's associahedron $\mathbb{A}\mathrm{sso}(n)$ [Lod04] and the zonotope $\mathbb{Z}\mathrm{ono}^1(n)$ coincides with the parallelepiped $\mathbb{P}\mathrm{ara}(n)$ generated by the simple roots $\boldsymbol{e}_{i+1} - \boldsymbol{e}_i$. See Section 1.2.2.

The lattices studied in Section 2.1 naturally appear in the geometry of these polytopes. Namely, recall the direction $\boldsymbol{\omega} := (n, n-1, \dots, 2, 1) - (1, 2, \dots, n-1, n) = \sum_{i\in[n]}(n+1-2i)\,\boldsymbol{e}_i$.

Proposition 2.26. *When oriented in the direction $\boldsymbol{\omega}$, the 1-skeleta of the permutahedron $\mathbb{P}\mathrm{erm}(n)$ (resp. of the brick polytope $\mathbb{B}\mathrm{rick}^k(n)$, resp. of the zonotope $\mathbb{Z}\mathrm{ono}^k(n)$) is the Hasse diagram of the weak order on permutations (resp. of the increasing flip lattice on acyclic (k, n)-twists, resp. of the increasing flip lattice on acyclic orientations of G_n^k).*

2.2.2 The geometry of the surjections $\mathbf{twi}^k$, $\mathbf{can}^k$, $\mathbf{rec}^k$

The main geometric connection between the three polytopes $\mathbb{P}\mathrm{erm}(n)$, $\mathbb{B}\mathrm{rick}^k(n)$ and $\mathbb{Z}\mathrm{ono}^k(n)$ is given by their normal fans. For a permutation $\sigma \in \mathfrak{S}_n$ (resp. for a twist $T \in \mathfrak{AT}_n^k$, resp. for an orientation $O \in \mathfrak{AO}_n^k$), we denote by $\boldsymbol{C}(\sigma)$ (resp. $\boldsymbol{C}(T)$, resp. $\boldsymbol{C}(O)$) the incidence cone of the chain $\sigma_1 \lhd \cdots \lhd \sigma_n$ (resp. of the transitive closure $\lhd_T$ of the contact graph $T^\#$, resp. of the transitive closure of O). We define similarly the braid cone $\boldsymbol{C}^\diamond(\sigma)$ (resp. $\boldsymbol{C}^\diamond(T)$, resp. $\boldsymbol{C}^\diamond(O)$). See Section 1.2.2 for the general definitions of these cones for posets.

Proposition 2.27. *Together with all their faces, the cones $\{\boldsymbol{C}^\diamond(\sigma) \mid \sigma \in \mathfrak{S}_n\}$, $\{\boldsymbol{C}^\diamond(T) \mid T \in \mathfrak{AT}_n^k\}$, and $\{\boldsymbol{C}^\diamond(O) \mid O \in \mathfrak{AO}_n^k\}$ respectively form the normal fans of the permutahedron $\mathbb{P}\mathrm{erm}(n)$, of the brick polytope $\mathbb{B}\mathrm{rick}^k(n)$ and of the zonotope $\mathbb{Z}\mathrm{ono}^k(n)$.*

Using these normal fans, we interpret geometrically the maps $\mathbf{twi}^k$, $\mathbf{can}^k$, and $\mathbf{rec}^k$ as follows.

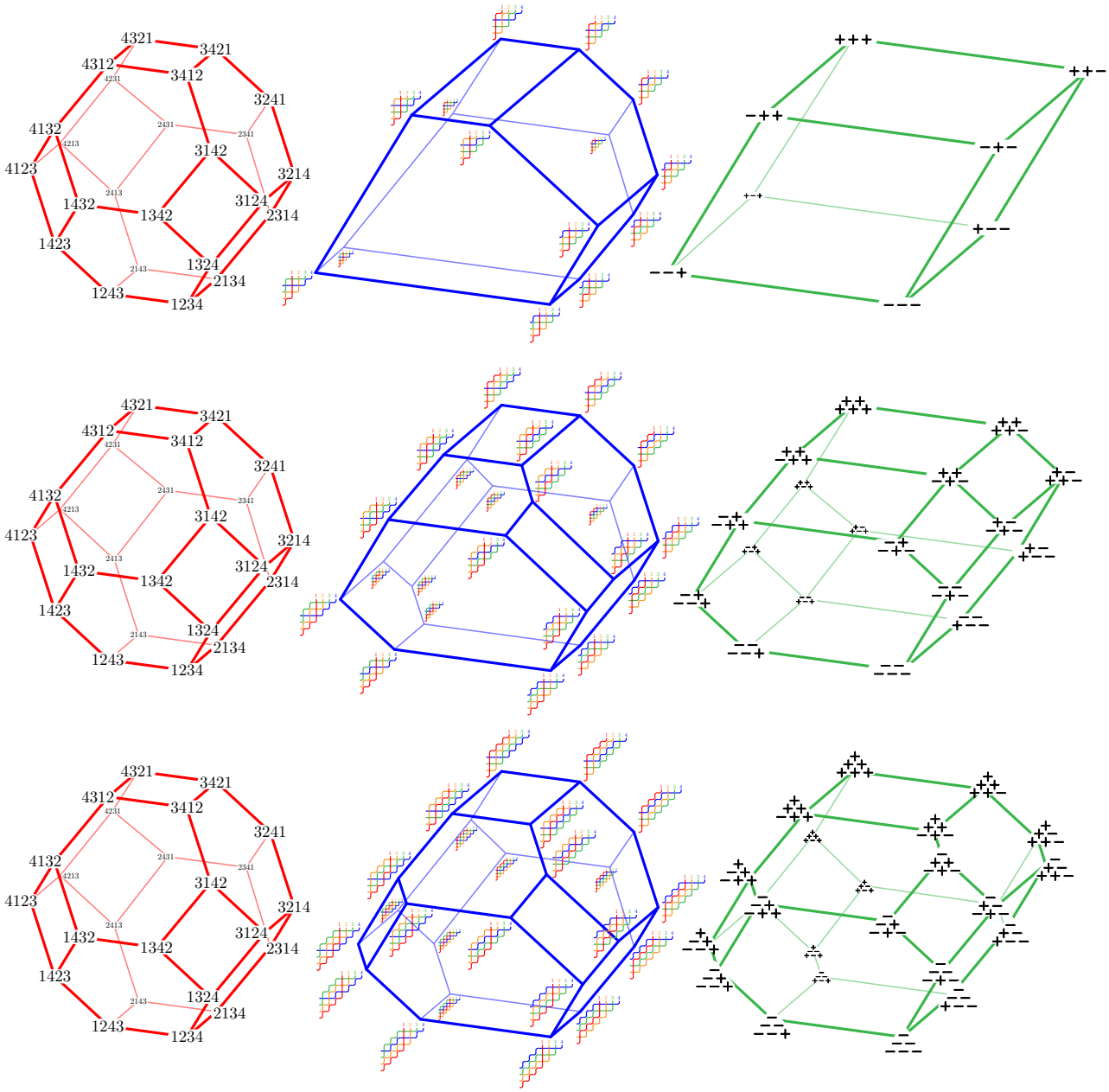

Figure 2.5: The permutahedron $\mathbb{P}\mathrm{erm}(4)$ (left), the brick polytope $\mathbb{B}\mathrm{rick}^k(4)$ (middle) and the zonotope $\mathbb{Z}\mathrm{ono}^k(4)$ (right) for $k = 1$ (top), $k = 2$ (middle) and $k = 3$ (bottom). For readibility, we represent orientations of G_n^k by pyramids of signs (a $-$ sign means an increasing relation).

Proposition 2.28. *The insertion map* $\mathbf{twi}^k : \mathfrak{S}_n \to \mathfrak{AT}_n^k$*, the* k*-canopy* $\mathbf{can}^k : \mathfrak{AT}_n^k \to \mathfrak{AO}_n^k$ *and the* k*-recoil map* $\mathbf{rec}^k : \mathfrak{S}_n \to \mathfrak{AO}_n^k$ *are characterized by:*

$$T = \mathbf{twi}^k(\sigma) \iff \boldsymbol{C}(T) \subseteq \boldsymbol{C}(\sigma) \iff \boldsymbol{C}^\diamond(T) \supseteq \boldsymbol{C}^\diamond(\sigma),$$
$$O = \mathbf{can}^k(T) \iff \boldsymbol{C}(O) \subseteq \boldsymbol{C}(T) \iff \boldsymbol{C}^\diamond(O) \supseteq \boldsymbol{C}^\diamond(T),$$
$$O = \mathbf{rec}^k(\sigma) \iff \boldsymbol{C}(O) \subseteq \boldsymbol{C}(\sigma) \iff \boldsymbol{C}^\diamond(O) \supseteq \boldsymbol{C}^\diamond(\sigma).$$

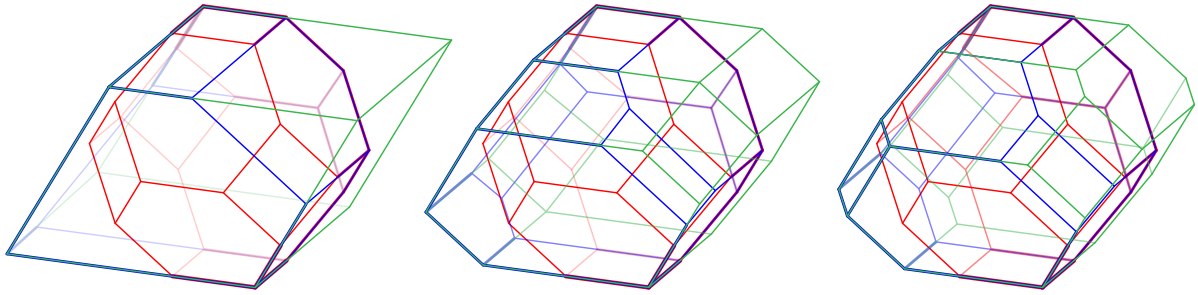

Figure 2.6: The inclusions $\mathbb{P}\mathrm{erm}(4) \subseteq \underline{\mathbb{B}\mathrm{rick}}^k(4) \subseteq \underline{\mathbb{Z}\mathrm{ono}}^k(4)$ for $k = 1$ (left), $k = 2$ (middle) and $k = 3$ (right). The permutahedron $\mathbb{P}\mathrm{erm}(4)$ is in red, the brick polytope $\underline{\mathbb{B}\mathrm{rick}}^k(4)$ in blue and the zonotope $\underline{\mathbb{Z}\mathrm{ono}}^k(4)$ in green.

Remark 2.29. In fact, one can even visualize these normal fan inclusions at the level of polytopes. It requires however to slightly transform the brick polytope $\mathbb{B}\mathrm{rick}^k(n)$ and the zonotope $\mathbb{Z}\mathrm{ono}^k(n)$ to:

- the polytope $\underline{\mathbb{B}\mathrm{rick}}^k(n)$ obtained by translating and scaling the brick polytope $\mathbb{B}\mathrm{rick}^k(n)$ so that its minimal and maximal vertices in the direction $\boldsymbol{\omega}$ coincide with the vertices $(1, \dots, n)$ and $(n, \dots, 1)$ of $\mathbb{P}\mathrm{erm}(n)$.
- the zonotope $\underline{\mathbb{Z}\mathrm{ono}}^k(n)$ obtained similarly from the Minkowski sum of the segments $[\boldsymbol{e}_i, \boldsymbol{e}_j]$ dilated with certain suitable factors. The precise dilation factors are not relevant and can be found in [Pil18, Sect. 1.2.1].

Note that these normalizations (translations, scalings and dilations) do not alter the normal fans of these polytopes: $\mathbb{B}\mathrm{rick}^k(n)$ and $\underline{\mathbb{B}\mathrm{rick}}^k(n)$ have the same normal fans, and $\mathbb{Z}\mathrm{ono}^k(n)$ and $\underline{\mathbb{Z}\mathrm{ono}}^k(n)$ have the same normal fans. These normalizations are chosen so that the polytopes $\mathbb{P}\mathrm{erm}(n)$, $\underline{\mathbb{B}\mathrm{rick}}^k(n)$ and $\underline{\mathbb{Z}\mathrm{ono}}^k(n)$ all live in the hyperplane $\mathbb{H} := \{\boldsymbol{x} \in \mathbb{R}^n \mid \sum_{i\in[n]} x_i = 0\}$ and fulfill the inclusions:

$$\begin{array}{ccccc}
\underline{\mathbb{B}\mathrm{rick}}^k(n) & & \subseteq & & \underline{\mathbb{B}\mathrm{rick}}^\ell(n) \\
& \supseteq & & \subseteq & \\
\cap\!| & & \mathbb{P}\mathrm{erm}(n) & & \cap\!| \\
& \supseteq & & \subseteq & \\
\underline{\mathbb{Z}\mathrm{ono}}^k(n) & & \subseteq & & \underline{\mathbb{Z}\mathrm{ono}}^\ell(n)
\end{array}$$

for $k > \ell$. Compare to Proposition 2.24. These inclusions are illustrated in Figures 2.5 to 2.7. Moreover the rescaled polytopes $\underline{\mathbb{B}\mathrm{rick}}^k(n)$ and $\underline{\mathbb{Z}\mathrm{ono}}^k(n)$ both converge to $\mathbb{P}\mathrm{erm}(n)$ when k tend to ∞, as illustrated in Figure 2.7.

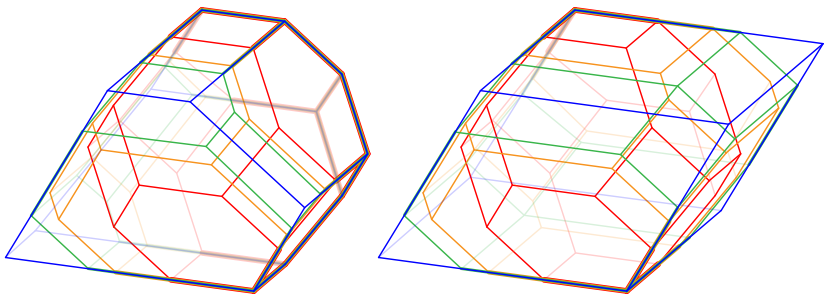

Figure 2.7: The inclusions of the brick polytopes $\underline{\mathbb{B}\mathrm{rick}}^k(4)$ (left) and of the zonotopes $\underline{\mathbb{Z}\mathrm{ono}}^k(4)$ (right) for $k = 1$ (blue), $k = 2$ (green) and $k = 3$ (orange). Both tend to the classical permutahedron $\mathbb{P}\mathrm{erm}(4)$ (red) when k tends to ∞.

2.3 The twist Hopf algebra

We now use the twist congruences to construct some relevant Hopf subalgebras of C. Malvenuto and C. Reutenauer's algebra $\boldsymbol{k}\mathfrak{S}$ on permutations [MR95]. We describe the product and coproduct in these Hopf algebras and their duals in terms of twists. Further algebraic directions, in particular product decompositions, multiplicative bases and integer point transforms, are explored in [Pil18].

2.3.1 Hopf subalgebra

We denote by $\boldsymbol{k}\mathfrak{AT}^k$ the vector subspace of $\boldsymbol{k}\mathfrak{S}$ generated by the elements $\mathbb{P}_T := \sum_{\substack{\tau\in\mathfrak{S}\\ \mathbf{twi}^k(\tau)=T}} \mathbb{F}_\tau = \sum_{\mathcal{L}(T^\#)} \mathbb{F}_\tau$, for all acyclic k-twists T of any size. Here are some examples:

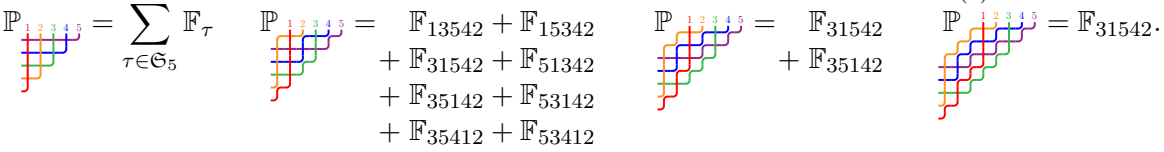

Theorem 2.30. *The vector subspace $\boldsymbol{k}\mathfrak{AT}^k$ is a Hopf subalgebra of $\boldsymbol{k}\mathfrak{S}$, called k-twist Hopf algebra.*

Example 2.31.
- For $k = 0$, the bijection which sends the unique $(0, n)$-twist to $X^n/n!$ defines an isomorphism from the 0-twist Hopf algebra $\boldsymbol{k}\mathfrak{AT}^0$ to the polynomial ring $\mathbb{K}[X]$.
- For $k = 1$, the bijection of Remark 2.3 defines an isomorphism from the 1-twist Hopf algebra $\boldsymbol{k}\mathfrak{AT}^1$ to M. Ronco and J.-L. Loday's Hopf algebra $\boldsymbol{k}\mathfrak{T}$ on planar binary trees [LR98, HNT05].

We now aim at understanding the product and the coproduct in $\boldsymbol{k}\mathfrak{AT}^k$ directly on k-twists. Although they are not always as satisfactory, our descriptions naturally extend classical results on the planar binary tree Hopf algebra described in [LR98, AS06, HNT05].

Product. To describe the product in $\boldsymbol{k}\mathfrak{AT}^k$, we need the following notation, which is illustrated in Figure 2.8. For a (k, m)-twist R and a (k, n)-twist S, we denote by $R\backslash S$ the $(k, m + n)$-twist obtained by inserting R in the first rows and columns of S and by R/S the $(k, m + n)$-twist obtained by inserting S in the last rows and columns of R. The following statement is illustrated in Figure 2.9.

Proposition 2.32. *For any acyclic k-twists $R \in \mathfrak{AT}^k_m$ and $S \in \mathfrak{AT}^k_n$, we have $\mathbb{P}_R \cdot \mathbb{P}_S = \sum_T \mathbb{P}_T$, where T runs over the interval between $R\backslash S$ and R/S in the acyclic $(k, m + n)$-twist lattice.*

Remark 2.33. The products of $\boldsymbol{k}\mathfrak{S}$ and $\boldsymbol{k}\mathfrak{T}$ are *dendriform*, meaning that they can be decomposed into two operations $\prec$ and $\succ$ satisfying $x \prec (y \cdot z) = (x \prec y) \prec z$, $x \succ (y \prec z) = (x \succ y) \prec z$ and $x \succ (y \succ z) = (x \cdot y) \succ z$. It was observed in [Pil18] that the product of $\boldsymbol{k}\mathfrak{AT}^k$ admits a decomposition into 2^k operations satisfying similar relations. This motivated the introduction of the signaletic operads and their Koszul dual citelangis operads. We refer to [HP19] without further details.

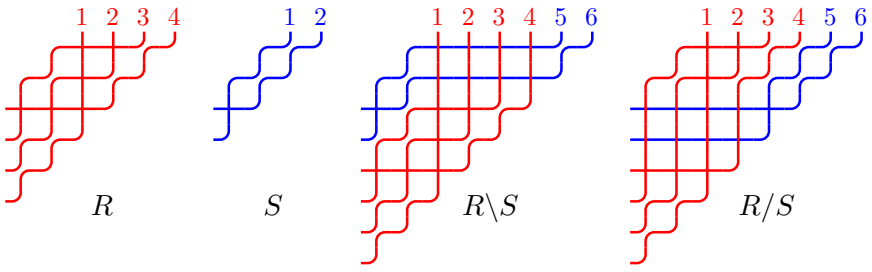

Figure 2.8: Two twists R, S (left) and the two twists $R\backslash S$ and R/S (right).

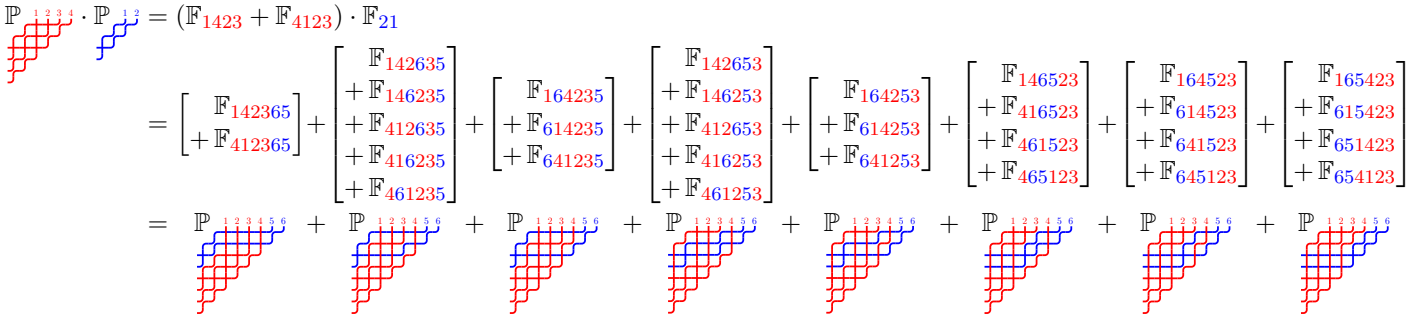

Figure 2.9: An example of product in the 2-twist Hopf algebra $\boldsymbol{k}\mathfrak{AT}^2$.

Coproduct. Our description of the coproduct in $\boldsymbol{k}\mathfrak{AT}^k$ is unfortunately not as simple as the coproduct in the planar binary tree algebra. We need the following definition. A *cut* in a k-twist T is a set γ of edges of the contact graph $T^\#$ such that any path in $T^\#$ from a leaf to the root contains precisely one edge of γ. We then denote by $A^\#(T,\gamma)$ (resp. $B^\#(T,\gamma)$) the restriction of the contact graph $T^\#$ to the nodes above (resp. below) γ. Moreover, $A^\#(T,\gamma)$ is the contact graph of the k-twist $A(T,\gamma)$ obtained from T by deleting all pipes below γ in $T^\#$. Nevertheless, note that $B^\#(T,\gamma)$ is not *a priori* the contact graph of a k-twist. The following statement is illustrated in Figure 2.10.

Proposition 2.34. *For any acyclic k-twist $T \in \mathfrak{AT}^k_p$, we have $\triangle\mathbb{P}_T = \sum_\gamma \left(\sum_\tau \mathbb{P}_{\mathbf{twi}^k(\tau)}\right) \otimes \mathbb{P}_{A(T,\gamma)}$, where γ runs over all cuts of T and τ runs over a set of representatives of the k-twist congruence classes of the linear extensions of $B^\#(T,\gamma)$.*

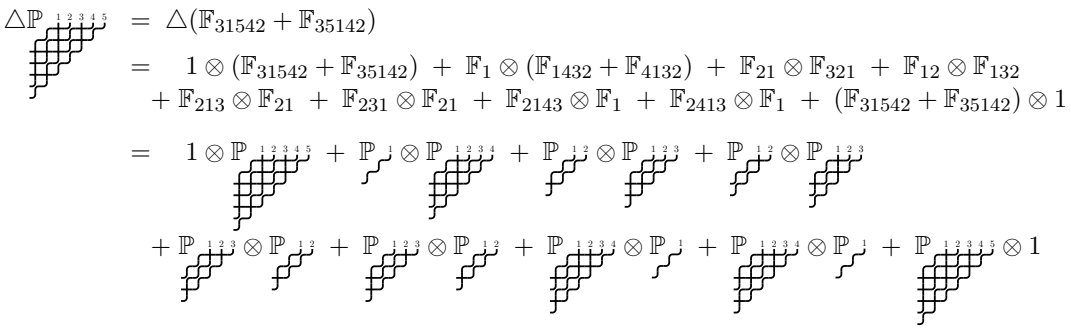

Figure 2.10: An example of coproduct in the 2-twist Hopf algebra $\boldsymbol{k}\mathfrak{AT}^2$.

k-recoil algebra. Consider the Hopf algebra $\boldsymbol{k}\mathfrak{AO}^k$ defined in [NRT11] as the Hopf subalgebra of $\boldsymbol{k}\mathfrak{S}$ generated by the elements $\mathbb{X}_O := \sum_{\mathbf{rec}^k(\tau)=O} \mathbb{F}_\tau$, for all acyclic orientations O of the graph G^k_n for all $n \in \mathbb{N}$. The commutative diagram of Proposition 2.24 gives $\mathbb{X}_O = \sum_{\mathbf{can}^k(T)=O} \mathbb{P}_T$, which shows that $\boldsymbol{k}\mathfrak{AO}^k$ is also a Hopf subalgebra of $\boldsymbol{k}\mathfrak{AT}^k$.

2.3.2 Quotient Hopf algebra

The following statement is automatic from Theorem 2.30.

Theorem 2.35. *The dual $\boldsymbol{k}\mathfrak{AT}^{k*}$ of the k-twist Hopf algebra is the quotient of $\boldsymbol{k}\mathfrak{S}^*$ under the k-twist congruence $\equiv^k$. The dual basis $\mathbb{Q}_T$ of $\mathbb{P}_T$ is expressed as $\mathbb{Q}_T = \pi(\mathbb{G}_\tau)$, where π is the quotient map and τ is any permutation such that $\mathbf{twi}^k(\tau) = T$.*

As in the previous section, we try to describe combinatorially the product and coproduct of $\mathbb{Q}$-basis elements of $\boldsymbol{k}\mathfrak{AT}^{k*}$ in terms of operations on acyclic k-twists.

Product. Once more, our description of the product in the dual twist Hopf algebra is not as simple as the product in the dual planar binary tree algebra, and is very close to the description of the direct computation using the product of $\boldsymbol{k}\mathfrak{S}^*$. For $X = \{x_1 < \ldots < x_m\} \in \binom{[m+n]}{m}$, $\rho \in \mathfrak{S}_m$, and $S \in \mathfrak{AT}_n^k$, we denote by $S \Rightarrow (\rho \cdot X)$ the result of iteratively inserting $x_{\rho_n}, \ldots, x_{\rho_1}$ in the k-twist S relabeled increasingly by $[m+n] \smallsetminus X$. The following statement is illustrated in Figure 2.11.

Proposition 2.36. *For any acyclic k-twists $R \in \mathfrak{AT}_m^k$ and $S \in \mathfrak{AT}_n^k$, we have $\mathbb{Q}_R \cdot \mathbb{Q}_S = \sum_X \mathbb{Q}_{S \Rightarrow (\rho \cdot X)}$ where X runs over $\binom{[m+n]}{m}$ and ρ is an arbitrary permutation such that $\mathbf{twi}^k(\rho) = R$.*

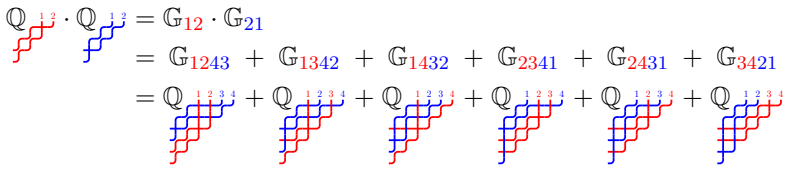

Figure 2.11: An example of product in the dual 2-twist Hopf algebra $\boldsymbol{k}\mathfrak{AT}^{2*}$.

Coproduct. Our description of the coproduct is more satisfactory. It is a special case of a coproduct on arbitrary pipe dreams studied in [BCP18]. We need the following notations, illustrated in Figure 2.12. For an acyclic (k,p)-twist T and a position $q \in \{0, \ldots, p\}$, we define two acyclic k-twists $L(T,q) \in \mathfrak{AT}_q^k$ and $R(T,q) \in \mathfrak{AT}_{p-q}^k$ as follows. The twist $L(T,q)$ is obtained by erasing the last $p-q$ pipes in T and glide the elbows of the remaining pipes as northwest as possible. More precisely, each elbow e of one of the first q pipes is translated one step north (resp. west) for each of the last $p-q$ pipes passing north (resp. west) of e. The definition is similar for $R(T,q)$, except that we erase the first q pipes instead of the last $p-q$ pipes. The next statement is illustrated in Figure 2.13.

Proposition 2.37. *For any acyclic k-twist $T \in \mathfrak{AT}_p^k$, we have $\triangle \mathbb{Q}_T = \sum_{0 \le q \le p} \mathbb{Q}_{L(T,q)} \otimes \mathbb{Q}_{R(T,q)}$.*

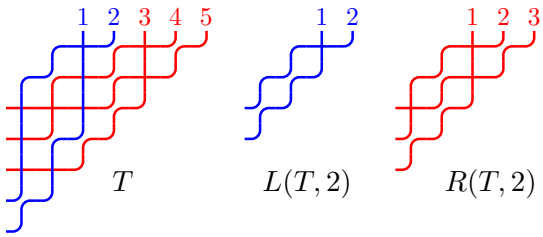

Figure 2.12: A 2-twist T (left) and the two 2-twists $L(T,2)$ (middle) and $R(T,2)$ (right).

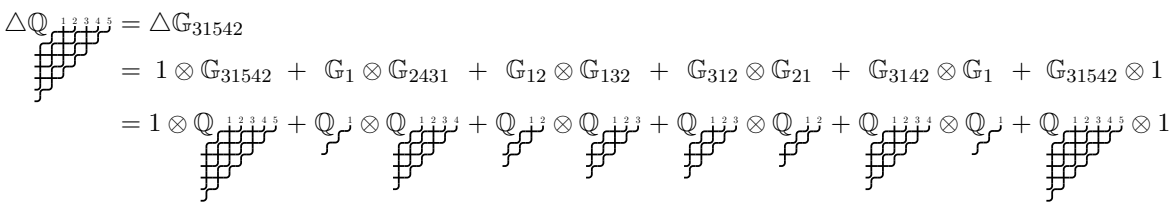

Figure 2.13: An example of coproduct in the dual 2-twist Hopf algebra $\boldsymbol{k}\mathfrak{AT}^{2*}$.

Chapter Three

PERMUTREEHEDRA

This chapter presents permutrees, a combinatorial object that generalizes and interpolates permutations, binary trees, and binary sequences. Extending the combinatorial, geometric and algebraic properties seen in Chapter 1, we show that the permutrees are endowed with a lattice structure (Section 3.1), correspond to the vertices of a polytope called permutreehedron (Section 3.2), and index the basis of a relevant Hopf subalgebra of a decorated version of C. Malvenuto and C. Reutenauer's Hopf algebra $\boldsymbol{k}\mathfrak{S}$ on permutations (Section 3.3). This chapter is adapted from a joint work with V. Pons [PP18].

3.1 PERMUTREE LATTICES

3.1.1 Permutrees

Definition 3.1. *A* permutree *is a directed tree T with vertex set $[n]$ such that for each vertex $j \in [n]$,*

(i) j has one or two parents (outgoing neighbors), and one or two children (incoming neighbors);

(ii) if j has two parents (resp. children), then all vertices in its left ancestor (resp. descendant) subtree are smaller than j while all labels in its right ancestor (resp. descendant) subtree are larger than j.

Figure 3.1 provides four examples of permutrees. We use the following conventions:

- All edges are oriented bottom-up and the vertices appear from left to right in natural order.
- We decorate the vertices with ⏀, ☮, ⍦, ⊗ depending on their number of parents and children. The sequence of these symbols, from left to right, is the *decoration* $\delta(T)$ of the permutree T.
- We often draw a vertical red wall below (resp. above) the vertices labeled by ☮ or ⊗ (resp. by ⍦ or ⊗) to mark the separation between the left and right descendant (resp. ancestor) subtrees.

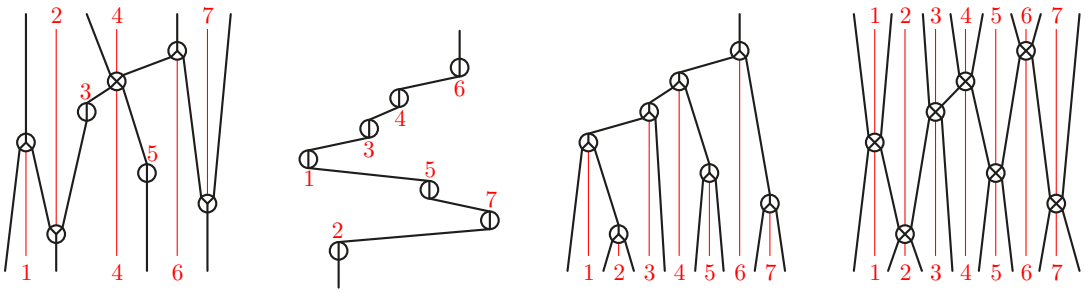

Figure 3.1: Four examples of permutrees. While the first is generic, the last three use specific decorations corresponding to permutations, binary trees, and binary sequences.

Example 3.2. As illustrated in Figure 3.1, δ-permutrees extend and interpolate between various combinatorial families, including permutations when $\delta = \oplus^n$, binary trees when $\delta = \curlywedge^n$, and binary sequences when $\delta = \otimes^n$. In fact, permutrees arose by pushing further the combinatorics of Cambrian trees developed in [CP17] to provide combinatorial models to the type A Cambrian lattices [Rea06].

3.1.2 Permutree correspondence

We now define a bijective correspondence between decorated permutations and leveled permutrees. We start with a *decorated permutation* σ, given by

- a permutation table[1], with rows labeled by positions from bottom to top and columns labeled by values from left to right, and with a dot at row i and column σ_i for all $i \in [n]$,
- a decoration of $\{\oplus, \curlywedge, \curlyvee, \otimes\}$ for each dot in the table[2],
- a vertical red wall below (resp. above) the vertices labeled by $\curlywedge$ or $\otimes$ (resp. by $\curlyvee$ or $\otimes$).

We then sweep the table from bottom to top (thus reading the permutation σ from left to right) as follows. We start with an incoming strand in between any two consecutive down values. At each step, we sweep the next vertex and proceed to the following operations depending on its decoration:

(i) a vertex decorated by $\oplus$ or $\curlyvee$ catches the only incoming strands it sees, while a vertex decorated by $\curlywedge$ or $\otimes$ connects the two incoming strands just to its left and to its right,

(ii) a vertex decorated by $\oplus$ or $\curlywedge$ creates a unique outgoing strand, while a vertex decorated by $\curlyvee$ or $\otimes$ creates two outgoing strands just to its left and to its right.

We end with an outgoing strand in between any two consecutive up values. See Figure 3.2. As strands cannot cross red walls during the algorithm, the result $\mathbf{lpt}(\sigma)$ of this procedure is a *leveled permutree*, *i.e.* a permutree whose vertices are ordered by one of its linear extensions.

Proposition 3.3. *The map* $\mathbf{lpt}$ *is a bijection from δ-decorated permutations to leveled δ-permutrees.*

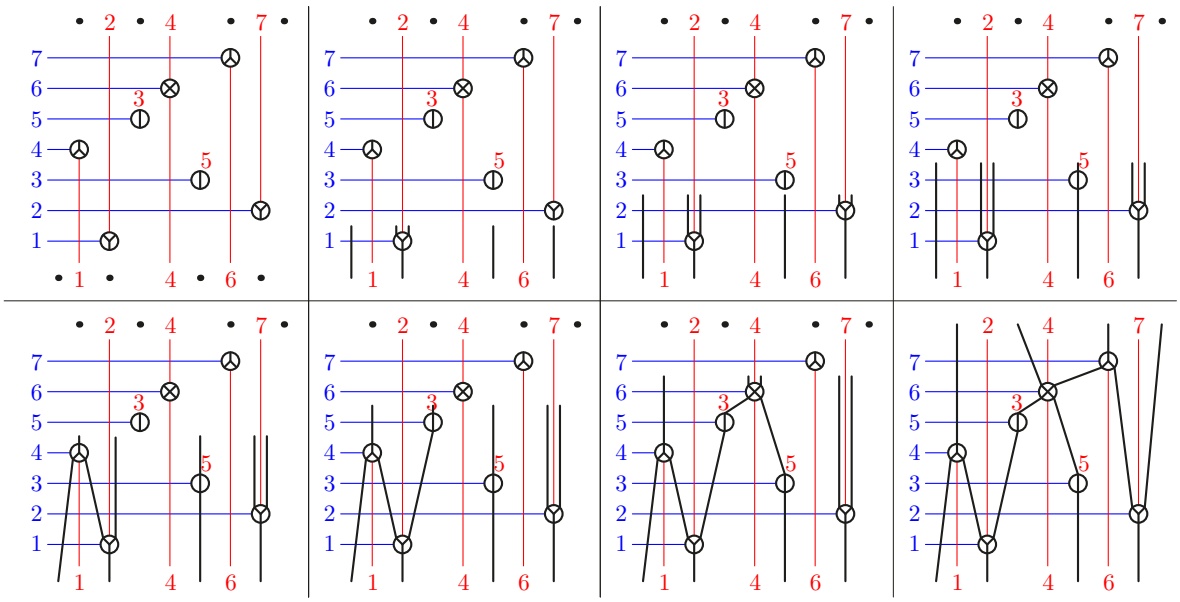

Figure 3.2: The permutree insertion algorithm on the decorated permutation $\overline{27}51\underline{3}\overline{\underline{46}}$.

[1] This unusual convention of orientation fits the existing constructions [LR98, HNT05, CP17].

[2] We could equivalently think of a permutation where the positions or the values receive a decoration, but it will be useful later to switch the decoration from positions to values.

3.1.3 Permutree congruences

In the rest of the chapter, we forget the order of the leveled permutree $\mathbf{lpt}(\sigma)$ and we denote the resulting permutree by $\mathbf{pt}(\sigma)$. We can think of the surjection $\mathbf{pt}$ as an insertion algorithm from decorated permutations to permutrees. We are interested in the fibers of this surjection.

Proposition 3.4. *The decorated permutations σ such that $\mathbf{pt}(\sigma) = T$ are precisely the linear extensions of (the transitive closure of) the permutree T.*

We then characterize the decorated permutations in the same fiber in terms of a congruence relation defined by a rewriting rule. This extends the trivial congruence when $\delta = (\wedge)^n$, the sylvester congruence [HNT05] when $\delta = (\curlywedge)^n$, the Cambrian congruences [Rea04, Rea06, CP17] when $\delta \in \{(\curlywedge), (\curlyvee)\}^n$, and the hypoplactic congruence [KT97, Nov00] when $\delta = (\otimes)^n$.

Definition 3.5. *For a decoration $\delta \in \{(\wedge), (\curlywedge), (\curlyvee), (\otimes)\}^n$, the δ-permutree congruence is the equivalence relation on δ-decorated permutations defined as the transitive closure of the rewriting rules*

$$\begin{aligned} UacVbW &\equiv_\delta UcaVbW \quad \text{if } a < b < c \text{ and } \delta_b = (\curlywedge) \text{ or } (\otimes), \\ UbVacW &\equiv_\delta UbVcaW \quad \text{if } a < b < c \text{ and } \delta_b = (\curlyvee) \text{ or } (\otimes), \end{aligned}$$

where a, b, c are elements of $[n]$ while U, V, W are words on $[n]$. Note that the decorations of a and c do not matter, only that of the witness b of the rewriting rule.

Proposition 3.6. *The classes of $\equiv_\delta$ are the fibers of $\mathbf{pt}$, i.e. $\sigma \equiv_\delta \tau \iff \mathbf{pt}(\sigma) = \mathbf{pt}(\tau)$.*

Proposition 3.7. *The δ-permutree congruence $\equiv_\delta$ is a lattice congruence of the weak order.*

3.1.4 Rotations and permutree lattices

We now define the rotation on permutrees, a local operation that only exchanges the orientation of an edge and rearranges the endpoints of two other edges. See Figure 3.3 for some examples.

Definition 3.8. *Let $i \to j$ be an edge in a δ-permutree T with $i < j$. Let D denote the only (resp. the right) descendant subtree of vertex i if $\delta_i \in \{(\wedge), (\curlyvee)\}$ (resp. if $\delta_i \in \{(\curlywedge), (\otimes)\}$) and let U denote the only (resp. the left) ancestor subtree of vertex j if $\delta_j \in \{(\wedge), (\curlywedge)\}$ (resp. if $\delta_j \in \{(\curlyvee), (\otimes)\}$). Let T' be the oriented tree obtained from T just reversing the orientation of $i \to j$ and attaching the subtree U to i and the subtree D to j as illustrated above. The transformation from T to T' is an increasing rotation.*

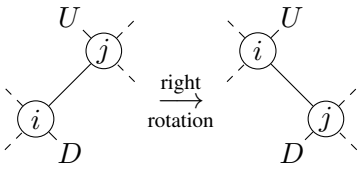

The rotation of an edge $i \to j$ exchanges the orientation of this edge while preserving all other edge cuts. An *edge cut* in a permutree T is the partition $(I \parallel J)$ of the vertices of T into the set I of vertices in the source set and the set $J = [n] \setminus I$ of vertices in the target set of an oriented edge of T.

Proposition 3.9. *The result T' of the rotation of an edge $i \to j$ in a δ-permutree T is a δ-permutree. Moreover, T' is the unique δ-permutree with the same edge cuts as T, except the cut defined by $i \to j$.*

Proposition 3.10. *The transitive closure of the increasing rotation graph on δ-permutrees is a lattice, called δ-permutree lattice. It isomorphic to the quotient of the weak order by the δ-permutree congruence $\equiv_\delta$. The map $\mathbf{pt}$ is a thus morphism from the weak order to the permutree lattice.*

Example 3.11. The δ-permutree lattice specializes to the weak order when $\delta = (\wedge)^n$, the Tamari lattice when $\delta = (\curlywedge)^n$, the Cambrian lattices [Rea06] when $\delta \in \{(\curlywedge), (\curlyvee)\}^n$ and the boolean lattice when $\delta = (\otimes)^n$.

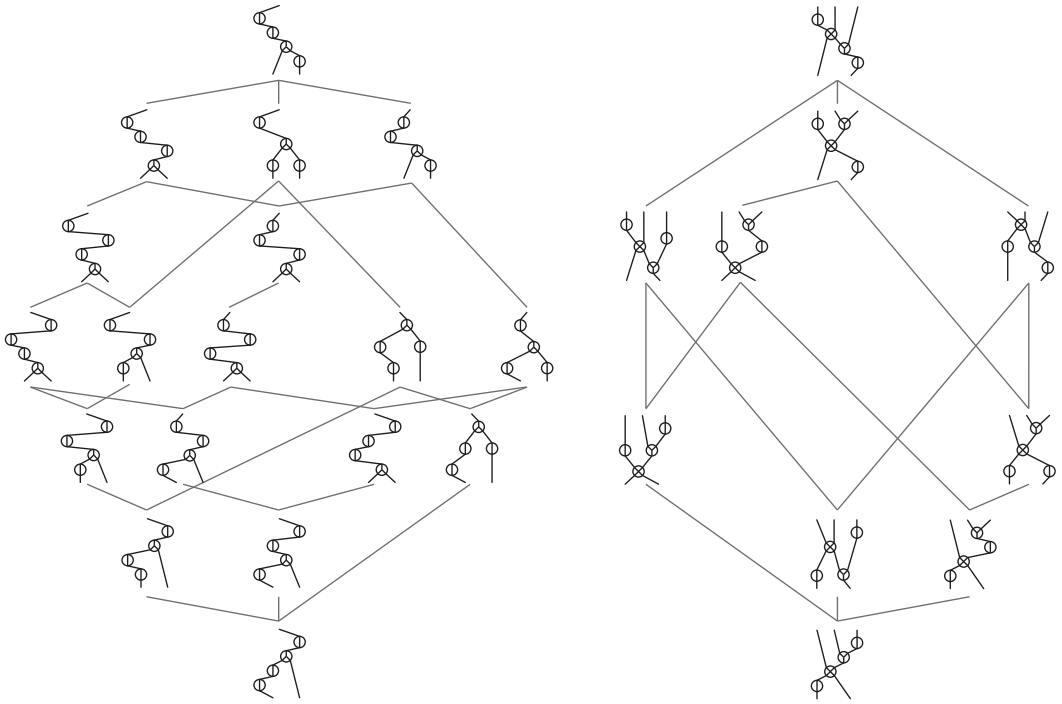

Figure 3.3: The δ-permutree lattices, for $\delta = \text{◐◐✇◐}$ (left) and $\delta = \text{◐⊗⋎◐}$ (right).

3.1.5 Decoration refinements

For two decorations $\delta, \delta' \in \{\text{◐}, \text{✇}, \text{⋎}, \otimes\}^n$, we say that δ *refines* δ' and we write $\delta \preccurlyeq \delta'$ if $\delta_i \preccurlyeq \delta'_i$ for all $i \in [n]$ for the order $\text{◐} \preccurlyeq \{\text{✇}, \text{⋎}\} \preccurlyeq \otimes$. In this case, the δ-permutree congruence refines the δ'-permutree congruence: $\sigma \equiv_\delta \tau$ implies $\sigma \equiv_{\delta'} \tau$ for any two permutations $\sigma, \tau \in \mathfrak{S}_n$. This defines a natural surjection map $\Psi_\delta^{\delta'}$ from δ-permutrees to δ'-permutrees.

Proposition 3.12. *The map $\Psi_\delta^{\delta'}$ is a morphism from the δ-permutree lattice to the δ'-permutree lattice.*

This surjection can be described visually as follows, see Figure 3.4 where $\delta = \text{✇◐◐⋎◐◐⋎}$ and $\delta' = \text{✇⋎◐⊗◐✇⋎}$. We start from a δ-permutree, with vertices labeled from left to right as usual. We then redecorate its vertices according to δ' and place the corresponding vertical red walls. The result is not a permutree at the moment as some edges of the tree cross some red walls. In order to fix it, we cut the edges crossing red walls and reconnect them with vertical segments as illustrated in Figure 3.4 (middle right). Finally, we stretch the picture to see a δ'-permutree with straight edges.

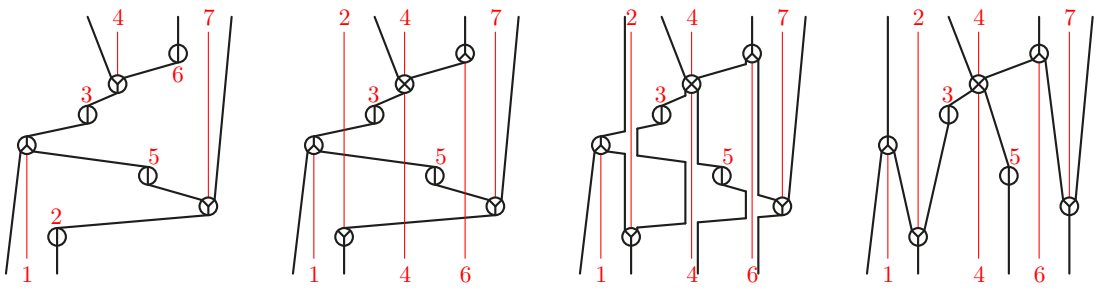

Figure 3.4: Decoration refinement by cut and stretch.

3.2 PERMUTREEHEDRA

We now construct permutree fans and permutreehedra, which provide geometric realizations of the permutree lattices. As for J.-L. Loday's or C. Hohlweg and C. Lange's associahedra [Lod04, HL07], the permutree fans are obtained by coarsening the braid arrangement $\mathcal{F}(n)$ and the permutreehedra are obtained by deleting certain inequalities in the facet description of the permutahedron $\mathbb{P}\mathrm{erm}(n)$.

3.2.1 Permutree fans

Recall that the *incidence cone* $\boldsymbol{C}(T)$ and the *braid cone* $\boldsymbol{C}^\diamond(T)$ of a permutree T are the cones:

$$\boldsymbol{C}(T) := \mathbb{R}_{\geq 0}\{\boldsymbol{e}_i - \boldsymbol{e}_j \mid \forall\, i \to j \text{ in } T\} = \left\{\boldsymbol{x} \in \mathbb{1}^\perp \;\middle|\; \sum_{j\in J} \frac{x_j}{|J|} \leq \sum_{i\in I} \frac{x_i}{|I|},\ \forall\, (I \parallel J) \text{ cut in } T\right\}$$

$$\boldsymbol{C}^\diamond(T), := \{\boldsymbol{x} \in \mathbb{1}^\perp \mid x_i \leq x_j,\ \forall\, i \to j \text{ in } T\} = \mathbb{R}_{\geq 0}\left\{\sum_{j\in J} \frac{\boldsymbol{e}_j}{|J|} - \sum_{i\in I} \frac{\boldsymbol{e}_i}{|I|} \;\middle|\; \forall\, (I \parallel J) \text{ cut in } T\right\}.$$

Note that these two cones both lie in the space $\mathbb{1}^\perp := \{\boldsymbol{x} \in \mathbb{R}^n \mid \sum_{i\in[n]} x_i = 0\}$, are simplicial, and are polar to each other. We use the braid cones to construct the δ-permutree fan.

Proposition 3.13. *The set of cones $\{\boldsymbol{C}^\diamond(T) \mid T$ δ-permutree$\}$, together with all their faces, forms a complete simplicial fan $\mathcal{F}(\delta)$ of $\mathbb{1}^\perp$ called δ-permutree fan.*

Example 3.14. The δ-permutree fan specializes to the braid fan when $\delta = \bigoplus^n$, the (type A) Cambrian fans of N. Reading and D. Speyer [RS09] when $\delta \in \{\circledcirc, \circledast\}^n$, the fan defined by the hyperplane arrangement $x_i = x_{i+1}$ for each $i \in [n-1]$ when $\delta = \bigotimes^n$, and the fan defined by the hyperplane arrangement $x_i = x_j$ for each $i < j \in [n-1]$ such that $\delta_{|(i,j)} = \bigoplus^{j-i-1}$ when $\delta \in \{\bigoplus, \bigotimes\}^n$.

Moreover, the decoration refinements of Section 3.1.5 translate to permutree fan refinements.

Proposition 3.15. *If $\delta \preccurlyeq \delta'$, the δ-permutree fan $\mathcal{F}(\delta)$ refines the δ'-permutree fan $\mathcal{F}(\delta')$. More precisely, $\boldsymbol{C}(T) \supseteq \boldsymbol{C}(T')$ and $\boldsymbol{C}^\diamond(T) \subseteq \boldsymbol{C}^\diamond(T')$ for any δ-permutree T with image $T' = \Psi_\delta^{\delta'}(T)$.*

3.2.2 Permutreehedra

We are now ready to construct the *δ-permutreehedron* $\mathbb{PT}(\delta)$ whose normal fan is the δ-permutree fan $\mathcal{F}(\delta)$. We provide both its vertex and facet descriptions:

(i) The vertices of $\mathbb{PT}(\delta)$ correspond to δ-permutrees. Namely, we associate to a δ-permutree T a point $\boldsymbol{p}(T) \in \mathbb{R}^n$ whose ith coordinate is defined by $\boldsymbol{p}(T)_i = 1 + d + \underline{\ell}\underline{r} - \overline{\ell}\overline{r}$, where d denotes the number of descendants of i in T, $\underline{\ell}$ and $\underline{r}$ denote the sizes of the left and right descendant subtrees of i in T when $\delta_i \in \{\circledast, \bigotimes\}$ (otherwise, $\underline{\ell} = \underline{r} = 0$), and $\overline{\ell}$ and $\overline{r}$ denote the sizes of the left and right ancestor subtrees of i in T when $\delta_i \in \{\circledcirc, \bigotimes\}$ (otherwise, $\overline{\ell} = \overline{r} = 0$). Note that $\boldsymbol{p}(T)$ is independent of the decorations of the first and last vertices of T.

(ii) The facets of $\mathbb{PT}(\delta)$ correspond to the *δ-building blocks*, that is, to all subsets $B \subseteq [n]$ such that there exists a δ-permutree T which admits $(B \parallel [n] \smallsetminus B)$ as an edge cut. We associate to a δ-building block B the halfspace $\boldsymbol{H}^{\geq}(B) := \{\boldsymbol{x} \in \mathbb{R}^n \mid \sum_{i\in B} x_i \geq \binom{|B|+1}{2}\}$.

As an illustration, the vertex corresponding to the permutree of Figure 3.1 (left) is $[7, -4, 3, 8, 1, 12, 1]$ and the facet corresponding to the edge $3 \to 4$ in the permutree of Figure 3.1 (left) is $x_1 + x_2 + x_3 \geq 6$.

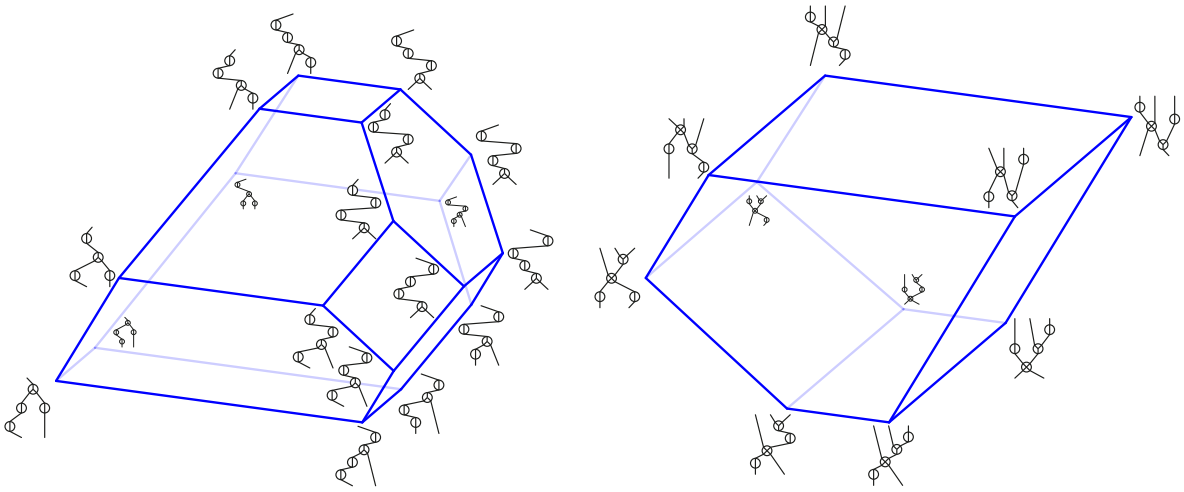

Figure 3.5: The permutreehedra $\mathbb{PT}(\bigoplus\bigoplus\curlywedge\bigoplus)$ (left) and $\mathbb{PT}(\bigoplus\otimes\curlyvee\bigoplus)$ (right).

Theorem 3.16. *The permutree fan $\mathcal{F}(\delta)$ is the normal fan of the* permutreehedron *$\mathbb{PT}(\delta)$ defined as*
(i) either the convex hull of the points $\boldsymbol{p}(T)$ for all δ-permutrees T,
(ii) or the intersection of the hyperplane $\mathbb{H}$ with the halfspaces $\boldsymbol{H}^{\geq}(B)$ for all δ-building blocks B.

Example 3.17. The δ-permutreehedron $\mathbb{PT}(\delta)$ specializes to the permutahedron $\mathbb{P}\mathrm{erm}(n)$ when $\delta = \bigoplus^n$, J.-L. Loday's associahedron $\mathbb{A}\mathrm{sso}(n)$ [SS93, Lod04] when $\delta = \curlywedge^n$, C. Hohlweg and C. Lange's associahedra $\mathbb{A}\mathrm{sso}(\delta)$ [HL07, LP18] when $\delta \in \{\curlywedge, \curlyvee\}^n$, the parallelepiped $\mathbb{P}\mathrm{ara}(n)$ with directions $\boldsymbol{e}_i - \boldsymbol{e}_{i+1}$ for each $i \in [n-1]$ when $\delta = \otimes^n$, the graphical zonotope $\mathbb{Z}\mathrm{ono}(\delta)$ generated by the vectors $\boldsymbol{e}_i - \boldsymbol{e}_j$ for each $i < j \in [n-1]$ such that $\delta_{|(i,j)} = \bigoplus^{j-i-1}$ when $\delta \in \{\bigoplus, \otimes\}^n$.

The δ-permutree lattice studied in Section 3.1.4 naturally appears in the geometry of the δ-permutreehedron $\mathbb{PT}(\delta)$. Recall that $\boldsymbol{\omega} := (n, n-1, \dots, 2, 1) - (1, 2, \dots, n-1, n) = \sum_{i\in[n]}(n+1-2i)\,\boldsymbol{e}_i$.

Proposition 3.18. *When oriented in the direction $\boldsymbol{\omega}$, the 1-skeleton of the δ-permutreehedron $\mathbb{PT}(\delta)$ is the Hasse diagram of the δ-permutree lattice.*

Finally, decoration refinements of Section 3.1.5 translates to permutreehedra containement, as illustrated in Figure 3.6.

Proposition 3.19. *For any two decorations $\delta \preccurlyeq \delta'$, the permutreehedron $\mathbb{PT}(\delta')$ is obtained by deleting inequalities in the facet description of the permutreehedron $\mathbb{PT}(\delta')$. Thus, $\mathbb{PT}(\delta) \subseteq \mathbb{PT}(\delta')$.*

Further geometric topics are studied in [PP18, Sect. 3.3], in particular pairs of parallel facets and isometries of permutreehedra, and common vertices of permutreehedra for distinct decorations.

3.3 The permutree Hopf algebra

We have used that the binary tree insertion to construct J.-L. Loday and M. Ronco's Hopf algebra $\boldsymbol{k}\mathfrak{T}$ on binary trees as a subalgebra of C. Malvenuto and C. Reutenauer's Hopf algebra $\boldsymbol{k}\mathfrak{S}$ on permutations. We now use the permutree insertion to construct a Hopf algebra on permutrees as a subalgebra of a Hopf algebra on decorated permutations. We then provide combinatorial interpretations of the products and coproducts both in the permutree Hopf algebra and its dual in terms of cutting operations in permutrees. Further algebraic directions, in particular multiplicative bases, are explored in [PP18].

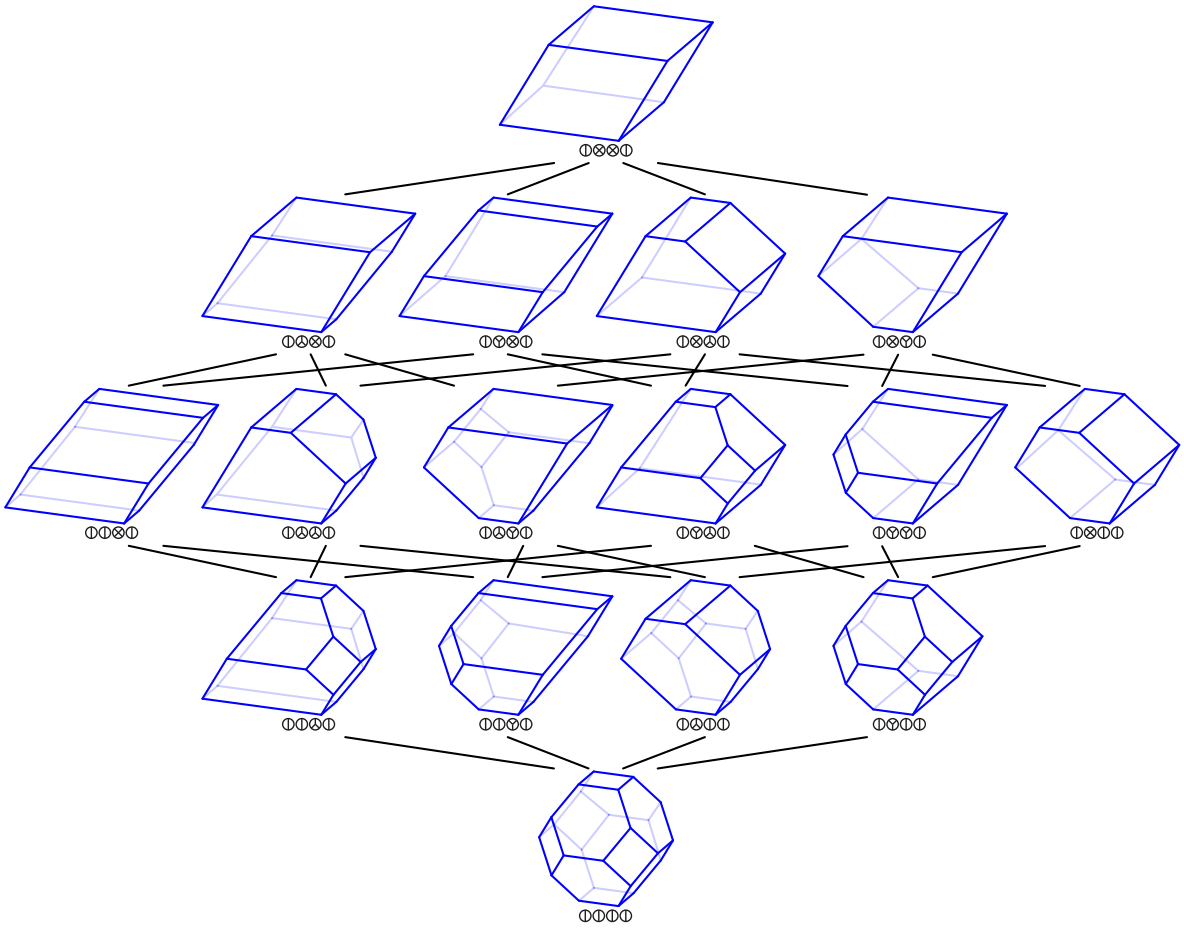

Figure 3.6: The δ-permutreehedra, for all decorations $\delta \in ⓓ \cdot \{ⓓ, ⓐ, ⓨ, ⊗\}^2 \cdot ⓓ$.

3.3.1 The Hopf algebra on decorated permutations

The *decorated shifted shuffle* $\sigma \,\bar{⧢}\, \tau$ is defined as the shifted shuffle of the permutations where decorations travel with their values, while the *decorated convolution* $\sigma \star \tau$ is defined as the convolution of the permutations where decorations stay at their positions.

E.g., $\overline{1}\underline{2} \,\bar{⧢}\, \underline{2}\overline{3}\overline{1} = \{\overline{1}\underline{2}\underline{4}\overline{5}\overline{3}, \overline{1}\underline{4}\overline{2}\overline{5}\overline{3}, \overline{1}\underline{4}\underline{5}\overline{2}\overline{3}, \overline{1}\underline{4}\underline{5}\overline{3}\overline{2}, \underline{4}\overline{1}\underline{2}\overline{5}\overline{3}, \underline{4}\overline{1}\underline{5}\overline{2}\overline{3}, \underline{4}\overline{1}\underline{5}\overline{3}\overline{2}, \underline{4}\underline{5}\overline{1}\underline{2}\overline{3}, \underline{4}\underline{5}\overline{1}\underline{3}\overline{2}, \underline{4}\underline{5}\overline{3}\overline{1}\overline{2}\}$,
$\overline{1}\underline{2} \star \underline{2}\overline{3}\overline{1} = \{\overline{1}\underline{2}\underline{4}\overline{5}\overline{3}, \overline{1}\underline{3}\underline{4}\overline{5}\overline{2}, \overline{1}\underline{4}\underline{3}\overline{5}\overline{2}, \overline{1}\underline{5}\underline{3}\underline{4}\overline{2}, \overline{2}\underline{3}\underline{4}\overline{5}\overline{1}, \overline{2}\underline{4}\underline{3}\overline{5}\overline{1}, \overline{2}\underline{5}\underline{3}\underline{4}\overline{1}, \overline{3}\underline{4}\underline{2}\overline{5}\overline{1}, \overline{3}\underline{5}\underline{2}\underline{4}\overline{1}, \overline{4}\underline{5}\underline{2}\overline{3}\overline{1}\}$.

As shown by J.-C. Novelli and J.-Y. Thibon in [NT10a], these operations define a decorated version of C. Malvenuto and C. Reutenauer's Hopf algebra $\boldsymbol{k}\mathfrak{S}$ on permutations [MR95].

Definition 3.20. *We denote by* $\boldsymbol{k}\mathfrak{S}^{\{ⓓ,ⓐ,ⓨ,⊗\}}$ *the Hopf algebra with basis* $\mathbb{F}_\tau$ *indexed by decorated permutations with product* $\mathbb{F}_\rho \cdot \mathbb{F}_\sigma = \sum_{\tau \in \rho \,\bar{⧢}\, \sigma} \mathbb{F}_\tau$ *and coproduct* $\triangle \mathbb{F}_\tau = \sum_{\tau \in \rho \star \sigma} \mathbb{F}_\rho \otimes \mathbb{F}_\sigma$.

We will also consider the dual Hopf algebra of $\boldsymbol{k}\mathfrak{S}^{\{ⓓ,ⓐ,ⓨ,⊗\}}$.

Definition 3.21. *We denote by* $(\boldsymbol{k}\mathfrak{S}^{\{ⓓ,ⓐ,ⓨ,⊗\}})^*$ *the Hopf algebra with basis* $\mathbb{G}_\tau$ *indexed by decorated permutations with product* $\mathbb{G}_\rho \cdot \mathbb{G}_\sigma = \sum_{\tau \in \rho \star \sigma} \mathbb{G}_\tau$ *and coproduct* $\triangle \mathbb{G}_\tau = \sum_{\tau \in \rho \,\bar{⧢}\, \sigma} \mathbb{G}_\rho \otimes \mathbb{G}_\sigma$.

3.3.2 Hopf subalgebra

We denote by $\boldsymbol{k}\mathfrak{Pmt}$ the vector subspace of $\boldsymbol{k}\mathfrak{S}^{\{\textcircled{1},\textcircled{2},\textcircled{3},\otimes\}}$ generated by $\mathbb{P}_T := \sum_{\substack{\tau\in\mathfrak{S}^{\{\textcircled{1},\textcircled{2},\textcircled{3},\otimes\}}\\ \mathbf{pt}(\tau)=T}} \mathbb{F}_\tau = \sum_{\tau\in\mathcal{L}(T)} \mathbb{F}_\tau$ for all permutrees T. For example:

$\mathbb{P}$ 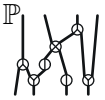 $= \mathbb{F}_{\overline{2}1\underline{3}\overline{5}\underline{4}\overline{7}\underline{6}} + \mathbb{F}_{\overline{2}1\underline{3}\overline{5}\overline{7}\underline{4}\underline{6}} + \mathbb{F}_{\overline{2}1\underline{3}\overline{7}\underline{5}\underline{4}\underline{6}} + \cdots + \mathbb{F}_{\overline{7}\overline{5}\overline{2}\underline{3}1\underline{4}\underline{6}} + \mathbb{F}_{\overline{7}\overline{5}\overline{2}\underline{3}\underline{4}\overline{1}\underline{6}} + \mathbb{F}_{\overline{7}\overline{5}\overline{2}\underline{3}\underline{4}\underline{6}\underline{1}}$ (90 terms).

The following statement is similar to [CP17, Thm. 24], which was inspired from similar arguments for Hopf algebras arising from lattice quotients of the weak order [Rea05].

Theorem 3.22. *The vector subspace $\boldsymbol{k}\mathfrak{Pmt}$ is a Hopf subalgebra of the decorated permutation Hopf algebra $\boldsymbol{k}\mathfrak{S}^{\{\textcircled{1},\textcircled{2},\textcircled{3},\otimes\}}$, called* permutree Hopf algebra.

Once we have observed this property, we want to describe the product and coproduct in the permutree Hopf algebra $\boldsymbol{k}\mathfrak{Pmt}$ directly in terms of permutrees. We briefly do it in the next two statements. This generalizes know rules for the binary tree Hopf algebra $\boldsymbol{k}\mathfrak{T}$ described in [LR98, AS06, HNT05].

Product. For any permutrees R, S, denote by $R\backslash S$ (resp. by R/S) the permutree obtained by grafting the rightmost outgoing (resp. incoming) edge of R to the leftmost incoming (resp. outgoing) edge of S while shifting all labels of S. An example is given in Figure 3.7 (left).

Proposition 3.23. *For any permutrees R, S, we have $\mathbb{P}_R \cdot \mathbb{P}_S = \sum_T \mathbb{P}_T$, where T runs over the interval between $R\backslash S$ and R/S in the $\delta(R)\delta(S)$-permutree lattice.*

Remark 3.24. Note that there are natural dendriform structures and integer point transform interpretations of the product in the permutree Hopf algebra restricted to decorations in $\{\textcircled{1},\textcircled{3}\}^*$, see [PP18, Sects. 4.4.2 & 4.4.3]. However, these properties are lost for arbitrary decorations in $\{\textcircled{1},\textcircled{2},\textcircled{3},\otimes\}^*$.

Coproduct. Define a *cut* of a permutree T to be a set γ of edges such that any geodesic vertical path in T from a down leaf to an up leaf contains precisely one edge of γ. Such a cut separates the permutree T into two forests, one above γ and one below γ, denoted $A(T,\gamma)$ and $B(T,\gamma)$, respectively. An example is given in Figure 3.7 (right).

Proposition 3.25. *For any permutree T, we have $\triangle\mathbb{P}_T = \sum_\gamma \Big(\prod_{R\in B(T,\gamma)} \mathbb{P}_R\Big) \otimes \Big(\prod_{S\in A(T,\gamma)} \mathbb{P}_S\Big)$, where γ runs over all cuts of T and both products are computed from left to right.*

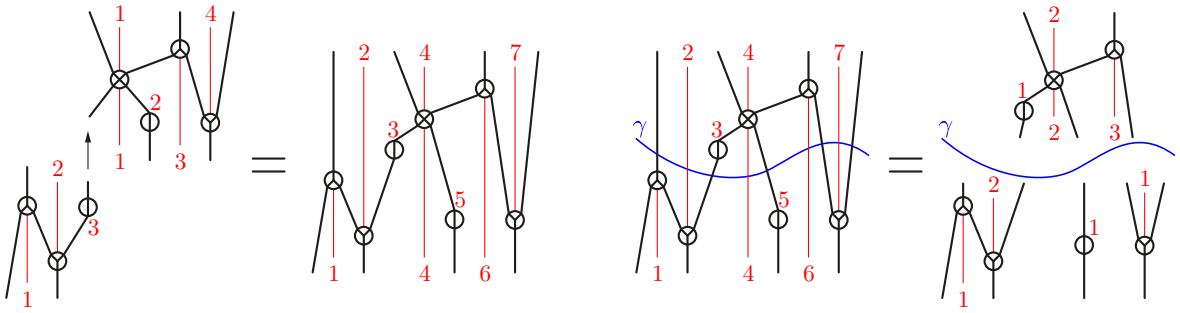

Figure 3.7: Grafting two permutrees (left) and cutting a permutree (right).

Remark 3.26. Let us underline relevant Hopf subalgebras of the permutree Hopf algebra $\boldsymbol{k}\mathfrak{Pmt}$. Namely, for any set $\boldsymbol{\delta}$ of decorations in $\{\textcircled{\scriptsize 1}, \textcircled{\scriptsize 2}, \textcircled{\scriptsize 3}, \textcircled{\scriptsize 4}\}^*$ stable by shuffle, the linear subspace of $\boldsymbol{k}\mathfrak{Pmt}$ generated by the elements $\mathbb{P}_\delta$ for $\delta \in \boldsymbol{\delta}$ forms a Hopf subalgebra $\boldsymbol{k}\mathfrak{Pmt}_{\boldsymbol{\delta}}$ of $\boldsymbol{k}\mathfrak{Pmt}$. In particular, $\boldsymbol{k}\mathfrak{Pmt}$ contains all algebras $\boldsymbol{k}\mathfrak{Pmt}_{D^*}$ for any subset D of the decorations $\{\textcircled{\scriptsize 1}, \textcircled{\scriptsize 2}, \textcircled{\scriptsize 3}, \textcircled{\scriptsize 4}\}$. Note that:

(i) $\boldsymbol{k}\mathfrak{Pmt}_{\{\textcircled{\scriptsize 1}\}^*}$ is C. Malvenuto and C. Reutenauer's Hopf algebra $\boldsymbol{k}\mathfrak{S}$ on permutations [MR95],

(ii) $\boldsymbol{k}\mathfrak{Pmt}_{\{\textcircled{\scriptsize 4}\}^*}$ is J.-L. Loday and M. Ronco's Hopf algebra $\boldsymbol{k}\mathfrak{T}$ of on binary trees [LR98],

(iii) $\boldsymbol{k}\mathfrak{Pmt}_{\{\textcircled{\scriptsize 2},\textcircled{\scriptsize 3}\}^*}$ is the Hopf algebra on Cambrian trees [CP17],

(iv) $\boldsymbol{k}\mathfrak{Pmt}_{\{\textcircled{\scriptsize 4}\}^*}$ is the recoil Hopf algebra algebra $\boldsymbol{k}\mathfrak{B}$ on binary sequences [GKL$^+$95].

Interestingly, the rules for the product and the coproduct in the permutree Hopf algebra $\boldsymbol{k}\mathfrak{Pmt}$ provide uniform product and coproduct rules for all these Hopf algebras.

3.3.3 Quotient Hopf algebra

We now consider the dual Hopf algebra of the permutree Hopf algebra $\boldsymbol{k}\mathfrak{Pmt}$. The following statement is automatic by duality from Theorem 3.22.

Theorem 3.27. *The dual $\boldsymbol{k}\mathfrak{Pmt}^*$ of the permutree Hopf algebra $\boldsymbol{k}\mathfrak{Pmt}$ is the quotient of $(\boldsymbol{k}\mathfrak{S}^{\{\textcircled{\scriptsize 1},\textcircled{\scriptsize 2},\textcircled{\scriptsize 3},\textcircled{\scriptsize 4}\}})^*$ under the permutree congruence $\equiv$. The dual basis $\mathbb{Q}_T$ of $\mathbb{P}_T$ is expressed as $\mathbb{Q}_T = \pi(\mathbb{G}_\tau)$, where π is the quotient map and τ is any linear extension of T.*

Similarly as in the previous section, we can describe combinatorially the product and coproduct of $\mathbb{Q}$-basis elements of $\boldsymbol{k}\mathfrak{Pmt}^*$ in terms of operations on permutrees. This generalizes know rules for the binary tree Hopf algebra $\boldsymbol{k}\mathfrak{T}$ described in [LR98, AS06, HNT05].

Product. Call *gaps* the $n+1$ positions between two consecutive integers of $[n]$, including the position before 1 and the position after n. A gap γ defines a *geodesic vertical path* $\lambda(T, \gamma)$ in a permutree T from the bottom leaf which lies in the same interval of consecutive down labels as γ to the top leaf which lies in the same interval of consecutive up labels as γ. See Figure 3.9. A multiset Γ of gaps therefore defines a *lamination* $\lambda(T, \Gamma)$ of T, *i.e.* a multiset of pairwise non-crossing geodesic vertical paths in T from down leaves to up leaves. When cut along the paths of a lamination, the permutree T splits into a forest.

Consider two Cambrian trees R and S of sizes $[m]$ and $[n]$ respectively. For any shuffle s of their decorations $\delta(R)$ and $\delta(S)$, consider the multiset Γ of gaps of $[m]$ given by the positions of the down labels of $\delta(S)$ in s and the multiset Ω of gaps of $[n]$ given by the positions of the up labels of $\delta(R)$ in s. We denote by $R\,{}_s\backslash S$ the Cambrian tree obtained by connecting the up leaves of the forest defined by the lamination $\lambda(R, \Gamma)$ to the down leaves of the forest defined by the lamination $\lambda(S, \Omega)$.

Example 3.28. Consider the permutrees $T^{\textcircled{\scriptsize 1}}$ and $T^{\square}$ of Figure 3.8. To distinguish decorations in $T^{\textcircled{\scriptsize 1}}$ and $T^{\square}$, we circle the symbols in $\delta(T^{\textcircled{\scriptsize 1}}) = \textcircled{\scriptsize 4}\textcircled{\scriptsize 2}\textcircled{\scriptsize 3}$ and square the symbols in $\delta(T^{\square}) = \square\boxtimes\square\square\square$. Consider now an arbitrary shuffle $s = \square\boxtimes\textcircled{\scriptsize 4}\textcircled{\scriptsize 2}\square\square\textcircled{\scriptsize 3}\square$ of these two decorations. The resulting laminations of $T^{\textcircled{\scriptsize 1}}$ and $T^{\square}$, as well as the permutree $T^{\textcircled{\scriptsize 1}}{}_s\backslash T^{\square}$ are represented in Figure 3.8.

Proposition 3.29. *For any permutrees R, S, we have $\mathbb{Q}_R \cdot \mathbb{Q}_S = \sum_s \mathbb{Q}_{R\,{}_s\backslash S}$, where s runs over all shuffles of the decorations of R and S.*

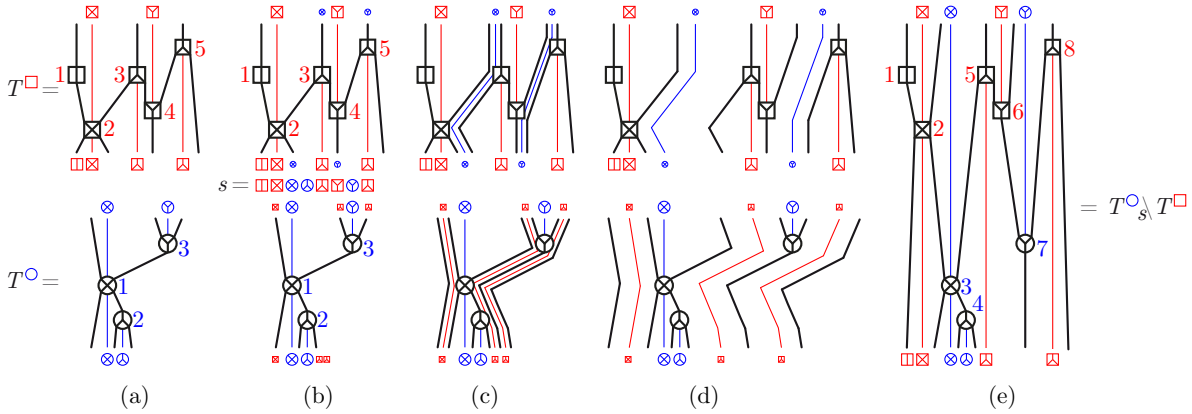

Figure 3.8: (a) The two initial permutrees $T^{\bigcirc}$ and $T^{\square}$. (b) Given the shuffle $s = \square\boxtimes\otimes\textcircled{Y}\boxplus\boxtimes\textcircled{Y}\boxplus$, the positions of the $\boxplus$ and $\boxtimes$ are reported in $T^{\bigcirc}$ and the positions of the $\textcircled{Y}$ and $\otimes$ are reported in $T^{\square}$. (c) The corresponding laminations. (d) The permutrees are split according to the laminations. (e) The resulting permutree $T^{\bigcirc}{}_s\backslash T^{\square}$.

Coproduct For a gap γ, we denote by $L(T,\gamma)$ and $R(T,\gamma)$ the left and right subpermutrees of T when split along the path $\lambda(T,\gamma)$. An example is given in Figure 3.9.

Proposition 3.30. *For any permutree T, we have $\triangle\mathbb{Q}_T = \sum_\gamma \mathbb{Q}_{L(T,\gamma)} \otimes \mathbb{Q}_{R(T,\gamma)}$, where γ runs over all gaps between vertices of T.*

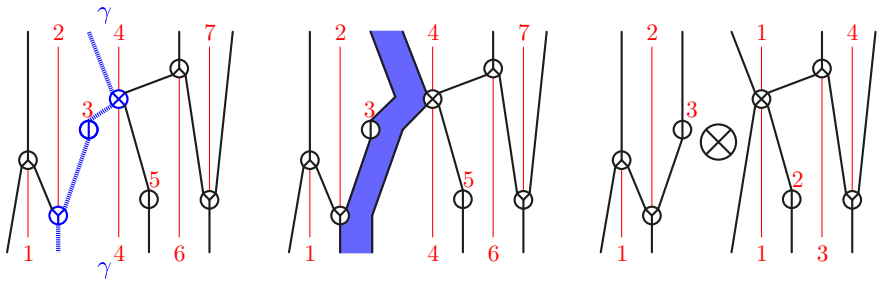

Figure 3.9: A gap γ (left) defines a vertical cut (middle) which splits the permutree vertically (right).

Remark 3.31. We conclude this chapter with an innocent operation, that we call *tuplization*, which yields many relevant polytopes and Hopf algebras. The motivation comes from S. Law and N. Reading's work on diagonal quadrangulations [LR12] and S. Giraudo's work on twin binary trees [Gir12]. For a k-tuple $\boldsymbol{\delta} := (\delta_1, \dots, \delta_k)$ of decorations $\delta_i \in \{\textcircled{I}, \textcircled{X}, \textcircled{Y}, \otimes\}^n$, define a ***$\boldsymbol{\delta}$-permutree tuple*** to be a k-tuple $\boldsymbol{T} := (T_1, \dots, T_k)$ where T_i is a δ_i-permutree and such that the union of the permutrees $T_1, \dots, T_k$ is acyclic (in other words, the permutrees $T_1, \dots, T_k$ admit a common linear extension). Then these $\boldsymbol{\delta}$-permutree tuples label:

- the classes of the congruence of the weak order defined as the intersection of permutree congruences $\equiv_{\delta_1} \cap \cdots \cap \equiv_{\delta_k}$,
- the vertices of the Minkowski sum of permutreehedra $\mathbb{PT}(\delta_1) + \cdots + \mathbb{PT}(\delta_k)$,
- the basis of a Hopf subalgebra of a tuple generalization of the decorated Malvenuto–Reutenauer algebra (where the products and coproducts are performed coordinatewise).

Chapter Four

QUOTIENTOPES

In this chapter, we finally deal simultaneously with all lattice congruences of the weak order. In Section 4.1, we briefly review non-crossing arc diagrams [Rea15], which provide a powerful combinatorial model for congruences classes of lattice congruences of the weak order. Using the geometry of shards, we then construct in Section 4.2 the quotientopes [PS19], which provide polytopal realizations of these quotients. Finally in Section 4.3, we show a general approach to construct Hopf algebra structures on all lattice quotients of the weak order, using further decorated versions of C. Malvenuto and C. Reutenauer's Hopf algebra $\boldsymbol{k}\mathfrak{S}$ on permutations. Section 4.2 is adapted from a joint work with F. Santos [PS19], Section 4.2.3 is a work in progress with A. Padrol and J. Ritter [PPR20], and Section 4.3 is adapted from [Pil19].

4.1 LATTICE QUOTIENTS AND ARC DIAGRAMS

4.1.1 Canonical representations and non-crossing arc diagrams

Let $(L, \leq, \wedge, \vee)$ be a finite lattice. A *join representation* of $x \in L$ is a subset $J \subseteq L$ such that $x = \bigvee J$. It is *irredundant* if $x \neq \bigvee J'$ for $J' \subsetneq J$. Irredundant join representations of $x \in L$ are ordered by $J \leq J'$ if and only if for any $y \in J$ there exists $y' \in J'$ with $y \leq y'$. The minimum element of this order, if it exists, is the *canonical join representation* of x. The lattice is *semidistributive* if any element admits canonical join and meet representations. The weak order on $\mathfrak{S}_n$ is a semidistributive lattice, whose canonical join and meet representations were explicitly described by N. Reading in [Rea15] as follows. A *descent* (resp. *ascent*) in $\sigma = \sigma_1 \dots \sigma_n \in \mathfrak{S}_n$ is a position $i \in [n-1]$ such that $\sigma_i > \sigma_{i+1}$ (resp. $\sigma_i < \sigma_{i+1}$). For a descent i of σ, consider the permutation $\underline{\lambda}(\sigma, i)$ with entries $1, \dots, (\sigma_{i+1} - 1)$ followed by $\{\sigma_j \,|\, j < i,\ \sigma_j \in]\sigma_{i+1}, \sigma_i[\}$ increasingly, then $\sigma_i\sigma_{i+1}$, then $\{\sigma_j \,|\, j > i+1,\ \sigma_j \in]\sigma_{i+1}, \sigma_i[\}$ increasingly, and finally $(\sigma_i + 1), \dots, n$. For each ascent i of σ, define dually $\overline{\lambda}(\sigma, i) := \omega_\circ \underline{\lambda}(\omega_\circ \sigma, i)$, where $\omega_\circ := [n, n-1, \dots, 2, 1]$ is the longest permutation of $\mathfrak{S}_n$.

Theorem 4.1 ([Rea15, Thm. 2.4]). *The canonical join and meet representations of a permutation $\sigma = \sigma_1 \dots \sigma_n$ are given by $\bigvee \{\underline{\lambda}(\sigma, i) \,|\, \sigma_i > \sigma_{i+1}\}$ and $\bigwedge \{\overline{\lambda}(\sigma, i) \,|\, \sigma_i < \sigma_{i+1}\}$.*

As observed in [Rea15], the permutation $\underline{\lambda}(\sigma, i)$ is determined by the values σ_i and σ_{i+1} and by the set $\{\sigma_j \,|\, j < i,\ \sigma_j \in]\sigma_{i+1}, \sigma_i[\}$. This data can be recorded in the following combinatorial gadgets. An *arc* is a quadruple (a, b, n, S) where $1 \leq a < b \leq n$ are integers and $S \subseteq]a, b[$. We denote by $\mathcal{A}_n := \{(a, b, n, S) \,|\, 1 \leq a < b \leq n \text{ and } S \subseteq]a, b[\}$ the set of arcs of length n, and by $\mathcal{A} := \bigsqcup_{n \in \mathbb{N}} \mathcal{A}_n$ the set of all arcs. We denote by $\underline{\alpha}(i, i+1, \sigma) := (\sigma_{i+1}, \sigma_i, n, \{\sigma_j \,|\, j < i \text{ and } \sigma_j \in]\sigma_{i+1}, \sigma_i[\})$ the arc associated to a descent i of a permutation σ and by $\underline{\delta}(\sigma) := \{\underline{\alpha}(i, i+1, \sigma) \,|\, \sigma_i > \sigma_{i+1}\}$ the set of arcs corresponding to all descents of σ. Define $\overline{\alpha}$ and $\overline{\delta}$ dually for ascents.

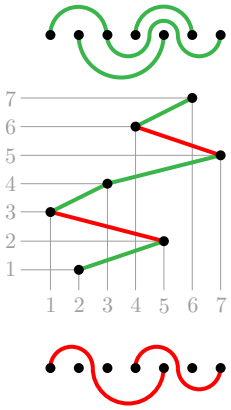

An arc (a, b, n, S) is visually represented as an x-monotone continuous curve wiggling around the horizontal axis, with endpoints a and b, and passing above the points of S and below the points of $]a, b[\smallsetminus S$. With this representation, N. Reading provided a convenient visual interpretation of $\underline{\delta}$ and $\overline{\delta}$. For this, represent the permutation σ by its *permutation table* (σ_i, i). Draw arcs between any two consecutive dots (σ_i, i) and $(\sigma_{i+1}, i+1)$, colored green if $\sigma_i < \sigma_{i+1}$ is an ascent and red if $\sigma_i > \sigma_{i+1}$ is a descent. Then move all dots down to the horizontal axis, allowing the segments to curve, but not to cross each other nor to pass through any dot. The set of red (resp. green) arcs is then the set $\underline{\delta}(\sigma)$ (resp. $\overline{\delta}(\sigma)$) corresponding to the canonical join (resp. meet) representation of σ.

Two arcs *cross* if the interior of the two curves representing these arcs intersect. A *non-crossing arc diagram* is a set $\mathcal{D}$ of arcs of $\mathcal{A}_n$ such that any two arcs of $\mathcal{D}$ do not cross and have distinct left endpoints and distinct right endpoints. Theorem 4.1 yields the following.

Theorem 4.2 ([Rea15, Thm. 3.1]). *The maps $\underline{\delta}$ and $\overline{\delta}$ are bijections from permutations of $\mathfrak{S}_n$ to non-crossing arc diagrams of $\mathcal{A}_n$.*

4.1.2 Lattice quotients of the weak order and arc ideals

Let $\equiv$ be lattice congruence of L (see Section 1.1.1). An element $x \in L$ is *contracted* by $\equiv$ if it is not minimal in its $\equiv$-equivalence class. As each class of $\equiv$ is an interval of L, it contains a unique uncontracted element, and the quotient $L/\equiv$ is isomorphic to the subposet of L induced by its uncontracted elements. Moreover, the canonical join representations in the quotient $L/\equiv$ are precisely the canonical join representations of L that do not involve any contracted join-irreducible. This yields the following.

Theorem 4.3 ([Rea15, Thm. 4.1]). *Consider a lattice congruence $\equiv$ of the weak order on $\mathfrak{S}_n$, and let $\mathcal{I}_\equiv$ denote the arcs corresponding to the join-irreducible permutations not contracted by $\equiv$.*

1. *A permutation σ is minimal in its $\equiv$-congruence class if and only if $\underline{\delta}(\sigma) \subseteq \mathcal{I}_\equiv$.*
2. *Sending a $\equiv$-congruence class with minimal permutation σ to the arc diagram $\underline{\delta}(\sigma)$ defines a bijection between the congruence classes of $\equiv$ and the non-crossing arc diagrams in $\mathcal{I}_\equiv$.*
3. *The congruence $\equiv$ is the transitive closure of the rewriting rule $\sigma \to \sigma \cdot (i\ i+1)$ where i is a descent of σ such that $\underline{\alpha}(i, i+1, \sigma) \notin \mathcal{I}_\equiv$.*

It remains to characterize the sets of arcs $\mathcal{I}_\equiv$ corresponding to the uncontracted join-irreducible permutations of a lattice congruence $\equiv$ of the weak order. This is again transparent on the arc representation. An arc $\alpha := (a, d, n, S)$ is *forced* by an arc $\beta := (b, c, n, T)$, denoted $\alpha \prec \beta$, if $a \le b < c \le d$ and $T = S \cap]b, c[$. Graphically, it means that β is obtained by restricting the arc α to the interval $[b, c]$. See on the right for the forcing order on $\mathcal{A}_4$. An *arc ideal* is any upper ideal $\mathcal{I}$ of the forcing order: $(a, d, n, S) \in \mathcal{I}$ implies $(b, c, n, S \cap]b, c[) \in \mathcal{I}$ for all $a \le b < c \le d$ and $S \subseteq]a, d[$. We denote by $\mathfrak{I}_n$ the set of arc ideals of $\mathcal{A}_n$.

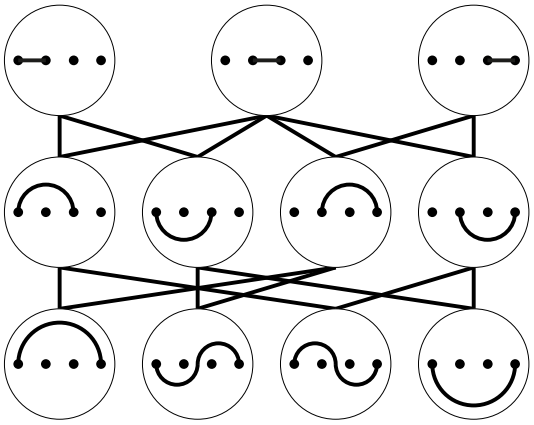

Theorem 4.4 ([Rea15, Coro. 4.5]). *A set of arcs $\mathcal{I} \subseteq \mathcal{A}_n$ is the set $\mathcal{I}_\equiv$ for some lattice congruence $\equiv$ of the weak order on $\mathfrak{S}_n$ if and only if it is an arc ideal of $\mathfrak{I}_n$.*

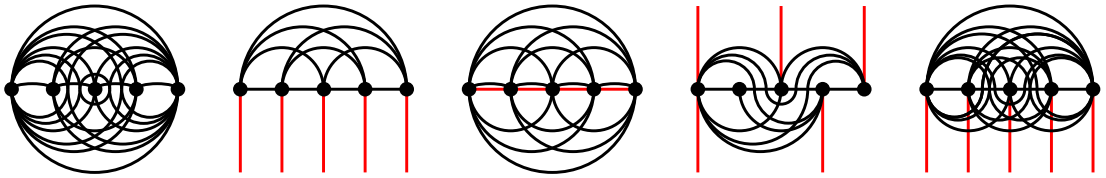

Figure 4.1: Examples of arc ideals $\mathcal{A}^{<k}_{\mathbf{n},\mathbf{s},\mathbf{e},\mathbf{w}}$. The associated lattice congruences correspond from left to right to permutations, binary trees, diagonal rectangulations, δ-permutrees, and acyclic 2-twists.

Example 4.5. The sets of all arcs $\mathcal{A}_n$, the set of upper arcs $\mathcal{A}_n^+ := \{(a,b,n,]a,b[) \,|\, 1 \le a < b \le n\}$, the set of lower arcs $\mathcal{A}_n^- := \{(a,b,n,\varnothing) \,|\, 1 \le a < b \le n\}$, or the union $\mathcal{A}_n^+ \cup \mathcal{A}_n^-$ are all arc ideals. More generally, fix four functions $\mathbf{n}, \mathbf{s}, \mathbf{e}, \mathbf{w} : [n] \to \mathbb{N}$ and choose $k \in \mathbb{N}$. For each $a \in [n]$, draw $\mathbf{n}(a)$ upper vertical walls above a, $\mathbf{s}(a)$ lower vertical walls below a, and $\min\big(\mathbf{e}(a), \mathbf{w}(a+1)\big)$ horizontal walls from a and $a+1$. Then the set $\mathcal{A}^{<k}_{\mathbf{n},\mathbf{s},\mathbf{e},\mathbf{w}}$ of arcs that cross at most $k-1$ of all these walls is an arc ideal. For certain choices of $\mathbf{n}, \mathbf{s}, \mathbf{e}, \mathbf{w}$ and k, the resulting arc ideals can correspond to:

- the weak order ($\mathbf{n} = \mathbf{s} = \mathbf{e} = \mathbf{w} = 0$ and $k = 1$),
- the Tamari lattice [Tam51] ($\mathbf{n} = \mathbf{e} = \mathbf{w} = 0$ and $\mathbf{s} = k = 1$),
- the boolean lattice ($\mathbf{e} = \mathbf{w} = 0$ and $\mathbf{n} = \mathbf{s} = k = 1$),
- the lattice of diagonal rectangulations [LR12] ($\mathbf{n} = \mathbf{s} = 0$ and $\mathbf{e} = \mathbf{w} = k = 1$),
- the permutree lattices [PP18] ($\mathbf{e} = \mathbf{w} = 0$, $\mathbf{n} \le 1$, $\mathbf{s} \le 1$ and $k = 1$),
- the lattice of sashes [Law14] ($\mathbf{e} = \mathbf{w} = 0$, $\mathbf{n} = 1$, $\mathbf{s} = 2$ and $k = 2$),
- the lattice of acyclic k-twists [Pil18] ($\mathbf{n} = \mathbf{e} = \mathbf{w} = 0$, $\mathbf{s} = 1$ and $k \ge 1$),
- the lattice of k-descent schemes [NRT11, Pil18] ($\mathbf{e} = \mathbf{w} = 0$, $\mathbf{n} = \mathbf{s} = 1$ and $k \ge 1$).

4.2 QUOTIENTOPES

4.2.1 Quotient fans

Recall that the cones of the braid fan $\mathcal{F}(n)$ are labeled by ordered partitions of $[n]$ (see also Section 5.1.1): an ordered partition $\pi = \pi_1|\pi_2|\dots|\pi_k$ of $[n]$ into k parts corresponds to the $(k-1)$-dimensional cone $\boldsymbol{C}^\diamond(\pi) := \big\{\boldsymbol{x} \in \mathbb{1}^\perp \mid x_u \le x_v \text{ for all } i \le j,\ u \in \pi_i \text{ and } v \in \pi_j\big\}$. In particular, the braid fan $\mathcal{F}(n)$ has a maximal cone $\boldsymbol{C}^\diamond(\sigma)$ for each permutation $\sigma \in \mathfrak{S}_n$, and a ray $\boldsymbol{C}^\diamond(R)$ for each subset $\varnothing \ne R \subsetneq [n]$.

The arcs of Section 4.1 have geometric counterparts called shards, due to by N. Reading [Rea03] (see also his survey chapters [Rea16b, Rea16a]). For an arc $\alpha := (a,b,n,S) \in \mathcal{A}_n$, the *shard* $\Sigma(\alpha)$ is the cone $\Sigma(\alpha) := \big\{\boldsymbol{x} \in \mathbb{1}^\perp \,\big|\, x_a = x_b,\ x_a \ge x_k \text{ for all } k \in S,\ x_a \le x_k \text{ for all } k \in]a,b[\smallsetminus S\big\}$. Each hyperplane $\boldsymbol{H}_{ab} := \big\{\boldsymbol{x} \in \mathbb{1}^\perp \,\big|\, x_a = x_b\big\}$ of the braid fan is thus decomposed into the 2^{b-a-1} shards $\Sigma(a,b,n,S)$ for all $S \subseteq]a,b[$. The shards are thus pieces of the hyperplanes of the braid arrangement. See Figures 4.2 and 4.3 (middle).

Reading proved in [Rea05] that any lattice congruence of the weak order defines a fan coarsening the braid fan in the following two equivalent ways. See Figures 4.2 and 4.3 (right).

Theorem 4.6 ([Rea05])**.** *For any lattice congruence $\equiv$ of the weak order on $\mathfrak{S}_n$, the cones obtained by*

- *glueing together the cones of the braid fan that belong to the same congruence class of $\equiv$,*
- *keeping the connected components of $\mathbb{1}^\perp \smallsetminus \bigcup_{\alpha \in \mathcal{I}_\equiv} \Sigma(\alpha)$,*

coincide and define a fan $\mathcal{F}(\equiv)$ whose dual graph is the Hasse diagram of the quotient $\mathfrak{S}_n/\equiv$.

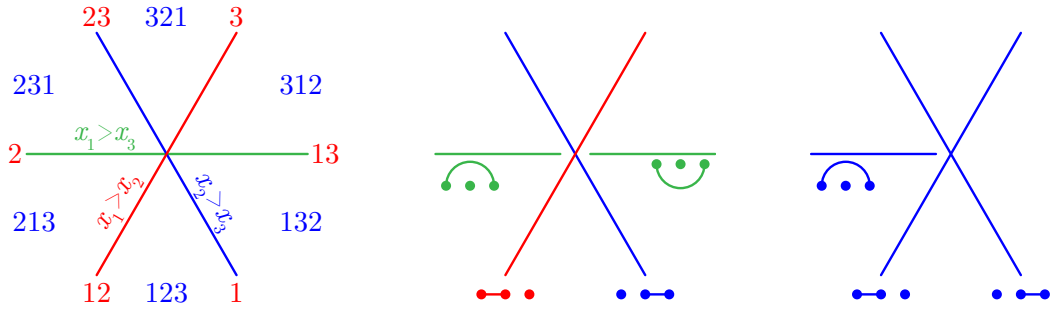

Figure 4.2: The braid fan $\mathcal{F}(3)$ (left), the corresponding shards (middle), and the quotient fan given by the sylvester congruence $\equiv^{\text{sylv}}$ (right).

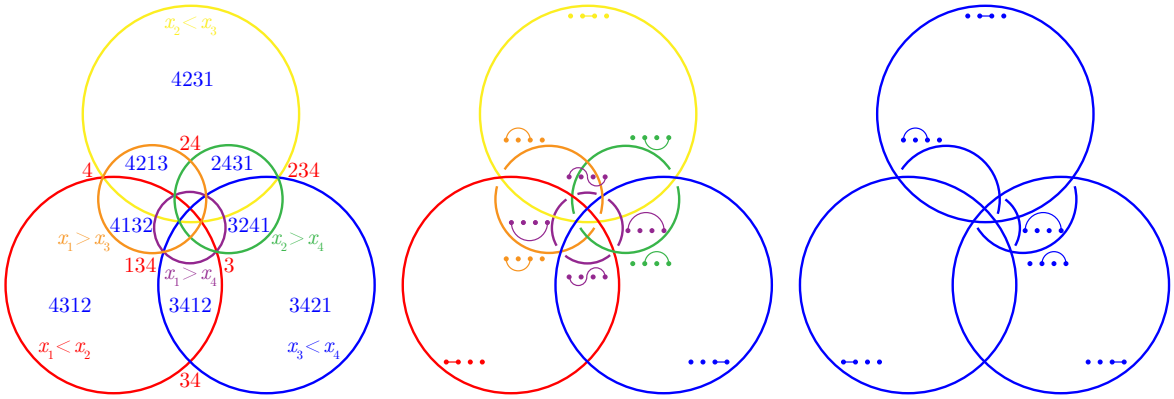

Figure 4.3: A stereographic projection of the braid fan $\mathcal{F}(4)$ (left), the corresponding shards (middle), and the quotient fan given by the sylvester congruence $\equiv^{\text{sylv}}$ (right).

4.2.2 Quotientopes

Closing an open question of [Rea05], we now use arcs to construct a polytopal realization of the quotient fan $\mathcal{F}(\equiv)$. A function $f : \mathcal{A}_n \to \mathbb{R}_{>0}$ is *forcing dominant* if $f(\alpha) > \sum_{\beta \prec \alpha} f(\beta)$ for any arc $\alpha \in \mathcal{A}_n$. Note that such functions clearly exist since $\prec$ is a poset, *e.g.* $f(a, b, n, S) = n^{-(b-a)^2}$. For an arc $\alpha = (a, b, n, S) \in \mathcal{A}_n$ and a subset $R \subseteq [n]$, we define the *contribution* $\gamma(\alpha, R)$ of α to R to be 1 if $|R \cap \{a, b\}| = 1$ and $S = R \cap]a, b[$, and 0 otherwise. For a subset $R \subseteq [n]$, we pick a representative vector $\boldsymbol{r}(R) = \mathbb{1}_{k \in R} - \mathbb{1}_{k+1 \in R}$ of the ray $\boldsymbol{C}^\diamond(R)$, and we define the *height* $h^f_\equiv(R) \in \mathbb{R}_{>0}$ to be $h^f_\equiv(R) := \sum_{\alpha \in \mathcal{I}_\equiv} f(\alpha)\, \gamma(\alpha, R)$. This height function has been chosen to fulfill the following property, proved in [PS19].

Lemma 4.7. *Let σ, σ' be two adjacent permutations. Let $\varnothing \neq R \subsetneq [n]$ (resp. $\varnothing \neq R' \subsetneq [n]$) be such that $\boldsymbol{r}(R)$ (resp. $\boldsymbol{r}(R')$) is the ray of $\boldsymbol{C}^\diamond(\sigma)$ not in $\boldsymbol{C}^\diamond(\sigma')$ (resp. of $\boldsymbol{C}^\diamond(\sigma')$ not in $\boldsymbol{C}^\diamond(\sigma)$). Then*

- *the (unique up to rescaling) linear dependence among the rays of the cones $\boldsymbol{C}^\diamond(\sigma)$ and $\boldsymbol{C}^\diamond(\sigma')$ is $\boldsymbol{r}(R) + \boldsymbol{r}(R') = \boldsymbol{r}(R \cap R') + \boldsymbol{r}(R \cup R')$,*
- *the height function satisfies $h^f_\equiv(R) + h^f_\equiv(R') \geq h^f_\equiv(R \cap R') + h^f_\equiv(R \cup R')$ with equality if and only if the chambers $\boldsymbol{C}^\diamond(\sigma)$ and $\boldsymbol{C}^\diamond(\sigma')$ belongs to the same cone of $\mathcal{F}(\equiv)$.*

This property is a standard characterization of polytopality of fans, see Proposition 7.28 and [PS19, Prop. 3]. The resulting realizations of $\mathcal{F}(\equiv)$, called *quotientopes*, are illustrated in Figures 4.4 and 4.5.

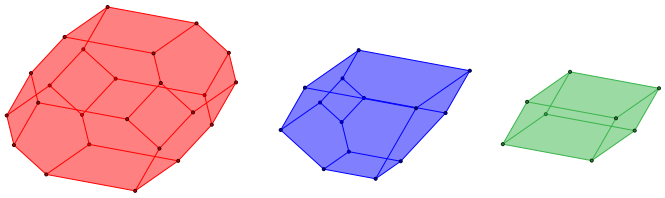

Figure 4.4: Permutahedron (left), associahedron (middle) and cube (right) as quotientopes.

Theorem 4.8. *For any lattice congruence $\equiv$ of the weak order on $\mathfrak{S}_n$, and any forcing dominant function $f : \mathcal{A}_n \to \mathbb{R}_{>0}$, the quotient fan $\mathcal{F}(\equiv)$ is the normal fan of the polytope*

$$\mathbb{QT}^f(\equiv) := \left\{ \boldsymbol{x} \in \mathbb{R}^n \mid \langle \boldsymbol{r}(R) \,|\, \boldsymbol{x} \rangle \leq h^f_{\equiv}(R) \text{ for all } \varnothing \neq R \subsetneq [n] \right\}.$$

In particular, when oriented in the direction $\boldsymbol{\omega} := (n, \dots, 1) - (1, \dots, n) = \sum_{i \in [n]} (n + 1 - 2i)\, \boldsymbol{e}_i$, the graph of $\mathbb{QT}^f(\equiv)$ is the Hasse diagram of the quotient of the weak order by $\equiv$.

Remark 4.9. Note that the definition of the height function ensures that $h^f_{\equiv}(R) \leq h^f_{\equiv'}(R)$ and thus $\mathbb{QT}^f(\equiv) \subseteq \mathbb{QT}^f(\equiv')$ when $\equiv$ coarsens $\equiv'$. See Figure 4.5.

4.2.3 Minkowski sums of associahedra or shard polytopes

We conclude with an alternative approach to quotientopes recently developed in [PPR20] to study the polytopality of quotient fans beyond the braid arrangement (see also Section A.3).

Lemma 4.10. *For any lattice congruence $\equiv$ of the weak order, the quotient fan $\mathcal{F}(\equiv)$ is the common refinement of the quotient fans $\mathcal{F}(\equiv_1), \dots, \mathcal{F}(\equiv_p)$ of the lattice congruences whose arc ideals $\mathcal{I}_{\equiv_1}, \dots, \mathcal{I}_{\equiv_p}$ are the principal upper ideals of the forcing order generated by the minimal elements of the arc ideal $\mathcal{I}_{\equiv}$ of $\equiv$.*

Lemma 4.11. *An arc ideal is principal if and only if it corresponds to a Cambrian congruence (possibly of low dimension).*

Corollary 4.12. *For any lattice congruence $\equiv$ of the weak order, the quotient fan $\mathcal{F}_{\equiv}$ is the normal fan of a Minkowski sum of associahedra.*

In fact, this idea can even been pushed further to obtain realizations of all quotientopes (including associahedra) as Minkowski sums of elementary summands, defined as follows.

Definition 4.13. *For an arc $\alpha = (a, b, n, S)$, we define*

- *an α-alternating matching as a (possibly empty) sequence $M = \{a_1, b_1, \dots, a_k, b_k\}$ where $a \leq a_1 < b_1 < \dots < a_k < b_k \leq b$ and $a_i \in S \cup \{a\}$ while $b_i \notin S$ for all $i \in [k]$.*
- *the characteristic vector of this α-alternating matching as $\chi(M) = \sum_{i \in [k]} \boldsymbol{e}_{a_i} - \boldsymbol{e}_{b_i}$,*
- *the shard polytope $\mathbb{SP}(\alpha)$ as the convex hull of the characteristic vectors of all α-alternating matchings.*

Proposition 4.14. *For any arc α, the union of the walls of the normal fan of the shard polytope $\mathbb{SP}(\alpha)$ contains the shard $\Sigma(\alpha)$ and is contained in the union of the shards $\Sigma(\beta)$ for the arcs β forced by α.*

Corollary 4.15. *For any lattice congruence $\equiv$ of the weak order, the quotient fan $\mathcal{F}_{\equiv}$ is the normal fan of the Minkowski sum of the shard polytopes $\mathbb{SP}(\alpha)$ over all $\alpha \in \mathcal{I}_{\equiv}$.*

Example 4.16. For the arc $\alpha = (a, b, n,]a, b[)$, the α-alternating matchings are given by $\varnothing$ and $\{i, b\}$ for $a \leq i < b$, so that the corresponding shard polytope $\mathbb{SP}(\alpha)$ is the translation of the standard simplex $\triangle_{[a,b]}$ by the vector $-\boldsymbol{e}_b$. We obtain thus the classical realization of Loday's associahedron as the Minkowski sum of all faces of the standard simplex corresponding to the intervals of $[n]$.

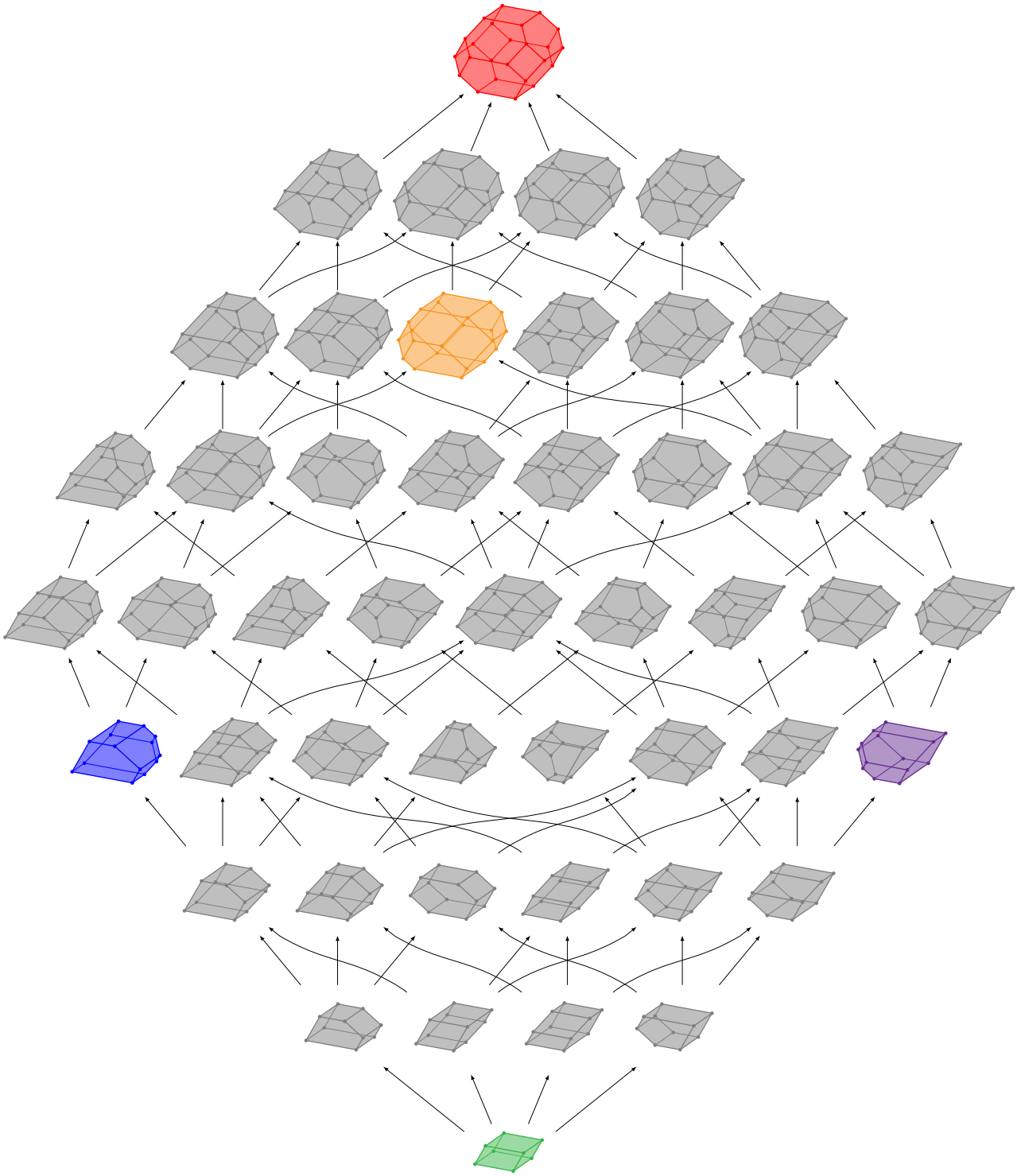

Figure 4.5: The quotientope lattice for $n = 4$: all quotientopes ordered by inclusion (which corresponds to refinement of the lattice congruences). We only consider lattice congruences whose arcs include all basic arcs $(i, i+1, 4, \varnothing)$, since otherwise their fan is not essential. We have highlighted the cube (green), J.-L. Loday's associahedron [Lod04] (blue), another one of C. Hohlweg and C. Lange's associahedra [HL07] (purple), the diagonal rectangulation polytope [LR12] (orange), and the permutahedron (red).

4.3 HOPF ALGEBRA STRUCTURES

4.3.1 Decorated permutations

The Cambrian and permutree Hopf algebras [CP17, PP18] were constructed as subalgebras of generalizations of the Malvenuto–Reutenauer Hopf algebra to signed or decorated permutations [NT10b]. Following this prototype, we will obtain Hopf algebras on non-crossing arc diagrams from algebras on permutations decorated with more complicated structures.

Definition 4.17. *A decoration set is a graded set* $\mathfrak{X} := \bigsqcup_{n\geq 0} \mathfrak{X}_n$ *endowed with*
- *a concatenation* $\mathbf{conc} : \mathfrak{X}_m \times \mathfrak{X}_n \longrightarrow \mathfrak{X}_{m+n}$ *for all* $m, n \in \mathbb{N}$,
- *a selection* $\mathbf{sel} : \mathfrak{X}_p \times \binom{[p]}{q} \longrightarrow \mathfrak{X}_q$ *for all* $p, q \in \mathbb{N}$,

such that
1. $\mathbf{conc}(\mathcal{X}, \mathbf{conc}(\mathcal{Y}, \mathcal{Z})) = \mathbf{conc}(\mathbf{conc}(\mathcal{X}, \mathcal{Y}), \mathcal{Z})$ *for any* $\mathcal{X}, \mathcal{Y}, \mathcal{Z} \in \mathfrak{X}$,
2. $\mathbf{sel}(\mathbf{sel}(\mathcal{X}, R), S) = \mathbf{sel}(\mathcal{X}, \{r_s \,|\, s \in S\})$ *for any* $\mathcal{X} \in \mathfrak{X}_p$, $R = \{r_1, \dots, r_q\} \subseteq [p]$, $S \subseteq [q]$,
3. $\mathbf{conc}(\mathbf{sel}(\mathcal{X}, R), \mathbf{sel}(\mathcal{Y}, S)) = \mathbf{sel}(\mathbf{conc}(\mathcal{X}, \mathcal{Y}), R \cup S^{\to m})$ *for any* $\mathcal{X} \in \mathfrak{X}_m$, $\mathcal{Y} \in \mathfrak{X}_n$, *and any* $R \subseteq [m]$, $S \subseteq [n]$, *where* $S^{\to m} := \{s + m \,|\, s \in S\}$.

Example 4.18. A typical decoration set is the set of words $\mathcal{A}^*$ on a finite alphabet $\mathcal{A}$, graded by length, with the concatenation of words $\mathbf{conc}(u_1 \dots u_m, v_1 \dots v_n) = u_1 \dots u_m v_1 \dots v_n$ and the selection defined by subwords $\mathbf{sel}(w_1 \dots w_p, \{r_1, \dots, r_q\}) = w_{r_1} \dots w_{r_q}$. Among many other examples, let us also mention the set of labeled graphs, graded by their number of vertices, with the concatenation defined as the shifted union, and the selection defined by standardized induced subgraphs. Further examples will appear in Section 4.3.3.

For $n \geq 0$, we denote by $\mathfrak{S}_n^{\mathfrak{X}} := \mathfrak{S}_n \times \mathfrak{X}_n$ the set of *$\mathfrak{X}$-decorated permutations* of size n, *i.e.* of pairs $(\sigma, \mathcal{X})$ with $\sigma \in \mathfrak{S}_n$ and $\mathcal{X} \in \mathfrak{X}_n$. We consider the graded set $\mathfrak{S}^{\mathfrak{X}} := \bigsqcup_{n\geq 0} \mathfrak{S}_n^{\mathfrak{X}}$ and the graded vector space $\boldsymbol{k}\mathfrak{S}^{\mathfrak{X}} := \bigoplus_{n\geq 0} \boldsymbol{k}\mathfrak{S}_n^{\mathfrak{X}}$, where $\boldsymbol{k}\mathfrak{S}_n^{\mathfrak{X}}$ is a vector space with basis $(\mathbb{F}_{(\sigma,\mathcal{X})})_{(\sigma,\mathcal{X})\in\mathfrak{S}_n^{\mathfrak{X}}}$ indexed by $\mathfrak{X}$-decorated permutations of size n. For two decorated permutations $(\sigma, \mathcal{X})$ and $(\tau, \mathcal{Y})$, we define the *product* $\mathbb{F}_{(\sigma,\mathcal{X})} \cdot \mathbb{F}_{(\tau,\mathcal{Y})}$ by

$$\mathbb{F}_{(\sigma,\mathcal{X})} \cdot \mathbb{F}_{(\tau,\mathcal{Y})} := \sum_{\rho \in \sigma \,⧢\, \tau} \mathbb{F}_{(\rho, \mathbf{conc}(\mathcal{X},\mathcal{Y}))}.$$

Proposition 4.19. *The product* $\cdot$ *defines an associative algebra on* $\boldsymbol{k}\mathfrak{S}^{\mathfrak{X}}$.

Let the *standardization* of a decorated permutation $(\rho, \mathcal{Z}) \in \mathfrak{S}_p^{\mathfrak{X}}$ at a subset $R \subseteq [p]$ be

$$\mathbf{std}((\rho, \mathcal{Z}), R) := \big(\mathbf{stdp}(\rho, R), \mathbf{sel}(\mathcal{Z}, \rho^{-1}(R))\big),$$

where $\mathbf{stdp}(\rho, R)$ is the position standardization on $\mathfrak{S}$ and $\mathbf{sel}(\mathcal{Z}, \rho^{-1}(R))$ is the selection on $\mathfrak{X}$. For a decorated permutation $(\rho, \mathcal{Z}) \in \mathfrak{S}_p^{\mathfrak{X}}$, we define the *coproduct* $\triangle\mathbb{F}_{(\rho,\mathcal{Z})}$ by

$$\triangle\mathbb{F}_{(\rho,\mathcal{Z})} := \sum_{k=0}^{p} \mathbb{F}_{\mathbf{std}((\rho,\mathcal{Z}),[k])} \otimes \mathbb{F}_{\mathbf{std}((\rho,\mathcal{Z}),[p]\setminus[k])}.$$

Proposition 4.20. *The coproduct* $\triangle$ *defines a coassociative coalgebra on* $\boldsymbol{k}\mathfrak{S}^{\mathfrak{X}}$.

Theorem 4.21. *The product* $\cdot$ *and the coproduct* $\triangle$ *define a combinatorial Hopf algebra on* $\boldsymbol{k}\mathfrak{S}^{\mathfrak{X}}$.

Example 4.22. When $\mathfrak{X}$ is the set of words $\mathcal{A}^*$ on a finite alphabet $\mathcal{A}$ as in Example 4.18, the Hopf algebra of decorated permutations was studied in detail by J.-C. Novelli and J.-Y. Thibon in [NT10b]. In particular, if $\mathfrak{X} = \{\bullet\}^*$, then $\boldsymbol{k}\mathfrak{S}^{\mathfrak{X}}$ is just C. Malvenuto and C. Reutenauer's Hopf algebra $\boldsymbol{k}\mathfrak{S}$ on permutations.

4.3.2 Decorated non-crossing arc diagrams

We now use our Hopf algebra on decorated permutations to construct Hopf algebras on decorated non-crossing arc diagrams. As in the previous section, we consider a decoration set $(\mathfrak{X}, \mathbf{conc}, \mathbf{sel})$ and the corresponding Hopf algebra $(\boldsymbol{k}\mathfrak{S}^{\mathfrak{X}}, \cdot, \triangle)$ on $\mathfrak{X}$-decorated permutations. Recall from Section 4.1.2 that $\mathfrak{I}_n$ denotes the set of arc ideals of $\mathcal{A}_n$.

For an arc $\alpha = (a, b, m, S)$ and $n \in \mathbb{N}$, define the *augmented arc* $\alpha^{+n} := (a, b, m+n, S)$ and the *shifted arc* $\alpha^{\to n} := (a+n, b+n, m+n, \{s+n \,|\, s \in S\})$. Graphically, the arc α^{+n} (resp. $\alpha^{\to n}$) is obtained from the arc α by adding n points to its right (resp. to its left). For $\mathcal{I} \subseteq \mathcal{A}_m$ and $n \in \mathbb{N}$, define $\mathcal{I}^{+n} := \{\alpha^{+n} \,|\, \alpha \in \mathcal{I}\}$ and $\mathcal{I}^{\to n} := \{\alpha^{\to n} \,|\, \alpha \in \mathcal{I}\}$.

Definition 4.23. *A graded function $\Psi : \mathfrak{X} = \bigsqcup_{n\geq 0} \mathfrak{X}_n \longrightarrow \mathfrak{I} = \bigsqcup_{n\geq 0} \mathfrak{I}_n$ is* conservative *if*

1. *$\Psi(\mathcal{X})^{+n}$ and $\Psi(\mathcal{Y})^{\to m}$ are both subsets of $\Psi(\mathbf{conc}(\mathcal{X}, \mathcal{Y}))$ for any $\mathcal{X} \in \mathfrak{X}_m$, $\mathcal{Y} \in \mathfrak{X}_n$,*
2. *$(r_a, r_b, p, S) \in \Psi(\mathcal{Z})$ implies $(a, b, q, \{c \in [q] \,|\, r_c \in S\}) \in \Psi(\mathbf{sel}(\mathcal{Z}, R))$ for any $\mathcal{Z} \in \mathfrak{X}_p$, any $R = \{r_1 < \ldots < r_q\} \subseteq [p]$, any $1 \leq a < b \leq q$ and any $S \subseteq]r_a, r_b[$.*

Example 4.24. If $\mathfrak{X} = \{\bullet\}^*$ is the decoration set of words on a one element alphabet, then the maps $\bullet^n \mapsto \mathcal{A}_n$ and $\bullet^n \mapsto \mathcal{A}_n^{\varnothing} := \{(a, b, n, \varnothing) \,|\, 1 \leq a < b \leq n\}$ are both conservative.

From now on, we assume that we are given a conservative function $\Psi : \mathfrak{X} \longrightarrow \mathfrak{I}$. For $n \geq 0$, we denote by $\mathfrak{D}_n^{\mathfrak{X}}$ the set of *$\mathfrak{X}$-decorated non-crossing arc diagrams* of size n, *i.e.* of pairs $(\mathcal{D}, \mathcal{X})$ where $\mathcal{X} \in \mathfrak{X}_n$ and $\mathcal{D}$ is a non-crossing arc diagram contained in $\Psi(\mathcal{X})$.

We now define a Hopf algebra on $\mathfrak{X}$-decorated non-crossing arc diagrams. By Theorem 4.4, any lattice congruence $\equiv$ of the weak order on $\mathfrak{S}_n$ corresponds to an arc ideal $\mathcal{I}_{\equiv} \in \mathfrak{I}_n$. We consider the map $\underline{\eta}_{\mathcal{I}_{\equiv}} : \mathfrak{S}_n \to \mathcal{I}_{\equiv}$ which associates to any permutation $\tau \in \mathfrak{S}_n$ the non-crossing arc diagram of $\mathcal{I}_{\equiv}$ corresponding to the $\equiv$-congruence class of τ. By Theorem 4.3, $\underline{\eta}_{\mathcal{I}_{\equiv}}(\tau) = \underline{\delta}(\sigma)$ where σ is the minimal permutation in the $\equiv$-congruence class of τ. We denote by $\boldsymbol{k}\mathfrak{D}^{\mathfrak{X}} := \bigoplus_{n\geq 0} \boldsymbol{k}\mathfrak{D}_n^{\mathfrak{X}}$ the graded vector subspace of $\boldsymbol{k}\mathfrak{S}^{\mathfrak{X}}$ generated by the elements

$$\mathbb{P}_{(\mathcal{D},\mathcal{X})} := \sum_{\substack{\sigma \in \mathfrak{S} \\ \underline{\eta}_{\Psi(\mathcal{X})}(\sigma) = \mathcal{D}}} \mathbb{F}_{(\sigma,\mathcal{X})},$$

for all $\mathfrak{X}$-decorated non-crossing arc diagrams $(\mathcal{D}, \mathcal{X})$. Our main result is the following.

Theorem 4.25. *The vector subspace $\boldsymbol{k}\mathfrak{D}^{\mathfrak{X}}$ is a Hopf subalgebra of $\boldsymbol{k}\mathfrak{S}^{\mathfrak{X}}$.*

Example 4.26. Let $\mathfrak{X} = \{\bullet\}^*$, so that $\boldsymbol{k}\mathfrak{S}^{\mathfrak{X}}$ is C. Malvenuto and C. Reutenauer's Hopf algebra $\boldsymbol{k}\mathfrak{S}$ on permutations by Example 4.22 and consider the two conservative functions of Example 4.24. If $\Psi(\bullet^n) = \mathcal{A}_n$, then $\boldsymbol{k}\mathfrak{D}^{\mathfrak{X}} = \boldsymbol{k}\mathfrak{S}^{\mathfrak{X}}$ is also C. Malvenuto and C. Reutenauer's Hopf algebra $\boldsymbol{k}\mathfrak{S}$. If $\Psi(\bullet^n) = \mathcal{A}_n^{\varnothing}$, then $\boldsymbol{k}\mathfrak{D}^{\mathfrak{X}}$ is J.-L. Loday and M. Ronco's Hopf algebra $\boldsymbol{k}\mathfrak{T}$ on binary trees [LR98] (as non-crossing arc diagrams in $\mathcal{A}_n^{\varnothing}$ are just non-crossing partitions, in bijection with binary trees).

We now state an analogue of Proposition 1.2 for decorated non-crossing arc diagrams.

Proposition 4.27. *Consider two $\mathfrak{X}$-decorated non-crossing arc diagrams $(\mathcal{D}, \mathcal{X})$ and $(\mathcal{E}, \mathcal{Y})$, and their weak order intervals $[\underline{\rho}, \overline{\rho}]_{\mathsf{W}} := \underline{\eta}^{-1}_{\Psi(\mathcal{X})}(\mathcal{D})$ and $[\underline{\sigma}, \overline{\sigma}]_{\mathsf{W}} := \underline{\eta}^{-1}_{\Psi(\mathcal{Y})}(\mathcal{E})$. Then*

$$\mathbb{P}_{(\mathcal{D},\mathcal{X})} \cdot \mathbb{P}_{(\mathcal{E},\mathcal{Y})} = \sum\nolimits_{\mathcal{F}} \mathbb{P}_{(\mathcal{F},\mathbf{conc}(\mathcal{X},\mathcal{Y}))},$$

where $\mathcal{F}$ ranges in the interval from $\mathcal{D} \backslash \mathcal{E} := \underline{\eta}_{\Psi(\mathbf{conc}(\mathcal{X},\mathcal{Y}))}(\underline{\rho} \backslash \underline{\sigma})$ to $\mathcal{E}/\mathcal{D} := \underline{\eta}_{\Psi(\mathbf{conc}(\mathcal{X},\mathcal{Y}))}(\overline{\rho}/\overline{\sigma})$ in the lattice of non-crossing arc diagrams in $\Psi(\mathbf{conc}(\mathcal{X}, \mathcal{Y}))$ (see 2 in Theorem 4.3).

4.3.3 Three applications

We conclude with three applications of Sections 4.3.1 and 4.3.2 that produce relevant Hopf algebras on non-crossing arc diagrams.

4.3.3.1 Insertional, translational, and Hopf families of congruences

For each $n \in \mathbb{N}$, fix a lattice congruence $\equiv_n$ of the weak order on $\mathfrak{S}_n$, with arc ideal $\mathcal{I}_n$. As a first application of Theorem 4.25, we obtain sufficient conditions for the family $(\equiv_n)_{n\in\mathbb{N}}$ to define a Hopf subalgebra of $\boldsymbol{k}\mathfrak{S}$, which essentially coincide with the translational and insertional conditions given by N. Reading in [Rea05, Thm. 1.2 & 1.3]. Note that this situation covers various families of lattice congruences, producing Hopf algebra on permutations [MR95], on binary trees [LR98, HNT05], on diagonal quadragulations [LR12], on k-twists [Pil18], etc.

Corollary 4.28 ([Rea05, Thm. 1.2 & 1.3])**.** *For all $n \in \mathbb{N}$, consider a lattice congruence $\equiv_n$ of the weak order on $\mathfrak{S}_n$, with arc ideal $\mathcal{I}_n$. If*

- *both $\mathcal{I}_m^{+n}$ and $\mathcal{I}_n^{\to m}$ are contained in $\mathcal{I}_{m+n}$ for all $m, n \in \mathbb{N}$,*
- *$(r_a, r_b, p, S) \in \mathcal{I}_p$ implies $(a, b, q, \{c \in [q] \,|\, r_c \in S\}) \in \mathcal{I}_q$ for any $1 \leq a < b \leq q$, any $R = \{r_1 < \ldots < r_q\} \subseteq [p]$, and any $S \subseteq]r_a, r_b[$,*

then the subvector space of $\boldsymbol{k}\mathfrak{S}$ generated by the sums $\sum_\sigma \mathbb{F}_\sigma$ over the classes of the congruences $\equiv_n$ is a Hopf subalgebra of C. Malvenuto and C. Reutenauer Hopf algebra $\boldsymbol{k}\mathfrak{S}$ on permutations.

4.3.3.2 Bounded crossings

We now consider the family of arc ideals $\mathcal{A}^{<k}_{\mathbf{n},\mathbf{s},\mathbf{e},\mathbf{w}}$ defined in Example 4.5. Consider the decoration set $\mathfrak{X} = \bigsqcup_{n\in\mathbb{N}} \mathfrak{X}_n$, where $\mathfrak{X}_n$ is the set of quadruples of functions $[n] \to \mathbb{N}$, and where the concatenation is defined by:

$$\mathbf{conc}((\mathbf{n},\mathbf{s},\mathbf{e},\mathbf{w}),(\mathbf{n}',\mathbf{s}',\mathbf{e}',\mathbf{w}'))(a) = \begin{cases} \big(\mathbf{n}(a),\mathbf{s}(a),\mathbf{e}(a),\mathbf{w}(a)\big) & \text{if } a \leq m \\ \big(\mathbf{n}'(a),\mathbf{s}'(a),\mathbf{e}'(a),\mathbf{w}'(a)\big) & \text{if } a > m \end{cases}$$

(in other words, the usual concatenation of words in $(\mathbb{N}^4)^*$), and the selection is defined by

$$\mathbf{sel}((\mathbf{n},\mathbf{s},\mathbf{e},\mathbf{w}),R)(a) = \big(\mathbf{n}(r_a),\ \mathbf{s}(r_a),\ \min\{\mathbf{e}(s) \,|\, s \in]r_{a-1}, r_a]\},\ \min\{\mathbf{w}(s) \,|\, s \in [r_a, r_{a+1}[\}\big).$$

Choose $k \in \mathbb{N}$ and define the function $\Psi : \mathfrak{X}_n \to \mathcal{A}_n$ by $\Psi(\mathbf{n},\mathbf{s},\mathbf{e},\mathbf{w}) = \mathcal{A}^{<k}_{\mathbf{n},\mathbf{s},\mathbf{e},\mathbf{w}}$. Recall from Example 4.5 that for each $a \in [n]$, we place $\mathbf{n}(a)$ upper vertical walls above a, $\mathbf{s}(a)$ lower vertical walls below a and $\min\big(\mathbf{e}(a), \mathbf{w}(a+1)\big)$ horizontal walls between a and $a+1$, and that an arc belongs to $\mathcal{A}^{<k}_{\mathbf{n},\mathbf{s},\mathbf{e},\mathbf{w}}$ if it crosses at most $k-1$ of these walls. The function Ψ is conservative since:

- for any $u \in \mathfrak{X}_m$, $v \in \mathfrak{X}_n$, $\alpha \in \Psi(u)$ and $\beta \in \Psi(v)$, the walls of uv crossed by α^{+n} are precisely the walls of u crossed by α, while the walls of uv crossed by $\beta^{\to m}$ are precisely the m-translates of the walls of v crossed by β,
- for any $w \in \mathfrak{X}_p$, $R = \{r_1, \ldots, r_q\} \subseteq [p]$, $1 \leq a < b \leq q$ and $S \subseteq]r_a, r_b[$, the walls crossed by the arc $(a, b, q, \{c \,|\, r_c \in S\})$ are walls crossed by the arc (r_a, r_b, p, S) (but the latter might cross more walls than the former).

We therefore obtain a Hopf algebra $\boldsymbol{k}\mathfrak{D}^{<k}$ on the classes of all lattice congruences $\mathcal{A}^{<k}_{\mathbf{n},\mathbf{s},\mathbf{e},\mathbf{w}}$ simultaneously. Moreover, any subset of $\mathfrak{X}$ stable by concatenation and selection provides a Hopf subalgebra $\boldsymbol{k}\mathfrak{D}^{<k}$. In particular, $\boldsymbol{k}\mathfrak{D}^{<1}$ contains *simultaneously* Hopf subalgebras on permutations [MR95], binary trees [LR98, HNT05], binary sequences [GKL$^+$95], Cambrian trees [CP17], permutrees [PP18], and diagonal rectangulations [LR12, Gir12], while $\boldsymbol{k}\mathfrak{D}^{<k}$ contains subalgebras on k-twists [Pil18] and on k-descent schemes [NRT11, Pil18].

4.3.3.3 All arc diagrams

To conclude, we define a Hopf algebra $\boldsymbol{k}\mathfrak{D}^\star$ simultaneously involving the classes of all lattice congruences of the weak order, and containing the permutree Hopf algebra of Section 3.3. An *extended arc* is a quadruple (a, b, n, S) with integers $0 \leq a < b \leq n + 1$, and $S \subseteq]a, b[$. We denote by $\mathcal{A}^\star_n$ the set of all extended arcs. The representation of arcs, the notions of crossing and forcing, as well as the operations α^{+n} and $\alpha^{\to n}$, are defined as for classical arcs. We denote by $\mathfrak{I}^\star_n$ the set of extended arc ideals (*i.e.* upper ideals of the forcing order $\prec$ on $\mathcal{A}^\star_n$).

The *juxtaposition* $\alpha\beta$ of two extended arcs $\alpha := (a, b, p, R)$ and $\beta := (c, d, p, S)$ is the singleton $\alpha\beta := \{(a, d, p, R \cup S)\}$ if $b = c + 1$, and $\varnothing$ otherwise. For $\mathcal{I}, \mathcal{J} \subseteq \mathcal{A}^\star_p$, we define the *juxtaposition* $\mathcal{I}\mathcal{J}$ by $\mathcal{I}\mathcal{J} := \mathcal{I} \cup \mathcal{J} \cup \bigcup_{\alpha\in\mathcal{I},\beta\in\mathcal{J}} \alpha\beta$. As illustrated in Figure 4.6, we define the *concatenation* of two extended arc ideals $\mathcal{I} \subseteq \mathcal{A}^\star_m$ and $\mathcal{J} \subseteq \mathcal{A}^\star_n$ by $\mathbf{conc}(\mathcal{I}, \mathcal{J}) := \mathcal{I}^{+n}\mathcal{J}^{\to m}$.

Consider an extended arc ideal $\mathcal{K} \subseteq \mathcal{A}^\star_p$ and a subset $X := \{x_1 < \ldots < x_q\}$ of $[p]$. Define by convention $x_0 := 0$ and $x_{q+1} := p + 1$. As illustrated in Figure 4.6, we define the *selection* $\mathbf{sel}(\mathcal{K}, X)$ as the set of all arcs (a, b, q, S) such that there exist:

- positions $y_0 < \ldots < y_r \in [p]$ with $x_a = y_0$ and $x_b = y_r$ while $y_1, \ldots, y_{r-1} \notin X$, and
- arcs $(y_0, y_1, p, S_1), \ldots, (y_{r-1}, y_r, p, S_r) \in \mathcal{K}$ such that $S = \{\ell \in [q] \,|\, x_\ell \in \bigcup S_k\}$.

Figure 4.6: The concatenation and selection for extended arc ideals.

Proposition 4.29. *The set $\mathfrak{I}^\star := \bigsqcup_{n\in\mathbb{N}} \mathfrak{I}^\star_n$ of all extended arcs ideals, endowed with the concatenation* **conc** *and selection* **sel***, is a decoration set.*

We now consider the map $\Psi : \mathfrak{I}^\star \to \mathfrak{I}$ which sends an extended arc ideal to the arc ideal of its strict arcs (not starting at 0 or ending at $n + 1$). It is clearly conservative so that we obtain a Hopf algebra $\boldsymbol{k}\mathfrak{D}^\star$ on pairs $(\mathcal{D}, \mathcal{I})$, where $\mathcal{I}$ is any extended arc ideal and $\mathcal{D}$ is a non-crossing arc diagram containing only strict arcs of $\mathcal{I}$. The Hopf algebra $\boldsymbol{k}\mathfrak{D}^\star$ involves the classes of all lattice congruences of the weak order, and the concatenation and selection were chosen to fulfill the following statement.

Proposition 4.30. *The permutree Hopf algebra [PP18] is a Hopf subalgebra of $\boldsymbol{k}\mathfrak{D}^\star$.*

II

Part Two

BEYOND THE WEAK ORDER

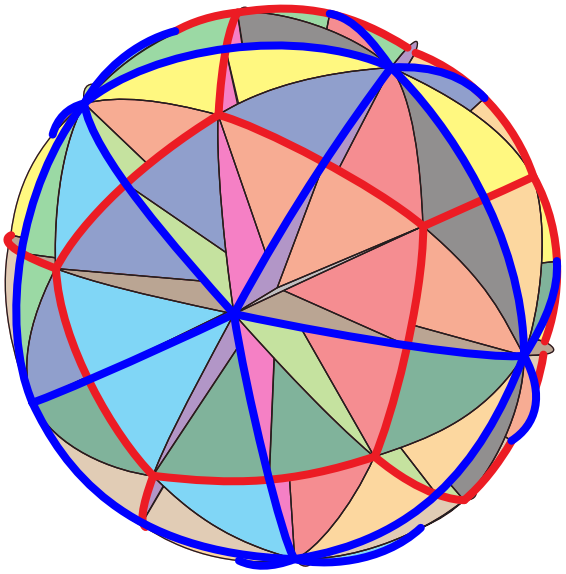

Beyond the weak order in two directions. In Part I, we have used lattice quotients of the weak order to extend the combinatorial, geometric and algebraic properties of the permutahedra, associahedra and cubes presented in Chapter 1. The objective of this part of the document is to extend these properties in a drastically different manner in the following two directions:

⋆ **Beyond the braid arrangement:** On the one hand, we consider classical generalizations of the braid arrangement, first to the Coxeter arrangements of finite Coxeter groups, then to arbitrary hyperplane arrangements.

⋆ **Beyond the vertices of the permutahedron:** On the other hand, we study the combinatorics of geometric objects beyond the vertices of the permutahedron, namely intervals of the weak order, faces of the permutahedron, or arbitrary cones of the braid (and Coxeter) arrangement.

We discuss further these two directions below.

Coxeter arrangements and hyperplane arrangements. This part of the document is the occasion to introduce two classical generalizations of the braid arrangement, with a very geometric flavor.

First, we consider finite Coxeter groups. These are finite groups generated by reflections of an Euclidean vector space, such as the isometry group of the Platonic solids or their higher dimensional analogues. Coxeter groups appear in several places in mathematics, in particular in Lie theory in the classification of crystallographic root systems. For our purposes, the essential features of a finite Coxeter group W are:

- the weak order $\leq_{\mathsf{W}}$, which is a lattice structure on the elements of W,
- the Coxeter arrangement formed by the reflection hyperplanes of W, defining the Coxeter fan $\mathcal{F}(W)$ which is the normal fan of the W-permutahedron $\mathbb{P}\mathrm{erm}(W)$. Each element of W corresponds to a maximal cone of $\mathcal{F}(W)$, thus to a vertex of $\mathbb{P}\mathrm{erm}(W)$. Moreover, the Hasse diagram of the weak order $\leq_{\mathsf{W}}$ is an orientation of the graph of the W-permutahedron $\mathbb{P}\mathrm{erm}(W)$.

We refer to Section 5.2.1 for a brief presentation of finite Coxeter groups and to the textbooks of J. Humphreys [Hum90] and A. Björner and F. Brenti [BB05] for a more detailed treatment and some historical background. It turns out that the weak order on a finite Coxeter group and its lattice quotients share many of the properties of the classical weak order on permutations discussed in Part I. In particular, we introduce in Section 5.2.6 the Cambrian congruences of the weak order, defined by N. Reading [Rea06]. They provide a fundamental lattice structure on the clusters of the finite type cluster algebras, which can be realized as an orientation of the generalized associahedra of [HLT11], as will be studied in Part III.

Second, we consider arbitrary hyperplane arrangements. Introduced by P. Edelman in [Ede84], the poset of regions $\mathsf{R}(\mathcal{H}, B)$ of a hyperplane arrangement $\mathcal{H}$ with respect to a base region B is the poset on all regions of $\mathcal{H}$ ordered by their combinatorial distance to B. A polytopal realization of its Hasse diagram is given by the graph of the zonotope $\mathbb{Z}\mathrm{ono}(\mathcal{H}) := \sum_{H\in\mathcal{H}} \boldsymbol{e}_H$ directed away from B, where $\boldsymbol{e}_H$ is an arbitrary normal vector to the hyperplane H. In [BEZ90], A. Björner, P. Edelman, and G. Ziegler proved that the poset of regions $\mathsf{R}(\mathcal{H}, B)$ of a simplicial hyperplane arrangement is always a lattice. We will see in Section 5.3.1 that some relevant combinatorial aspects of the Coxeter arrangements extend in this setting.

Facial weak order. Our first relevant generalization of the weak order is a lattice structure on all faces of the permutahedron $\mathbb{P}\mathrm{erm}(n)$. Some properties of permutations studied in Part I were already extended to ordered partitions as follows:

⋆ **Combinatorics:** In [KLN+01], D. Krob, M. Latapy, J.-C. Novelli, H.-D. Phan and S. Schwer introduced the pseudopermutahedron, a lattice structure on ordered partitions that extends the weak order on permutations (see Section 5.1.2).

⋆ **Geometry:** Ordered partitions of $[n]$ are in natural bijection with faces of the classical permutahedron $\mathbb{P}\mathrm{erm}(n)$ (see Section 5.1.1).

⋆ **Algebra:** F. Chapoton defined in [Cha00] a Hopf algebra structure on ordered partitions that extends C. Malvenuto and C. Reutenauer's Hopf algebra $\boldsymbol{k}\mathfrak{S}$ on permutations (see Section 5.1.3).

As in Part I, a rich combinatorics then arises from congruences of the pseudopermutahedron. For instance, the faces of J.-L. Loday's associahedron $\mathbb{A}\mathrm{sso}(n)$ correspond to Schröder trees (*i.e.* planar trees where each node has at least two children). Moreover, there is a simple insertion algorithm $\mathbf{st}$ from ordered partitions to Schröder trees, and the fibers of $\mathbf{st}$ define a lattice congruence of the pseudopermutahedron. This yields a lattice structure and a Hopf algebra on the faces of the associahedron $\mathbb{A}\mathrm{sso}(n)$.

In Chapter 5 we study the structure of the faces of the permutahedron beyond the braid arrangement. We consider a poset on these faces, called facial weak order, first in the context of finite Coxeter groups as introduced by P. Palacios and M. Ronco [PR06] and studied in [DHP18] and then for arbitrary hyperplane arrangements as introduced and studied in [DHMP19]. In both settings, we provide various interpretations of this facial weak order (see Sections 5.2.3 and 5.3.2):

- describing the cover relations of the facial weak order,
- using certain sets of roots of the Coxeter group (or normal vectors of the hyperplanes),
- comparing the minimal and maximal elements of the faces in weak order (or in the poset of regions for hyperplane arrangements).

Although not apparent in this document, these different points of view are instrumental to prove that the facial weak order is a lattice for finite Coxeter groups and more generally for hyperplane arrangements whose poset of regions is a lattice. Finally, we observe that each lattice congruence $\equiv_{\mathsf{W}}$ of the weak order naturally extends to a lattice congruence $\equiv_{\mathsf{F}}$ of the facial weak order. Exactly as the classes of $\equiv_{\mathsf{W}}$ correspond to the maximal cones of the quotient fan $\mathcal{F}(\equiv_{\mathsf{W}})$, the classes of $\equiv_{\mathsf{F}}$ correspond to all cones of $\mathcal{F}(\equiv_{\mathsf{W}})$. This defines in particular lattice structures on the faces of the generalized associahedra of [HLT11].

Weak order on posets. In Chapter 6, we generalize the weak order even beyond the faces of the permutahedron $\mathbb{P}\mathrm{erm}(n)$. We consider the set of integer posets, *i.e.* of posets on $[n]$. Our motivation is the geometry of the braid arrangement: integer posets correspond to convex cones in the braid arrangement (not cones of the braid arrangement, but cones obtained by glueing some regions of the braid arrangement), see Chapter 1. In particular, these integer posets provide relevant combinatorial models for the elements, the intervals, and the faces of the weak order and its quotients.

Motivated by our study of the facial weak order, we define a poset on the set of integer posets on $[n]$ (see Section 6.1), obtained by comparing separately the increasing relations and the decreasing relations of the posets. Again, this poset turns out to be a lattice as was shown in [CPP19]. This enables to reinterpret the classical lattice structures on permutations, binary trees, permutrees, ordered partitions, among others as induced subposets of the weak order on integer posets.

We then define a Hopf algebra on all integer posets (see Section 6.2) defined in [PP20]. We show that C. Malvenuto and C. Reutenauer's Hopf algebra on permutations [MR95], and F. Chapoton's algebra on ordered partitions [Cha00] are quotients of the integer poset algebra. Interestingly, we also construct a Hopf algebra on weak order intervals as another quotient of the integer poset algebra. Moreover, as in the usual setting, congruences on the weak order on posets give rise to relevant subalgebras.

Finally, we discuss possible generalizations of the weak order on posets in the context of Coxeter groups studied in [GP18]. Surprisingly, while it extends to crystallographic root systems, natural generalizations of the weak order on posets fail to define lattices beyond crystallographic root systems.

Chapter Five

FACIAL WEAK ORDER

The weak order is a lattice structure on permutations, thus on the vertices of the permutahedron. In this chapter, we discuss the facial weak order, a similar lattice structure on all the faces of the permutahedron, introduced in [KLN+01] for the symmetric group. After a brief review on the classical case (see Section 5.1), we study this order in further generality: first for arbitrary finite Coxeter groups as introduced in [PR06] (see Section 5.2), then for arbitrary hyperplane arrangements whose poset of regions is a lattice (see Section 5.3). While the former setting is a subcase of the later setting, the tools and vocabulary are quite different in the two settings, and we have chosen to present the Coxeter group setting as the results of Chapter 6 will not extend beyond Coxeter groups. In both settings, we provide various interpretations of the facial weak order. This kaleidoscopic perspective then enables us to show that the facial weak order defines a lattice structure on the faces of the permutahedron, which contains the classical weak order (or poset of region) as a sublattice. This chapter is based on joint works with A. Dermenjian, C. Hohlweg and T. McConville [DHP18, DHMP19].

5.1 ORDERED PARTITIONS AND PSEUDOPERMUTAHEDRON

5.1.1 Permutahedron faces

As illustrated in Figure 5.1, the $(n-k)$-dimensional faces of the permutahedron $\mathbb{P}\mathrm{erm}(n)$ correspond to the *ordered partitions* of $[n]$ into k parts, or equivalently to the *surjections* from $[n]$ to $[k]$.

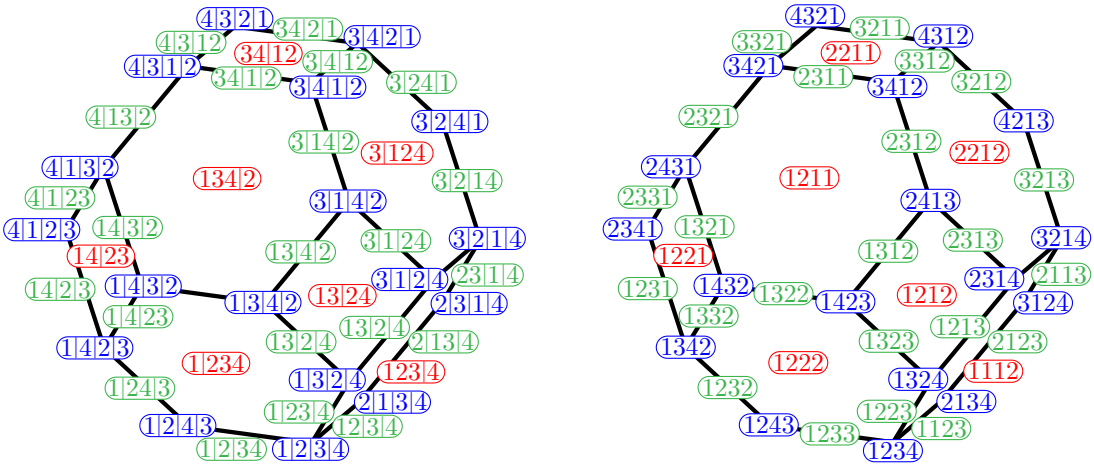

Figure 5.1: The faces of the permutahedron labeled by ordered partitions (left) and surjections (right).

For instance, the vertices of the permutahedron $\mathbb{P}\mathrm{erm}(n)$ correspond to the permutations of $\mathfrak{S}_n$ and its facets corresponds to proper subsets of $[n]$. In fact, the face lattice of the permutahedron is the refinement lattice on ordered partitions. The bijections between these three families are elementary:

- the fibers of a surjection from $[n]$ to $[k]$ define an ordered partition of $[n]$ with k parts,
- the positions in an ordered partition of $[n]$ with k parts define a surjection from $[n]$ to $[k]$,
- an ordered partition λ of $[n]$ into k parts corresponds the $(n-k)$-dimensional face of $\mathbb{P}\mathrm{erm}(n)$ given by $\boldsymbol{F}(\lambda) := \mathrm{conv}\{\sigma \in \mathfrak{S}_n \,|\, \sigma \prec \lambda\}$ (where $\prec$ is the refinement on partitions),
- a surjection ρ from $[n]$ to $[k]$ corresponds to the $(n-k)$-dimensional face of $\mathbb{P}\mathrm{erm}(n)$ whose normal cone is $\boldsymbol{C}^\diamond(\rho) := \big\{\boldsymbol{x} \in \mathbb{1}^\perp \,\big|\, x_i \le x_j \text{ for all } i,j \text{ with } \rho(i) < \rho(j)\big\}$.

In this section, we will work with ordered partitions rather than with surjections to fit with the presentation in Part I. We denote by $\mathfrak{P}_n$ the set of ordered partitions of $[n]$. Abusing notation, we denote by λ^{-1} the surjection corresponding to an ordered partition λ.

5.1.2 Pseudopermutahedron and its quotients

We now introduce a lattice structure on the ordered partitions of $\mathfrak{P}_n$ that extend the weak order on permutations of $\mathfrak{S}_n$. This order was defined in [KLN+01], and its representation theoretic properties were studied in [BHKN01]. It is illustrated for $\mathfrak{P}_3$ on the right.

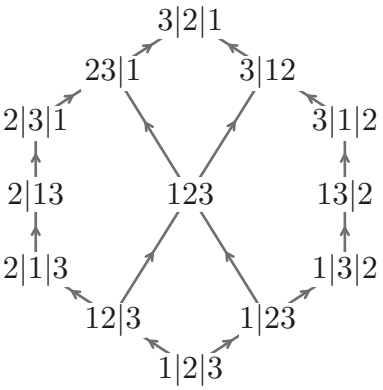

Definition 5.1 ([KLN+01]). *The (right)* inversion map $\mathrm{inv}(\lambda,\cdot,\cdot)$ *of an ordered partition $\lambda \in \mathfrak{P}_n$ is the map from $\binom{[n]}{2}$ to $\{-1,0,1\}$ defined for $i<j$ by $\mathrm{inv}(\lambda,i,j) = \mathrm{sign}\big(\lambda^{-1}(i) - \lambda^{-1}(j)\big)$. The* facial weak order *is the poset $\leq_{\mathsf{F}}$ on the set $\mathfrak{P}_n$ of ordered partitions of $[n]$ defined by $\lambda \leq_{\mathsf{F}} \lambda'$ if $\mathrm{inv}(\lambda,i,j) \le \mathrm{inv}(\lambda',i,j)$ for all $i<j$.*

This poset was called "pseudopermutahedron" in [KLN+01], we prefer the name "facial weak order" to recall that it gives an order on the faces of the permutahedron $\mathbb{P}\mathrm{erm}(n)$.

Note that the restriction of the facial weak order to $\mathfrak{S}_n$ is the classical weak order on permutations, which is a lattice. This property was extended to the facial weak order on $\mathfrak{P}_n$ in [KLN+01].

Theorem 5.2 ([KLN+01]). *The facial weak order $\leq_{\mathsf{F}}$ on the set of ordered partitions $\mathfrak{P}_n$ is a lattice.*

Proposition 5.3 ([KLN+01]). *The cover relations $\lessdot_{\mathsf{F}}$ of the facial weak order $\leq_{\mathsf{F}}$ on $\mathfrak{P}_n$ are:*

$$\begin{aligned}
\lambda_1|\cdots|\lambda_i|\lambda_{i+1}|\cdots|\lambda_k &\lessdot_{\mathsf{F}} \lambda_1|\cdots|\lambda_i\lambda_{i+1}|\cdots|\lambda_k && \text{if } \lambda_i \ll \lambda_{i+1},\\
\lambda_1|\cdots|\lambda_i\lambda_{i+1}|\cdots|\lambda_k &\lessdot_{\mathsf{F}} \lambda_1|\cdots|\lambda_i|\lambda_{i+1}|\cdots|\lambda_k && \text{if } \lambda_{i+1} \ll \lambda_i,
\end{aligned}$$

where $X \ll Y$ means $\max(X) < \min(Y)$ or equivalently $x < y$ for all $x \in X$ and $y \in Y$.

Remark 5.4. As for the weak order on permutations, the lattice quotients of the facial weak order $\leq_{\mathsf{F}}$ on ordered partitions correspond to the faces of some relevant families of polytopes. For instance:

1. faces of the associahedron $\mathbb{A}\mathrm{sso}(n)$ of Chapter 1 correspond to *Schröder trees* with $n+1$ leaves, *i.e.* planar trees where each node has at least two children,
2. faces of the brick polytope $\mathbb{B}\mathrm{rick}^k(n)$ of Chapter 2 correspond to *acyclic hypertwists*, see [Pil18],
3. faces of the permutreehedron $\mathbb{PT}(\delta)$ of Chapter 3 correspond to Schröder δ-permutrees, *i.e.* trees obtained by contracting edges in δ-permutrees. Their nodes are labeled by a partition of $[n]$, and satisfy local conditions around each node similar to that of Definition 3.1. See [PP18, Def. 5.1] for a precise definition and Figure 5.2 for an illustration.

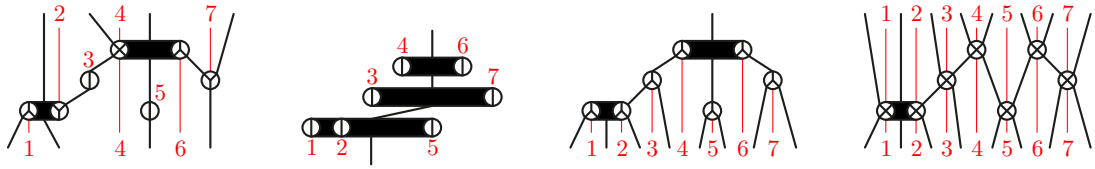

Figure 5.2: Four examples of Schröder permutrees. While the first is generic, the last three use specific decorations corresponding to ordered partitions, Schröder trees, and ternary sequences.

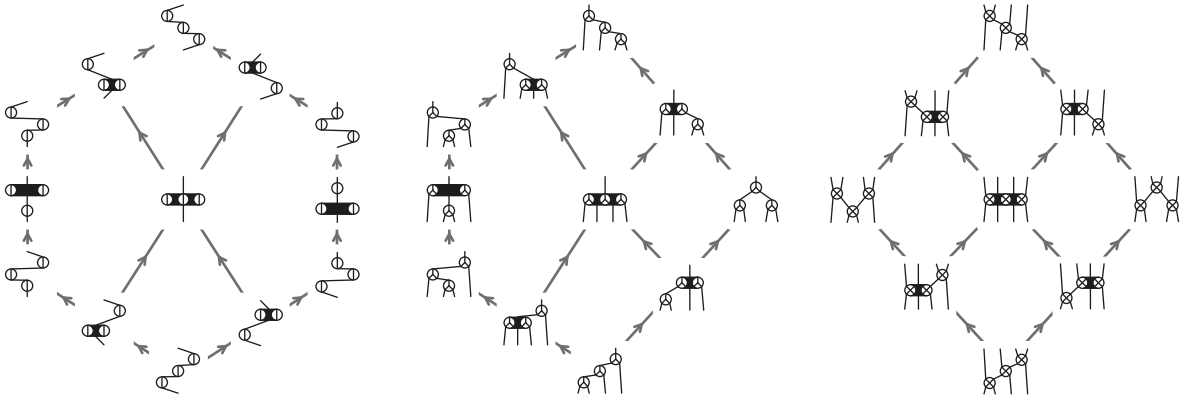

Figure 5.3: The Schröder δ-permutree lattices for $\delta = \bigcirc^3$ (left), $\curlywedge^3$ (middle) and $\otimes^3$ (right).

Moreover, in these three families of examples, there are insertion algorithms (see [Pil18] and [PP18]) similar to the ones of Part I, whose fibers define lattice congruences of the facial weak order on ordered partitions, and thus induce lattice structures on the faces of these polytopes. For instance, Figure 5.3 illustrates lattice structures on the faces of the permutahedron $\mathbb{P}\mathrm{erm}(n)$, associahedron $\mathbb{A}\mathrm{sso}(n)$ and parallelepiped $\mathbb{P}\mathrm{ara}(n)$ seen as lattices on specific families of Schröder permutrees.

5.1.3 Hopf algebras

We now define natural analogues of the shifted shuffle and convolution products of Section 1.3.2 on ordered partitions. Equivalent definitions in the terms of surjections can be found in [Cha00].

We first define two standardizations on ordered partitions. Consider an ordered partition μ of $[n]$ into k parts. We represent graphically μ by the $(k \times n)$-table with a dot in row i and column j for each $j \in \mu_i$. In other words, positions appear on the vertical axis while values appear on the horizontal axis. The *standardization* of a table with some empty rows and columns is the ordered partition table whose dots are in the same horizontal and vertical order. For an ordered partition $\lambda \in \mathfrak{P}_\ell$ and a subset $R \subseteq [\ell]$, we define $\mathbf{stdp}(\lambda, R)$ (resp. $\mathbf{stdv}(\lambda, R)$) as the standardization of the table of λ after deleting all entries whose positions or rows (resp. values or columns) are not in R. See Figure 5.4 for illustrations of these operations. For two ordered partitions $\mu \in \mathfrak{P}_m$ and $\nu \in \mathfrak{P}_n$, define the *shifted shuffle* $\mu \,\bar{\sqcup}\, \nu$ and the *convolution* $\mu \star \nu$ by:

$$\mu \,\bar{\sqcup}\, \nu := \{\lambda \in \mathfrak{P}_{m+n} \,|\, \mathbf{stdv}(\lambda, [m]) = \mu \text{ and } \mathbf{stdv}(\lambda, [m+n] \smallsetminus [m]) = \nu\},$$
$$\text{and} \qquad \mu \star \nu := \{\lambda \in \mathfrak{P}_{m+n} \,|\, \mathbf{stdp}(\lambda, [m]) = \mu \text{ and } \mathbf{stdp}(\lambda, [m+n] \smallsetminus [m]) = \nu\}.$$

E.g., $1|2 \,\bar{\sqcup}\, 2|13 = \{1|2|4|35,\ 1|24|35,\ 1|4|2|35,\ \dots \text{ (12 terms) } \dots,\ 4|1|35|2,\ 4|135|2,\ 4|35|1|2\}$,
$1|2 \star 2|13 = \{1|2|4|35,\ 1|3|4|25,\ 1|4|3|25,\ \dots \text{ (10 terms) } \dots,\ 3|4|2|15,\ 3|5|2|14,\ 4|5|2|13\}$.

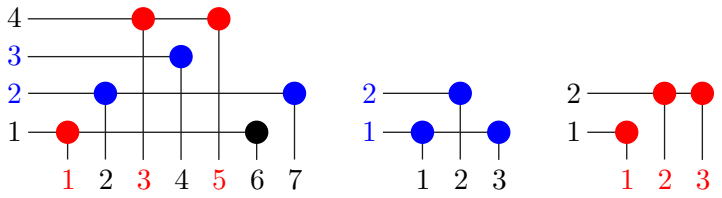

Figure 5.4: The tables of the ordered partitions $\mu = 16|27|4|35$ (left) and of its restrictions $\mathbf{stdp}(\mu, \{2,3\}) = 13|2$ (middle) and $\mathbf{stdv}(\mu, \{1,3,5\}) = 1|23$ (right).

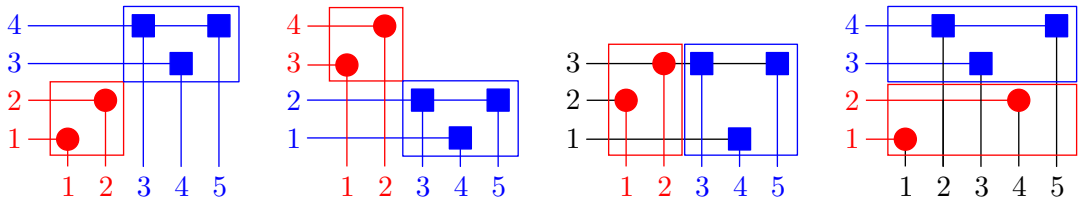

Figure 5.5: The tables of the products $\mu\backslash\nu$ (left) and μ/ν (middle left) have two blocks containing the tables of $\mu = 1|2$ and $\nu = 2|31$. Elements of the shifted shuffle product $\mu \,\bar{\sqcup}\, \nu$ (middle right) and the convolution product $\mu \star \nu$ (right) are obtained by shuffling the rows and columns of the table of $\mu\backslash\nu$.

This is illustrated in Figure 5.5 on ordered partition tables. These operations yield a natural generalization of C. Malvenuto and C. Reutenauer's Hopf algebra $\boldsymbol{k}\mathfrak{S}$ on permutations to all ordered partitions, introduced in [Cha00]. Note that the ordered partition Hopf algebra is the dual of the algebra of word quasi-symmetric functions, see [BZ09, NT06].

Proposition 5.5 (Adapted from [Cha00])**.** *The vector space $\boldsymbol{k}\mathfrak{P}$ with basis $(\mathbb{F}_\lambda)_{\lambda\in\mathfrak{P}}$ endowed with the product $\mathbb{F}_\mu \cdot \mathbb{F}_\nu = \sum_{\lambda\in\mu\,\bar{\sqcup}\,\nu} \mathbb{F}_\lambda$ and the coproduct $\triangle\mathbb{F}_\lambda = \sum_{\lambda\in\mu\star\nu} \mathbb{F}_\mu \otimes \mathbb{F}_\nu$ is a Hopf algebra.*

The product in $\boldsymbol{k}\mathfrak{P}$ behaves nicely with the facial weak order $\leq_{\mathsf{F}}$ on $\mathfrak{P}_n$. For two ordered partitions μ of m with p parts and ν or n with q parts, consider the ordered partitions $\mu\backslash\nu$ and μ/ν of $m+n$ with $p+q$ parts defined by:

$$(\mu\backslash\nu)_i = \begin{cases} \mu_i & \text{if } i \in [p] \\ m + \nu_{i-p} & \text{otherwise} \end{cases} \quad \text{and} \quad (\mu/\nu)_i = \begin{cases} m + \nu_i & \text{if } i \in [q] \\ \mu_{i-q} & \text{otherwise,} \end{cases}$$

where $x+Y = \{x+y \,|\, y \in Y\}$ for $x \in \mathbb{N}$ and $Y \subset \mathbb{N}$. These notations should be clear on the ordered partition tables of $\mu\backslash\nu$ and μ/ν, illustrated in Figure 5.5 (remember our unconventional orientation!). The shifted shuffle $\mu \,\bar{\sqcup}\, \nu$ is then the interval between $\mu\backslash\nu$ and μ/ν in the facial weak order $\leq_{\mathsf{F}}$ on $\mathfrak{P}_{m+n}$. This extends to a product of facial weak order intervals.

Proposition 5.6. *A product of facial weak order intervals in $\boldsymbol{k}\mathfrak{P}$ is a facial weak order interval: for two intervals $[\underline{\mu}, \overline{\mu}]_{\mathsf{F}} \subseteq \mathfrak{P}_m$ and $[\underline{\nu}, \overline{\nu}]_{\mathsf{F}} \subseteq \mathfrak{P}_n$, we have* $\sum_{\underline{\mu}\leq_{\mathsf{F}}\mu\leq_{\mathsf{F}}\overline{\mu}} \mathbb{F}_\mu \cdot \sum_{\underline{\nu}\leq_{\mathsf{F}}\nu\leq_{\mathsf{F}}\overline{\nu}} \mathbb{F}_\nu = \sum_{\underline{\mu}\backslash\underline{\nu}\leq_{\mathsf{F}}\lambda\leq_{\mathsf{F}}\overline{\mu}/\overline{\nu}} \mathbb{F}_\lambda.$

Remark 5.7. As in Part I, relevant congruences of the facial weak order yield relevant Hopf subalgebras of the ordered partition Hopf algebra $\boldsymbol{k}\mathfrak{P}$. For instance, there is:

1. a Hopf subalgebra indexed by Schröder trees (already considered in [Cha00]), analogue to J.-L. Loday and M. Ronco's Hopf algebra $\boldsymbol{k}\mathfrak{T}$ on binary trees,
2. a Hopf subalgebra indexed by acyclic hypertwists [Pil18], analogue to the twist Hopf algebra,
3. a Hopf algebra on Schröder permutrees [PP18] obtained as a Hopf subalgebra of the Hopf algebra on decorated ordered partitions, analogue to the permutree Hopf algebra.

5.2 Facial weak order on finite Coxeter groups

5.2.1 Finite Coxeter groups

We start by fixing notations on finite Coxeter groups. Detailled treatments and historical perspectives can be found in textbooks by J. Humphreys [Hum90] and A. Björner and F. Brenti [BB05].

Finite reflection groups and Coxeter systems. Let $(V, \langle \cdot \,|\, \cdot \rangle)$ be an n-dimensional Euclidean vector space. For any vector $v \in V \setminus \{0\}$, we denote by s_v the reflection interchanging v and $-v$ while fixing pointwise the orthogonal hyperplane. We consider a *finite reflection group* W acting on V, that is, a finite group generated by reflections in the orthogonal group $O(V)$. For instance, the Coxeter groups of types A_3, B_3, and H_3 represented in Figure 5.6 are the reflection groups of the tetrahedron, the cube or its dual octahedron, and the dodecahedron or its dual icosahedron respectively. The *Coxeter arrangement* of W is the collection of all reflecting hyperplanes. Its complement in V is a union of open polyhedral cones whose closures are called *chambers*. The *Coxeter fan* is the polyhedral fan $\mathcal{F}(W)$ formed by the chambers together with all their faces. It is complete and simplicial, and we can assume without loss of generality that it is essential. We fix an arbitrary chamber C which we call the *fundamental chamber*. The n reflections orthogonal to the facet defining hyperplanes of C are called *simple reflections*. The set S of simple reflections generates W. In particular, the set of *reflections* is the set $T = \left\{ wsw^{-1} \,\middle|\, w \in W \text{ and } s \in S \right\}$. The pair (W, S) forms a *Coxeter system*.

Roots and weights. We consider a *root system* Φ for W, *i.e.* a set of vectors invariant under the action of W and containing precisely two opposite roots orthogonal to each reflecting hyperplane of W. The *simple roots* Δ are the roots orthogonal to the defining hyperplanes of C and pointing towards C. They form a linear basis of V. The root system Φ splits into the *positive roots* $\Phi^+ := \Phi \cap \mathbb{R}_{\geq 0}\Delta$ and the *negative roots* $\Phi^- := \Phi \cap \mathbb{R}_{\leq 0}\Delta = -\Phi^+$. In other words, the positive roots are the roots whose scalar product with any vector of the interior of the fundamental chamber C is positive, and the simple roots form the basis of the cone generated by Φ^+. More generally, for $R \subseteq \Phi$, we denote by $R^+ := R \cap \Phi^+$ and by $R^- := R \cap \Phi^-$. Each reflecting hyperplane is orthogonal to one positive and one negative root. For a reflection $s \in T$, we set α_s to be the unique positive root orthogonal to the reflecting hyperplane of s, *i.e.* such that $s = s_{\alpha_s}$.

The *Cartan matrix* of the simple system $\Delta = \{\alpha_1, \ldots, \alpha_n\}$ is the matrix $A = [a_{ij}]_{i,j \in [n]}$ defined by $a_{ij} := 2\langle \alpha_i \,|\, \alpha_j \rangle / \langle \alpha_j \,|\, \alpha_j \rangle$. It records the angles between the reflection hyperplanes of Δ.

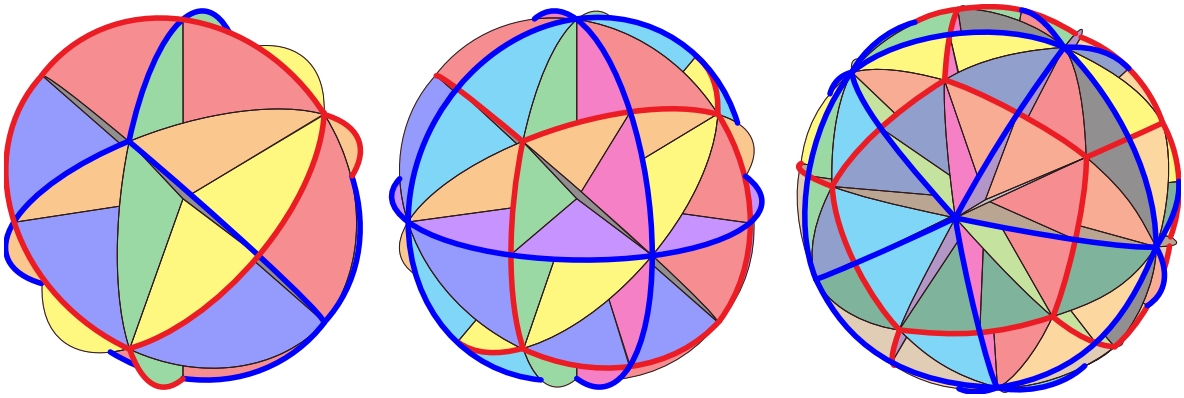

Figure 5.6: The type A_3, B_3, and H_3 Coxeter arrangements.

We denote by $\alpha_s^\vee := 2\alpha_s/\langle \alpha_s \,|\, \alpha_s\rangle$ the *coroot* corresponding to $\alpha_s \in \Delta$, and by $\Delta^\vee := \{\alpha_s^\vee \,|\, s \in S\}$ the coroot basis. The vectors of its dual basis $\nabla := \{\omega_s \,|\, s \in S\}$ are called *fundamental weights* (thus $\langle \alpha_s^\vee \,|\, \omega_t\rangle = \delta_{s=t}$ for all $s, t \in S$). Equivalently, the simple roots of Δ and the fundamental weights of ∇ are two bases[1] of V related by the Cartan matrix. Geometrically, the fundamental weight ω_s gives the direction of the ray of the fundamental chamber C not contained in the reflecting hyperplane of s. We let $\Omega := W(\nabla) = \{w(\omega_s) \,|\, w \in W, s \in S\}$ denote the set of all weights of W, obtained as the orbit of the fundamental weights under W.

Length, reduced words and weak order. The *length* $\ell(w)$ of an element $w \in W$ is the length of the smallest word for w as a product of generators in S. A word $w = s_1 \cdots s_k$ with $s_1, \dots, s_k \in S$ is called *reduced* if $k = \ell(w)$. For $u, v \in W$, the product uv is said to be *reduced* if the concatenation of a reduced word for u and of a reduced word for v is a reduced word for uv, *i.e.* if $\ell(uv) = \ell(u) + \ell(v)$. We say that $u \in W$ is a *prefix* of $v \in W$ if there is a reduced word for u that is the prefix of a reduced word for v, *i.e.* if $\ell(u^{-1}v) = \ell(v) - \ell(u)$.

The (right) *weak order* is the order on W defined by $u \leq_{\mathsf{W}} v$ if and only if $\ell(u) + \ell(u^{-1}v) = \ell(v)$, or equivalently if and only if u is a prefix of v. By a result of A. Björner [Bjö84], the weak order defines a lattice structure on W, with minimal element e and maximal element $w_\circ$ (which sends all positive roots to negative ones and all positive simple roots to negative simple ones). The conjugation $w \mapsto w_\circ w w_\circ$ defines an automorphism while the left and right multiplications $w \mapsto w_\circ w$ and $w \mapsto w w_\circ$ define anti-automorphisms of the weak order. See [BB05, Chap. 3] for more details.

The weak order encodes the combinatorics of reduced words and enjoys a useful geometric characterization within the root system, which we explain now. The (left) *inversion set* of w is the set $\boldsymbol{N}(w) := \Phi^+ \cap w(\Phi^-)$ of positive roots sent to negative ones by w^{-1}. If $w = uv$ is reduced then $\boldsymbol{N}(w) = \boldsymbol{N}(u) \sqcup u\big(\boldsymbol{N}(v)\big)$. In particular, we have $\boldsymbol{N}(w) = \big\{\alpha_{s_1}, s_1(\alpha_{s_2}), \dots, s_1 s_2 \cdots s_{p-1}(\alpha_{s_k})\big\}$ for any reduced word $w = s_1 \cdots s_k$, and therefore $\ell(w) = |\boldsymbol{N}(w)|$. Moreover, the weak order is characterized in term of inversion sets by: $u \leq_{\mathsf{W}} v$ if and only if $\boldsymbol{N}(u) \subseteq \boldsymbol{N}(v)$ for any $u, v \in W$.

We say that $s \in S$ is a *left ascent* of $w \in W$ if $\ell(sw) = \ell(w) + 1$ and a *left descent* of w if $\ell(sw) = \ell(w) - 1$. We denote by $D_L(w)$ the set of left descents of w. Note that for $s \in S$ and $w \in W$, we have $s \in D_L(w) \iff \alpha_s \in \boldsymbol{N}(w) \iff s \leq_{\mathsf{W}} w$. Similarly, $s \in S$ is a *right descent* of $w \in W$ if $\ell(ws) = \ell(w) - 1$, and we denote by $D_R(w)$ the set of right descents of w.

Parabolic subgroups and cosets. Consider a subset $I \subseteq S$. The *standard parabolic subgroup* W_I is the subgroup of W generated by I. It is also a Coxeter group with simple generators I, simple roots $\Delta_I := \{\alpha_s \,|\, s \in I\}$, root system $\Phi_I = W_I(\Delta_I) = \Phi \cap \mathrm{span}(\Delta_I)$, length function $\ell_I = \ell\,|_{W_I}$, longest element $w_{\circ,I}$, etc. For example, $W_\varnothing = \{e\}$ while $W_S = W$.

We denote by $W^I := \{w \in W \,|\, \ell(ws) > \ell(w) \text{ for all } s \in I\}$ the set of elements of W with no right descents in I. For example, $W^\varnothing = W$ while $W^S = \{e\}$. Observe that for any $x \in W^I$, we have $x(\Delta_I) \subseteq \Phi^+$ and thus $x(\Phi_I^+) \subseteq \Phi^+$.

Any element $w \in W$ admits a unique factorization $w = w^I \cdot w_I$ with $w^I \in W^I$ and $w_I \in W_I$, and moreover, $\ell(w) = \ell(w^I) + \ell(w_I)$, see [BB05, Prop. 2.4.4]. Therefore, W^I is the set of *minimal length coset representatives* of the *standard parabolic coset* W/W_I. Throughout the chapter, we will always implicitly assume that $x \in W^I$ when writing that xW_I. Note that any standard parabolic coset $xW_I = [x, xw_{\circ,I}]$ is an interval in the weak order. We denote by $\mathscr{F}_W$ the set of all standard parabolic cosets of W, or equivalently of faces of the W-permutahedron $\mathbb{P}\mathrm{erm}(W)$ defined next.

[1] As we work in finite dimension, we always implicitly identify the Euclidean vector space V with its dual $V^\vee$. In particular, we consider that the roots, coroots, weights and coweights all live in the same space V.

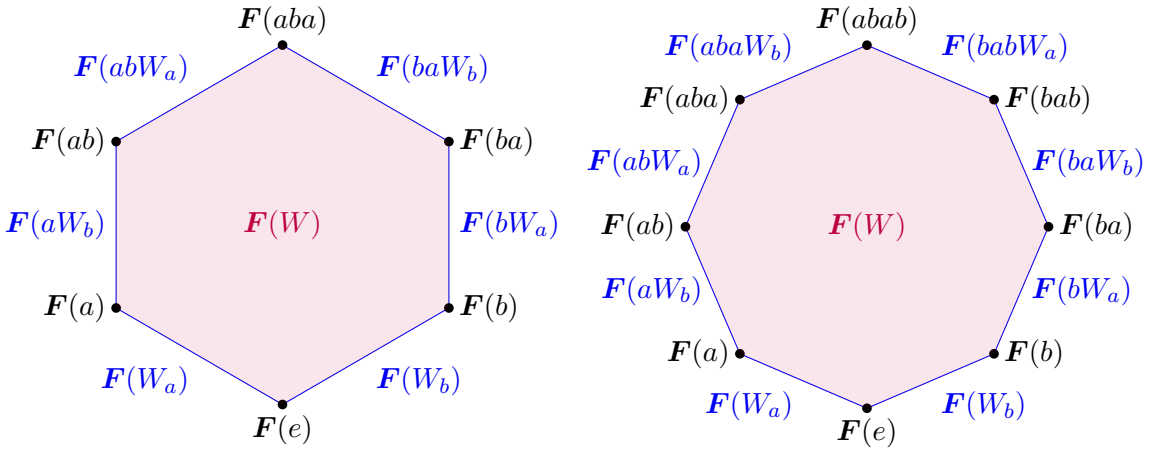

Figure 5.7: Standard parabolic cosets of the type A_2 and B_2 Coxeter groups and the corresponding faces on their permutahedra.

Permutahedron. The *W-permutahedron* $\mathbb{P}\mathrm{erm}^p(W)$ is the convex hull of the orbit under W of a generic point $p \in V$ (not located on a reflection hyperplane of W). Its vertex and facet descriptions are

$$\mathbb{P}\mathrm{erm}^p(W) = \operatorname{conv}\big\{w(p) \mid w \in W\big\} = \bigcap_{\substack{s\in S\\ w\in W}} \big\{v \in V \mid \langle w(\omega_s) \,|\, v\rangle \le \langle \omega_s \,|\, p\rangle\big\}.$$

Examples in types A_2, B_2, A_3, B_3, and H_3 are represented in Figures 5.7 and 5.8.

We often write $\mathbb{P}\mathrm{erm}(W)$ instead of $\mathbb{P}\mathrm{erm}^p(W)$ as the combinatorics of the W-permutahedron is independent of the choice of the point p. Namely, each standard parabolic coset xW_I corresponds to a face $\boldsymbol{F}(xW_I) = x\big(\mathbb{P}\mathrm{erm}^p(W_I)\big) = \mathbb{P}\mathrm{erm}^{x(p)}(xW_Ix^{-1})$ of $\mathbb{P}\mathrm{erm}^p(W)$. Therefore, the k-dimensional faces of $\mathbb{P}\mathrm{erm}^p(W)$ correspond to the cosets xW_I with $|I| = k$ and the face lattice of $\mathbb{P}\mathrm{erm}^p(W)$ is isomorphic to the inclusion poset $(\mathscr{F}_W, \subseteq)$. The normal fan of $\mathbb{P}\mathrm{erm}^p(W)$ is the Coxeter fan $\mathcal{F}(W)$. The graph of the permutahedron $\mathbb{P}\mathrm{erm}^p(W)$ is isomorphic to the Cayley graph of the Coxeter system (W, S). Moreover, when oriented in the linear direction $\boldsymbol{\omega} := w_\circ(p) - p$, it coincides with the Hasse diagram of the (right) weak order on W. We refer to [Hoh12] for more details on the W-permutahedron $\mathbb{P}\mathrm{erm}(W)$.

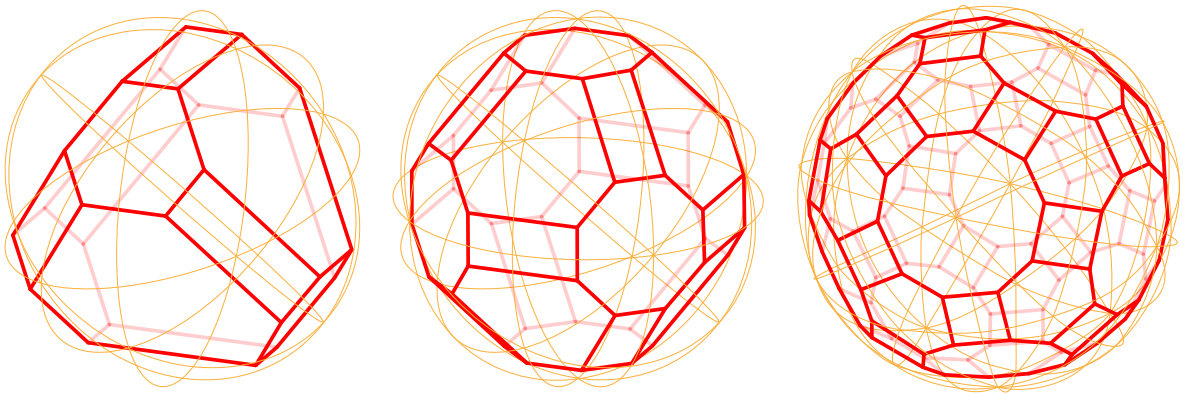

Figure 5.8: The type A_3, B_3, and H_3 permutahedra.

Example 5.8. The Coxeter group of type A_{n-1} is the symmetric group $\mathfrak{S}_n$. Its simple generators are the simple transpositions $\tau_i = (i\ i{+}1)$ for $i \in [n{-}1]$ with relations $\tau_i^2 = 1$ and $\tau_i\tau_{i+1}\tau_i = \tau_{i+1}\tau_i\tau_{i+1}$. Its elements are permutations of $[n]$ and its standard parabolic cosets are ordered partitions of $[n]$. A root system for $\mathfrak{S}_n$ consists in the set of vectors $\{\boldsymbol{e}_i - \boldsymbol{e}_j \,|\, i \neq j \in [n]\}$ where $(\boldsymbol{e}_1, \dots, \boldsymbol{e}_n)$ is the canonical basis of $\mathbb{R}^n$. Finally, $\mathcal{F}(A_{n-1}) = \mathcal{F}(n)$ and $\mathbb{P}\mathrm{erm}(A_{n-1}) = \mathbb{P}\mathrm{erm}(n)$. See Figure 5.6 (left) for the type A_3 arrangement, and Figures 5.7 (left) and 5.8 (left) for the type A_2 and A_3 permutahedra.

5.2.2 Root and weight sets of a face

As we are interested in the faces of the W-permutahedron $\mathbb{P}\mathrm{erm}(W)$, it is natural to consider the primal and normal cones of these faces. As we work in a Coxeter group, these cones can be completely encoded by the following collections of roots and weights.

Definition 5.9. *The root set $\boldsymbol{R}(xW_I)$ and weight set $\boldsymbol{W}(xW_I)$ of a standard parabolic coset xW_I are*

$$\boldsymbol{R}(xW_I) := x\big(\Phi^- \cup \Phi_I^+\big) \subseteq \Phi \qquad \text{and} \qquad \boldsymbol{W}(xW_I) := x\big(\nabla_{S \smallsetminus I}\big) \subseteq \Omega.$$

The following statement gives the precise connection of the root and weight sets to the geometry of the W-permutahedron $\mathbb{P}\mathrm{erm}(W)$ and is illustrated on Figure 5.9 for the Coxeter group of type A_2.

Proposition 5.10. *Let xW_I be a standard parabolic coset of W. Then:*
(i) the cone $\mathbb{R}_{\geq 0}\,\boldsymbol{R}(xW_I)$ is the inner primal cone of the face $\boldsymbol{F}(xW_I)$ of $\mathbb{P}\mathrm{erm}(W)$,
(ii) the cone $\mathbb{R}_{\geq 0}\,\boldsymbol{W}(xW_I)$ is the outer normal cone of the face $\boldsymbol{F}(xW_I)$ of $\mathbb{P}\mathrm{erm}(W)$,
(iii) the cones generated by the root set and by the weight set of xW_I are polar to each other.

Our next statement connects the root set $\boldsymbol{R}(xW_\varnothing)$ to the inversion set and reduced words of $x \in W$. For brevity we write $\boldsymbol{R}(x)$ instead of $\boldsymbol{R}(xW_\varnothing)$.

Proposition 5.11. *For any $x \in W$, we have:*
(i) $\boldsymbol{R}(x) = \boldsymbol{N}(x) \cup -\big(\Phi^+ \smallsetminus \boldsymbol{N}(x)\big)$ where $\boldsymbol{N}(x) = \Phi^+ \cap x(\Phi^-)$ is the inversion set of x.
(ii) If $x = s_1 s_2 \cdots s_k$ is reduced, then $\boldsymbol{R}(xW_\varnothing) = \Phi^- \triangle \{\pm\alpha_{s_1}, \pm s_1(\alpha_{s_2}), \dots, \pm s_1 \cdots s_{k-1}(\alpha_{s_k})\}$.
(iii) $\boldsymbol{R}(xw_\circ) = -\,\boldsymbol{R}(x)$ and $\boldsymbol{R}(w_\circ x) = w_\circ\big(\boldsymbol{R}(x)\big)$.

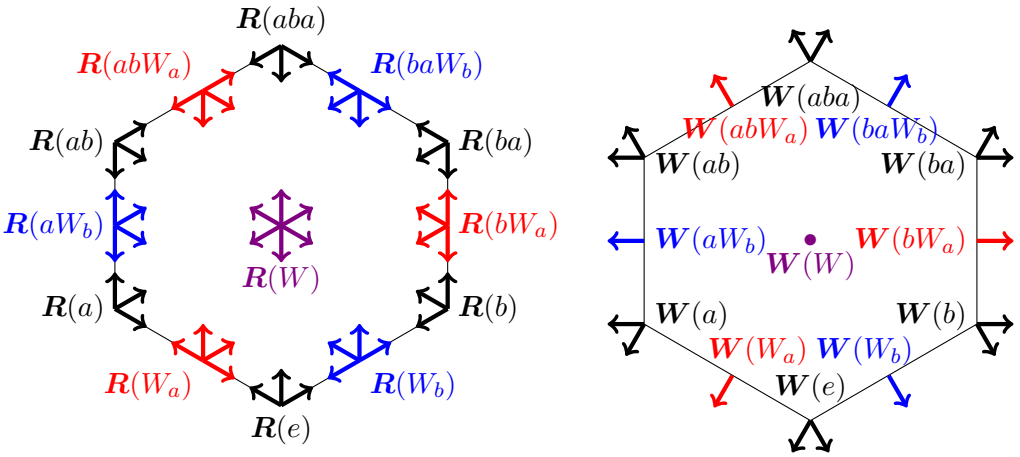

Figure 5.9: The root set (left) and weight set (right) of the standard parabolic cosets in type A_2. Note that positive roots point downwards.

The next statement gives a characterization of the weak order on W in terms of root sets, which translates the characterization of the weak order in term of inversion sets.

Corollary 5.12. *For $x, y \in W$, we have:*

$$\begin{aligned} x \leq_{\mathsf{W}} y &\iff \boldsymbol{R}(x) \smallsetminus \boldsymbol{R}(y) \subseteq \Phi^- \quad \text{and} \quad \boldsymbol{R}(y) \smallsetminus \boldsymbol{R}(x) \subseteq \Phi^+, \\ &\iff \boldsymbol{R}(x)^+ \subseteq \boldsymbol{R}(y)^+ \quad \text{and} \quad \boldsymbol{R}(x)^- \supseteq \boldsymbol{R}(y)^-. \end{aligned}$$

Finally, we observe that the root and weight sets of a parabolic coset xW_I can be computed from that of its minimal and maximal length representatives x and $xw_{\circ,I}$.

Proposition 5.13. *The root and weight sets of xW_I can be computed from those of x and $xw_{\circ,I}$ by:*

$$\boldsymbol{R}(xW_I) = \boldsymbol{R}(x) \cup \boldsymbol{R}(xw_{\circ,I}) \qquad \text{and} \qquad \boldsymbol{W}(xW_I) = \boldsymbol{W}(x) \cap \boldsymbol{W}(xw_{\circ,I}).$$

5.2.3 Three equivalent definitions of the facial weak order

We are now ready to define the facial weak order on $\mathscr{F}_W$. We start with the original definition of P. Palacios and M. Ronco [PR06], illustrated in Figure 5.10.

Definition 5.14 ([PR06])**.** *The (right) facial weak order is the order $\leq_{\mathsf{F}}$ on $\mathscr{F}_W$ defined by cover relations of two types: for $I \subseteq S$ and $x \in W^I$,*

$$\begin{aligned} &(1) \qquad xW_I \lessdot_{\mathsf{F}} xW_{I\cup\{s\}} \qquad \text{if } s \notin I \text{ and } x \in W^{I\cup\{s\}}, \\ &(2) \qquad xW_I \lessdot_{\mathsf{F}} xw_{\circ,I}w_{\circ,I\smallsetminus\{s\}}W_{I\smallsetminus\{s\}} \qquad \text{if } s \in I. \end{aligned}$$

Note that these cover relations translate to the following geometric conditions on faces of the permutahedron $\mathbb{P}\mathrm{erm}(W)$: a face F is covered by a face G if and only if either F is a facet of G with the same weak order minimum, or G is a facet of F with the same weak order maximum.

This original definition is difficult to manipulate as it relies on cover relations. The following statement provides two equivalent definitions of the facial weak order, proved in [DHP18].

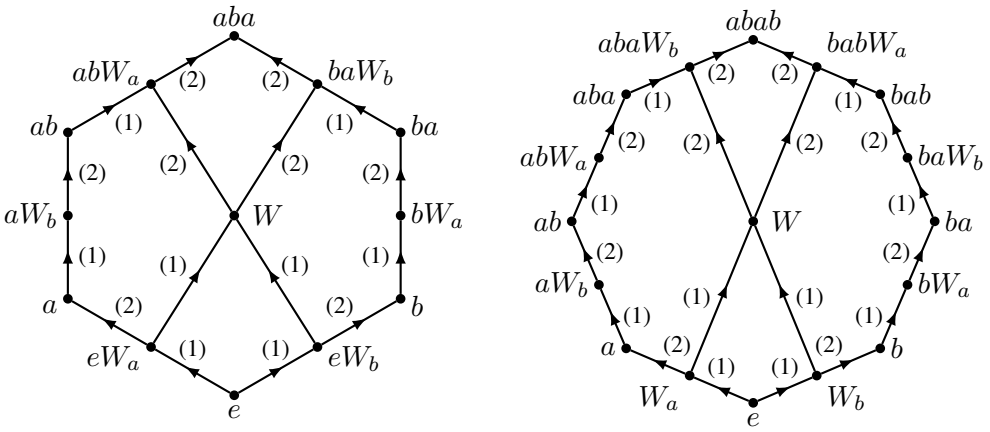

Figure 5.10: The facial weak order on the standard parabolic cosets of the Coxeter group of types A_2 and B_2. Edges are labelled with the cover relations of type (1) or (2) as in Definition 5.14.

Theorem 5.15. *The following conditions are equivalent for two standard parabolic cosets xW_I and yW_J of $\mathscr{F}_W$:*
(i) $xW_I \leq_{\mathsf{F}} yW_J$ *in facial weak order of Definition 5.14,*
(ii) $\boldsymbol{R}(xW_I)^+ \subseteq \boldsymbol{R}(yW_J)^+$ *and* $\boldsymbol{R}(xW_I)^- \supseteq \boldsymbol{R}(yW_J)^-$,
(iii) $x \leq_{\mathsf{W}} y$ *and* $xw_{\circ,I} \leq_{\mathsf{W}} yw_{\circ,J}$ *in weak order.*

Remark 5.16. Three quick observations about the conditions of Theorem 5.15:
- An alternative way to write (ii) is $\boldsymbol{R}(xW_I) \smallsetminus \boldsymbol{R}(yW_J) \subseteq \Phi^-$ and $\boldsymbol{R}(yW_J) \smallsetminus \boldsymbol{R}(xW_I) \subseteq \Phi^+$.
- Recall that the set $\{[x, X] \,|\, x, X \in P,\ x \leq X\}$ of all intervals of any poset P is itself ordered by $[x, X] \leq_{\mathsf{I}} [y, Y] \iff x \leq y$ and $X \leq Y$. Therefore, (iii) states that the facial weak order $\leq_{\mathsf{F}}$ on $\mathscr{F}_W$ is the subposet of the poset of intervals of the weak order $\leq_{\mathsf{W}}$ induced by the facial intervals (*i.e.* of the form $[x, xw_{\circ,I}]_{w_\circ}$ for all standard parabolic cosets $xW_I \in \mathscr{F}_W$).
- (iii) implies the following statements, not obvious with the cover relations from Definition 5.14.

Corollary 5.17. *The weak order $\leq_{\mathsf{W}}$ is the subposet of the facial weak order $\leq_{\mathsf{F}}$ induced by $W_\varnothing$-cosets. In other words, $x \leq_{\mathsf{W}} y$ if and only if $xW_\varnothing \leq_{\mathsf{F}} yW_\varnothing$ for any $x, y \in W$.*

Corollary 5.18. *The maps $xW_I \mapsto w_\circ x w_{\circ,I} W_I$ and $xW_I \mapsto xw_{\circ,I}w_\circ W_{w_\circ I w_\circ}$ are anti-automorphisms of the facial weak order $\leq_{\mathsf{F}}$. Hence, the map $xW_I \mapsto w_\circ x w_\circ W_{w_\circ I w_\circ}$ is an automorphism.*

Example 5.19. The facial weak order of the Coxeter group A_{n-1} is isomorphic to the facial weak order on ordered partitions of $[n]$. Compare for instance the facial weak order in type A_2 represented in Figure 5.10 (left) with the facial weak order on ordered partitions of $[3]$ represented in the right of Definition 5.1. Observe in particular that:
- the cover relations of Definition 5.14 translate to that of Proposition 5.3 on ordered partitions,
- condition (ii) of Theorem 5.15 translate to that of Definition 5.1 on ordered partitions,
- in contrast, condition (iii) of Theorem 5.15 was not observed earlier in type A.

5.2.4 The facial weak order is a lattice

The following statement is the central result of [DHP18], generalizing the result of [KLN+01] stated in Theorem 5.2. The characterizations of Theorem 5.15 are instrumental in the proof.

Theorem 5.20. *The facial weak order $\leq_{\mathsf{F}}$ is a lattice. The meet $\wedge_{\mathsf{F}}$ and join $\vee_{\mathsf{F}}$ of two standard parabolic cosets xW_I and yW_J are given by:*
- $xW_I \wedge_{\mathsf{F}} yW_J = z_\wedge W_{K_\wedge}$, *where* $z_\wedge = x \wedge_{\mathsf{W}} y$ *and* $K_\wedge = D_L\big(z_\wedge^{-1}(xw_{\circ,I} \wedge_{\mathsf{W}} yw_{\circ,J})\big)$,
- $xW_I \vee_{\mathsf{F}} yW_J = z_\vee W_{K_\vee}$, *where* $z_\vee = xw_{\circ,I} \vee_{\mathsf{W}} yw_{\circ,J}$ *and* $K_\vee = D_L\big(z_\vee^{-1}(x \vee_{\mathsf{W}} y)\big)$.

Remark 5.21. Two important observations on this statement:
- In the second point, the minimal representative of the coset $z_\vee W_{K_\vee}$ is in fact $z_\vee w_{\circ,K_\vee}$, not $z_\vee$. We take the liberty to use another coset representative than the minimal one to underline the symmetry between meet and join in facial weak order.
- The expressions for the meet and join can be interpreted in the lattice of weak order intervals. Indeed, the poset $\leq_{\mathsf{I}}$ on intervals of a lattice L is again a lattice whose meet and join are given by $[x, X] \wedge_{\mathsf{I}} [y, Y] = [x \wedge y, X \wedge Y]$ and $[x, X] \vee_{\mathsf{I}} [y, Y] = [x \vee y, X \vee Y]$. However, the meet interval $[x, xw_{\circ,I}]_{\mathsf{W}} \wedge_{\mathsf{I}} [y, yw_{\circ,J}]_{\mathsf{W}} = [x \wedge_{\mathsf{W}} y, xw_{\circ,I} \wedge_{\mathsf{W}} yw_{\circ,J}]_{\mathsf{W}}$ of two cosets xW_I and yW_J is not anymore a standard parabolic coset. The meet $xW_I \wedge_{\mathsf{F}} yW_J$ in the facial weak order is obtained as the biggest parabolic coset in this meet interval containing $x \wedge_{\mathsf{W}} y$. Similarly, the join $xW_I \vee_{\mathsf{F}} yW_J$ is obtained as the biggest parabolic coset in the join interval $[x, xw_{\circ,I}]_{\mathsf{W}} \vee_{\mathsf{I}} [y, yw_{\circ,J}]_{\mathsf{W}} = [x \vee_{\mathsf{W}} y, xw_{\circ,I} \vee_{\mathsf{W}} yw_{\circ,J}]_{\mathsf{W}}$ containing $xw_{\circ,I} \vee_{\mathsf{W}} yw_{\circ,J}$.

Corollary 5.22. *The weak order $\leq_{\mathsf{W}}$ is the sublattice of the facial weak order $\leq_{\mathsf{F}}$ induced by $W_\varnothing$-cosets. In other words, $xW_\varnothing \wedge_{\mathsf{F}} yW_\varnothing = (x \wedge_{\mathsf{W}} y)W_\varnothing$ and $xW_\varnothing \vee_{\mathsf{F}} yW_\varnothing = (x \vee_{\mathsf{W}} y)W_\varnothing$ for any $x, y \in W$.*

5.2.5 Lattice quotients of the facial weak order

In this section we observe that any lattice congruence $\equiv_{\mathsf{W}}$ of the weak order $\leq_{\mathsf{W}}$ on W extends to a lattice congruence $\equiv_{\mathsf{F}}$ of the facial weak order $\leq_{\mathsf{F}}$ on $\mathscr{F}_W$. Consider a lattice congruence $\equiv_{\mathsf{W}}$ of the weak order $\leq_{\mathsf{W}}$ on W with up and down projections $\pi^{\uparrow}$ and $\pi_{\downarrow}$. We want to extend $\equiv_{\mathsf{W}}$ to a lattice congruence $\equiv_{\mathsf{F}}$ of the facial weak order on $\mathscr{F}_W$. We need the following technical statement.

Lemma 5.23. *There exist unique subsets $\Sigma^{\uparrow}(xW_I) \subseteq S \smallsetminus D_R\big(\pi^{\uparrow}(x)\big)$ and $\Sigma_{\downarrow}(xW_I) \subseteq D_R\big(\pi_{\downarrow}(xw_{\circ,I})\big)$ such that $xw_{\circ,I} \leq_{\mathsf{W}} \pi^{\uparrow}(x)w_{\circ,\Sigma^{\uparrow}(x,I)} \leq_{\mathsf{W}} \pi^{\uparrow}(xw_{\circ,I})$ and $\pi_{\downarrow}(x) \leq_{\mathsf{W}} \pi_{\downarrow}(xw_{\circ,I})w_{\circ,\Sigma_{\downarrow}(x,I)} \leq_{\mathsf{W}} x$.*

Based on this lemma, we can define two projection maps $\Pi^{\uparrow}$ and $\Pi_{\downarrow}$ from $\mathscr{F}_W$ to itself by $\Pi^{\uparrow}(xW_I) = \pi^{\uparrow}(x)W_{\Sigma^{\uparrow}(x,I)}$ and $\Pi_{\downarrow}(xW_I) = \pi_{\downarrow}(xw_{\circ,I})W_{\Sigma_{\downarrow}(x,I)}$. We again take the liberty to write $\Pi_{\downarrow}(xW_I) = \pi_{\downarrow}(xw_{\circ,I})W_{\Sigma_{\downarrow}(x,I)}$ instead of $\Pi_{\downarrow}(xW_I) = \pi_{\downarrow}(xw_{\circ,I})\, w_{\circ,\Sigma^{\uparrow}(x,I)}W_{\Sigma_{\downarrow}(x,I)}$ to make apparent the symmetry between $\Pi^{\uparrow}$ and $\Pi_{\downarrow}$.

Theorem 5.24. *The maps $\Pi^{\uparrow}$ and $\Pi_{\downarrow}$ fulfill the following properties:*
(i) $\Pi_{\downarrow}(xW_I) \leq_{\mathsf{F}} xW_I \leq_{\mathsf{F}} \Pi^{\uparrow}(xW_I)$ *for any coset xW_I.*
(ii) $\Pi^{\uparrow} \circ \Pi^{\uparrow} = \Pi^{\uparrow} \circ \Pi_{\downarrow} = \Pi^{\uparrow}$ *and* $\Pi_{\downarrow} \circ \Pi_{\downarrow} = \Pi_{\downarrow} \circ \Pi^{\uparrow} = \Pi_{\downarrow}$.
(iii) $\Pi^{\uparrow}$ *and* $\Pi_{\downarrow}$ *are order preserving.*
Therefore, the fibers of $\Pi^{\uparrow}$ and $\Pi_{\downarrow}$ coincide and define a lattice congruence $\equiv_{\mathsf{F}}$ of the facial weak order $\leq_{\mathsf{F}}$ on $\mathscr{F}_W$.

In fact, this congruence can also be understood in the lattice of weak order intervals. Indeed, note that a lattice congruence $\equiv$ on a lattice L yields a lattice congruence $\equiv_{\mathsf{I}}$ on the lattice $\leq_{\mathsf{I}}$ of intervals of L, defined by $[x, X] \equiv_{\mathsf{I}} [y, Y] \iff x \equiv y$ and $X \equiv Y$. The following statement affirms that this congruence $\equiv_{\mathsf{I}}$ on the lattice $\leq_{\mathsf{I}}$ of weak order intervals restricts to a lattice congruence on the facial weak order $\leq_{\mathsf{F}}$. However, note that we have not been able to use this statement as the definition of the congruence $\equiv_{\mathsf{F}}$, as the proof of Theorem 5.24 really requires to understand the projections $\Pi^{\uparrow}$ and $\Pi_{\downarrow}$.

Proposition 5.25. *For any standard parabolic cosets xW_I and $yW_J \in \mathscr{F}_W$,*

$$xW_I \equiv_{\mathsf{F}} yW_J \iff x \equiv_{\mathsf{W}} y \text{ and } xw_{\circ,I} \equiv_{\mathsf{W}} yw_{\circ,J}.$$

Corollary 5.26. *The weak order congruence $\equiv_{\mathsf{W}}$ is the restriction to W of the facial weak order congruence $\equiv_{\mathsf{F}}$. In other words, we have $x \equiv_{\mathsf{W}} y$ if and only if $xW_\varnothing \equiv_{\mathsf{F}} yW_\varnothing$ for any $x, y \in W$.*

This corollary says that the congruence $\equiv_{\mathsf{F}}$ of the facial weak order $\leq_{\mathsf{F}}$ on $\mathscr{F}_W$ indeed extends the congruence $\equiv_{\mathsf{W}}$ of the weak order $\leq_{\mathsf{W}}$ on W. Nevertheless, observe that not all congruences of the facial weak order arise as congruences of the weak order (consider for instance the congruence on $\mathscr{F}_{A_2}$ that only contracts sW_t with $stW_\varnothing$).

We now discuss the geometry of the lattice congruences of the facial weak order $\leq_{\mathsf{F}}$ on $\mathscr{F}_W$ defined by Theorem 5.24. As already mentioned in Chapter 4, the congruence $\equiv_{\mathsf{W}}$ of the weak order $\leq_{\mathsf{W}}$ on W defines a complete simplicial fan $\mathcal{F}(\equiv_{\mathsf{W}})$, called *quotient fan*, which coarsens the Coxeter fan $\mathcal{F}(W)$ [Rea05]. Each maximal cone of $\mathcal{F}(\equiv_{\mathsf{W}})$ corresponds to a congruence class of $\equiv_{\mathsf{W}}$, and is obtained by glueing together the regions of the Coxeter fan $\mathcal{F}(W)$ that belong to this congruence class. We now use the congruence $\equiv_{\mathsf{F}}$ of the facial weak order $\leq_{\mathsf{F}}$ on $\mathscr{F}_W$ to describe all cones of $\mathcal{F}(\equiv_{\mathsf{W}})$ (not only the maximal ones). This shows that the lattice structure on the maximal faces of $\mathcal{F}(\equiv_{\mathsf{W}})$ extends to a lattice structure on all cones of $\mathcal{F}(\equiv_{\mathsf{W}})$. As in Section 5.2.2, we first introduce the root and weight sets of the congruence classes of $\equiv_{\mathsf{F}}$.

Definition 5.27. *The root set* $\boldsymbol{R}(\Gamma)$ *and the weight set* $\boldsymbol{W}(\Gamma)$ *of a congruence class* Γ *of* $\equiv_{\mathsf{F}}$ *are defined by* $\boldsymbol{R}(\Gamma) = \bigcap_{xW_I \in \Gamma} \boldsymbol{R}(xW_I)$ *and* $\boldsymbol{W}(\Gamma) = \bigcup_{xW_I \in \Gamma} \boldsymbol{W}(xW_I)$.

As in Theorem 5.15, the root sets enable to recover the order relations in the lattice quotient $\leq_{\mathsf{F}}/\equiv_{\mathsf{F}}$.

Proposition 5.28. *For any two congruence classes* Γ *and* Λ *of* $\equiv_{\mathsf{F}}$*, we have* $\Gamma \leq \Lambda$ *in the quotient of the facial weak order by* $\equiv_{\mathsf{F}}$ *if and only if* $\boldsymbol{R}(\Gamma)^+ \subseteq \boldsymbol{R}(\Lambda)^+$ *and* $\boldsymbol{R}(\Gamma)^- \supseteq \boldsymbol{R}(\Lambda)^-$.

Finally, the weight sets enable to reconstruct the quotient fan $\mathcal{F}(\equiv_{\mathsf{W}})$.

Theorem 5.29. *The quotient fan* $\mathcal{F}(\equiv_{\mathsf{W}})$ *is the collection of cones* $\{\mathbb{R}_{\geq 0}\, \boldsymbol{W}(\Gamma) \,|\, \Gamma \in \mathscr{F}_W/\equiv_{\mathsf{F}}\}$.

5.2.6 Two relevant lattice congruences

5.2.6.1 Facial Cambrian lattices

Fix a *Coxeter element* c, *i.e.* the product of all simple reflections in S in an arbitrary order. A simple reflection $s \in S$ is *initial* in c if $\ell(sc) < \ell(c)$. For s initial in c, note that scs is another Coxeter element for W while sc is a Coxeter element for $W_{S \smallsetminus \{s\}}$.

In [Rea06, Rea07b], N. Reading defines the c-Cambrian lattice as a lattice quotient of the weak order (by the c-Cambrian congruence) or as a sublattice of the weak order (induced by c-sortable elements). There are several ways to present his constructions. We choose to start from the projection maps of the c-Cambrian congruence. These maps are defined by an induction both on the length of the elements and on the rank of the underlying Coxeter group. Namely, define the projection $\pi_{\downarrow}^{c} : W \to W$ inductively by $\pi_{\downarrow}^{c}(e) = e$ and for any s initial in c,

$$\pi_{\downarrow}^{c}(w) = \begin{cases} s \cdot \pi_{\downarrow}^{scs}(sw) & \text{if } \ell(sw) < \ell(w), \\ \pi_{\downarrow}^{sc}(w_{\langle s \rangle}) & \text{if } \ell(sw) > \ell(w), \end{cases}$$

where $w = w_{\langle s \rangle} \cdot {}^{\langle s \rangle}w$ is the unique factorization of w such that $w_{\langle s \rangle} \in W_{S \smallsetminus \{s\}}$ and $\ell(t^{\langle s \rangle}w) > \ell({}^{\langle s \rangle}w)$ for all $t \in S \smallsetminus \{s\}$. The projection $\pi_{c}^{\uparrow} : W \to W$ is defined similarly, or using the weak order anti-morphism by $\pi_{c}^{\uparrow}(w) = \big(\pi_{\downarrow}^{(c^{-1})}(ww_\circ)\big)w_\circ$. N. Reading proves in [Rea07b] that these projection maps $\pi_{c}^{\uparrow}$ and $\pi_{\downarrow}^{c}$ define a congruence $\equiv_{\mathsf{W}}^{c}$ of the weak order $\leq_{\mathsf{W}}$ on W, called *c-Cambrian congruence*. The quotient of the weak order by the c-Cambrian congruence is called the *c-Cambrian lattice*.

Cambrian congruences are relevant in the context of finite type cluster algebras, generalized associahedra, and W-Catalan combinatorics. Without details, let us point out the following facts:

(i) The fan $\mathcal{F}(\equiv_{\mathsf{W}}^{c})$ associated to the c-Cambrian congruence $\equiv_{\mathsf{W}}^{c}$ is the *Cambrian fan* studied by N. Reading and D. Speyer [RS09]. Is was proved to be the normal fan of a *generalized associahedra* by C. Hohlweg, C. Lange and H. Thomas [HLT11], see also [Ste13, PS15a, HPS18] for further geometric properties. The resulting polytope $\mathbb{A}\mathrm{sso}(c)$ is called *c-associahedra*. See Figure 5.12 and Chapters 7 and 8 for more details.

(ii) These polytopes realize the *c-cluster complexes* of type W. When W is crystallographic, these complexes were defined from the theory of finite type *cluster algebras* of S. Fomin and A. Zelevinsky [FZ02, FZ03a]. See also Part III.

(iii) The minimal elements in the c-Cambrian congruence classes are precisely the *c-sortable elements*, defined as the elements $w \in W$ such that there exists nested subsets $K_1 \supseteq K_2 \supseteq \cdots \supseteq K_r$ of S such that $w = c_{K_1} c_{K_2} \dots c_{K_r}$ where c_K is the product of the elements in K in the order given by c. They are connected to various W-Catalan families: c-clusters, vertices of the c-associahedron, W-non-crossing partitions. See [Rea07a] for precise definitions.

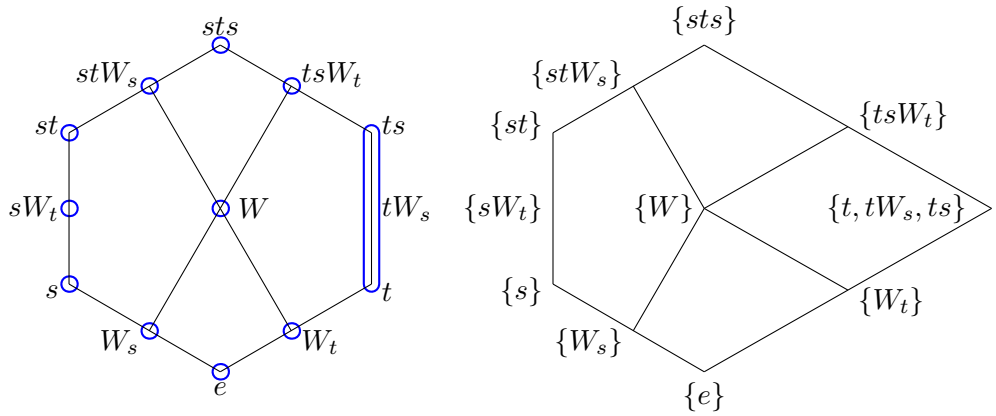

Figure 5.11: The st-Cambrian congruence classes of the standard parabolic cosets in type A_2 (left) and the resulting quotient (right).

The results presented in this chapter translate to the following statement.

Theorem 5.30. *For any Coxeter element c of W, the facial c-Cambrian congruence $\equiv^c_{\mathsf{F}}$ on $\mathscr{F}_W$, defined by*

$$xW_I \equiv^c_{\mathsf{F}} yW_J \iff x \equiv^c_{\mathsf{W}} y \text{ and } xw_{\circ,I} \equiv^c_{\mathsf{W}} yw_{\circ,J},$$

satisfies the following properties:

(i) The c-Cambrian congruence $\equiv^c_{\mathsf{W}}$ is the restriction to W of the facial c-Cambrian congruence $\equiv^c_{\mathsf{F}}$.

(ii) The quotient of the facial weak order by the facial c-Cambrian congruence $\equiv^c_{\mathsf{F}}$ defines a lattice structure on the cones of the c-Cambrian fan of [RS09], or equivalently on the faces of the c-associahedron $\mathbb{A}\mathrm{sso}(c)$ of [HLT11].

(iii) A coset xW_I is minimal (resp. maximal) in its facial c-congruence class if and only if $xw_{\circ,I}$ is c-sortable (resp. x is c-antisortable). In particular, a Coxeter cone $\mathbb{R}_{\geq 0}\,\boldsymbol{W}(xW_I)$ is a cone of the c-Cambrian fan if and only if x is c-antisortable and $xw_{\circ,I}$ is c-sortable.

Examples of facial Cambrian congruences in type A_2, A_3, and B_3 appear in Figures 5.11 and 5.12.

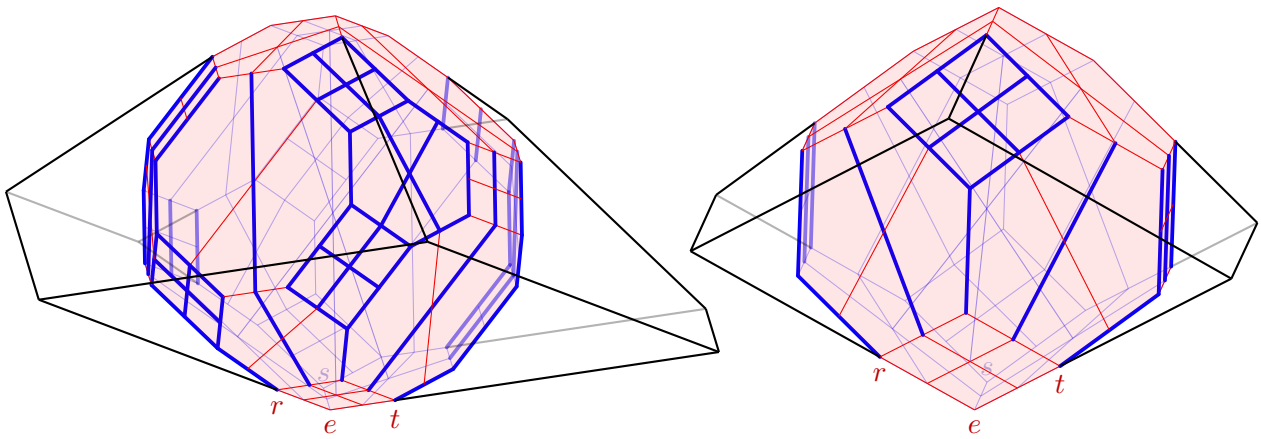

Figure 5.12: The srt-Cambrian congruence on the standard parabolic cosets in type A_3 (left) and B_3 (right) and the resulting quotient. Bold blue edges are contracted edges. The quotient is given the geometry of the type A_3 and B_3 srt-associahedra $\mathbb{A}\mathrm{sso}(srt)$ of [HLT11].

Example 5.31. In type A, the sylvester congruence classes correspond to binary trees, while the facial sylvester congruence classes correspond to Schröder trees. The quotient of the facial weak order by the facial sylvester congruence was already described in [PR06, NT06]. The Cambrian counterparts of binary trees and Schröder trees were described in [CP17], and used to introduce the facial type A Cambrian lattices.

5.2.6.2 Facial boolean lattice

The *descent congruence* is the congruence of the weak order defined by $x \equiv_{\mathsf{W}}^{\mathrm{des}} y$ if and only if $D_L(x) = D_L(y)$, where $D_L(x)$ denotes the left descent set of x, see Section 5.2.1. The corresponding up and down projections are given by $\pi_{\downarrow}(x) = w_{\circ,D_L(x)}$ and $\pi^{\uparrow}(x) = w_\circ w_{\circ,S\smallsetminus D_L(x)}$. The quotient of the weak order by $\equiv_{\mathsf{W}}^{\mathrm{des}}$ is isomorphic to the boolean lattice on S. The fan $\mathcal{F}(\equiv_{\mathsf{W}}^{\mathrm{des}})$ is given by the arrangement of the hyperplanes orthogonal to the simple roots of Δ. It is the normal fan of the parallelepiped $\mathbb{P}\mathrm{ara}(W)$ generated by the simple roots of Δ. Denote by $\equiv_{\mathsf{F}}^{\mathrm{des}}$ the facial weak order congruence induced by $\equiv_{\mathsf{W}}^{\mathrm{des}}$ as defined in Section 5.2.5. According to Theorem 5.29, the $\equiv_{\mathsf{F}}^{\mathrm{des}}$ congruence classes correspond to all faces of the parallelepiped $\mathbb{P}\mathrm{ara}(W)$. In the next few statements, we provide a direct criterion to test whether two cosets are $\equiv_{\mathsf{F}}^{\mathrm{des}}$-congruent. For this, we need to extend to all cosets the notion of descent sets.

Definition 5.32. *The descent set of a coset xW_I is the set of roots $\boldsymbol{D}(xW_I) := \boldsymbol{R}(xW_I) \cap \pm\Delta \subseteq \Phi$.*

The following statement is similar to Propositions 5.11 and 5.13.

Proposition 5.33. *For any $x \in W$, the root descent set $\boldsymbol{D}(x)$ has the following properties:*
(i) $\boldsymbol{D}(x) = \big(\Delta \cap \boldsymbol{N}(x)\big) \cup -\big(\Delta \smallsetminus \boldsymbol{N}(x)\big)$, *where $\boldsymbol{N}(x) = \Phi^+ \cap x(\Phi^-)$ is the inversion set of x.*
(ii) $\boldsymbol{D}(xw_\circ) = -\boldsymbol{D}(x)$ *and* $\boldsymbol{D}(w_\circ x) = w_\circ\big(\boldsymbol{D}(x)\big)$.
(iii) The descent set of xW_I is given by those of x and $xw_{\circ,I}$ by $\boldsymbol{D}(xW_I) = \boldsymbol{D}(x) \cup \boldsymbol{D}(xw_{\circ,I})$.

We get that the $\equiv_{\mathsf{F}}^{\mathrm{des}}$-equivalence class of xW_I is determined by the root descent set $\boldsymbol{D}(xW_I)$.

Proposition 5.34. *For any xW_I, yW_J, we have $xW_I \equiv_{\mathsf{F}}^{\mathrm{des}} yW_J$ if and only if $\boldsymbol{D}(xW_I) = \boldsymbol{D}(yW_J)$.*

Example 5.35. In type A, the *descent vector* $\mathrm{des}(\lambda) \in \{-1, 0, 1\}^{n-1}$ of an ordered partition λ of $[n]$ is defined by $\mathrm{des}(\lambda)_i = \mathrm{sign}\,\big(\lambda^{-1}(i) - \lambda^{-1}(i+1)\big)$. These descent vectors where used by J.-C. Novelli and J.-Y. Thibon in [NT06] to see that the facial weak order on the cube is a lattice. See also [CP17].

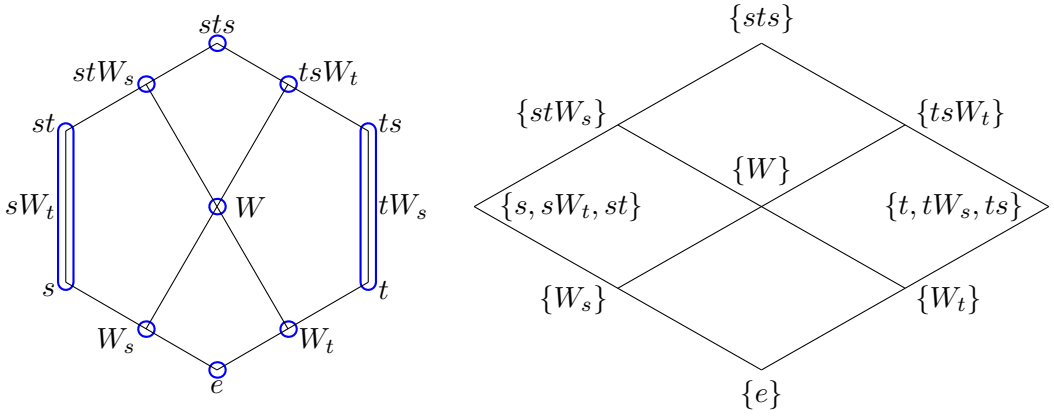

Figure 5.13: The descent congruence classes of the standard parabolic cosets in type A_2 (left) and the resulting quotient (right).

5.3 FACIAL WEAK ORDER ON ARRANGEMENTS

5.3.1 Poset of regions of a hyperplane arrangement

Let $(V, \langle \cdot \,|\, \cdot \rangle$ be an Euclidean vector space. A (real, central) *hyperplane arrangement* is a collection $\mathcal{H}$ of linear hyperplanes of V. We assume without loss of generality that the arrangement is *essential*, *i.e.* that the intersection $\bigcap \mathcal{H}$ of all its hyperplanes is reduced to the origin. The *regions* of $\mathcal{H}$ are the closures of the connected components of its complement $V \smallsetminus \bigcup \mathcal{H}$. The *faces* of $\mathcal{H}$ are all faces of the regions of $\mathcal{H}$. We denote by $\mathscr{R}_{\mathcal{H}}$ and $\mathscr{F}_{\mathcal{H}}$ the sets of regions and faces of $\mathcal{H}$. The faces of $\mathcal{H}$ form a complete fan $\mathcal{F}(\mathcal{H})$ and a lattice for the inclusion, called the *face lattice* of $\mathcal{H}$. The arrangement $\mathcal{H}$ is called *simplicial* when the fan $\mathcal{F}(\mathcal{H})$ is.

Call *separating set* of two regions R, S of $\mathcal{H}$ the set $\mathbf{sep}(R, S)$ of hyperplanes of $\mathcal{H}$ that separate R from S. We now fix a *base region* B of $\mathcal{H}$ and abbreviate $\mathbf{sep}(B, R)$ to $\mathbf{sep}(R)$. The fundamental poset of this section is the following.

Definition 5.36 ([Ede84])**.** *The* poset of regions $\mathsf{R}(\mathcal{H}, B) := (\mathscr{R}_{\mathcal{H}}, \leq_{\mathsf{R}})$ *is the poset on all regions of $\mathcal{H}$ ordered by inclusion of separating sets* $\mathbf{sep}(R)$.

In other words, the cover relations of $\mathsf{R}(\mathcal{H}, B)$ are the pairs (R, R') of adjacent regions of $\mathcal{H}$ such that R and B lie on the same side of the separating hyperplane of R and R'. The poset $\mathsf{R}(\mathcal{H}, B)$ clearly has a minimal element B (with empty separating set) and a maximal element $-B$ (with separating set $\mathcal{H}$), and the antipodal map $R \mapsto -R$ is an anti-automorphism corresponding to the complementation of separating sets. The following result is due to A. Björner, P. Edelman, and G. Ziegler [BEZ90].

Theorem 5.37 ([BEZ90, Thm. 3.4])**.** *For any simplicial hyperplane arrangement $\mathcal{H}$, and any base region B of $\mathcal{H}$, the poset of regions $\mathsf{R}(\mathcal{H}, B)$ is a lattice.*

Note that this sufficient condition is not necessary. One the one hand, N. Reading extended this result when the hyperplane arrangement $\mathcal{H}$ is *tight* with respect to the base region B [Rea16b, Thm. 9.3.2], meaning that for any region R, every pair of lower (resp. upper) facets of R with respect to B intersect in a codimension 2 face of R. On the other hand, A. Björner, P. Edelman, and G. Ziegler proved that the base region B must be simplicial when the poset of regions $\mathsf{R}(\mathcal{H}, B)$ is a lattice [BEZ90, Thm. 3.1], but that there exist arrangements $\mathcal{H}$ with simplicial base regions B for which the poset of regions $\mathsf{R}(\mathcal{H}, B)$ is not a lattice (although this can only happen in dimension $d \geq 4$ by [BEZ90, Thm. 3.2]).

5.3.2 Facial weak order of a hyperplane arrangement

We now extend the poset of regions to an order on all regions of the arrangement $\mathcal{H}$. As in Section 5.2, we provide several perspectives on this order and discuss its lattice properties.

Facial intervals. Our first approach is to interpret the faces of $\mathscr{F}_{\mathcal{H}}$ as intervals of the poset of regions and to compare the minimum and maximum elements of these intervals as in Theorem 5.15 (iii). In other words, we define the facial weak order as the subposet of the interval poset of the poset of regions induced by facial intervals.

Proposition 5.38. *For any face $F \in \mathscr{F}_{\mathcal{H}}$, the set $\{R \in \mathscr{R}_{\mathcal{H}} \,|\, F \subseteq R\}$ is an interval of the poset of regions $\mathsf{R}(\mathcal{H}, B)$. We denote it $[m_F, M_F]$ and call it the* facial interval *of F.*

Definition 5.39. *The* facial weak order $\mathsf{F}(\mathcal{H}, B) := (\mathscr{F}_{\mathcal{H}}, \leq_{\mathsf{F}})$ *is the poset on all faces of $\mathcal{H}$ defined by:*

$$F \leq_{\mathsf{F}} G \quad \Longleftrightarrow \quad m_F \leq_{\mathsf{R}} m_G \quad \text{and} \quad M_F \leq_{\mathsf{R}} M_G.$$

Sign function. We now use sign functions to describe the facial weak order. The underlying context is the more general theory of oriented matroids [BLS+99, Bok06], to which the facial weak order extend. We fix a normal vector $\boldsymbol{e}_H$ to each hyperplane $H \in \mathcal{H}$, so that $H = \{v \in V \mid \langle \boldsymbol{e}_H \mid v \rangle = 0\}$. We consider the open half spaces $H^+ = \{v \in V \mid \langle \boldsymbol{e}_H \mid v \rangle > 0\}$ and $H^- = \{v \in V \mid \langle \boldsymbol{e}_H \mid v \rangle < 0\}$. We choose the direction of the vector $\boldsymbol{e}_H$ such that the base region B lies in H^+.

For any face $F \in \mathscr{F}_{\mathcal{H}}$, we let $F(H) \in \{-, 0, +\}$ be such that $F \subseteq H^{F(H)}$, or equivalently, $\langle \boldsymbol{e}_H \mid v \rangle = F(H)$ for any v in the interior $\mathring{F}$ of F. The *sign vector* of F is $\sigma(F) := (F(H))_{H \in \mathcal{H}}$. The facial weak order is then obtained by the natural componentwise order on the sign vectors.

Proposition 5.40. *For any $F, G \in \mathscr{F}_{\mathcal{H}}$, we have $F \leq_{\mathsf{F}} G \iff F(H) \geq G(H)$ for all $H \in \mathcal{H}$.*

Cover relations. We can describe the facial weak order by its cover relations as in Definition 5.14.

Proposition 5.41. *The cover relations $\lessdot_{\mathsf{F}}$ of the facial weak order $\leq_{\mathsf{F}}$ are precisely of the form $F \lessdot_{\mathsf{F}} G$ for $F, G \in \mathscr{F}_{\mathcal{H}}$ such that either F is a facet of G and $m_F = m_G$, or G is a facet of F and $M_F = M_G$.*

Root sets. We now interpret the facial weak order on root sets as in Theorem 5.15 (ii). By analogy with the Coxeter setting, let $\Phi^+_{\mathcal{H}} := \{\boldsymbol{e}_H \mid H \in \mathcal{H}\}$, $\Phi^-_{\mathcal{H}} := \{-\boldsymbol{e}_H \mid H \in \mathcal{H}\}$ and $\Phi_{\mathcal{H}} := \Phi^+_{\mathcal{H}} \cup \Phi^-_{\mathcal{H}}$. For $X \subseteq \Phi_{\mathcal{H}}$, we still denote by $X^+ := X \cap \Phi^+_{\mathcal{H}}$ the positive part and $X^- := X \cap \Phi^-_{\mathcal{H}}$ the negative part.

Definition 5.42. *The root set of a face $F \in \mathscr{F}_{\mathcal{H}}$ is $\boldsymbol{R}(F) := \{\boldsymbol{e} \in \Phi_{\mathcal{H}} \mid \langle \boldsymbol{e} \mid x \rangle \leq 0$, for some $x \in \mathring{F}\}$.*

Theorem 5.43. *For any $F, G \in \mathscr{F}_{\mathcal{H}}$, we have $F \leq_{\mathsf{F}} G \iff \boldsymbol{R}(F)^+ \subseteq \boldsymbol{R}(G)^+$ and $\boldsymbol{R}(F)^- \supseteq \boldsymbol{R}(G)^-$.*

Zonotopes. We now provide an alternative geometric interpretation of the root sets in terms of the geometry of zonotopes associated to hyperplane arrangements.

Definition 5.44. *The zonotope $\mathbb{Z}\mathrm{ono}(\mathcal{H})$ is the Minkowski sum of the normal vectors to the hyperplanes of $\mathcal{H}$, i.e. $\mathbb{Z}\mathrm{ono}(\mathcal{H}) := \sum_{H \in \mathcal{H}} [-\boldsymbol{e}_H, \boldsymbol{e}_H] = \{ \sum_{H \in \mathcal{H}} \lambda_H \boldsymbol{e}_H \mid -1 \leq \lambda_H \leq 1$ for all $H \in \mathcal{H}\}$.*

This zonotope depends upon the choice of the normal vectors $\boldsymbol{e}_H$ of the hyperplanes $H \in \mathcal{H}$, but its combinatorics does not. Namely, P. H. Edelman gives in [Ede84, Lem. 3.1] a bijection between the non-empty faces of the zonotope $\mathbb{Z}\mathrm{ono}(\mathcal{H})$ and the the faces $\mathscr{F}_{\mathcal{H}}$ of the arrangement $\mathcal{H}$ using the map in the following lemma.

Lemma 5.45 ([McM71])**.** *The map $\tau : F \mapsto \{ \sum_{F \not\subseteq H} F(H) \boldsymbol{e}_H + \sum_{F \subseteq H} \lambda_H \boldsymbol{e}_H \mid -1 \leq \lambda_H \leq 1 \}$ is a bijection from the faces $\mathscr{F}_{\mathcal{H}}$ to the non-empty faces of the zonotope $\mathbb{Z}\mathrm{ono}(\mathcal{H})$. Moreover, F is the outer normal cone of $\tau(F)$, so that the fan $\mathcal{F}(\mathcal{H})$ of the arrangement $\mathcal{H}$ is the normal fan of $\mathbb{Z}\mathrm{ono}(\mathcal{H})$.*

Proposition 5.46. *The cone $\mathbb{R}_{\geq 0}\, \boldsymbol{R}(F)$ of the root set $\boldsymbol{R}(F)$ is the inner primal cone of the face $\tau(F)$ in the zonotope $\mathbb{Z}\mathrm{ono}(\mathcal{H})$.*

Lattice. We conclude with the main results of [DHMP19], extending Theorem 5.20 and Corollary 5.22. The proof is very different from that of Theorem 5.20 and requires to emancipate from the Coxeter group technology. It is based on the BEZ lemma [BEZ90] and on a property that enables to determine the meet of two faces from meets of their projections in some subarrangements.

Theorem 5.47. *For any arrangement $\mathcal{H}$ whose poset of regions $\mathsf{R}(\mathcal{H}, B)$ is a lattice, the facial weak order $\mathsf{F}(\mathcal{H}, B)$ is a lattice as well.*

Proposition 5.48. *When $\mathcal{H}$ is simplicial, the poset of regions $\mathsf{R}(\mathcal{H}, B)$ is a sublattice of the facial weak order $\mathsf{F}(\mathcal{H}, B)$.*

Chapter Six

WEAK ORDER ON INTEGER POSETS

This chapter goes beyond the facial weak order presented in Chapter 5. Namely, we endow the set of integer posets with a lattice structure in Section 6.1 and a Hopf algebra structure in Section 6.2. We then show that the lattice and Hopf algebra structures on permutations, binary trees, permutrees, ordered partitions, among others can be interpreted as substructures of these structures on integer posets. Finally, in Section 6.3 we discuss the possible extensions of the weak order on integer posets to Coxeter groups. Surprisingly, it fails to define a lattice beyond crystallographic root systems. This chapter is adapted from joint works with G. Chatel, J. Gay and V. Pons [CPP19, GP18, PP20].

6.1 WEAK ORDER ON INTEGER POSETS

In this section, we introduce the weak order on integer binary relations which restricts to a lattice structure on integer posets. We then show that it restricts further to several relevant families of posets.

6.1.1 Weak order on integer binary relations and integer posets

Recall that a binary relation on X is a subset R of X^2. As usual, we write $(a, b) \in R$ or $a \, R \, b$.

Definition 6.1. *An integer binary relation of size n is a binary relation on $[n] := \{1, \dots, n\}$. We only consider reflexive relations and let $\mathfrak{R}_n$ be the set of all reflexive binary relations on $[n]$.*

Definition 6.2. *The increasing and decreasing subrelations of an integer relation $R \in \mathfrak{R}_n$ are the relations defined by $R^{\mathsf{Inc}} := \{(a, b) \in R \,|\, a \leq b\}$ and $R^{\mathsf{Dec}} := \{(b, a) \in R \,|\, a \leq b\}$.*

In our pictures, we always represent an integer relation $R \in \mathfrak{R}_n$ as follows: we write the numbers $1, \dots, n$ from left to right and we draw the increasing relations of R above in blue and the decreasing relations of R below in red, omitting the reflexive relations (i, i). See *e.g.* Figure 6.1.

Definition 6.3. *The weak order on $\mathfrak{R}_n$ is the order defined by $R \leq_{\mathsf{R}} S$ if $R^{\mathsf{Dec}} \subseteq S^{\mathsf{Dec}}$ and $R^{\mathsf{Inc}} \supseteq S^{\mathsf{Inc}}$. It is a lattice with meet and join*

$$R \wedge_{\mathsf{R}} S = (R^{\mathsf{Dec}} \cap S^{\mathsf{Dec}}) \cup (R^{\mathsf{Inc}} \cup S^{\mathsf{Inc}}) \qquad \text{and} \qquad R \vee_{\mathsf{R}} S = (R^{\mathsf{Dec}} \cup S^{\mathsf{Dec}}) \cup (R^{\mathsf{Inc}} \cap S^{\mathsf{Inc}}).$$

We now use this order to define a similar order on integer posets. An *integer poset* is an integer relation which is a poset. We denote by $\mathfrak{Pos}_n$ the set of integer posets on $[n]$. We want to show that the subposet of the weak order induced by integer posets is a lattice. Note that $\wedge_{\mathsf{R}}$ and $\vee_{\mathsf{R}}$ preserve antisymmetry but not transitivity, so that $\mathfrak{Pos}_n$ does not induce a sublattice of the weak order on $\mathfrak{R}_n$.

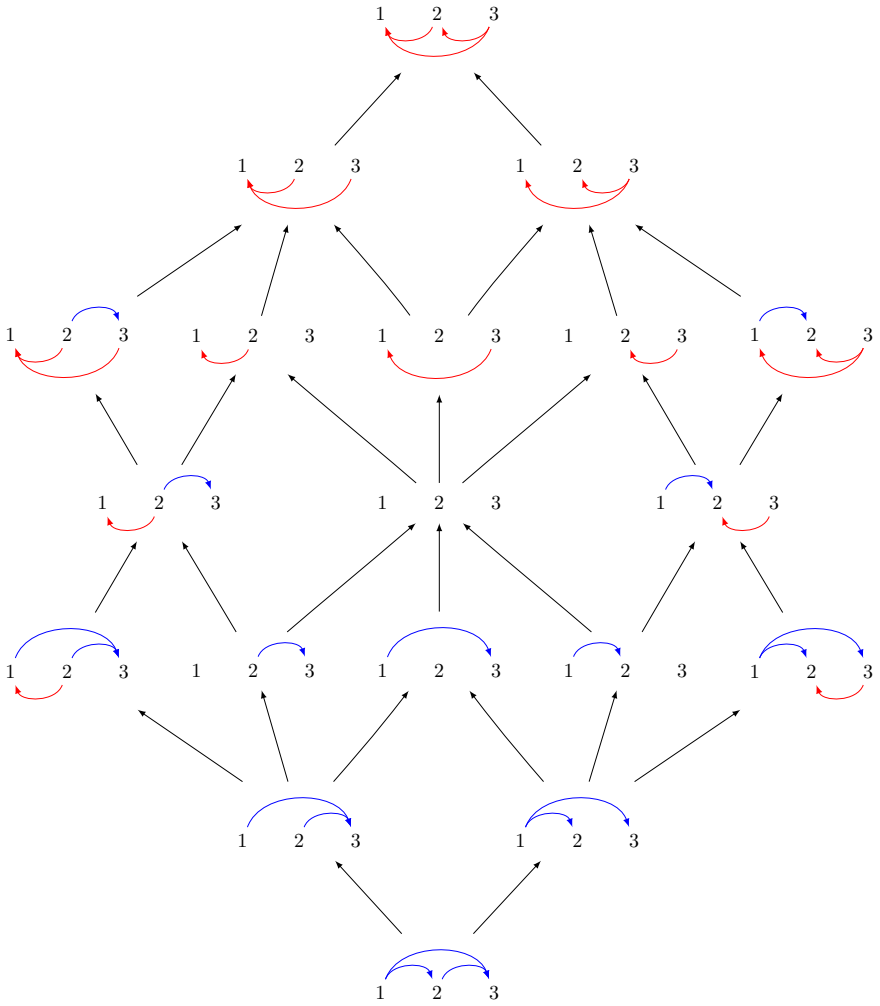

Figure 6.1: The weak order on integer posets of size 3.

Definition 6.4. *For $R \in \mathfrak{R}_n$, define the* transitive closure R^{tc}*, the* transitive decreasing deletion R^{tdd} *and the* transitive increasing deletion R^{tid} *as*

$$R^{\mathsf{tc}} := \{(u, w) \in [n]^2 \mid \exists\, v_1, \ldots, v_p \in [n] \text{ such that } u = v_1\, R\, v_2\, R \ldots R\, v_{p-1}\, R\, v_p = w\},$$
$$R^{\mathsf{tdd}} := R \smallsetminus \{(b, a) \in R^{\mathsf{Dec}} \mid \exists\, i \leq b \text{ and } j \geq a \text{ such that } i\, R\, b\, R\, a\, R\, j \text{ while } i \not R\, j\},$$
$$R^{\mathsf{tid}} := R \smallsetminus \{(a, b) \in R^{\mathsf{Inc}} \mid \exists\, i \geq a \text{ and } j \leq b \text{ such that } i\, R\, a\, R\, b\, R\, j \text{ while } i \not R\, j\}.$$

Note that in these definitions, i and j may coincide with a and b (since we assumed that all our relations are reflexive). The following central result of [CPP19] is illustrated below and in Figure 6.1.

Theorem 6.5. *The subposet of the weak order induced by integer posets is a lattice with meet and join*

$$R \wedge_{\mathsf{P}} S = \big((R^{\mathsf{Dec}} \cap S^{\mathsf{Dec}}) \cup (R^{\mathsf{Inc}} \cup S^{\mathsf{Inc}})^{\mathsf{tc}}\big)^{\mathsf{tdd}} \quad \text{and} \quad R \vee_{\mathsf{P}} S = \big((R^{\mathsf{Dec}} \cup S^{\mathsf{Dec}})^{\mathsf{tc}} \cup (R^{\mathsf{Inc}} \cap S^{\mathsf{Inc}})\big)^{\mathsf{tid}}.$$

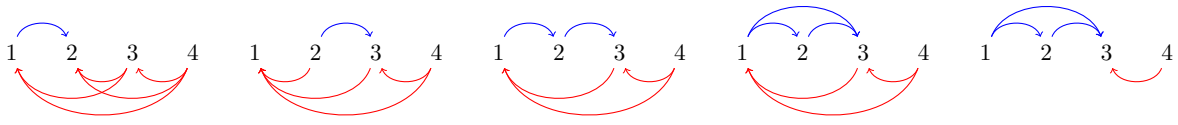

$R \in \mathfrak{Pos}_4$ | $S \in \mathfrak{Pos}_4$ | $(R^{\mathsf{Inc}} \cup S^{\mathsf{Inc}}) \cup (R^{\mathsf{Dec}} \cap S^{\mathsf{Dec}})$ | $(R^{\mathsf{Inc}} \cup S^{\mathsf{Inc}})^{\mathsf{tc}} \cup (R^{\mathsf{Dec}} \cap S^{\mathsf{Dec}})$ | $R \wedge_{\mathsf{P}} S \in \mathfrak{Pos}_4$

6.1.2 Weak order on relevant families of integer posets

In this section, we observe that certain relevant combinatorial objects can be interpreted by specific integer posets and that the subposets of the weak order induced by these integer posets correspond to classical lattice structures on these combinatorial objects. For each of these special families of posets, we try to consistently present (1) a characterization of the posets of this family, (2) an interpretation of the weak order on these posets, and (3) whether it is a sublattice of the weak order on all posets.

6.1.2.1 Permutations, weak order intervals, and ordered partitions

We first reinterpret the classical weak order, its interval lattice and its facial interval lattice using specific posets. As illustrated in Figure 6.2, each permutation $\sigma \in \mathfrak{S}_n$ corresponds to a *weak order element poset* $\lhd_\sigma$ defined by $u \lhd_\sigma v$ if $\sigma^{-1}(u) \leq \sigma^{-1}(v)$. Define $\mathfrak{Woep}_n := \{\lhd_\sigma \mid \sigma \in \mathfrak{S}_n\}$. The following statement motivates Definition 6.3. For a permutation $\sigma \in \mathfrak{S}_n$, a pair $(a, b) \in [n]^2$ is a *version* if $a \leq b$ and $\sigma^{-1}(a) \leq \sigma^{-1}(b)$, and an *inversion* if $a \geq b$ and $\sigma^{-1}(a) \leq \sigma^{-1}(b)$. Note that we order the entries of the inversions in a strange way, and that we borrow the versions from [KLR03].

Proposition 6.6. *1. A poset $\lhd$ is in $\mathfrak{Woep}_n$ if and only if $a \lhd b$ or $a \rhd b$ for all $a, b \in [n]$.*
2. For any $\sigma \in \mathfrak{S}_n$, the increasing (resp. decreasing) relations of $\lhd_\sigma$ are the versions (resp. inversions) of σ. Therefore, for any $\sigma, \tau \in \mathfrak{S}_n$, we have $\lhd_\sigma \leq_{\mathsf{R}} \lhd_\tau \iff \sigma \leq_{\mathsf{W}} \tau$.
3. Moreover, the weak order on $\mathfrak{Woep}_n$ is a sublattice of the weak order on $\mathfrak{Pos}_n$.

We now present a similar approach to intervals of the weak order. For $\underline{\sigma} \leq_{\mathsf{W}} \overline{\sigma} \in \mathfrak{S}_n$, consider the weak order interval $[\underline{\sigma}, \overline{\sigma}]_{\mathsf{W}} := \{\tau \in \mathfrak{S}_n \mid \underline{\sigma} \leq_{\mathsf{W}} \tau \leq_{\mathsf{W}} \overline{\sigma}\}$. The permutations of $[\underline{\sigma}, \overline{\sigma}]_{\mathsf{W}}$ are the linear extensions of the *weak order interval poset* $\lhd_{[\underline{\sigma},\overline{\sigma}]} := \bigcap_{\underline{\sigma} \leq_{\mathsf{W}} \tau \leq_{\mathsf{W}} \overline{\sigma}} \lhd_\tau = \lhd_{\underline{\sigma}} \cap \lhd_{\overline{\sigma}} = \lhd_{\overline{\sigma}}^{\mathsf{Inc}} \cup \lhd_{\underline{\sigma}}^{\mathsf{Dec}}$. Define $\mathfrak{Woip}_n := \{\lhd_{[\underline{\sigma},\overline{\sigma}]} \mid \underline{\sigma}, \overline{\sigma} \in \mathfrak{S}_n,\ \underline{\sigma} \leq_{\mathsf{W}} \overline{\sigma}\}$.

Proposition 6.7. *1. A poset $\lhd$ is in $\mathfrak{Woip}_n$ if and only if it satisfies $a \lhd c \Rightarrow (a \lhd b$ or $b \lhd c)$ and $a \rhd c \Rightarrow (a \rhd b$ or $b \rhd c)$ for all $a < b < c$ [BW91, Thm. 6.8].*
2. For any $\sigma \leq_{\mathsf{W}} \overline{\sigma}$ and $\underline{\tau} \leq_{\mathsf{W}} \overline{\tau}$ in $\mathfrak{S}_n$, we have $\lhd_{[\underline{\sigma},\overline{\sigma}]} \leq_{\mathsf{R}} \lhd_{[\underline{\tau},\overline{\tau}]} \iff \underline{\sigma} \leq_{\mathsf{W}} \underline{\tau}$ and $\overline{\sigma} \leq_{\mathsf{W}} \overline{\tau}$.
3. The weak order on $\mathfrak{Woip}_n$ is a lattice with meet $\lhd_{[\underline{\sigma},\overline{\sigma}]} \wedge_{\mathsf{WOIP}} \lhd_{[\underline{\tau},\overline{\tau}]} = \lhd_{[\underline{\sigma} \wedge_{\mathsf{W}} \underline{\tau},\, \overline{\sigma} \wedge_{\mathsf{W}} \overline{\tau}]}$ and join $\lhd_{[\underline{\sigma},\overline{\sigma}]} \vee_{\mathsf{WOIP}} \lhd_{[\underline{\tau},\overline{\tau}]} = \lhd_{[\underline{\sigma} \vee_{\mathsf{W}} \underline{\tau},\, \overline{\sigma} \vee_{\mathsf{W}} \overline{\tau}]}$. However, the weak order on $\mathfrak{Woip}_n$ is not a sublattice of the weak order on $\mathfrak{Pos}_n$.

Finally, we consider a face of the permutahedron, that is, an ordered partition π of $[n]$. As illustrated in Figure 6.3, we see π as a *weak order face poset* $\lhd_\pi$ defined by $u \lhd_\pi v$ if $\pi^{-1}(u) < \pi^{-1}(v)$. Define $\mathfrak{Wofp}_n := \{\lhd_\pi \mid \pi \text{ ordered partition of } [n]\}$.

Proposition 6.8. *1. A poset $\lhd$ is in $\mathfrak{Wofp}_n$ if and only if $\lhd \in \mathfrak{Woip}_n$ and $(a \lhd b \Leftrightarrow b \rhd c)$ and $(a \rhd b \Leftrightarrow b \lhd c)$ for all $a < b < c$ with $a \not\lhd c$ and $a \not\rhd c$.*
2. For any μ, ν in $\mathfrak{P}_n$, we have $\lhd_\mu \leq_{\mathsf{R}} \lhd_\nu \iff \mu \leq_{\mathsf{F}} \nu$ in the facial weak order of [KLN+01, PR06, DHP18], see Section 5.1.
3. The weak order on $\mathfrak{Wofp}_n$ is a lattice with meet $\lhd_\mu \wedge_{\mathsf{WOFP}} \lhd_\nu = \lhd_{\mu \wedge_{\mathsf{F}} \nu}$ and join $\lhd_\mu \vee_{\mathsf{WOFP}} \lhd_\nu = \lhd_{\mu \vee_{\mathsf{F}} \nu}$. However, the weak order on $\mathfrak{Wofp}_n$ is not a sublattice of the weak order on $\mathfrak{Pos}_n$, nor on $\mathfrak{Woip}_n$.

6.1.2.2 Binary trees, Tamari intervals, and Schröder trees

We now reinterpret the Tamari lattice, its interval lattice and its facial interval lattice using specific posets. As illustrated in Figure 6.2, each binary tree $T \in \mathfrak{T}_n$ corresponds to a *Tamari order element poset* $\lhd_T$, defined by $i \lhd_T j$ when i is a descendant of j in T. In other words, the Hasse diagram of $\lhd_T$ is the tree T oriented towards its root. Define $\mathfrak{Toep}_n := \{\lhd_T \mid T \in \mathfrak{T}_n\}$.

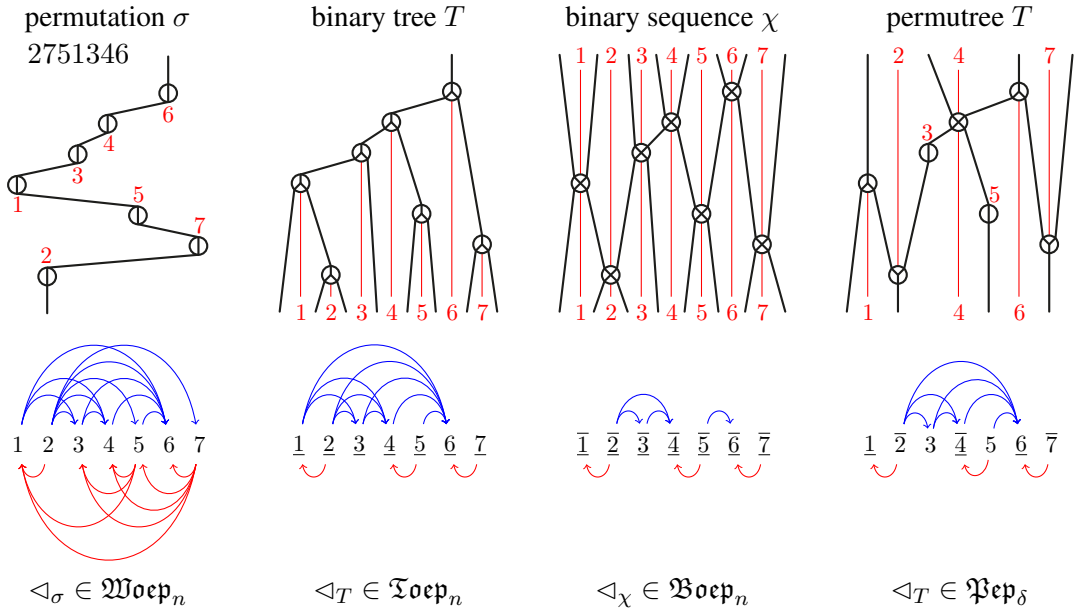

Figure 6.2: Posets for permutations, binary trees, binary sequences, and permutrees.

Proposition 6.9. *1. A poset $\lhd$ is in $\mathfrak{Toep}_n$ if and only if*
(i) $(a \lhd c \Rightarrow b \lhd c)$ and $(a \rhd c \Rightarrow a \rhd b)$ for all $a < b < c$ and
(ii) there exists $a < b < c$ such that $a \lhd b \rhd c$ for all $a < c$ incomparable in $\lhd$.
2. For any binary trees $S, T \in \mathfrak{T}_n$, we have $\lhd_S \leq_\mathsf{R} \lhd_T \iff S \leq_\mathsf{T} T$.
3. Moreover, the Tamari lattice on $\mathfrak{Toep}_n$ is a sublattice of the weak order on $\mathfrak{Pos}_n$.

For $\underline{T} \leq_\mathsf{T} \overline{T} \in \mathfrak{T}_n$, consider the Tamari interval $[\underline{T}, \overline{T}]_\mathsf{T} := \{S \in \mathfrak{T}_n \,|\, \underline{T} \leq_\mathsf{T} S \leq_\mathsf{T} \overline{T}\}$. We see it as the *Tamari order interval poset* $\lhd_{[\underline{T},\overline{T}]} := \bigcap_{\underline{T} \leq_\mathsf{T} S \leq_\mathsf{T} \overline{T}} \lhd_S = \lhd_{\underline{T}} \cap \lhd_{\overline{T}} = \lhd_{\overline{T}}^{\mathsf{Inc}} \cup \lhd_{\underline{T}}^{\mathsf{Dec}}$. Define $\mathfrak{Toip}_n := \{\lhd_{[\underline{T},\overline{T}]} \mid \underline{T}, \overline{T} \in \mathfrak{T}_n, \underline{T} \leq_\mathsf{R} \overline{T}\}$.

Proposition 6.10. *1. A poset $\lhd$ is in $\mathfrak{Toip}_n$ if and only if $(a \lhd c \Rightarrow b \lhd c)$ and $(a \rhd c \Rightarrow a \rhd b)$ for all $a < b < c$.*
2. For any $\underline{S} \leq_\mathsf{T} \overline{S}$ and $\underline{T} \leq_\mathsf{T} \overline{T}$ in $\mathfrak{T}_n$, we have $\lhd_{[\underline{S},\overline{S}]} \leq_\mathsf{R} \lhd_{[\underline{T},\overline{T}]} \iff \underline{S} \leq_\mathsf{T} \underline{T}$ and $\overline{S} \leq_\mathsf{T} \overline{T}$.
3. Moreover, the weak order on $\mathfrak{Toip}_n$ is a sublattice of the weak order on $\mathfrak{Pos}_n$.

Consider now a face of the associahedron, that is, a Schröder tree S (a rooted tree where each internal node has at least two children). We label the angles between two consecutive children in inorder, meaning that each angle is labeled after the angles in its left child and before the angles in its right child. As illustrated in Figure 6.3, we associate to S the poset $\lhd_S$ where $i \lhd_S j$ if and only if the angle labeled i belongs to the left or to the right child of the angle labeled j. Note that $\lhd_S = \lhd_{[T^{\min}, T^{\max}]}$, where $T^{\min}$ (resp. $T^{\max}$) is obtained by replacing the nodes of S by left (resp. right) combs. Define $\mathfrak{Tofp}_n := \{\lhd_S \mid S \text{ Schröder tree on } [n]\}$.

Proposition 6.11. *1. A poset $\lhd$ is in $\mathfrak{Tofp}_n$ if and only if $\lhd \in \mathfrak{Toip}_n$ and for all $a < c$ incomparable in $\lhd$, either there exists $a < b < c$ such that $a \not\rhd b \not\lhd c$, or for all $a < b < c$ we have $a \rhd b \lhd c$.*
2. For any Schröder trees R, S, we have $\lhd_R \leq_\mathsf{R} \lhd_S \iff R \leq_\mathsf{F} S$ in the facial weak order on the associahedron $\mathbb{A}\mathrm{sso}(n)$ (see Section 5.1).
3. The weak order on $\mathfrak{Tofp}_n$ is a lattice but not a sublattice of the weak order on $\mathfrak{Pos}_n$, nor on $\mathfrak{Woip}_n$, nor on $\mathfrak{Toip}_n$.

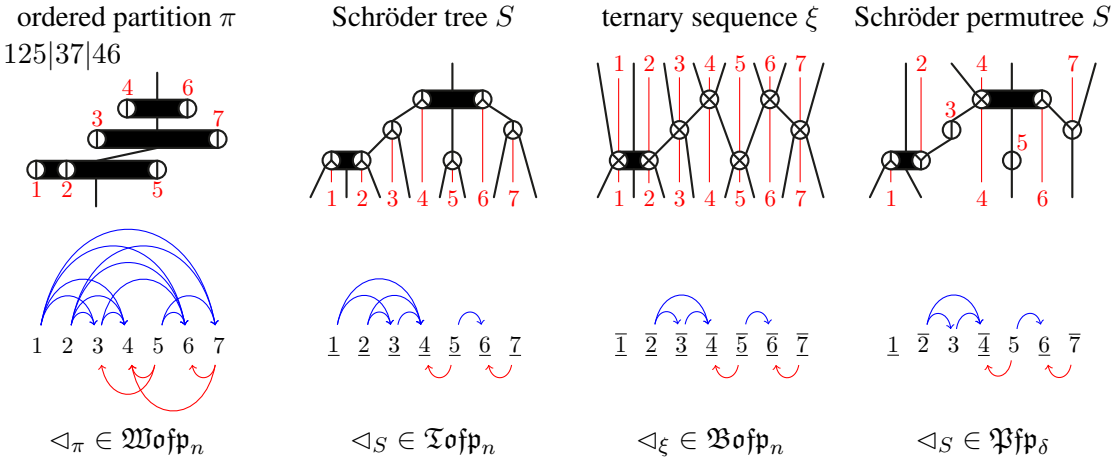

Figure 6.3: Posets for ordered partitions, Schröder trees, ternary sequences, and Schröder permutrees.

Finally, we want to show that the binary tree insertion $\mathbf{bt}$ and the Schröder tree insertion $\mathbf{st}$ can as well be directly understood at the level of posets. For this, define the $\mathfrak{Toip}$ *deletion* on integer posets by $\lhd^{\mathsf{TOIPd}} := \lhd \smallsetminus (\{(a,c) \,|\, \exists\ a<b<c,\ b \not\lhd c\} \cup \{(c,a) \,|\, \exists\ a<b<c,\ a \not\rhd b\})$.

Proposition 6.12. *For any permutation σ, weak order interval $\underline{\sigma} \leq_{\mathsf{W}} \overline{\sigma}$, and ordered partition π,*

$$(\lhd_\sigma)^{\mathsf{TOIPd}} = \lhd_{\mathbf{bt}(\sigma)}, \qquad (\lhd_{[\underline{\sigma},\overline{\sigma}]})^{\mathsf{TOIPd}} = \lhd_{[\mathbf{bt}(\underline{\sigma}),\, \mathbf{bt}(\overline{\sigma})]} \qquad \text{and} \qquad (\lhd_\pi)^{\mathsf{TOIPd}} = \lhd_{\mathbf{st}(\pi)}.$$

6.1.2.3 Permutrees, permutree intervals, and Schröder permutrees

To conclude this section, we want to mention that the statements of Sections 6.1.2.1 and 6.1.2.2 extend to the permutrees of Chapter 3. As illustrated in Figure 6.2, we associate to each permutree T its *permutree element poset* $\lhd_T$ where $i \lhd_T j$ if there is an oriented path from i to j in T. Define $\mathfrak{Pep}_\delta := \{\lhd_T \,|\, T\ \delta\text{-permutree}\}$. The next statement extends Propositions 6.6 and 6.9. A decoration $\delta \in \{\textcircled{\scriptsize I}, \textcircled{\scriptsize /}, \textcircled{\scriptsize \textbackslash}, \textcircled{\scriptsize X}\}^n$ is *covering* if $\delta_i \neq \textcircled{\scriptsize I}$ for any $i \in \{2, \dots, n-1\}$.

Proposition 6.13. *1. $\mathfrak{Pep}_\delta$ is characterized by local conditions*[1] *as in Propositions 6.6 and 6.9.*

2. For any δ-permutrees S, T, we have $\lhd_S \leq_{\mathsf{R}} \lhd_T \iff S \leq_{\mathsf{PT}} T$.

3. The permutree lattice on $\mathfrak{Pep}_\delta$ is always a sublattice of the weak order on $\mathfrak{Woip}_n$. Moreover, it is a sublattice of the weak order on $\mathfrak{Pos}_n$ when δ is covering, but not in general.

We now consider intervals in the permutree lattice. For two δ-permutrees $\underline{T} \leq_{\mathsf{PT}} \overline{T}$, consider the permutree interval $[\underline{T}, \overline{T}]_{\mathsf{PT}} := \{S\ \delta\text{-permutree} \,|\, \underline{T} \leq_{\mathsf{PT}} S \leq_{\mathsf{PT}} \overline{T}\}$. It corresponds to the *permutree interval poset* $\lhd_{[\underline{T},\overline{T}]} := \lhd_{\underline{T}} \cap \lhd_{\overline{T}} = \lhd^{\mathsf{Inc}}_{\overline{T}} \cup \lhd^{\mathsf{Dec}}_{\underline{T}}$. Define $\mathfrak{Pip}_\delta := \{\lhd_{[\underline{T},\overline{T}]} \mid \underline{T} \leq_{\mathsf{PT}} \overline{T}\ \delta\text{-permutrees}\}$. The next statement extends Propositions 6.7 and 6.10.

Proposition 6.14. *1. A poset $\lhd$ is in $\mathfrak{Pip}_\delta$ if and only if $\lhd \in \mathfrak{Woip}_n$ and for any $a<b<c$, we have $(a \lhd c \Rightarrow a \lhd b)$ and $(a \rhd c \Rightarrow b \rhd c)$ when $\delta_b \in \{\textcircled{\scriptsize X}, \textcircled{\scriptsize \textbackslash}\}$, and $(a \lhd c \Rightarrow b \lhd c)$ and $(a \rhd c \Rightarrow a \rhd b)$ when $\delta_b \in \{\textcircled{\scriptsize /}, \textcircled{\scriptsize \textbackslash}\}$.*

2. For any δ-permutrees $\underline{S} \leq_{\mathsf{PT}} \overline{S}$ and $\underline{T} \leq_{\mathsf{PT}} \overline{T}$, we have $\lhd_{[\underline{S},\overline{S}]} \leq_{\mathsf{R}} \lhd_{[\underline{T},\overline{T}]} \iff \underline{S} \leq_{\mathsf{PT}} \underline{T}$ and $\overline{S} \leq_{\mathsf{PT}} \overline{T}$.

3. The weak order on $\mathfrak{Pip}_\delta$ is always a sublattice of the weak order on $\mathfrak{Woip}_n$. Moreover, it is a sublattice of the weak order on $\mathfrak{Pos}_n$ when δ is covering, but not in general.

[1] The detailed conditions are quite intricate but can be found in [CPP19, Prop. 2.3.12].

To extend Propositions 6.8 and 6.11, we now consider facial intervals of the permutree lattice. The faces of the permutreehedron $\mathbb{PT}(\delta)$ correspond to the Schröder δ-permutrees, which are obtained from the δ-permutrees by edge contractions. As illustrated in Figure 6.3, we define the *permutree face poset* $\lhd_S = \lhd_{[T^{\min}, T^{\max}]}$, where $T^{\min}$ (resp. $T^{\max}$) is obtained by replacing the nodes of S by left (resp. right) combs (with the correct orientations). Define $\mathfrak{Pfp}_\delta := \{\lhd_S \mid S \text{ Schröder } \delta\text{-permutree}\}$.

Proposition 6.15. *1. $\mathfrak{Pfp}_\delta$ is characterized by local conditions[2] as in Propositions 6.8 and 6.11.*
2. *For any Schröder permutrees R, S, we have $\lhd_R \leq_{\mathsf{R}} \lhd_S \iff R \leq_{\mathsf{F}} S$ in the facial weak order on the permutreehedron $\mathbb{PT}(\delta)$ (see Section 5.1).*
3. *The weak order on $\mathfrak{Pfp}_\delta$ is a lattice but not a sublattice of the weak order on $\mathfrak{Pos}_n$, nor on $\mathfrak{Woip}_n$, nor on $\mathfrak{Pip}_\delta$.*

Finally, for $\lhd \in \mathfrak{Pos}_n$, we define its $\mathfrak{Pip}_\delta$ *deletion* $\lhd^{\mathsf{PIP}_\delta\mathsf{d}}$ to be the poset obtained by removing simultaneously from $\lhd$ all increasing relations (a, c) such that:
- either $\exists\, a < b_1 < \ldots < b_k < c$ with $a \not\lhd b_1 \not\lhd \cdots \not\lhd b_k \not\lhd c$ (preventing $\lhd \in \mathfrak{Woip}$),
- or $\exists\, a \leq n < p \leq c$ with $n = a$ or $\delta_n \in \{\circledcirc, \otimes\}$, while $p = c$ or $\delta_n \in \{\circledcirc, \otimes\}$, and $n \not\lhd p$.

and their analogue decreasing relations. We now give an analogue of Proposition 6.12.

Proposition 6.16. *For any permutation σ, weak order interval $\underline{\sigma} \leq_{\mathsf{R}} \overline{\sigma}$, and ordered partition π,*

$$(\lhd_\sigma)^{\mathsf{PIP}_\delta\mathsf{d}} = \lhd_{\Psi_\delta^{\delta'}(\sigma)}, \quad (\lhd_{[\underline{\sigma},\overline{\sigma}]})^{\mathsf{PIP}_\delta\mathsf{d}} = \lhd_{[\Psi_\delta^{\delta'}(\underline{\sigma}),\, \Psi_\delta^{\delta'}(\overline{\sigma})]} \quad \text{and} \quad (\lhd_\pi)^{\mathsf{PIP}_\delta\mathsf{d}} = \lhd_{\Psi_\delta^{\delta'}(\pi)},$$

where $\Psi_\delta^{\delta'}(\sigma)$ (resp. $\Psi_\delta^{\delta'}(\pi)$) is the permutree (resp. Schröder permutree) associated to σ (resp. π).

To conclude, note that this section provides in particular an interpretation of the boolean lattice and its interval lattice (and thus of its facial interval lattice) in terms of integer posets. The corresponding families of integer posets $\mathfrak{Boep}_n$ and $\mathfrak{Boip}_n = \mathfrak{Bofp}_n$ are illustrated in Figures 6.2 and 6.3.

6.2 Hopf algebra on integer posets

We now construct a Hopf algebra on integer posets. We then show that the permutations, the weak order intervals, and the ordered partitions index certain quotients of the integer poset algebra, and that the binary trees, the Tamari intervals, and the Schröder trees index subalgebras of these quotients. Define $\mathfrak{R} := \bigsqcup_{n\geq 0} \mathfrak{R}_n$ and similarly for the other families of relations considered in this chapter.

6.2.1 Hopf algebras on binary relations and integer posets

As for the weak order, we first define our Hopf algebra at the level of binary relations. We consider the vector space $\boldsymbol{k}\mathfrak{R} := \bigoplus_{n\geq 0} \boldsymbol{k}\mathfrak{R}_n$ indexed by all integer binary relations of arbitrary size. We denote by $R_X := \{(i, j) \in [k]^2 \mid x_i\, R\, x_k\}$ the *restriction* of an integer relation $R \in \mathfrak{R}_n$ to a subset $X = \{x_1, \ldots, x_k\} \subseteq [n]$. We define:
1. the *product* of two integer relations $R \in \mathfrak{R}_m$ and $S \in \mathfrak{R}_n$ by $R \cdot S := \sum T$ where T ranges over all integer relations $T \in \mathfrak{R}_{m+n}$ with $T_{[m]} = R$ and $T_{[n+m]\smallsetminus[m]} = S$,
2. the *coproduct* of an integer relation $T \in \mathfrak{R}(p)$ by $\triangle(T) := \sum T_X \otimes T_Y$ where the sum ranges over all partitions $X \sqcup Y \subseteq [p]$ such that $x\, T\, y$ and $y \not T\, x$ for all $(x, y) \in X \times Y$.

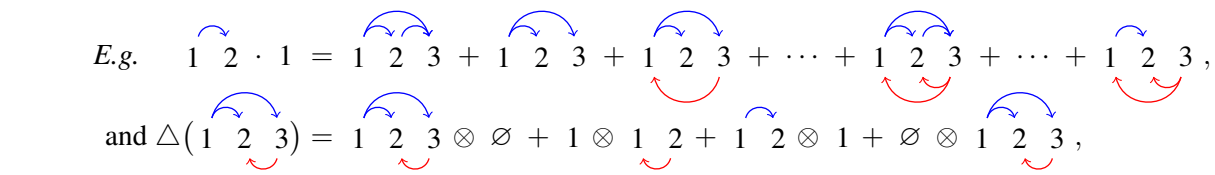

where the terms in the coproduct arise from X ranging in $\{1, 2, 3\}$, $\{1\}$, $\{1, 3\}$, and $\varnothing$.

[2] The detailed conditions are quite intricate but can be found in [CPP19, Prop. 2.3.17].

Proposition 6.17. *For $R \in \mathfrak{R}_m$ and $S \in \mathfrak{R}_n$, the product $R \cdot S$ is the sum over the interval between $R \backslash S := R \cup S^{\to m} \cup ([m] \times [n]^{\to m})$ and $R/S := R \cup S^{\to m} \cup ([n]^{\to m} \times [m])$ in the weak order on $\mathfrak{R}_{m+n}$ (where $S^{\to m} := \{(m+i, m+j) \,|\, (i,j) \in S\}$ and $[n]^{\to m} := [m+n] \smallsetminus [m]$).*

Proposition 6.18. *The product $\cdot$ and coproduct $\triangle$ endow $\boldsymbol{k}\mathfrak{R}$ with a Hopf algebra structure.*

We now use this Hopf algebra on binary relations to get a Hopf algebra on posets.

Proposition 6.19. *If $R \in \mathfrak{R}$ is not a poset, then none of the summands in $R \cdot S$ (resp. $\triangle(R)$) is a poset (resp. the tensor product of two posets). In other words, the vector subspace of $\boldsymbol{k}\mathfrak{R}$ generated by integer relations which are not posets is a Hopf ideal of $\boldsymbol{k}\mathfrak{R}$. The quotient of $\boldsymbol{k}\mathfrak{R}$ by this ideal is thus a Hopf algebra $\boldsymbol{k}\mathfrak{Pos}$ on integer posets.*

E.g. 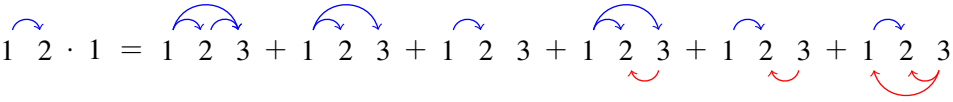 in $\boldsymbol{k}\mathfrak{Pos}$.

Proposition 6.20. *For $\lhd \in \mathfrak{Pos}_m$ and $\blacktriangleleft \in \mathfrak{Pos}_n$, the product $\lhd \cdot \blacktriangleleft$ is the interval between $\lhd \backslash \blacktriangleleft$ and $\lhd / \blacktriangleleft$ in the weak order on $\mathfrak{Pos}_{m+n}$.*

6.2.2 Hopf algebras on relevant families of integer posets

We now use the families of integer posets defined in Section 6.1.2 to define relevant Hopf algebras.

6.2.2.1 Permutations, weak order intervals, and ordered partitions

We first want to construct Hopf algebras on $\mathfrak{Woep}$, $\mathfrak{Woip}$ and $\mathfrak{Wofp}$ as quotients of the integer poset Hopf algebra $\boldsymbol{k}\mathfrak{Pos}$. The important point is that all these families of posets are defined by local conditions on their relations, and that a contradiction to these conditions cannot be destroyed by the product or the coproduct.

We start with weak order element posets $\mathfrak{Woep}$, interpreting C. Malvenuto and C. Reutenauer's Hopf algebra on permutations [MR95] as a quotient of the integer poset Hopf algebra $\boldsymbol{k}\mathfrak{Pos}$.

Proposition 6.21. *1. The vector subspace of $\boldsymbol{k}\mathfrak{Pos}$ generated by non-total integer posets is a Hopf ideal of $\boldsymbol{k}\mathfrak{Pos}$. The quotient of the poset Hopf algebra $\boldsymbol{k}\mathfrak{Pos}$ by this ideal is thus a Hopf algebra $\boldsymbol{k}\mathfrak{Woep}$ on total orders.*

2. The map $\sigma \mapsto \lhd_\sigma$ defines a Hopf algebra isomorphism from C. Malvenuto and C. Reutenauer's Hopf algebra $\boldsymbol{k}\mathfrak{S}$ on permutations [MR95] to $\boldsymbol{k}\mathfrak{Woep}$.

3. For any permutations $\sigma \in \mathfrak{S}_m$ and $\tau \in \mathfrak{S}_n$, the product $\lhd_\sigma \cdot \lhd_\tau$ is the interval between $\lhd_\sigma \backslash \lhd_\tau$ and $\lhd_\sigma / \lhd_\tau$ in the weak order on $\mathfrak{Woep}_{m+n}$.

E.g. 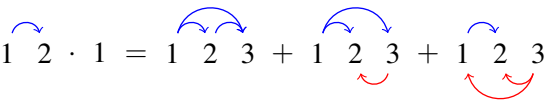 in $\boldsymbol{k}\mathfrak{Woep}$.

We now consider weak order interval posets $\mathfrak{Woip}$, characterized in Proposition 6.7.

Proposition 6.22. *1. The vector subspace of $\boldsymbol{k}\mathfrak{Pos}$ generated by $\mathfrak{Pos} \smallsetminus \mathfrak{Woip}$ is a Hopf ideal of $\boldsymbol{k}\mathfrak{Pos}$. The quotient of the integer poset algebra $\boldsymbol{k}\mathfrak{Pos}$ by this ideal is thus a Hopf algebra $\boldsymbol{k}\mathfrak{Woip}$ on weak order intervals.*

2. For any $\underline{\sigma} \leq_{\mathsf{R}} \overline{\sigma} \in \mathfrak{S}_m$ and $\underline{\tau} \leq_{\mathsf{R}} \overline{\tau} \in \mathfrak{S}_n$, the product $\lhd_{[\underline{\sigma},\overline{\sigma}]} \cdot \lhd_{[\underline{\tau},\overline{\tau}]}$ is the interval between $\lhd_{[\underline{\sigma},\overline{\sigma}]} \backslash \lhd_{[\underline{\tau},\overline{\tau}]}$ and $\lhd_{[\underline{\sigma},\overline{\sigma}]} / \lhd_{[\underline{\tau},\overline{\tau}]}$ in the weak order on $\mathfrak{Woip}_{m+n}$.

E.g. 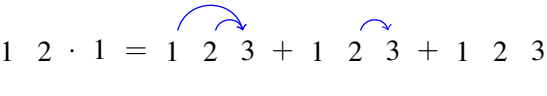 in $\boldsymbol{k}\mathfrak{Woip}$.

Finally, a similar statement holds for weak order face posets $\mathfrak{Wofp}$, characterized in Proposition 6.8. The resulting Hopf algebra is isomorphic to that of [Cha00] mentioned in Section 5.1.3.

Proposition 6.23. *1. The vector subspace of $\boldsymbol{k}\mathfrak{Pos}$ generated by $\mathfrak{Pos} \setminus \mathfrak{Woip}$ is a Hopf ideal of $\boldsymbol{k}\mathfrak{Pos}$. The quotient of the poset Hopf algebra $\boldsymbol{k}\mathfrak{Pos}$ by this ideal is thus a Hopf algebra $\boldsymbol{k}\mathfrak{Wofp}$ on faces of the permutahedron $\mathbb{P}\mathrm{erm}(n)$.*

2. The map $\pi \mapsto \lhd_\pi$ defines a Hopf algebra isomorphism from F. Chapoton's Hopf algebra $\boldsymbol{k}\mathfrak{P}$ on ordered partitions [Cha00] to $\boldsymbol{k}\mathfrak{Wofp}$ (see Section 5.1.3).

3. For any ordered partitions μ of $[m]$ and ν of $[n]$, the product $\lhd_\mu \cdot \lhd_\nu$ is the interval between $\lhd_\mu \backslash \lhd_\nu$ and $\lhd_\mu / \lhd_\nu$ in the weak order on $\mathfrak{Wofp}_{m+n}$.

E.g. $1\ 2 \cdot 1 = 1\ 2\ 3 + 1\ 2\ 3 + 1\ 2\ 3$ in $\boldsymbol{k}\mathfrak{Wofp}$.

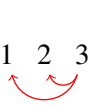

6.2.2.2 Binary trees, Tamari intervals, and Schröder trees

To conclude, we use the $\mathfrak{Toip}$ deletion defined in the end of Section 6.1.2.2 to construct Hopf subalgebras of $\boldsymbol{k}\mathfrak{Woep}$, $\boldsymbol{k}\mathfrak{Woip}$ and $\boldsymbol{k}\mathfrak{Wofp}$ respectively indexed by $\mathfrak{Toep}$, $\mathfrak{Toip}$ and $\mathfrak{Tofp}$. This idea mimics the construction of J.-L. Loday and M. Ronco's Hopf algebra $\boldsymbol{k}\mathfrak{T}$ on binary trees [LR98, HNT05], that can be defined as a Hopf subalgebra of the C. Malvenuto and C. Reutenauer's Hopf algebra $\boldsymbol{k}\mathfrak{S}$ on permutations [MR95].

Proposition 6.24. *1. The vector subspace $\boldsymbol{k}\mathfrak{Toep}$ of $\boldsymbol{k}\mathfrak{Woep}$ generated by the sums of the fibers $\left\{ \blacktriangleleft \in \mathfrak{Woep} \,\middle|\, \blacktriangleleft^{\mathsf{TOIPd}} = \lhd \right\}$ for all $\lhd \in \mathfrak{Toep}$ is stable by $\cdot$ and $\triangle$.*

2. For any binary trees $S \in \mathfrak{T}_m$ and $T \in \mathfrak{T}_n$, the product $\lhd_S \cdot \lhd_T$ is the interval between $\lhd_S \backslash \lhd_T$ and $\lhd_S / \lhd_T$ in the weak order on $\mathfrak{Toep}_{m+n}$.

3. The map $T \mapsto \lhd_T$ is a Hopf algebra isomorphism from the J.-L. Loday M. Ronco's Hopf algebra $\boldsymbol{k}\mathfrak{T}$ on binary trees [LR98, HNT05] to $\boldsymbol{k}\mathfrak{Toep}$.

We now proceed to the same construction for Tamari intervals. To the best of our knowledge, our approach provides the first Hopf algebra on Tamari intervals.

Proposition 6.25. *1. The vector subspace $\boldsymbol{k}\mathfrak{Toip}$ of $\boldsymbol{k}\mathfrak{Woip}$ generated by the sums of the fibers $\left\{ \blacktriangleleft \in \mathfrak{Woip} \,\middle|\, \blacktriangleleft^{\mathsf{TOIPd}} = \lhd \right\}$ for all $\lhd \in \mathfrak{Toip}$ is stable by $\cdot$ and $\triangle$.*

2. For any Tamari intervals $\underline{S} \leq_{\mathsf{R}} \overline{S} \in \mathfrak{T}_m$ and $\underline{T} \leq_{\mathsf{R}} \overline{T} \in \mathfrak{T}_n$, the product $\lhd_{[\underline{S},\overline{S}]} \cdot \lhd_{[\underline{T},\overline{T}]}$ is the interval between $\lhd_{[\underline{S},\overline{S}]} \backslash \lhd_{[\underline{T},\overline{T}]}$ and $\lhd_{[\underline{S},\overline{S}]} / \lhd_{[\underline{T},\overline{T}]}$ in the weak order on $\mathfrak{Woip}_{m+n}$.

The same construction for faces recovers F. Chapoton's Schröder trees Hopf Algebra [Cha00].

Proposition 6.26. *1. The vector subspace $\boldsymbol{k}\mathfrak{Tofp}$ of $\boldsymbol{k}\mathfrak{Wofp}$ generated by the sums of the fibers $\left\{ \blacktriangleleft \in \mathfrak{Wofp} \,\middle|\, \blacktriangleleft^{\mathsf{TOIPd}} = \lhd \right\}$ for all $\lhd \in \mathfrak{Tofp}$ is stable by $\cdot$ and $\triangle$.*

2. For any Schröder trees S on $[m]$ and T on $[n]$, the product $\lhd_S \cdot \lhd_T$ is the interval between $\lhd_S \backslash \lhd_T$ and $\lhd_S / \lhd_T$ in the weak order on $\mathfrak{Wofp}_{m+n}$.

3. The map $S \mapsto \lhd_S$ is a Hopf algebra isomorphism from F. Chapoton's algebra on Schröder trees [Cha00] to $\boldsymbol{k}\mathfrak{Tofp}$ (see Section 5.1.3).

Finally, let us mention that similar ideas can be used to uniformly construct Hopf algebra structures on permutrees, permutree intervals, and Schröder permutrees. Following [CP17, PP18], one first defines some decorated versions of the Hopf algebras $\boldsymbol{k}\mathfrak{Woep}$, $\boldsymbol{k}\mathfrak{Woip}$ and $\boldsymbol{k}\mathfrak{Wofp}$, where each poset on $[n]$ appears 4^n times with all possible different decorations. One then constructs Hopf algebras on $\boldsymbol{k}\mathfrak{Pep}$, $\boldsymbol{k}\mathfrak{Pip}$ and $\boldsymbol{k}\mathfrak{Pfp}$ using the fibers of the map $(\lhd, \delta) \mapsto \lhd^{\mathsf{PIP}_\delta\mathsf{d}}$. See [PP18, PP20]. This provides in particular Hopf algebra structures on the families $\mathfrak{Boep}$ and $\mathfrak{Boip} = \mathfrak{Bofp}$ of integer posets corresponding to the boolean lattice and its intervals.

6.3 Weak order on Coxeter posets

Similarly to Section 5.3, we conclude this chapter with a brief discussion of the possible extensions of the weak order on posets to finite Coxeter groups. More details can be found in [GP18].

6.3.1 Φ-posets

We consider certain specific families of collections of roots generalizing posets in type A. We start with the simple definition of symmetric and antisymmetric subsets of roots.

Definition 6.27. *A subset $R \subseteq \Phi$ is* symmetric *if $-R = R$ and* antisymmetric *if $R \cap -R = \varnothing$.*

We now want to define closed sets of roots. The next statement is proved by A. Pilkington [Pil06, Sect. 2] for subsets of positive roots but extends to subsets of all roots. Recall that a root system Φ is *crystallographic* if $\langle \alpha^\vee \,|\, \beta \rangle \in \mathbb{Z}$ for any $\alpha, \beta \in \Phi$. Equivalently, the Coxeter group W stabilizes the lattice $\mathbb{Z}\Phi$, and is called a *Weyl group*.

Lemma 6.28. *In a crystallographic root system Φ, the following conditions are equivalent for $R \subseteq \Phi$:*
(i) $\alpha + \beta \in R$ *for any* $\alpha, \beta \in R$ *such that* $\alpha + \beta \in \Phi$,
(ii) $m\alpha + n\beta \in R$ *for any* $\alpha, \beta \in R$ *and* $m, n \in \mathbb{N}$ *such that* $m\alpha + n\beta \in \Phi$,
(iii) $\alpha_1 + \cdots + \alpha_p \in R$ *for any* $\alpha_1, \dots, \alpha_p \in R$ *such that* $\alpha_1 + \cdots + \alpha_p \in \Phi$.

Definition 6.29. *In a crystallographic root system Φ, a subset $R \subseteq \Phi$ is* closed *if it satisfies the equivalent conditions of Lemma 6.28.*

Definition 6.30. *In a crystallographic root system Φ, the* closure *of $R \subseteq \Phi$ is the set $R^{\mathrm{cl}} := \mathbb{N}R \cap \Phi$.*

Remark 6.31. The map $R \mapsto R^{\mathrm{cl}}$ is a closure operator on Φ, meaning that $\varnothing^{\mathrm{cl}} = \varnothing$, $\Phi \subseteq \Phi^{\mathrm{cl}}$, $R \subseteq S \implies R^{\mathrm{cl}} \subseteq S^{\mathrm{cl}}$ and $(R^{\mathrm{cl}})^{\mathrm{cl}} = R^{\mathrm{cl}}$ for all $R, S \subseteq \Phi$. Moreover R^{cl} is closed and R is closed if and only if $R = R^{\mathrm{cl}}$.

Remark 6.32. Lemma 6.28 fails for non-crystallographic root systems. For example, consider the type $H_2 = I_2(5)$ Coxeter group and the roots $\alpha := \alpha_1$, $\beta := \alpha_2$, $\gamma := \psi\alpha_1 + \psi\alpha_2$ and $\delta := -\alpha_1 - \psi\alpha_2$, where $\psi = -2\cos(4\pi/5)$. Then the set $R := \{\alpha, \beta, \gamma, \delta\}$ satisfies (i) but not (iii).

Remark 6.33. As studied in details by A. Pilkington in [Pil06], even in crystallographic root systems, there are other possible notions of closed sets of roots. Namely, one says that $R \subseteq \Phi$ is
- $\mathbb{N}$*-closed* if $m\alpha + n\beta \in R$ for any $\alpha, \beta \in R$ and $m, n \in \mathbb{N}$ such that $m\alpha + n\beta \in \Phi$,
- $\mathbb{R}$*-closed* if $x\alpha + y\beta \in R$ for any $\alpha, \beta \in R$ and $x, y \in \mathbb{R}$ such that $x\alpha + y\beta \in \Phi$,
- *convex* if $R = \Phi \cap C$ for a convex cone C in V.

Note that convex implies $\mathbb{R}$-closed which implies $\mathbb{N}$-closed, but that the converse statements are wrong even for finite root systems [Pil06, p. 3192]. In this section, we will only work with the notion of $\mathbb{N}$-closedness in crystallographic root systems, as it is discussed in [Bou68]. Remark 6.40 justifies this restriction.

Example 6.34. In type A, we identify subsets of roots with integer binary relations via the bijection $(i, j) \in [n]^2 \longleftrightarrow \boldsymbol{e}_i - \boldsymbol{e}_j \in \Phi_A$. A subset of roots is symmetric (resp. antisymmetric, resp. closed) if the corresponding integer binary relation is symmetric (resp. antisymmetric, resp. transitive). (Note that here the three notions of closed sets of roots mentioned in Remark 6.33 coincide in type A.) This example motivates the following definition.

Definition 6.35. *In a crystallographic root system Φ, a* Φ-poset *is an antisymmetric and $\mathbb{N}$-closed subset of roots of Φ. We denote by $\mathfrak{Pos}(\Phi)$ the set of all Φ-posets.*

6.3.2 Weak order on Φ-posets

Let Φ be a finite root system (not necessarily crystallographic for the moment), with positive roots Φ^+ and negative roots Φ^-. We denote by $\mathfrak{R}(\Phi)$ the set of all subsets of Φ. For $R \in \mathfrak{R}(\Phi)$, we denote by $R^+ := R \cap \Phi^+$ its positive part and $R^- := R \cap \Phi^-$ its negative part. The following order extends the weak order on binary relations introduced in Definition 6.3.

Definition 6.36. *The weak order on $\mathfrak{R}(\Phi)$ is defined by $R \leq_{\mathsf{R}} S \iff R^+ \subseteq S^+$ and $R^- \supseteq S^-$. It is a lattice with meet and join*

$$R \wedge_{\mathsf{R}} S = (R^+ \cap S^+) \sqcup (R^- \cup S^-) \qquad \text{and} \qquad R \vee_{\mathsf{R}} S = (R^+ \cup S^+) \sqcup (R^- \cap S^-).$$

As in Section 6.1.1, $\wedge_{\mathsf{R}}$ and $\vee_{\mathsf{R}}$ preserve antisymmetric but not closed subsets of roots. We therefore need an analogue of the operators of Definition 6.4.

Definition 6.37. *For $R \in \mathfrak{R}(\Phi)$, we define the positive and negative closure deletions R^{pcd} and R^{ncd} by*

$$R^{\mathsf{pcd}} := R \smallsetminus \{\alpha \in R^+ \mid \exists\, X \subseteq R^- \text{such that } \alpha + \Sigma X \in \Phi \smallsetminus R\},$$
$$R^{\mathsf{ncd}} := R \smallsetminus \{\alpha \in R^- \mid \exists\, X \subseteq R^+ \text{such that } \alpha + \Sigma X \in \Phi \smallsetminus R\}.$$

These operators enable us to state the following extension of Theorem 6.5, illustrated in Figure 6.4.

Theorem 6.38. *When Φ is crystallographic, the subposet of the weak order induced by Φ-posets is a lattice with meet and join*

$$R \wedge_{\mathsf{P}} S = \big((R^+ \cap S^+) \sqcup (R^- \cup S^-)^{\mathrm{cl}}\big)^{\mathsf{pcd}} \quad \text{and} \quad R \vee_{\mathsf{P}} S = \big((R^+ \cup S^+)^{\mathrm{cl}} \sqcup (R^- \cap S^-)\big)^{\mathsf{ncd}}.$$

Remark 6.39. Surprisingly, this result fails for non-crystallographic root systems. In view of Remark 6.32, it might a priori depend of the notion of $\mathbb{N}$-closed subsets considered. However, the following example works for either of the notions (i), (ii) and (iii) of Lemma 6.28. Consider the Coxeter group of type H_3 with Dynkin diagram $1 \overset{5}{—} 2 — 3$. Consider the roots $\alpha := \alpha_1 \in \Phi^+$, $\beta := -\alpha_1 - \psi\alpha_2 \in \Phi^-$ and $\gamma := -\psi\alpha_1 - \alpha_2 - \alpha_3 \in \Phi^-$, where $\psi = -2\cos(4\pi/5)$. Note that $\beta + \gamma \in \Phi^-$ and $\alpha + \beta + \gamma \in \Phi^-$, while $\alpha + \beta \notin \Phi$ and $\alpha + \gamma \notin \Phi$. Consider the sets $R := \{\alpha,\ \beta,\ \gamma,\ \beta + \gamma,\ \alpha + \beta + \gamma\}$, $S := \{\beta,\ \gamma,\ \beta + \gamma\}$, $U := \{\alpha, \beta\}$ and $V := \{\alpha, \gamma\}$. Note that R, S, U and V are Φ-posets, and that both U and V are weak order larger than both R and S. Moreover, we claim that there is no Φ-poset T which is weak order smaller than both U and V and weak order larger than both R and S. Indeed, such a Φ-poset T should contain α, β, γ and thus $\beta + \gamma$ and $\alpha + \beta + \gamma$ by closedness, which would contradict $S \leq_{\mathsf{W}} T$. This implies that R and S have no join and that U and V have no meet in the weak order on Φ-posets, thus contradicting the result of Theorem 6.38 in the non-crystallographic type H_3.

Remark 6.40. As mentioned in Remark 6.33, even for crystallographic root systems, there are different possible notions of closed subsets (which all coincide in type A). Unfortunately, it turns out that Theorem 6.38 fails for the other notions of closed sets. The smallest counter-example is in type B_3. Consider the sets of roots $R := \{-\alpha_1,\ -\alpha_1 - \alpha_2,\ -\alpha_1 - \alpha_2 - \alpha_3,\ -\alpha_1 - 2\alpha_2 - 2\alpha_3,\ \alpha_3\}$, $S := \{-\alpha_1,\ -\alpha_1 - \alpha_2 - \alpha_3,\ -\alpha_1 - 2\alpha_2 - 2\alpha_3\}$, $U := \{-\alpha_1,\ \alpha_3\}$ and $V := \{-\alpha_1 - 2\alpha_2 - 2\alpha_3,\ \alpha_3\}$. Note that R, S, U and V are convex, and that both U and V are weak order smaller than both R and S. We have $R \vee_{\mathsf{P}} S = U \wedge_{\mathsf{P}} V = \{-\alpha_1,\ -\alpha_1 - 2\alpha_2 - 2\alpha_3,\ \alpha_3\}$ but this set is not convex. In fact, we claim that there is no convex subset T which is weak order smaller than both U and V and weak order larger than both R and S. Indeed, such a set T should contain $\{-\alpha_1,\ -\alpha_1 - 2\alpha_2 - 2\alpha_3,\ \alpha_3\}$ and thus also $-\alpha_1 - \alpha_2 = (-\alpha_1)/2 + (-\alpha_1 - 2\alpha_2 - 2\alpha_3)/2 + \alpha_3$, contradicting $T \leq_{\mathsf{W}} S$. This implies that R and S have no join and that U and V have no meet in the weak order on convex subsets of Φ.

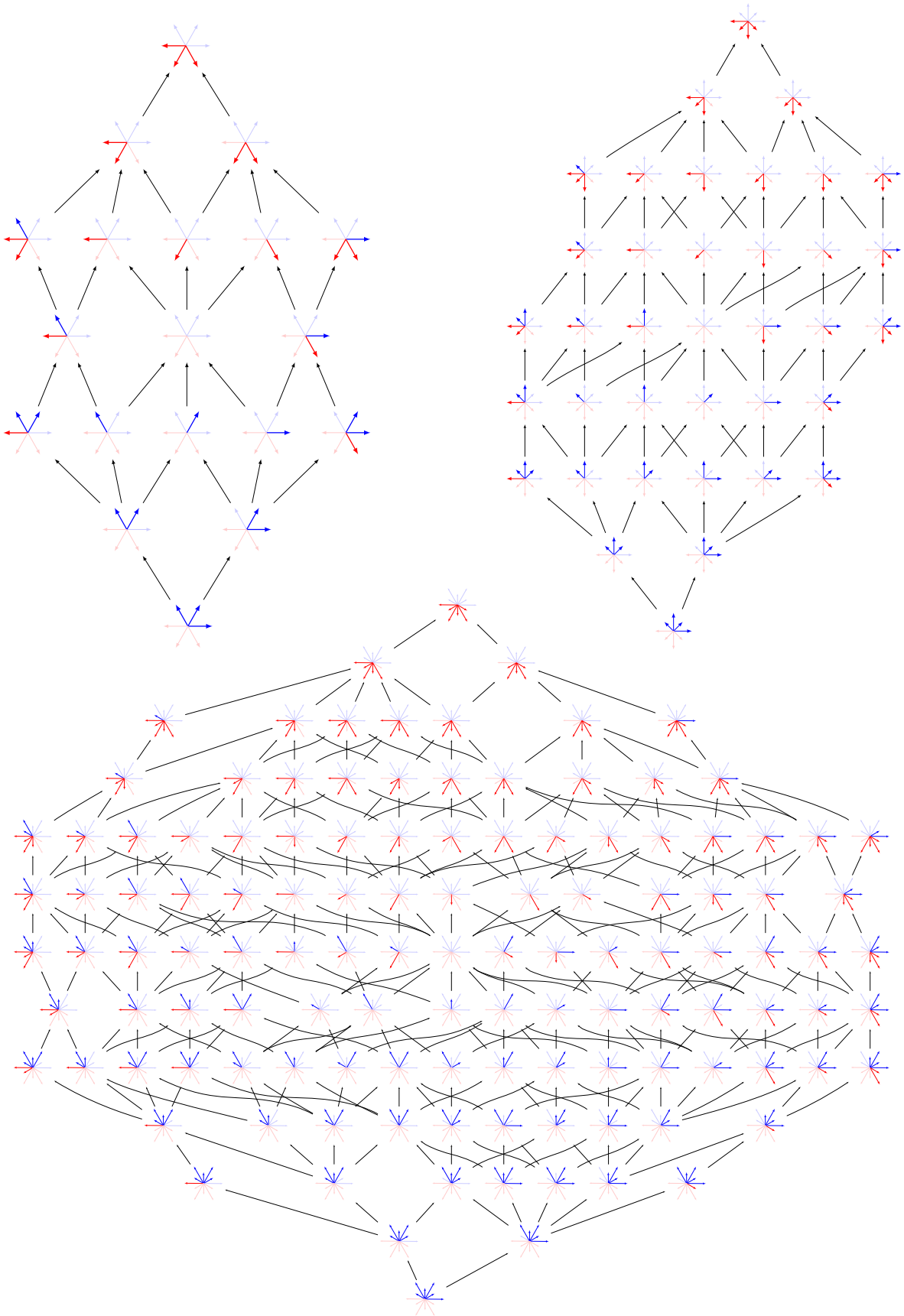

Figure 6.4: The weak order on A_2-posets (top left), B_2-posets (top right), and G_2-posets (bottom).

6.3.3 Weak order on relevant families of Φ-posets

As in Section 6.1.2, relevant families of Φ-posets correspond to the elements, the intervals, and the faces of the weak order on W. Again, for each of these special families of Φ-posets, we are interested in (1) a characterization of the Φ-posets of this family, (2) an interpretation of the weak order on these Φ-posets, and (3) whether it is a sublattice of the weak order on all Φ-posets. We start with the elements of W. Each element $w \in W$ defines a *weak order element poset* $R_w := w(\Phi^-)$. Define $\mathfrak{Woep}(\Phi) := \{R_w \mid w \in W\}$. Recall from Section 5.2.1 that the inversion set of $w \in W$ is the set of roots $\boldsymbol{N}(w) := \Phi^+ \cap w(\Phi^-)$.

Proposition 6.41. *1. A Φ-poset R is in $\mathfrak{Woep}(\Phi)$ if and only if $\alpha \in R$ or $-\alpha \in R$ for all $\alpha \in \Phi$.*
2. For $w \in W$, we have $\boldsymbol{N}(w) = \Phi^+ \cap R_w$ and $R_w = \big(\Phi^- \smallsetminus -\boldsymbol{N}(w)\big) \sqcup \boldsymbol{N}(w)$. Therefore, for any $v, w \in W$, we have $R_v \leq_{\mathsf{R}} R_w \iff v \leq_{\mathsf{W}} w$.
3. Moreover, the weak order on $\mathfrak{Woep}(\Phi)$ is a sublattice of the weak order on $\mathfrak{Pos}(\Phi)$.

For $\underline{w} \leq_{\mathsf{W}} \overline{w} \in W$, we consider the weak order interval $[\underline{w}, \overline{w}]_{\mathsf{W}} := \{v \in W \mid \underline{w} \leq_{\mathsf{W}} v \leq_{\mathsf{W}} \overline{w}\}$. It corresponds to the *weak order interval poset* $R_{[\underline{w},\overline{w}]} := \bigcap_{v \in [\underline{w},\overline{w}]} R_v = R_{\underline{w}} \cap R_{\overline{w}} = R^-_{\underline{w}} \sqcup R^+_{\overline{w}}$. Define $\mathfrak{Woip}(\Phi) := \big\{R_{[\underline{w},\overline{w}]} \,\big|\, \underline{w}, \overline{w} \in W,\ \underline{w} \leq_{\mathsf{W}} \overline{w}\big\}$.

Proposition 6.42. *1. A Φ-poset R is in $\mathfrak{Woip}(\Phi)$ if and only if $\alpha + \beta \in R$ implies $\alpha \in R$ or $\beta \in R$ for all $\alpha, \beta \in \Phi^-$ and all $\alpha, \beta \in \Phi^+$.*
2. For any $\underline{v} \leq_{\mathsf{W}} \overline{v}$ and $\underline{w} \leq_{\mathsf{W}} \overline{w}$ in W, we have $R_{[\underline{v},\overline{v}]} \leq_{\mathsf{R}} R_{[\underline{w},\overline{w}]} \iff \underline{v} \leq_{\mathsf{W}} \underline{w}$ and $\overline{v} \leq_{\mathsf{W}} \overline{w}$.
3. The weak order on $\mathfrak{Woip}(\Phi)$ is a lattice with meet $R_{[\underline{v},\overline{v}]} \wedge_{\mathsf{WOIP}} R_{[\underline{w},\overline{w}]} = R_{[\underline{v} \wedge_{\mathsf{W}} \underline{w}, \overline{v} \wedge_{\mathsf{W}} \overline{w}]}$ and join $R_{[\underline{v},\overline{v}]} \vee_{\mathsf{WOIP}} R_{[\underline{w},\overline{w}]} = R_{[\underline{v} \vee_{\mathsf{W}} \underline{w}, \overline{v} \vee_{\mathsf{W}} \overline{w}]}$. However, the weak order on $\mathfrak{Woip}(\Phi)$ is not a sublattice of the weak order on $\mathfrak{Pos}(\Phi)$.

Finally, we consider the faces of the permutahedron $\mathbb{P}\mathrm{erm}(W)$. In Section 5.2.2, we have already associated to each standard parabolic coset xW_I the root set $\boldsymbol{R}(xW_I) := x(\Phi^- \cup \Phi_I^+)$. We cannot use this root set here as it is not a Φ-poset (it is not antisymmetric in general). Instead, we consider the *weak order face poset* $R_{xW_I} := x(\Phi^- \smallsetminus \Phi_I) = \Phi \smallsetminus \big(-\boldsymbol{R}(xW_I)\big)$, which is always a Φ-poset. Define $\mathfrak{Wofp}(\Phi) := \{R_{xW_I} \mid xW_I \text{ standard parabolic coset of } W\}$.

Proposition 6.43. *1. A Φ-poset is in $\mathfrak{Wofp}(\Phi)$ if and only if it is convex closed and antisymmetric.*
2. For any standard parabolic cosets xW_I and yW_J, we have $R_{xW_I} \leq_{\mathsf{W}} R_{yW_J}$ in the weak order on $\mathfrak{Wofp}(\Phi)$ if and only if $xW_I \leq_{\mathsf{F}} yW_J$ in the facial weak order of [DHP18], see Section 5.2.
3. The weak order on $\mathfrak{Wofp}(\Phi)$ is a lattice with meet $R_{xW_I} \wedge_{\mathsf{WOFP}} R_{yW_J} = R_{xW_I \wedge_{\mathsf{F}} yW_J}$ and join $R_{xW_I} \vee_{\mathsf{WOFP}} R_{yW_J} = R_{xW_I \vee_{\mathsf{F}} yW_J}$. However, the weak order on $\mathfrak{Wofp}(\Phi)$ is not a sublattice of the weak order on $\mathfrak{Pos}(\Phi)$, nor on $\mathfrak{Woip}(\Phi)$.

Finally, as in Section 6.1.2, one can also construct special families of Φ-posets for the elements, the intervals, and the faces in the c-Cambrian lattices of Section 5.2.6.1 and in the boolean lattices of Section 5.2.6.2. Their characterizations and properties are natural extensions of that of Section 6.1.2 in type A. However, while the weak order on these families of posets is well understood, some characterizations remain conjectural and still deserve to be studied in details. We spare these laborious constructions to the reader and refer to [GP18, Sects. 4.2 & 4.3] for details.

III

Part Three

CLUSTER ALGEBRAS AND GENERALIZED ASSOCIAHEDRA

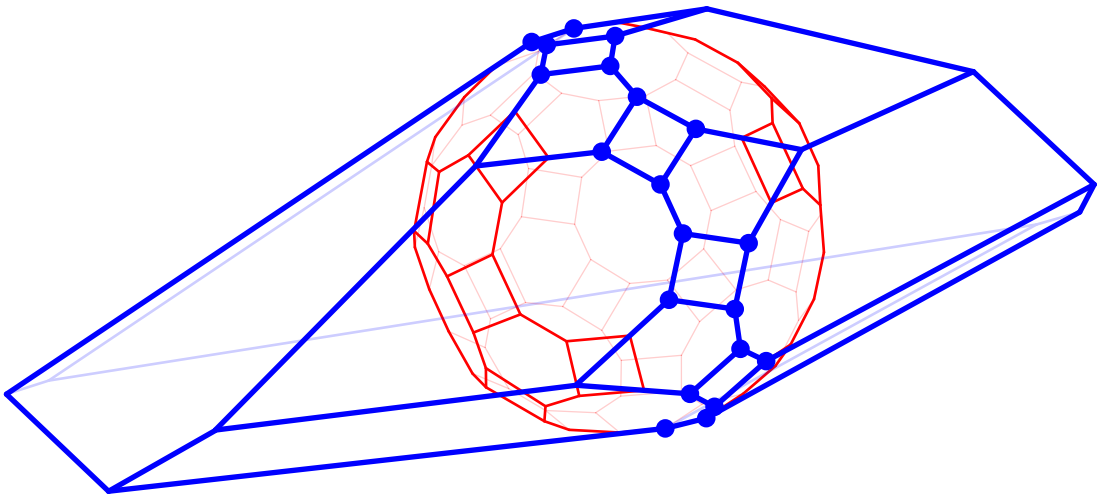

Cluster algebras. Cluster algebras were introduced by S. Fomin and A. Zelevinsky in the series of papers [FZ02, FZ03a, FZ05, FZ07] and have been widely studied in the last decades due to their connection with various areas of mathematics (see the cluster algebra portal [Fom]). They are commutative rings generated by a set of cluster variables grouped into overlapping clusters. Clusters are obtained from an initial seed by a mutation process controlled by a combinatorial object (a skew-symmetrizable matrix, or a weighted quiver). During a mutation, a single variable in the cluster is perturbed and the new variable is computed by an exchange relation. See Section 7.1.1 for a precise description of this dynamics. One fundamental aspect of this process is the Laurent phenomenon: all cluster variables are Laurent polynomials with respect to the cluster variables of the initial seed. An important combinatorial and geometric object associated to a cluster algebra is its cluster complex, the simplicial complex with cluster variables as vertices and clusters as facets.

In this document, we restrict our attention to finite type cluster algebras, *i.e.* whose cluster complexes are finite. They are classified by the Cartan-Killing classification for finite root systems [FZ03a]. See Section 7.1.2 for a precise statement of this classification. There are combinatorial models for the cluster variables and clusters of the cluster algebras of non-exceptional finite types. In particular, the cluster complex of the cluster algebra of type A_n is isomorphic to the simplicial associahedron: the cluster variables correspond to the internal diagonals of an $(n+3)$-gon, the clusters correspond to the triangulations of this polygon, the mutation between clusters correspond to the flip between triangulations, and the exchange relation can even be interpreted as a Ptolemy relation in a quadrilateral.

Generalized associahedra. A generalized associahedron is a polytope which realizes the cluster complex of a finite type cluster algebra. Generalized associahedra were first constructed by F. Chapoton, S. Fomin and A. Zelevinsky [CFZ02] using the $\boldsymbol{d}$-vector fans of [FZ03b]. Further realizations were obtained by C. Hohlweg, C. Lange and H. Thomas [HLT11] based on the Cambrian lattices of N. Reading [Rea06] and the Cambrian fans of N. Reading and D. Speyer [RS09]. These constructions were later revisited in [Ste13] with an approach similar to the original one of [CFZ02], in [PS15a] via brick polytopes, in [HPS18] using universal associahedra, and finally in [BMDM+18, PPPP19] using type cones of $\boldsymbol{g}$-vector fans. The objective of this part of the document is to present the last three approaches.

Similarly to the constructions of Section 1.2.2 in type A, the generalized associahedra $\mathbb{A}\mathrm{sso}(c)$ of [HLT11] is obtained by deleting well-chosen inequalities in the facet description of the W-permutahedron $\mathbb{P}\mathrm{erm}(W)$. An intruiguing property is that the vertex barycenters of the resulting generalized associahedron $\mathbb{A}\mathrm{sso}(c)$ and of the W-permutahedron $\mathbb{P}\mathrm{erm}(W)$ coincide at the origin. In type A, this property was observed by F. Chapoton for J.-L. Loday's realization of the classical associahedron [Lod04], conjectured for all associahedra of C. Hohlweg and C. Lange in [HL07], proved by C. Hohlweg, J. Lortie and A. Raymond [HLR10] and revisited in [LP18]. For arbitrary acyclic finite types, it was conjectured by C. Hohlweg, C. Lange and H. Thomas in [HLT11]. We will present here two independent proofs of this property: one using the universal associahedron approach of [HPS18] in Chapter 7, and the other using the brick polytope approach of [PS15a, PS15b] in Chapter 8.

Polytopality of $\boldsymbol{g}$-vector fans. Chapter 7 is devoted to the study of polytopal realizations of $\boldsymbol{g}$-vector fans of finite type cluster algebras.

The $\boldsymbol{g}$-vectors of cluster variables are essential geometric data defined implicitly in [FZ07], see Section 7.1.3. The cones generated by the $\boldsymbol{g}$-vectors of the clusters with respect to a given initial cluster $X_\circ$ form a fan $\mathcal{F}^{\boldsymbol{g}}(X_\circ)$, called $\boldsymbol{g}$-vector fan of the cluster algebra. Some properties of this fan are gathered in Section 7.1.4. When computed from an acyclic initial cluster $X_\circ$ of a cluster

algebra of finite type W, the $\boldsymbol{g}$-vector fan $\mathcal{F}^{\boldsymbol{g}}(X_\circ)$ coincides with the corresponding c-Cambrian fan of [RS09] and was realized as a generalized associahedron $\mathbb{A}\mathrm{sso}(c)$ in [HLT11, Ste13] by deleting well-chosen inequalities in the facet description of the W-permutahedron $\mathbb{P}\mathrm{erm}(W)$. This approach is unsuccessful for cyclic initial seeds, and the polytopality of cyclic finite type $\boldsymbol{g}$-vector fans remained an open problem for a long time.

In Chapter 7, we close this problem by constructing polytopal realizations of the $\boldsymbol{g}$-vector fan $\mathcal{F}^{\boldsymbol{g}}(X_\circ)$ of any finite type cluster algebra with respect to any initial cluster $X_\circ$. We actually use two different approaches with different advantages:

- Section 7.2 reports the approach of [HPS18]. We construct a polytopal realization $\mathbb{A}\mathrm{sso}^h(X_\circ)$ of the $\boldsymbol{g}$-vector fan $\mathcal{F}^{\boldsymbol{g}}(X_\circ)$ using specific right hand sides for the inequalities obtained from any function h that we call exchange submodular. For an acyclic initial cluster $X_\circ$, the resulting polytope $\mathbb{A}\mathrm{sso}^h(X_\circ)$ coincides with the generalized associahedron $\mathbb{A}\mathrm{sso}(c)$ of [HLT11]. While the $\boldsymbol{g}$-vector fan $\mathcal{F}^{\boldsymbol{g}}(X_\circ)$ depends on the initial cluster $X_\circ$, the properties required for the exchange submodular function h do not, which allows to construct a universal associahedron $\mathbb{U}\mathrm{ni}\mathbb{A}\mathrm{sso}^h(W)$ containing simultaneously all $\boldsymbol{g}$-vectors fans of the cluster algebra of a given finite type W. More precisely, the universal associahedron $\mathbb{U}\mathrm{ni}\mathbb{A}\mathrm{sso}^h(W)$ lives in a vector space indexed by all cluster variables of the type W cluster algebra, and the $\boldsymbol{g}$-vector fan $\mathcal{F}^{\boldsymbol{g}}(X_\star)$ with respect to any initial cluster $X_\star$ of the type W cluster algebra is the normal fan of the projection of the universal associahedron $\mathbb{U}\mathrm{ni}\mathbb{A}\mathrm{sso}^h(W)$ on the coordinate plane corresponding to the variables of $X_\star$. We observe moreover that this approach provides a first clean explanation of the barycenter property of the generalized associahedra mentioned above: in fact, the barycenter of the universal associahedron $\mathbb{U}\mathrm{ni}\mathbb{A}\mathrm{sso}^h(W)$ is at the origin and projects to the barycenter of any generalized associahedron $\mathbb{A}\mathrm{sso}(c)$ of [HLT11].
- Section 7.3 reports the approach of [PPPP19]. We study the space of all polytopal realizations of the $\boldsymbol{g}$-vector fan $\mathcal{F}^{\boldsymbol{g}}(X_\circ)$, called type cone of the fan as studied by P. McMullen [McM73]. Quite surprisingly, it turns out that for any initial cluster $X_\circ$ of any finite type cluster algebra, the type cone of the $\boldsymbol{g}$-vector fan $\mathcal{F}^{\boldsymbol{g}}(X_\circ)$ is simplicial. This property implies a very simple description of all the realizations of the $\boldsymbol{g}$-vector fan $\mathcal{F}^{\boldsymbol{g}}(X_\circ)$ in terms of sections of the positive orthant, extending results of [AHBHY18] in type A and [BMDM$^+$18] for acyclic initial seeds. This method relies on the fact that the linear dependence between the $\boldsymbol{g}$-vectors of any pair of adjacent clusters is positively generated by the linear dependences between the $\boldsymbol{g}$-vectors of certain special pairs of adjacent clusters called meshes. This result admits an easy combinatorial proof in type A (in fact, we will see that it extends to certain non-kissing complexes in Chapter 10), but unfortunately relies on a technical representation theoretic approach for arbitrary finite types that requires tools beyond the scope of this document, for which we prefer to refer the reader to [PPPP19].

Brick polytopes. Chapter 8 is devoted to yet another approach to the generalized associahedron $\mathbb{A}\mathrm{sso}(c)$ of [HLT11] based on brick polytopes of subword complexes.

As already mentioned in Chapter 2, brick polytopes were initially motivated by the question to find geometric realizations to the multiassociahedron. Based on the k-star decomposition of k-triangulations [PS09], one can interpret k-triangulations as pseudoline arrangements on sorting networks [PP12]. Brick polytopes of sorting networks were then constructed in [PS12], and were shown to be polytopal realizations of the simplicial complexes associated to certain class of sorting networks. In particular, it turns out that all type A associahedra of C. Hohlweg and C. Lange [HL07] appear as brick polytopes for well-chosen sorting networks.

Independently, multitriangulations were connected to pipe dreams and type A subword complexes in [Stu11, SS12], another language for pseudoline arrangements on sorting networks. Subword complexes were introduced by A. Knutson and E. Miller in the context of Gröbner geometry of Schubert varieties [KM05], and extended to all finite Coxeter groups in [KM04], see Section 8.1.1. They proved that these simplicial complexes are either topological balls or spheres, and raised the question of realizing spherical subword complexes as boundary complexes of convex polytopes. In [CLS14], C. Ceballos, J.-P. Labbé and C. Stump extended the subword complex interpretations of [PP12, Stu11, SS12] for triangulations and multitriangulations of convex polygons to arbitrary finite Coxeter groups. They proved in particular that all finite type cluster complexes are isomorphic to certain well-chosen subword complexes (see Section 8.3.1).

In Chapter 8, we define and study brick polytopes of subword complexes on finite Coxeter groups following [PS15a], see Section 8.2.1. We provide in Section 8.2.2 a simple combinatorial characterization of the class of subword complexes that are realized by their brick polytope, and deduce that it contains all finite type cluster complexes. For the latter, it turns out that the brick polytopes are indeed translates of the generalized associahedra of [HLT11].

This alternative interpretation provides an explicit vertex description of the generalized associahedra of [HLT11], and thus enables to easily derive some of their geometric properties. In particular, we show how we derived the original proof [PS15b] of the barycenter property of the generalized associahedra mentioned above, using a simple dictionary between natural operations on words and geometric symmetries on brick polytopes.

Chapter 7

POLYTOPAL REALIZATIONS OF FINITE TYPE $\boldsymbol{g}$-VECTOR FANS

In this chapter, we investigate the existence of generalized associahedra realizing finite type $\boldsymbol{g}$-vector fans. We start in Section 7.1 with a brief recollection on finite type cluster algebras and $\boldsymbol{g}$-vector fans. In Section 7.2, we show that for any finite type initial seed $B_\circ$, acyclic or not, the $\boldsymbol{g}$-vector fan with respect to $B_\circ$ is the normal fan of a generalized associahedron $\mathbb{A}\mathrm{sso}(B_\circ)$, extending results of [HLT11] for acyclic initial seeds. In fact, for any finite Dynkin type W, we even construct a universal associahedron $\mathbb{U}\mathrm{ni}\mathbb{A}\mathrm{sso}(W)$ with the property that any $\boldsymbol{g}$-vector fan of type W is the normal fan of a suitable projection of $\mathbb{U}\mathrm{ni}\mathbb{A}\mathrm{sso}(W)$. In Section 7.3, we investigate all polytopal realizations of the $\boldsymbol{g}$-vector fan, observe that they define a simplicial cone and deduce a very simple description of all the realizations in terms of sections of the positive orthant, extending results of [AHBHY18] in type A and [BMDM$^+$18] for acyclic initial seeds. The material presented in Section 7.2 is adapted from a joint work with C. Hohlweg and S. Stella [HPS18], while the approach of Section 7.3 is adapted from a joint work with A. Padrol, Y. Palu and P.-G. Plamondon [PPPP19].

7.1 CLUSTER ALGEBRAS AND $\boldsymbol{g}$-VECTOR FANS

We begin by recalling some standard notions on cluster algebras following the simplified presentation of [HPS18]. We refer to [FZ07] for a general treatment.

7.1.1 Cluster algebras

We work in the ambient field $\mathbb{Q}(x_1, \dots, x_n, p_1, \dots, p_m)$ of rational expressions in $n+m$ variables with coefficients in $\mathbb{Q}$ and we denote by $\mathbb{P}_m$ its abelian multiplicative subgroup generated by $\{p_i\}_{i\in[m]}$. For $p = \prod_{i\in[m]} p_i^{a_i} \in \mathbb{P}_m$ we write $\{p\}_+ := \prod_{i\in[m]} p_i^{\max(a_i,0)}$ and $\{p\}_- := \prod_{i\in[m]} p_i^{-\min(a_i,0)}$, so that $p = \{p\}_+ \{p\}_-^{-1}$.

A *seed* Σ is a triple (B, P, X) where:

- the *exchange matrix* B is an integer $n \times n$ skew-symmetrizable matrix, *i.e.* such that there exist a diagonal matrix D with $-BD = (BD)^T$,
- the *coefficient tuple* P is any subset of n elements of $\mathbb{P}_m$,
- the *cluster* X is a set of *cluster variables*, n rational functions in the ambient field that are algebraically independent over $\mathbb{Q}(p_1, \dots, p_m)$.

To shorten our notation we think of rows and columns of B, as well as elements of P, as being labeled by the elements of X: we write $B = (b_{xy})_{x,y\in X}$ and $P = \{p_x\}_{x\in X}$. Moreover we say that a cluster variable x (resp. a coefficient p) belongs to $\Sigma = (B, P, X)$ to mean $x \in X$ (resp. $p \in P$).

Given a seed $\Sigma = (B, P, X)$ and a cluster variable $x \in \Sigma$, we can construct a new seed $\mu_x(\Sigma) = \Sigma' = (B', P', X')$ by *mutation* in direction x, where:

- the new cluster X' is obtained from X by replacing x with the cluster variable x' defined by the *exchange relation*:
$$xx' = \{p_x\}_+ \prod_{\substack{y\in X\\ b_{xy}>0}} y^{b_{xy}} + \{p_x\}_- \prod_{\substack{y\in X\\ b_{xy}<0}} y^{-b_{xy}}$$
and leaving the remaining cluster variables unchanged so that $X \smallsetminus \{x\} = X' \smallsetminus \{x'\}$.
- the row (resp. column) of B' indexed by x' is the negative of the row (resp. column) of B indexed by x, while all the other entries satisfy $b'_{yz} = b_{yz} + \frac{1}{2}\big(|b_{yx}|b_{xz} + b_{yx}|b_{xz}|\big)$,
- the elements of the new coefficient tuple P' are given by $p'_y = p_x^{-1}$ if $y = x'$, and otherwise $p'_y = p_y \{p_x\}_-^{b_{xy}}$ if $b_{xy} \leq 0$ and $p'_y = p_y \{p_x\}_+^{b_{xy}}$ if $b_{xy} > 0$.

A straightforward computation shows that mutations are involutions, *i.e.* $\mu_{x'}\big(\mu_x(\Sigma)\big) = \Sigma$ so they define an equivalence relation on the collection of all seeds.

Fix a seed $\Sigma_\circ = (B_\circ, P_\circ, X_\circ)$ and call it *initial*. Up to an automorphism of the ambient field we will assume that $X_\circ = \{x_1, \dots, x_n\}$ and drop $X_\circ$ from our notations.

Definition 7.1 ([FZ07, Def. 2.11])**.** *The (geometric type)* cluster algebra $\mathcal{A}(B_\circ, P_\circ)$ *is the* $\mathbb{ZP}_m$*-subring of the ambient field generated by the set* $\mathcal{X}(B_\circ, P_\circ)$ *of all the cluster variables in all the seeds mutationally equivalent to the initial seed* $\Sigma_\circ$*.*

For instance, the simplest possible choice of coefficient tuple in the initial seed, namely $m = 0$ and $P_\circ = \{1\}_{i\in[n]}$, gives rise to the *cluster algebra without coefficients* which we will denote by $\mathcal{A}_{\mathrm{fr}}(B_\circ)$.

One of the most important feature of cluster algebras is the following Laurent phenomenon.

Theorem 7.2 ([FZ02, Thm. 3.1])**.** *Any cluster variable in the cluster algebra* $\mathcal{A}(B_\circ, P_\circ)$ *is expressed in terms of the initial cluster variables* $X_\circ$ *as a Laurent polynomial with coefficients in* $\mathbb{ZP}_m$*.*

7.1.2 Finite type

We will only be dealing with cluster algebras of *finite type i.e.* cluster algebras having only a finite number of cluster variables. Being of finite type is a property that depends only on the exchange matrix in the initial seed and not on the coefficient tuple. The *Cartan companion* of an exchange matrix B is the symmetrizable matrix $A(B)$ given by $a_{xy} = 2$ if $x = y$ and $a_{xy} = -|b_{xy}|$ otherwise.

Theorem 7.3 ([FZ03a, Thm. 1.4])**.** *The cluster algebra* $\mathcal{A}(B_\circ, P_\circ)$ *is of finite type if and only if there exists an exchange matrix* B *obtained by a sequence of mutations from* $B_\circ$ *such that its Cartan companion is a Cartan matrix of finite type. Moreover the type of* $A(B)$ *is uniquely determined by* $B_\circ$*: if* B' *is any other exchange matrix obtained by mutation from* $B_\circ$ *and such that* $A(B')$ *is a finite type Cartan matrix then* $A(B')$ *and* $A(B)$ *are related by a simultaneous permutation of rows and columns.*

In accordance with the above statement, when talking about the *(cluster) type* of $\mathcal{A}(B_\circ, P_\circ)$ or $B_\circ$ we will refer to the Cartan type of $A(B)$. We reiterate that the Cartan type of $A(B_\circ)$ need not be finite: being of finite type is a property of the mutation class.

For a finite type cluster algebra $\mathcal{A}(B_\circ, P_\circ)$, we consider the root system of $A(B_\circ)$. We keep the conventions of Section 5.2.1: simple roots $\{\alpha_x\}_{x\in X_\circ}$, fundamental weights $\{\omega_x\}_{x\in X_\circ}$, simple coroots $\{\alpha_x^\vee\}_{x\in X_\circ}$, and fundamental coweights $\{\omega_x^\vee\}_{x\in X_\circ}$ are four bases of the same vector space V. Roots and weights (resp. coroots and coweights) are related by the Cartan matrix $A(B_\circ)$ (resp. by the transpose of $A(B_\circ)$), and roots and coweights (resp. coroots and weights) are dual bases.

A finite type exchange matrix $B_\circ$ is said to be *acyclic* if $A(B_\circ)$ is itself a Cartan matrix of finite type and *cyclic* otherwise. An acyclic finite type exchange matrix is said to be *bipartite* if each of its rows (or equivalently columns) consists either of non-positive or non-negative entries.

7.1.3 Principal coefficients, g- and c-vectors

Among all the cluster algebras having a fixed initial exchange matrix, a central role is played by those with principal coefficients. Indeed, thanks to the results in [FZ07], they encode enough informations to understand all the other possible choices of coefficients.

Definition 7.4 ([FZ07, Def. 3.1])**.** *A cluster algebra is said to have* principal coefficients *(at the initial seed) if its ambient field is $\mathbb{Q}(x_1, \dots, x_n, p_1, \dots, p_n)$ and the initial coefficient tuple consists of the generators of $\mathbb{P}_n$ i.e. $P_\circ = \{p_i\}_{i\in[n]}$. In this case we will write $\mathcal{A}_{\mathrm{pr}}(B_\circ)$ for $\mathcal{A}\big(B_\circ, \{p_i\}_{i\in[n]}\big)$, and we reindex the generators $\{p_i\}_{i\in[n]}$ of $\mathbb{P}_n$ by $\{p_x\}_{x\in X_\circ}$.*

A notable property of cluster algebras with principal coefficients is that they are $\mathbb{Z}^n$-graded (in the basis $\{\omega_x\}_{x\in X_\circ}$ of V). The degree $\deg(B_\circ, \cdot)$ on $\mathcal{A}_{\mathrm{pr}}(B_\circ)$ is obtained by setting $\deg(B_\circ, x) := \omega_x$ and $\deg(B_\circ, p_x) := \sum_{y\in X_\circ} -b_{yx}\omega_y$ for any $x \in X_\circ$. This assignment makes all exchange relations and all cluster variables in $\mathcal{A}_{\mathrm{pr}}(B_\circ)$ homogeneous [FZ07] and it justifies the definition of the following family of integer vectors associated to cluster variables.

Definition 7.5 ([FZ07])**.** *The $\boldsymbol{g}$-vector $\boldsymbol{g}(B_\circ, x)$ of a cluster variable $x \in \mathcal{A}_{\mathrm{pr}}(B_\circ)$ is its degree. We denote by $\boldsymbol{g}(B_\circ, \Sigma) := \{\boldsymbol{g}(B_\circ, x) \,|\, x \in \Sigma\}$ the set of $\boldsymbol{g}$-vectors of a seed Σ of $\mathcal{A}_{\mathrm{pr}}(B_\circ)$.*

The next definition gives another family of integer vectors, introduced implicitly in [FZ07].

Definition 7.6 ([FZ07])**.** *Given a seed Σ in $\mathcal{A}_{\mathrm{pr}}(B_\circ)$, the $\boldsymbol{c}$-vector of a cluster variable $x \in \Sigma$ is the vector $\boldsymbol{c}(B_\circ, x \in \Sigma) := \sum_{y\in X_\circ} c_{yx}\,\alpha_y \in V$ of exponents of $p_x = \prod_{y\in X_\circ}(p_y)^{c_{yx}}$. We denote by $\boldsymbol{c}(B_\circ, \Sigma) := \{\boldsymbol{c}(B_\circ, x \in \Sigma) \,|\, x \in \Sigma\}$ the set of $\boldsymbol{c}$-vectors of a seed Σ of $\mathcal{A}_{\mathrm{pr}}(B_\circ)$ and by $\boldsymbol{C}(B_\circ) := \bigcup_\Sigma \boldsymbol{c}(B_\circ, \Sigma)$ the set of all $\boldsymbol{c}$-vectors in $\mathcal{A}_{\mathrm{pr}}(B_\circ)$.*

An important feature of $\boldsymbol{c}$-vectors is that their entries weekly agree in sign. This is one of the various reformulation of the *sign-coherence* conjecture of [FZ07] established in full generality by [GHKK18]. In the setting of finite type cluster algebras, this result can also be deduced in several ways from earlier works. Here we observe it as a corollary of the following statement.

Theorem 7.7 ([NS14, Thm. 1.3])**.** *The $\boldsymbol{c}$-vectors of the finite type cluster algebra $\mathcal{A}_{\mathrm{pr}}(B_\circ)$ are roots in the root system whose Cartan matrix is $A(B_\circ)$.*

Again note that, since $A(B_\circ)$ may not be of finite type, the root system in this statement is not finite in general. More precisely, it is finite if and only if $B_\circ$ is acyclic. For example, for the cyclic type A_3 exchange matrix, the Cartan companion $A(B_\circ)$ is of affine type $A_2^{(1)}$, see Figure 7.1 (middle right).

Our next task is to discuss a duality relation in between $\boldsymbol{c}$-vectors and $\boldsymbol{g}$-vectors. A first step is to recall the notion of the *cluster complex* of $\mathcal{A}(B_\circ, P_\circ)$: it is the simplicial complex $\mathcal{C}_{\mathrm{clu}}(B_\circ)$ whose vertices are the cluster variables of $\mathcal{A}(B_\circ, P_\circ)$ and whose facets are its clusters. As it turns out, at least in the finite type cases, this complex is independent of the choice of coefficients, see [FZ03a, Thm. 1.13] and [FZ07, Conj. 4.3]. In particular this means that, up to isomorphism, there is only one cluster complex for each finite type: the one associated to $\mathcal{A}_{\mathrm{fr}}(B_\circ)$. We will use this remark later on to relate cluster variables of different cluster algebras of the same finite type. Note also that, again when $\mathcal{A}(B_\circ, P_\circ)$ is of finite type, the cluster complex $\mathcal{C}_{\mathrm{clu}}(B_\circ)$ is a sphere [FZ03a].

For a skew-symmetrizable exchange matrix $B_\circ$, the matrix $B_\circ^\vee := -B_\circ^T$ is also skew-symmetrizable. The cluster algebras $\mathcal{A}_{\mathrm{pr}}(B_\circ)$ and $\mathcal{A}_{\mathrm{pr}}(B_\circ^\vee)$ can be thought as *dual* to each other. Moreover their cluster complexes are isomorphic: by performing the same sequence of mutations we can identify any cluster variable x of $\mathcal{A}_{\mathrm{pr}}(B_\circ)$ with a cluster variable $x^\vee$ of $\mathcal{A}_{\mathrm{pr}}(B_\circ^\vee)$, and any seed Σ in $\mathcal{A}_{\mathrm{pr}}(B_\circ)$ with a seed $\Sigma^\vee$ in $\mathcal{A}_{\mathrm{pr}}(B_\circ^\vee)$. More importantly the following crucial property holds.

Theorem 7.8 ([NZ12, Thm. 1.2])**.** *For any seed Σ of $\mathcal{A}_{\mathrm{pr}}(B_\circ)$, let $\Sigma^\vee$ be its dual in $\mathcal{A}_{\mathrm{pr}}(B_\circ^\vee)$. Then the $\boldsymbol{g}$-vectors $\boldsymbol{g}(B_\circ, \Sigma)$ of the cluster variables in Σ and the $\boldsymbol{c}$-vectors $\boldsymbol{c}(B_\circ^\vee, \Sigma^\vee)$ of the cluster variables in $\Sigma^\vee$ are dual bases, i.e. $\big\langle\, \boldsymbol{g}(B_\circ, x) \,\big|\, \boldsymbol{c}(B_\circ^\vee, y^\vee \in \Sigma^\vee) \,\big\rangle = \delta_{x=y}$ for any two cluster variables $x, y \in \Sigma$.*

In view of the above results, and since $A(B_\circ^\vee) = A(B_\circ)^T$, the $\boldsymbol{c}$-vectors of a finite type cluster algebra $\mathcal{A}_{\mathrm{pr}}(B_\circ^\vee)$ can be understood as coroots for $A(B_\circ)$ so that the $\boldsymbol{g}$-vectors of $\mathcal{A}_{\mathrm{pr}}(B_\circ)$ become weights. This justify our choice to define $\boldsymbol{g}$-vectors in the weight basis.

7.1.4 The g-vector fan

We now recast a well known fact concerning the cones spanned by the $\boldsymbol{g}$-vectors of a finite type cluster algebra with principal coefficients, illustrated in Figure 7.1.

Theorem 7.9. *For any finite type exchange matrix $B_\circ$, the cones $\big\{\boldsymbol{g}(B_\circ, \Sigma) \mid \Sigma \text{ seed of } \mathcal{A}_{\mathrm{pr}}(B_\circ)\big\}$, together with all their faces, forms a complete simplicial fan $\mathcal{F}^{\boldsymbol{g}}(B_\circ)$, called the $\boldsymbol{g}$-vector fan.*

There are several ways to find or deduce Theorem 7.9 from the literature. First, it was established in the acyclic case in [RS09, YZ08, Ste13], see Example 7.11. As already observed by N. Reading in [Rea14, Thm. 10.6], the general case then follows from the initial seed recursion on $\boldsymbol{g}$-vectors [NZ12, Prop. 4.2 (v)], valid thanks to sign-coherence. Another possible proof would be to use the following description of the linear dependence between the $\boldsymbol{g}$-vectors of two adjacent clusters, which will be crucial in the next section.

Lemma 7.10. *For any finite type exchange matrix $B_\circ$ and any adjacent seeds (B, P, X) and (B', P', X') in $\mathcal{A}_{\mathrm{pr}}(B_\circ)$ with $X \smallsetminus \{x\} = X' \smallsetminus \{x'\}$, the $\boldsymbol{g}$-vectors of $X \cup X'$ satisfy precisely one of the following two linear dependences*

$$\boldsymbol{g}(B_\circ, x) + \boldsymbol{g}(B_\circ, x') = \sum_{\substack{y \in X \cap X' \\ b_{xy} < 0}} -b_{xy}\, \boldsymbol{g}(B_\circ, y) \quad \text{or} \quad \boldsymbol{g}(B_\circ, x) + \boldsymbol{g}(B_\circ, x') = \sum_{\substack{y \in X \cap X' \\ b_{xy} > 0}} b_{xy}\, \boldsymbol{g}(B_\circ, y).$$

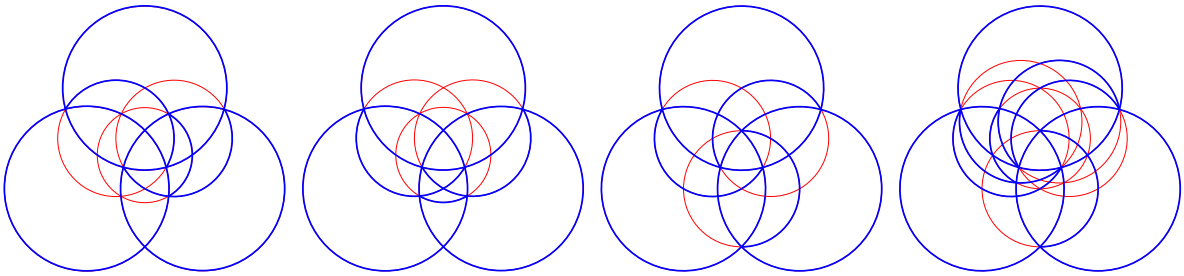

$$\begin{bmatrix} 0 & -1 & 0 \\ 1 & 0 & -1 \\ 0 & 1 & 0 \end{bmatrix} \quad \begin{bmatrix} 0 & -1 & 0 \\ 1 & 0 & 1 \\ 0 & -1 & 0 \end{bmatrix} \quad \begin{bmatrix} 0 & -1 & 1 \\ 1 & 0 & -1 \\ -1 & 1 & 0 \end{bmatrix} \quad \begin{bmatrix} 0 & -1 & 2 \\ 1 & 0 & -2 \\ -1 & 1 & 0 \end{bmatrix}$$

Figure 7.1: The dual $\boldsymbol{c}$-vector fan $\mathcal{F}^{\boldsymbol{c}}(B_\circ^\vee)$ (thin red) and $\boldsymbol{g}$-vector fan $\mathcal{F}^{\boldsymbol{g}}(B_\circ)$ (bold blue) for all type A_3 and the cyclic type C_3 initial exchange matrices. Each 3-dimensional fan is intersected with the unit sphere and stereographically projected to the plane from the pole $(-1, -1, -1)$.

Note that which of the two possible linear dependences is satisfied by the $\boldsymbol{g}$-vectors of $X \cup X'$ depends on the initial exchange matrix $B_\circ$. In particular, the geometry of the $\boldsymbol{g}$-vector fan $\mathcal{F}^{\boldsymbol{g}}(B_\circ)$ changes as $B_\circ$ varies within a given mutation class.

For any finite type exchange matrix $B_\circ$, the $\boldsymbol{g}$-vector fan $\mathcal{F}^{\boldsymbol{g}}(B_\circ)$ can be seen as a coarsening of two other fans naturally associated to $A(B_\circ)$. Denote by $\mathcal{F}^{\boldsymbol{Cox}}(B_\circ^\vee)$ the *dual Coxeter fan i.e.* the fan defined by the hyperplane arrangement given by the root system of $A(B_\circ^\vee)$. Similarly let $\mathcal{F}^{\boldsymbol{c}}(\bar{Q})$ be the *dual $\boldsymbol{c}$-vector fan i.e.* the fan defined by the arrangement of hyperplanes orthogonal to all the $\boldsymbol{c}$-vector of $\mathcal{A}_{\mathrm{pr}}(B_\circ^\vee)$. By Theorem 7.8, $\mathcal{F}^{\boldsymbol{g}}(B_\circ)$ coarsens $\mathcal{F}^{\boldsymbol{c}}(\bar{Q})$ which, in turn, coarsens $\mathcal{F}^{\boldsymbol{Cox}}(B_\circ^\vee)$ by Theorem 7.7. Figure 7.1 illustrates these $\boldsymbol{g}$- and $\boldsymbol{c}$-vector fans for all type A_3 and the cyclic type C_3 initial exchange matrices.

Example 7.11. When the exchange matrix $B_\circ$ is acyclic, the $\boldsymbol{g}$-vector fan is the Cambrian fan constructed by N. Reading and D. Speyer [RS09], while the dual $\boldsymbol{c}$-vector fan is the type $A(B_\circ^\vee)$ Coxeter fan. See the first two fans of Figure 7.1 for examples in type A_3.

7.1.5 Coefficient specialization and universal cluster algebra

We now want to relate, within a given finite type, cluster algebras with different choices of coefficients. Pick a finite type exchange matrix $B_\circ$ and let $\mathcal{A}(B_\circ, P_\circ) \subset \mathbb{Q}(x_1, \dots, x_n, p_1, \dots, p_m)$ and $\mathcal{A}\big(B_\circ, \overline{P}_\circ\big) \subset \mathbb{Q}(\overline{x}_1, \dots, \overline{x}_n, \overline{p}_1, \dots, \overline{p}_\ell)$ be any two cluster algebras having $B_\circ$ as exchange matrix in their initial seed. As we said, cluster variables and seeds in these two algebras are in bijection because their cluster complexes are isomorphic. Let us write $x \longleftrightarrow \overline{x}$ and $\Sigma \longleftrightarrow \overline{\Sigma}$ for this bijection. We will say that $\mathcal{A}\big(B_\circ, \overline{P}_\circ\big)$ is obtained from $\mathcal{A}(B_\circ, P_\circ)$ by a *coefficient specialization* if there exist a map of abelian groups $\eta : \mathbb{P}_m \to \mathbb{P}_\ell$ such that, for any p_x in some seed Σ of $\mathcal{A}(B_\circ, P_\circ)$ we have $\eta(\{p_x\}_+) = \{\overline{p}_{\overline{x}}\}_+$ and $\eta(\{p_x\}_-) = \{\overline{p}_{\overline{x}}\}_-$, and which extends in a unique way to a map of algebras that satisfy $\eta(x) = \overline{x}$. Note that this is not the most general definition (see [FZ07, Def. 12.1 and Prop. 12.2]) but it will suffice here. Armed with the notion of coefficient specialization we can now introduce the last kind of cluster algebra of finite type we will need.

Definition 7.12 ([FZ07, Def. 12.3 and Thm. 12.4])**.** *Pick a finite type exchange matrix $B_\circ$. The cluster algebra with universal coefficients $\mathcal{A}_{\mathrm{un}}(B_\circ)$ is the unique (up to canonical isomorphism) cluster algebra such that any other cluster algebra of the same type as $B_\circ$ can be obtained from it by a unique coefficient specialization.*

Let us insist on the fact that, in view of the universal property it satisfies, $\mathcal{A}_{\mathrm{un}}(B_\circ)$ depends only on the type of $B_\circ$ and not on the exchange matrix $B_\circ$ itself. We again keep $B_\circ$ in the notation only to fix an embedding into the ambient field.

Rather than proving the existence and explaining the details of how such a universal algebra is built, we will recall here one of its remarkable properties that follows directly from the $\boldsymbol{g}$-vector recursion [NZ12, Prop. 4.2 (v)]. Denote by $\mathcal{X}(B_\circ)$ the set of all cluster variables in $\mathcal{A}_{\mathrm{un}}(B_\circ)$ and let $\{p[x]\}_{x \in \mathcal{X}(B_\circ)}$ be the generators of $\mathbb{P}_{|\mathcal{X}(B_\circ)|}$.

Theorem 7.13 ([Rea14, Thm. 10.12])**.** *The cluster algebra $\mathcal{A}_{\mathrm{un}}(B_\circ)$ can be realized over $\mathbb{P}_{|\mathcal{X}(B_\circ)|}$. The coefficient tuple $P = \{p_x\}_{x \in X}$ at each seed $\Sigma = (B, P, X)$ of $\mathcal{A}_{\mathrm{un}}(B_\circ)$ is given by the formula $p_x = \prod_{y \in \mathcal{X}(B_\circ)} \big(p[y]\big)^{[\boldsymbol{g}(B^T, y^T); x^T]}$ where $[\boldsymbol{v}; x]$ is the x-th coefficient of $\boldsymbol{v}$ in the weight basis $(\omega_x)_{x \in X}$.*

Remark 7.14. In view of this result, it is straightforward to produce the coefficient specialization morphism to get any cluster algebra with principal coefficients of type $B_\circ$ from $\mathcal{A}_{\mathrm{un}}(B_\circ)$. Namely, for any seed $\Sigma_\star = (B_\star, P_\star, X_\star)$ of $\mathcal{A}_{\mathrm{un}}(B_\circ)$, we obtain $\mathcal{A}_{\mathrm{pr}}(B_\star)$ by evaluating to 1 all the coefficients $p[y]$ corresponding to cluster variables y not in $\Sigma_\star$.

7.2 GENERALIZED ASSOCIAHEDRA FOR $\boldsymbol{g}$-VECTOR FANS

7.2.1 Polytopal realizations of $\boldsymbol{g}$-vector fans

In this section, we show that the $\boldsymbol{g}$-vector fan $\mathcal{F}^{\boldsymbol{g}}(B_\circ)$ is polytopal for any finite type exchange matrix $B_\circ$. As discussed in Example 7.18, this result was previously known for acyclic finite type exchange matrices [HLT11, Ste13, PS15a]. We first consider some convenient functions used in Theorem 7.16 to lift the $\boldsymbol{g}$-vector fan and discuss the existence of such functions in Proposition 7.17.

Definition 7.15. *A positive function h on the cluster variables of $\mathcal{A}(B_\circ, P_\circ)$ is* exchange submodular *if, for any pair of adjacent seeds (B, P, X) and (B', P', X') with $X \smallsetminus \{x\} = X' \smallsetminus \{x'\}$, it satisfies*

$$h(x) + h(x') > \max\Big(\sum_{\substack{y \in X \cap X' \\ b_{xy} < 0}} -b_{xy}\, h(y)\ ,\ \sum_{\substack{y \in X \cap X' \\ b_{xy} > 0}} b_{xy}\, h(y) \Big).$$

The following statement is the central result of this section. The proof is based on Lemma 7.10 and the standard characterization of polytopal realizations of simplicial fans given in Proposition 7.28.

Theorem 7.16. *For any finite type exchange matrix $B_\circ$ and any exchange submodular function h, the $\boldsymbol{g}$-vector fan $\mathcal{F}^{\boldsymbol{g}}(B_\circ)$ is the normal fan of the $B_\circ$-associahedron $\mathbb{A}\mathrm{sso}^h(B_\circ) \subseteq V$ defined as*

(i) either the convex hull of the points $\sum_{x \in \Sigma} h(x)\, \boldsymbol{c}(B_\circ^\vee, x^\vee \in \Sigma^\vee)$ for all seeds Σ of $\mathcal{A}_{\mathrm{pr}}(B_\circ)$,

(ii) or the intersection of the halfspaces $\{\boldsymbol{v} \in V \mid \langle \boldsymbol{g}(B_\circ, x) \,|\, \boldsymbol{v} \rangle \leq h(x)\}$ for all cluster variables x of $\mathcal{A}_{\mathrm{pr}}(B_\circ)$.

Our next step is to discuss the existence of exchange submodular functions for any finite type cluster algebra with principal coefficients. The important observation here is that the definition of exchange submodular function does not involve in any way the coefficients of $\mathcal{A}_{\mathrm{pr}}(B_\circ)$ so that it suffices to construct one in the coefficient free cases. We can therefore, without loss of generality, assume that $B_\circ$ is bipartite and directly deduce our result from [Ste13, Prop. 8.3] obtained as an easy consequence of [CFZ02, Lem. 2.4] which we recast here in our current setting.

When $B_\circ$ is acyclic, the Weyl group of $A(B_\circ)$ is finite and has a longest element $w_\circ$. A point $\lambda^\vee := \sum_{x \in X_\circ} \lambda_x^\vee\, \omega_x^\vee$ in the interior of the fundamental Weyl chamber of $A(B_\circ^\vee)$ (that is to say $\lambda_x^\vee > 0$ for all $x \in X_\circ$) is *fairly balanced* if $w_\circ(\lambda^\vee) = -\lambda^\vee$.

Proposition 7.17. *Let $\mathcal{A}_{\mathrm{fr}}(B_\circ)$ be a finite type cluster algebra without coefficients where $B_\circ$ is bipartite. To each fairly balanced point $\lambda^\vee$ corresponds an exchange submodular function $h_{\lambda^\vee}$ on $\mathcal{A}_{\mathrm{fr}}(B_\circ)$.*

A particular example of fairly balanced point is the point $\rho^\vee := \sum_{x \in X_\circ} \omega_x^\vee$. Note that $\rho^\vee$ is both the sum of the fundamental coweights and the half sum of all positive coroots of the root system of finite type $A(B_\circ)$. In particular $h_{\rho^\vee}$ is the *half compatibility sum* of x, *i.e.* the half sum of the compatibility degrees $h_{\rho^\vee}(x) := \frac{1}{2} \sum_{y \neq x} (y \,\|\, x)$ over all cluster variables distinct from x. (See [FZ03b, CP15b] for the definition and discussion of the relevant properties of compatibility degrees.) The point $\rho^\vee$ is particularly relevant in representation theory and its role in this context has already been observed in [CFZ02, Rem. 1.6]. We call *balanced $B_\circ$-associahedron* and denote by $\mathbb{A}\mathrm{sso}(B_\circ)$ the $B_\circ$-associahedron $\mathbb{A}\mathrm{sso}^{h_{\rho^\vee}}(B_\circ)$ for the exchange submodular function $h_{\rho^\vee}$. We have represented in Figure 7.2 the $B_\circ$-associahedra $\mathbb{A}\mathrm{sso}(B_\circ)$ for the same two initial exchange matrices. The third associahedron of Figure 7.2 appeared as a mysterious realization of the associahedron in [CSZ15].

Example 7.18. When $B_\circ$ is acyclic, the $B_\circ$-associahedron $\mathbb{A}\mathrm{sso}(B_\circ)$ was already constructed in [HLT11, Ste13, PS15a]. It is then obtained by deleting inequalities from the facet description of the permutahedron $\mathbb{P}\mathrm{erm}(B_\circ)$ of the Coxeter group of type $A(B_\circ)$. See the first two associahedra of Figure 7.2 for examples in type A_3, and Section 7.2.3.3 for a discussion of this property.

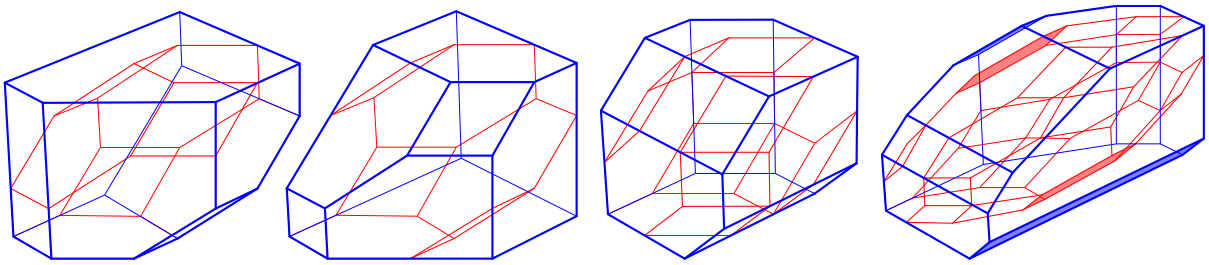

Figure 7.2: The zonotopes $\mathbb{Z}\mathrm{ono}(B_\circ)$ (thin red) and the associahedra $\mathbb{A}\mathrm{sso}(B_\circ)$ (bold blue) for all type A_3 and the cyclic type C_3 initial exchange matrices, realizing the $\boldsymbol{c}$-vector fans $\mathcal{F}^{\boldsymbol{c}}(B_\circ)$ and the $\boldsymbol{g}$-vector fans $\mathcal{F}^{\boldsymbol{g}}(B_\circ)$ of Figure 7.1. See Section 7.2.3.3 for the definition of $\mathbb{Z}\mathrm{ono}(B_\circ)$.

7.2.2 Universal associahedron

For each initial exchange matrix $B_\circ$ of a given type, we constructed in Section 7.2.1 a generalized associahedron $\mathbb{A}\mathrm{sso}^h(B_\circ)$ by lifting the $\boldsymbol{g}$-vector fan using an exchange submodular function h on the cluster variables of $\mathcal{A}_{\mathrm{pr}}(B_\circ)$. As already observed though, the function h is independent of the coefficients of $\mathcal{A}_{\mathrm{pr}}(B_\circ)$, so that all $\boldsymbol{g}$-vector fans can all be lifted with the same function h. This motivates the definition of a universal associahedron.

Consider the finite type cluster algebra $\mathcal{A}_{\mathrm{un}}(B_\circ)$ with universal coefficients, and let $\mathcal{X}(B_\circ)$ denote its set of cluster variables. Consider a $|\mathcal{X}(B_\circ)|$-dimensional Euclidean space U with a pair of dual bases $\{\beta_x\}_{x\in\mathcal{X}(B_\circ)}$ and $\{\beta^\vee_{x^\vee}\}_{x^\vee\in\mathcal{X}(B^\vee_\circ)}$. As before, the cluster variables of $\mathcal{A}_{\mathrm{un}}(B_\circ)$ and $\mathcal{A}_{\mathrm{un}}(B^\vee_\circ)$ are related by $x \leftrightarrow x^\vee$. For $X \subseteq \mathcal{X}(B_\circ)$, we denote by $\boldsymbol{H}_X$ the coordinate subspace of U spanned by $\{\beta_x\}_{x\in X}$.

Definition 7.19. *Given a seed Σ in $\mathcal{A}_{\mathrm{un}}(B_\circ)$, the $\boldsymbol{u}$-vector of a cluster variable $x \in \Sigma$ is the vector $\boldsymbol{u}(B_\circ, x \in \Sigma) := \sum_{y\in\mathcal{X}(B_\circ)} u_{yx}\,\beta_y \ \in U$ of exponents of $p_x = \prod_{y\in\mathcal{X}(B_\circ)}(p[y])^{u_{yx}}$.*

Remark 7.14 then reformulates geometrically in terms of $\boldsymbol{u}$- and $\boldsymbol{c}$-vectors as follows. Choose a seed $\Sigma_\star = (B_\star, P_\star, X_\star)$ in $\mathcal{A}_{\mathrm{un}}(B_\circ)$ that you want to make initial. Then, for any cluster variable x in a seed Σ, the $\boldsymbol{c}$-vector $\boldsymbol{c}(B_\star, x \in \Sigma)$ is the orthogonal projection of the $\boldsymbol{u}$-vector $\boldsymbol{u}(B_\circ, x \in \Sigma)$ on the coordinate subspace $\boldsymbol{H}_{X_\star}$. (Here and elsewhere we identify $\boldsymbol{H}_{X_\star}$ with V in the obvious way.) We are now ready to define the universal associahedron.

Definition 7.20. *For any finite type exchange matrix $B_\circ$ and any exchange submodular function h, the universal $B_\circ$-associahedron is the polytope $\mathbb{U}\mathrm{ni}\mathbb{A}\mathrm{sso}^h(B_\circ) \subseteq U$ defined as the convex hull of the points $\sum_{x\in\Sigma} h(x)\,\boldsymbol{u}(B^\vee_\circ, x^\vee \in \Sigma^\vee) \ \in U$ for each seed Σ of $\mathcal{A}_{\mathrm{un}}(B_\circ)$.*

Note that $\mathbb{U}\mathrm{ni}\mathbb{A}\mathrm{sso}^h(B_\circ)$ does not depend on $B_\circ$ but only on its cluster type. We keep $B_\circ$ in the notation since it fixes the indexing of the space U. Our interest in $\mathbb{U}\mathrm{ni}\mathbb{A}\mathrm{sso}^h(B_\circ)$ comes from the following property.

Theorem 7.21. *Fix a finite type exchange matrix $B_\circ$ and an exchange submodular function h. For any seed $(B_\star, P_\star, X_\star)$ of $\mathcal{A}_{\mathrm{un}}(B_\circ)$, the orthogonal projection of the universal associahedron $\mathbb{U}\mathrm{ni}\mathbb{A}\mathrm{sso}^h(B_\circ)$ on the coordinate subspace $\boldsymbol{H}_{X^\vee_\star}$ of U spanned by $\{\beta^\vee_{x^\vee}\}_{x^\vee\in X^\vee_\star}$ is the $B_\star$-associahedron $\mathbb{A}\mathrm{sso}^h(B_\star)$.*

Remark 7.22. We call *universal $\boldsymbol{g}$-vector fan* the normal fan $\mathcal{F}^{\boldsymbol{g}}_{\mathrm{un}}(B_\circ)$ of the universal $B_\circ$-associahedron $\mathbb{U}\mathrm{ni}\mathbb{A}\mathrm{sso}(B_\circ)$. For any seed $\Sigma_\star = (B_\star, P_\star, X_\star)$ in $\mathcal{A}_{\mathrm{un}}(B_\circ)$, the section of $\mathcal{F}^{\boldsymbol{g}}_{\mathrm{un}}(B_\circ)$ by the coordinate subspace $\boldsymbol{H}_{X_\star}$ of U spanned by $\{\beta_x\}_{x\in X_\star}$ is the $\boldsymbol{g}$-vector fan $\mathcal{F}^{\boldsymbol{g}}(B_\star)$. Besides this universality property, our understanding of this fan is, however, quite limited.

n	dimension of ambient space	dimension	# vertices	# facets	# vertices / facet	# facets / vertex
1	2	1	2	2	1	1
2	5	4	5	5	4	4
3	9	8	14	60	$9 \leq \cdot \leq 10$	$30 \leq \cdot \leq 42$
4	14	13	42	8960	$14 \leq \cdot \leq 28$	$3463 \leq \cdot \leq 4244$

Table 7.1: Some statistics for the universal associahedron of type A_n for $n \in [4]$.

As an immediate consequence of Theorem 7.21, we obtain that all seeds of the cluster algebra $\mathcal{A}_{\mathrm{un}}(B_\circ)$ appear as vertices of the universal associahedron $\mathbb{U}\mathrm{ni}\mathbb{A}\mathrm{sso}^h(B_\circ)$, and that the mutation graph of the cluster algebra $\mathcal{A}_{\mathrm{un}}(B_\circ)$ is a subgraph of the graph of the universal associahedron $\mathbb{U}\mathrm{ni}\mathbb{A}\mathrm{sso}^h(B_\circ)$. However, this inclusion is strict in general.

We conclude with three observations on the universal $B_\circ$-associahedron $\mathbb{U}\mathrm{ni}\mathbb{A}\mathrm{sso}^h(B_\circ)$ obtained by computer experiment:

- Although *a priori* defined in U, $\mathbb{U}\mathrm{ni}\mathbb{A}\mathrm{sso}^h(B_\circ)$ seems to be of codimension 1.
- In general $\mathbb{U}\mathrm{ni}\mathbb{A}\mathrm{sso}^h(B_\circ)$ is neither simple nor simplicial. Table 7.1 presents some statistics for the number of vertices per facet and facets per vertex in type A_n for $n \in [4]$.
- The face lattice (and thus the f-vector) of $\mathbb{U}\mathrm{ni}\mathbb{A}\mathrm{sso}^h(B_\circ)$ seems independent of h.

To conclude, let us insist on the fact that Theorem 7.21 describes the projection of the universal associahedron $\mathbb{U}\mathrm{ni}\mathbb{A}\mathrm{sso}^h(B_\circ)$ on coordinate subspaces corresponding to clusters of $\mathcal{A}_{\mathrm{un}}(B_\circ)$. It turns out that the projections on coordinate subspaces corresponding to all faces (not necessarily facets) of the cluster complex $\mathcal{C}_{\mathrm{clu}}(B_\circ)$ create relevant simplicial complexes, fans and polytopes [Cha16, GM18, MP19, PPP17], see Section 10.3.5. This naturally raises the question to understand all coordinate projections of the universal associahedron $\mathbb{U}\mathrm{ni}\mathbb{A}\mathrm{sso}^h(B_\circ)$.

7.2.3 Further properties of $\mathbb{A}\mathrm{sso}(B_\circ)$

7.2.3.1 Green mutations

We consider a natural orientation of mutations introduced by B. Keller in [Kel11]. For two adjacent seeds $\Sigma = (B, P, X)$ and $\Sigma' = (B', P', X')$ of $\mathcal{A}_{\mathrm{pr}}(B_\circ)$ with $X \smallsetminus \{x\} = X' \smallsetminus \{x'\}$, the mutation $\Sigma \to \Sigma'$ is a *green mutation* when the dual $\boldsymbol{c}$-vector $\boldsymbol{c}(B_\circ^\vee, x^\vee \in \Sigma^\vee) = -\boldsymbol{c}(B_\circ^\vee, x'^\vee \in \Sigma'^\vee)$ is positive. The directed graph $\mathcal{G}(B_\circ)$ of green mutations is known to be acyclic, and even the Hasse diagram of a lattice when the type of $B_\circ$ is simply laced, see [GM17b, Coro. 4.7] and the references therein. It turns out that this green mutation digraph $\mathcal{G}(B_\circ)$ is apparent in the $B_\circ$-associahedron.

Proposition 7.23. *For any finite type exchange matrix $B_\circ$, the graph of the associahedron $\mathbb{A}\mathrm{sso}^h(B_\circ)$, oriented in the linear direction $\boldsymbol{\omega} := -\sum_{x \in X_\circ} \omega_x$, is the graph $\mathcal{G}(B_\circ)$ of green mutations in $\mathcal{A}_{\mathrm{pr}}(B_\circ)$.*

Example 7.24. For instance, for an acyclic initial exchange matrix $B_\circ$, the lattice of green mutations is the c-Cambrian lattice of N. Reading [Rea06] (where c is the Coxeter element corresponding to $B_\circ$).

7.2.3.2 Vertex barycenter

For an acyclic initial exchange matrix $B_\circ$ of type W, it is known that the origin is the vertex barycenter of both the permutahedron $\mathbb{P}\mathrm{erm}(A(B_\circ))$ of the Coxeter group of type $A(B_\circ)$ and of the $B_\circ$-associahedron $\mathbb{A}\mathrm{sso}(B_\circ)$. In type A, this property was observed by F. Chapoton for J.-L. Loday's realization of the classical associahedron [Lod04] and conjectured for arbitrary Coxeter element in [HL07].

It was later proved in type A in [HLR10] and revisited in [LP18], both proofs using an orbit refinement of this property. For arbitrary finite types, it was conjectured in [HLT11] and proved using the brick polytope approach in [PS15b] (see Section 8.3.2). In fact, this result also extends to all associahedra $\mathbb{A}\mathrm{sso}^h(B_\circ)$ for any initial exchange matrix $B_\circ$ and any exchange submodular function h, as a consequence of the following stronger statement.

Theorem 7.25. *For any finite type exchange matrix $B_\circ$ and any exchange submodular function h, the origin is the vertex barycenter of the universal $B_\circ$-associahedron $\mathbb{U}\mathrm{ni}\mathbb{A}\mathrm{sso}^h(B_\circ)$.*

Corollary 7.26. *For any finite type exchange matrix $B_\circ$ and any exchange submodular function h, the origin is the vertex barycenter of the $B_\circ$-associahedron $\mathbb{A}\mathrm{sso}^h(B_\circ)$.*

7.2.3.3 Zonotope

Motivated by Example 7.18, it is natural to investigate whether there exists a zonotope $\mathbb{Z}\mathrm{ono}(B_\circ)$ whose facet description contains all inequalities of the associahedron $\mathbb{A}\mathrm{sso}(B_\circ)$. The natural choice is the zonotope $\mathbb{Z}\mathrm{ono}(B_\circ) := \sum_{\boldsymbol{c}\in\boldsymbol{C}(B_\circ^\vee)} \boldsymbol{c}$, which works in the following two specific cases.

Proposition 7.27. *All inequalities of the generalized associahedron $\mathbb{A}\mathrm{sso}(B_\circ)$ are inequalities of the zonotope $\mathbb{Z}\mathrm{ono}(B_\circ)$ when $B_\circ$ is either acyclic or of type A.*

In the acyclic case, $\mathbb{Z}\mathrm{ono}(B_\circ) = \mathbb{P}\mathrm{erm}(A(B_\circ))$ is the permutahedron of the Coxeter group W of type $A(B_\circ)$, and this statement was actually the way the associahedron $\mathbb{A}\mathrm{sso}(B_\circ)$ was initially constructed in [HLT11]. The cyclic type A case was shown in [HPS18, Sect. 6.2], were more details on type A associahedra can be found. Despite these two special cases, it turns out that the property of Proposition 7.27 does not extend in general. In fact, it already fails for the type C_3 cyclic initial exchange matrix $B_\circ$, see Figure 7.1 (right) and Figure 7.2 (right). One indeed checks that in the direction of the $\boldsymbol{g}$-vectors $(-1,1,0)$ and $(1,-1,0)$, the right hand sides of the inequalities are 4 in $\mathbb{A}\mathrm{sso}(B_\circ)$ and 3 in $\mathbb{Z}\mathrm{ono}(B_\circ)$. This is illustrated in Figure 7.2 (right) where the facets of $\mathbb{A}\mathrm{sso}(B_\circ)$ and $\mathbb{Z}\mathrm{ono}(B_\circ)$ orthogonal to the $\boldsymbol{g}$-vectors $(-1,1,0)$ and $(1,-1,0)$ are shaded. In fact, one can even show that there exist initial exchange matrices $B_\circ$ for which no zonotope contains all inequalities of the associahedron $\mathbb{A}\mathrm{sso}(B_\circ)$. See [HPS18, Sect. 7.4] for details.

7.3 Type cones of $\boldsymbol{g}$-vector fans

In this section, we consider the problem of the polytopality of the $\boldsymbol{g}$-vector fan $\mathcal{F}^{\boldsymbol{g}}(B_\circ)$ from another perspective. Namely, we consider the cone of all polytopal realizations of $\mathcal{F}^{\boldsymbol{g}}(B_\circ)$. Surprisingly, one can prove using representation theoretic tools that this cone is always simplicial. This enables us to extend results of [AHBHY18] in type A and [BMDM+18] for acyclic initial seeds. Much more details on this approach are available in [PPPP19].

7.3.1 Type cone of a simplicial fan

Fix an essential complete simplicial fan $\mathcal{F}$ in $\mathbb{R}^n$. Let $\boldsymbol{G}$ be the $N\times n$-matrix whose rows are the rays of $\mathcal{F}$ and let $\boldsymbol{K}$ be a $(N-n)\times N$-matrix that spans the left kernel of $\boldsymbol{G}$ (*i.e.* $\boldsymbol{K}\boldsymbol{G}=0$).

For any adjacent maximal cones $\mathbb{R}_{\geq 0}\boldsymbol{R}$ and $\mathbb{R}_{\geq 0}\boldsymbol{R}'$ of $\mathcal{F}$ with $\boldsymbol{R}\smallsetminus\{\boldsymbol{r}\} = \boldsymbol{R}'\smallsetminus\{\boldsymbol{r}'\}$, we denote by $\alpha_{\boldsymbol{R},\boldsymbol{R}'}(\boldsymbol{s})$ the coefficient of $\boldsymbol{s}$ in the unique linear dependence between the rays of $\boldsymbol{R}\cup\boldsymbol{R}'$, *i.e.* such that $\sum_{\boldsymbol{s}\in\boldsymbol{R}\cup\boldsymbol{R}'}\alpha_{\boldsymbol{R},\boldsymbol{R}'}(\boldsymbol{s})\,\boldsymbol{s}=0$. These coefficients are *a priori* defined up to rescaling, but we additionally fix the rescaling so that $\alpha_{\boldsymbol{R},\boldsymbol{R}'}(\boldsymbol{r})$ and $\alpha_{\boldsymbol{R},\boldsymbol{R}'}(\boldsymbol{r}')$ are positive, say $\alpha_{\boldsymbol{R},\boldsymbol{R}'}(\boldsymbol{r})+\alpha_{\boldsymbol{R},\boldsymbol{R}'}(\boldsymbol{r}')=2$.

The following classical statement characterizes the polytopal realizations of the fan $\mathcal{F}$. It is a reformulation of regularity of triangulations of vector configurations, introduced in the theory of secondary polytopes [GKZ08], see also [DRS10]. We present a convenient formulation from [CFZ02, Lem. 2.1].

Proposition 7.28. *Let $\mathcal{F}$ be an essential complete simplicial fan in $\mathbb{R}^n$. Then the following are equivalent for any height vector $\boldsymbol{h} \in \mathbb{R}^N$:*

1. *The fan $\mathcal{F}$ is the normal fan of the polytope $\mathbb{P}_{\boldsymbol{h}} := \{\boldsymbol{x} \in \mathbb{R}^n \,|\, \boldsymbol{G}\boldsymbol{x} \leq \boldsymbol{h}\}$.*
2. *For any two adjacent maximal cones $\mathbb{R}_{\geq 0}\boldsymbol{R}$ and $\mathbb{R}_{\geq 0}\boldsymbol{R}'$ of $\mathcal{F}$ we have $\sum_{\boldsymbol{s} \in \boldsymbol{R} \cup \boldsymbol{R}'} \alpha_{\boldsymbol{R},\boldsymbol{R}'}(\boldsymbol{s})\, \boldsymbol{h}_{\boldsymbol{s}} > 0$.*

In this section, we are interested in the set of all possible realizations of $\mathcal{F}$ as the normal fan of a polytope $\mathbb{P}_{\boldsymbol{h}}$. This was studied by P. McMullen in [McM73] (see [DRS10, Sect. 9.5] for a formulation in terms of chambers of triangulations of vector configurations).

Definition 7.29. *The type cone of $\mathcal{F}$ is the cone $\mathbb{TC}(\mathcal{F})$ of all height vectors $\boldsymbol{h} \in \mathbb{R}^N$ realizing $\mathcal{F}$:*

$$\begin{aligned}\mathbb{TC}(\mathcal{F}) &:= \left\{\boldsymbol{h} \in \mathbb{R}^N \,\middle|\, \mathcal{F} \text{ is the normal fan of } \mathbb{P}_{\boldsymbol{h}}\right\} \\ &= \left\{\boldsymbol{h} \in \mathbb{R}^N \,\middle|\, \sum_{\boldsymbol{s} \in \boldsymbol{R} \cup \boldsymbol{R}'} \alpha_{\boldsymbol{R},\boldsymbol{R}'}(\boldsymbol{s})\, \boldsymbol{h}_{\boldsymbol{s}} > 0 \quad \begin{array}{l}\text{for any adjacent maximal} \\ \text{cones } \mathbb{R}_{\geq 0}\boldsymbol{R} \text{ and } \mathbb{R}_{\geq 0}\boldsymbol{R}' \text{ of } \mathcal{F}\end{array} \right\}.\end{aligned}$$

Note that the type cone is an open cone and contains a linearity subspace of dimension n (it is invariant by translation in $\boldsymbol{G}\mathbb{R}^n$). It is sometimes useful to get rid of the linearity space by considering the projection $\boldsymbol{K}\mathbb{TC}(\mathcal{F})$. If $\mathcal{F}$ is the normal fan of the polytope $\mathbb{P}$, then the closure of the type cone $\mathbb{TC}(\mathcal{F})$ is called the *deformation cone* of $\mathbb{P}$ in [Pos09], see also [PRW08].

Definition 7.30. *An extremal adjacent pair of $\mathcal{F}$ is a pair of adjacent maximal cones $\{\mathbb{R}_{\geq 0}\boldsymbol{R}, \mathbb{R}_{\geq 0}\boldsymbol{R}'\}$ of $\mathcal{F}$ such that the corresponding inequality $\sum_{\boldsymbol{s} \in \boldsymbol{R} \cup \boldsymbol{R}'} \alpha_{\boldsymbol{R},\boldsymbol{R}'}(\boldsymbol{s})\, \boldsymbol{h}_{\boldsymbol{s}} \geq 0$ in the definition of the type cone $\mathbb{TC}(\mathcal{F})$ actually defines a facet of $\mathbb{TC}(\mathcal{F})$.*

In other words, extremal adjacent pairs define the extremal rays of the polar of the type cone $\mathbb{TC}(\mathcal{F})$. Understanding the extremal adjacent pairs of $\mathcal{F}$ enables to describe its type cone $\mathbb{TC}(\mathcal{F})$ and thus all its polytopal realizations.

Remark 7.31. Since the type cone is an N-dimensional cone with a linearity subspace of dimension n, it has at least $N - n$ facets (thus $N - n$ extremal adjacent pairs). The type cone is *simplicial* when it has precisely $N - n$ facets.

Finally, using the type cone, one can provide alternative polytopal realizations of the fan $\mathcal{F}$, which are particularly relevant in the situation when the type cone $\mathbb{TC}(\mathcal{F})$ is simplicial.

Proposition 7.32. *The affine map $\Psi : \mathbb{R}^n \to \mathbb{R}^N$ defined by $\Psi(\boldsymbol{x}) = \boldsymbol{h} - \boldsymbol{G}\boldsymbol{x}$ sends the polytope $\mathbb{P}_{\boldsymbol{h}} := \{\boldsymbol{x} \in \mathbb{R}^n \,|\, \boldsymbol{G}\boldsymbol{x} \leq \boldsymbol{h}\}$ to the polytope $\mathbb{Q}_{\boldsymbol{h}} := \left\{\boldsymbol{z} \in \mathbb{R}^N \,\middle|\, \boldsymbol{K}\boldsymbol{z} = \boldsymbol{K}\boldsymbol{h} \text{ and } \boldsymbol{z} \geq 0\right\}$.*

Corollary 7.33. *Assume that the type cone $\mathbb{TC}(\mathcal{F})$ is simplicial and let $\boldsymbol{K}$ be the $(N-n) \times N$-matrix whose rows are the inner normal vectors of the facets of $\mathbb{TC}(\mathcal{F})$. Then, for any positive vector $\boldsymbol{\ell} \in \mathbb{R}^{N-n}_{>0}$, the polytope $\mathbb{R}_{\boldsymbol{\ell}} := \left\{\boldsymbol{z} \in \mathbb{R}^N \,\middle|\, \boldsymbol{K}\boldsymbol{z} = \boldsymbol{\ell} \text{ and } \boldsymbol{z} \geq 0\right\}$ is a realization of the fan $\mathcal{F}$. Moreover, the polytopes $\mathbb{R}_{\boldsymbol{\ell}}$ for $\boldsymbol{\ell} \in \mathbb{R}^{N-n}_{>0}$ describe all polytopal realizations of $\mathcal{F}$.*

7.3.2 Type cones of g-vector fans

The linear dependences of Lemma 7.10 provide a redundant description of the type cone of the cluster fan $\mathcal{F}^{\boldsymbol{g}}(B_\circ)$. We denote by $\boldsymbol{n}(B_\circ, x, x')$ the normal vector of the inequality of the type cone corresponding to two exchangeable cluster variables x and x' (for cluster algebras, the linear dependence only depends on the pair of exchanged variables, not on the pair of adjacent clusters in which they are exchanged). In other words, depending on which of the two linear dependences of Lemma 7.10 holds,

$$\boldsymbol{n}(B_\circ, x, x') := \boldsymbol{f}_x + \boldsymbol{f}_{x'} - \sum_{\substack{y \in X \cap X' \\ b_{xy} < 0}} -b_{xy}\, \boldsymbol{f}_y \qquad \text{or} \qquad \boldsymbol{n}(B_\circ, x, x') := \boldsymbol{f}_x + \boldsymbol{f}_{x'} - \sum_{\substack{y \in X \cap X' \\ b_{xy} > 0}} b_{xy}\, \boldsymbol{f}_y,$$

where $(\boldsymbol{f}_x)_{x \in \mathcal{X}(B_\circ)}$ denotes the canonical basis of $\mathbb{R}^{\mathcal{X}(B_\circ)}$. We obtain the following statement.

Corollary 7.34. *For any finite type exchange matrix $B_\circ$, the type cone of $\mathcal{F}^{\boldsymbol{g}}(B_\circ)$ is given by*

$$\mathbb{TC}\big(\mathcal{F}^{\boldsymbol{g}}(B_\circ)\big) = \Big\{ \boldsymbol{h} \in \mathbb{R}^{\mathcal{X}(B_\circ)} \;\Big|\; \langle \boldsymbol{n}(B_\circ, x, x') \,|\, \boldsymbol{h} \rangle > 0 \text{ for all exchangeable cluster variables } x, x' \Big\}.$$

For instance, the type cone of the fan of Figure 7.1 (right) lives in $\mathbb{R}^{12}$ and has a linearity space of dimension 3. It has 9 facet-defining inequalities (given below), which correspond to the mesh mutations of Theorem 7.38 as illustrated in Figure 7.3.

variables	x_1	x_2	x_3	$\frac{x_2+x_3}{x_1}$	$\frac{x_1+x_3}{x_2}$	$\frac{x_1^2+x_2^2}{x_3}$	$\frac{x_1^2+x_2^2+x_1x_3}{x_2x_3}$	$\frac{x_1^2+x_2^2+x_2x_3}{x_1x_3}$	$\frac{x_1+x_2+x_3}{x_1x_2}$	$\frac{x_1^2+x_2^2+2x_1x_3+x_3^2}{x_2^2x_3}$	$\frac{x_1^2+x_2^2+2x_2x_3+x_3^2}{x_1^2x_3}$	$\frac{x_1^2+x_2^2+x_1x_3+x_2x_3}{x_1x_2x_3}$	
$\boldsymbol{g}$-vectors	$\begin{bmatrix}1\\0\\0\end{bmatrix}$	$\begin{bmatrix}0\\1\\0\end{bmatrix}$	$\begin{bmatrix}0\\0\\1\end{bmatrix}$	$\begin{bmatrix}-1\\0\\1\end{bmatrix}$	$\begin{bmatrix}1\\-1\\0\end{bmatrix}$	$\begin{bmatrix}0\\2\\-1\end{bmatrix}$	$\begin{bmatrix}0\\1\\-1\end{bmatrix}$	$\begin{bmatrix}-1\\1\\0\end{bmatrix}$	$\begin{bmatrix}0\\-1\\0\end{bmatrix}$	$\begin{bmatrix}0\\0\\-1\end{bmatrix}$	$\begin{bmatrix}-2\\0\\1\end{bmatrix}$	$\begin{bmatrix}-1\\0\\0\end{bmatrix}$	
facet defining inequalities	1	0	0	0	−1	0	0	0	1	0	0	0	Ⓐ
	0	0	−1	1	1	0	0	0	−1	0	0	0	Ⓑ
	0	0	1	−2	0	0	0	0	0	0	1	0	Ⓒ
	0	−1	0	1	0	0	0	1	0	0	−1	0	Ⓓ
	0	0	0	0	0	1	0	−2	0	0	1	0	Ⓔ
	0	1	0	0	0	0	0	−1	0	0	0	1	Ⓕ
	0	0	0	0	0	−1	1	1	0	0	0	−1	Ⓖ
	0	0	0	0	0	1	−2	0	0	1	0	0	Ⓗ
	−1	0	0	0	1	0	1	0	0	−1	0	0	Ⓘ

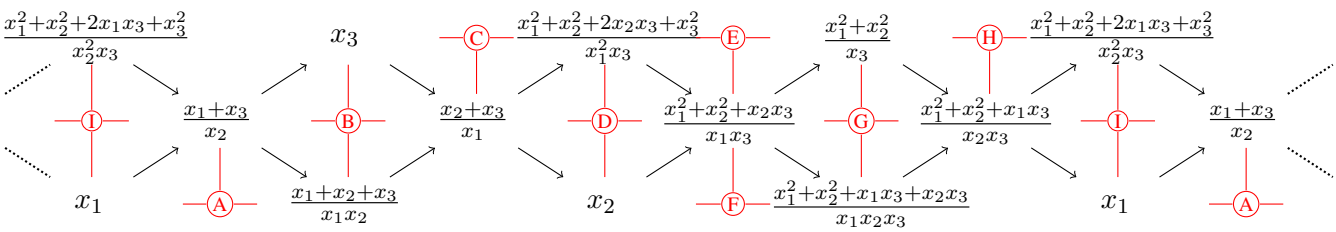

Figure 7.3: The facet-defining inequalities of the type cone $\mathbb{TC}\big(\mathcal{F}^{\boldsymbol{g}}(B_\circ)\big)$ of the cluster fan correspond to the mesh mutations described in Theorem 7.38.

In order to describe the facets of this type cone, we need the following special mutations.

Definition 7.35. *The mutation of a seed $\Sigma = (B, X)$ in the direction of a cluster variable $x \in X$ is a* mesh mutation *that* starts *(resp.* ends*) at x if the entries b_{xy} for $y \in X$ are all non-negative (resp. all non-positive). A mesh mutation is* initial *if it ends at a cluster variable of an initial seed. We denote by $\mathcal{M}(B_\circ)$ the set of all pairs $\{x, x'\}$ where x and x' are two cluster variables of $\mathcal{A}_{\mathrm{pr}}(B_\circ)$ which are exchangeable via a non-initial mesh mutation.*

Lemma 7.36. *Consider two adjacent seeds (B, X) and (B', X') with $X \smallsetminus \{x\} = X' \smallsetminus \{x'\}$ connected by a non-initial mesh mutation. Then, the $\boldsymbol{g}$-vectors of $X \cup X'$ with respect to $B_\circ$ satisfy the linear dependence $\boldsymbol{g}(B_\circ, x) + \boldsymbol{g}(B_\circ, x') = \sum_{y \in X \cap X'} |b_{xy}|\, \boldsymbol{g}(B_\circ, y)$.*

For $\{x, x'\} \in \mathcal{M}(B_\circ)$ and $y \in \mathcal{X}(B_\circ)$, we denote by $\alpha_{x,x',y}$ the coefficient of $\boldsymbol{g}(B_\circ, y)$ in the linear dependence between the $\boldsymbol{g}$-vectors $\boldsymbol{g}(B_\circ, x)$ and $\boldsymbol{g}(B_\circ, x')$. In other words, according to Lemma 7.36, if (B, X) and (B', X') are two adjacent seeds with $X \smallsetminus \{x\} = X' \smallsetminus \{x'\}$, we have $\alpha_{x,x',y} = |b_{xy}|$ for $y \in X \cap X'$ and $\alpha_{x,x',y} = 0$ otherwise. The following statement, proved in [PPPP19, Sect. 3] requires representation theory techniques far beyond the material discussed here.

Theorem 7.37. *For any finite type exchange matrix $B_\circ$ (acyclic or not, simply-laced or not), the linear dependence between the $\boldsymbol{g}$-vectors of any mutation can be decomposed into positive combinations of linear dependences between $\boldsymbol{g}$-vectors of non-initial mesh mutations.*

Using Theorem 7.37 as a blackbox, we can now describe the type cone, and thus all polytopal realizations, of the $\boldsymbol{g}$-vector fans of finite type cluster algebras.

Theorem 7.38. *For any finite type exchange matrix $B_\circ$ (acyclic or not, simply-laced or not), the type cone $\mathbb{TC}\big(\mathcal{F}^{\boldsymbol{g}}(B_\circ)\big)$ is simplicial and the non-initial mesh mutations precisely correspond to the extremal adjacent pairs of the cluster fan $\mathcal{F}^{\boldsymbol{g}}(B_\circ)$.*

Combining Corollary 7.33 and Theorem 7.38, we derive the following description of all polytopal realizations of the cluster fan $\mathcal{F}^{\boldsymbol{g}}(B_\circ)$. This result was stated in [AHBHY18] in type A, and extended in [BMDM+18] in the special situation of acyclic seeds in simply-laced types.

Theorem 7.39. *For any finite type exchange matrix $B_\circ$ (acyclic or not, simply-laced or not), and for any $\boldsymbol{\ell} \in \mathbb{R}_{>0}^{\mathcal{M}(B_\circ)}$, the polytope*

$$\mathbb{R}_{\boldsymbol{\ell}}(B_\circ) := \Big\{ \boldsymbol{z} \in \mathbb{R}^{\mathcal{X}(B_\circ)} \;\Big|\; \boldsymbol{z} \geq 0 \text{ and } \boldsymbol{z}_x + \boldsymbol{z}_{x'} - \sum_{y \in \mathcal{X}(B_\circ)} \alpha_{x,x',y}\, \boldsymbol{z}_y = \boldsymbol{\ell}_{\{x,x'\}} \text{ for all } \{x, x'\} \in \mathcal{M}(B_\circ) \Big\}$$

is a generalized associahedron, whose normal fan is the cluster fan $\mathcal{F}^{\boldsymbol{g}}(B_\circ)$. Moreover, the polytopes $\mathbb{R}_{\boldsymbol{\ell}}(B_\circ)$ for $\boldsymbol{\ell} \in \mathbb{R}_{>0}^{\mathcal{M}(B_\circ)}$ describe all polytopal realizations of $\mathcal{F}^{\boldsymbol{g}}(B_\circ)$.

Example 7.40. Let us translate to diagonals and triangulations the result of Theorem 7.39 in type A. Let $n \geq 3$. Consider a convex $(n+3)$-gon whose vertices are labeled modulo $n+3$ and whose (internal and boundary) diagonals are denoted by $\Delta(n) := \binom{\mathbb{Z}/(n+3)\mathbb{Z}}{2}$. Consider a triangulation T of this polygon, formed by the $n+3$ boundary edges and n internal diagonals of the $(n+3)$-gon. Then for any $\boldsymbol{\ell} \in \mathbb{R}_{>0}^{\Delta(n) \smallsetminus T}$, the polytope

$$\mathbb{R}_{\boldsymbol{\ell}}(T) := \left\{ \boldsymbol{z} \in \mathbb{R}^{\Delta(n)} \;\middle|\; \begin{array}{l} \boldsymbol{z} \geq 0 \quad \text{and} \quad \boldsymbol{z}_{(a,a+1)} = 0 \text{ for all } a \in Z/(n+3)\mathbb{Z} \quad \text{and} \\ \boldsymbol{z}_{(a,b)} + \boldsymbol{z}_{(a-1,b-1)} - \boldsymbol{z}_{(a,b-1)} - \boldsymbol{z}_{(a-1,b)} = \boldsymbol{\ell}_{(a,b)} \text{ for all } (a,b) \notin T \end{array} \right\}$$

is an associahedron whose normal fan is the $\boldsymbol{g}$-vector fan $\mathcal{F}^{\boldsymbol{g}}(T)$ with respect to the triangulation T. Moreover, the polytopes $\mathbb{R}_{\boldsymbol{\ell}}(T)$ for $\boldsymbol{\ell} \in \mathbb{R}_{>0}^{\Delta(n) \smallsetminus T}$ describe all polytopal realizations of $\mathcal{F}^{\boldsymbol{g}}(T)$.

Chapter Eight

BRICK POLYTOPES OF SUBWORD COMPLEXES

Brick polytopes were defined first on sorting networks as a tentative approach to construct polytopal realizations of the multiassociahedron [PS12], as already mentioned in Chapter 2. This chapter presents the general setting of brick polytopes of subword complexes on finite Coxeter groups. We first describe the combinatorics of subword complexes using the powerful tool of root functions. We then construct the brick polytopes using the analogous weight functions. These brick polytopes generalize and provide an alternative perspective on the generalized associahedra of [HLT11] discussed in Chapter 7. For instance, we show that it provides an elementary proof that their vertex barycenter is at the origin. This chapter is adapted from joint works with C. Stump [PS15a, PS15b].

8.1 COMBINATORICS OF SUBWORD COMPLEXES

8.1.1 Subword complex

Let (W, S) be a finite Coxeter system (W, S) (see Section 5.2.1 or [Hum90, BB05] for a presentation of Coxeter groups). We choose a word $M := m_1 \cdots m_\ell$ on S (not necessarily reduced) and an element $\rho \in W$. The following complex was introduced by A. Knutson and E. Miller in [KM04, KM05].

Definition 8.1 ([KM04]). *The subword complex $\mathcal{C}_{\mathrm{sub}}(M, \rho)$ is the simplicial complex of subwords of M whose complements contain a reduced expression of ρ.*

By definition, the subword complex $\mathcal{C}_{\mathrm{sub}}(M, \rho)$ is non-empty if and only if M contains at least one reduced expression for ρ as a subword. Its vertices are labeled by the positions $[\ell] := \{1, \dots, \ell\}$ of the letters in the word M, an its facets are the complements of the reduced expressions of ρ in M.

In this chapter, we always assume that ρ is the longest word $w_\circ$ of W, and we write $\mathcal{C}_{\mathrm{sub}}(M)$ instead of $\mathcal{C}_{\mathrm{sub}}(M, w_\circ)$ to simplify notations. The subword complex $\mathcal{C}_{\mathrm{sub}}(M)$ is then known to be a vertex-decomposable simplicial sphere [KM04].

For instance, the facets of the subword complex $\mathcal{C}_{\mathrm{sub}}(M)$ for the word $M = \tau_2\tau_3\tau_1\tau_3\tau_2\tau_1\tau_2\tau_3\tau_1$ are $\{2,3,5\}$, $\{2,3,9\}$, $\{2,5,6\}$, $\{2,6,7\}$, $\{2,7,9\}$, $\{3,4,5\}$, $\{3,4,9\}$, $\{4,5,6\}$, $\{4,6,7\}$ and $\{4,7,9\}$.

Example 8.2. Let $W = \mathfrak{S}_{n+1}$ and $S = \{\tau_p \,|\, p \in [n]\}$, where τ_p is the transposition $(p, p+1)$. We represent the word $M := m_1 m_2 \cdots m_\ell$ by a *sorting network* $\mathcal{N}_M$ as illustrated in Figure 8.1 (left). The network $\mathcal{N}_M$ is formed by $n+1$ horizontal lines (its *levels*, labeled from bottom to top) together with ℓ vertical segments (its *commutators*, labeled from left to right) corresponding to the letters of M. If $m_k = \tau_p$, the kth commutator of $\mathcal{N}_M$ lies between the pth and $(p+1)$th levels of $\mathcal{N}_M$.

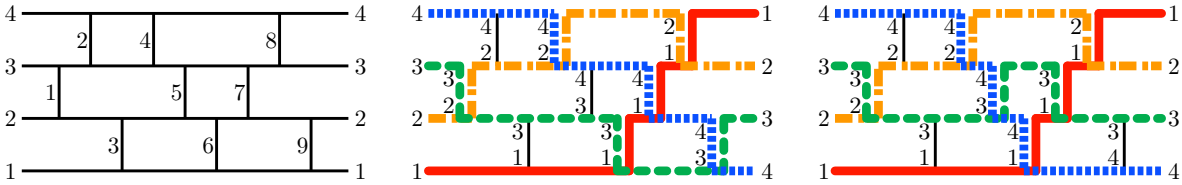

Figure 8.1: The sorting network $\mathcal{N}_M$ corresponding to the word $M = \tau_2\tau_3\tau_1\tau_3\tau_2\tau_1\tau_2\tau_3\tau_1$ (left) and the pseudoline arrangements corresponding to the facets $\{2,3,5\}$ (middle) and $\{2,3,9\}$ (right).

A *pseudoline* supported by $\mathcal{N}_M$ is an abscissa monotone path on $\mathcal{N}_M$. A commutator is a *crossing* between two pseudolines if it is traversed by both pseudolines, and a *contact* if its endpoints are contained one in each pseudoline. A *pseudoline arrangement* Λ is a set of $n+1$ pseudolines on $\mathcal{N}_M$, any two of which have precisely one crossing, possibly some contacts, and no other intersection. As a consequence of the definition, the pseudoline of Λ which starts at level p ends at level $n-p+2$, and is called the pth pseudoline of Λ. As illustrated in Figure 8.1 (middle and right), a facet I of $\mathcal{C}_{\text{sub}}(M)$ is represented by a pseudoline arrangement Λ_I supported by $\mathcal{N}_M$. Its contacts (resp. crossings) are the commutators of $\mathcal{N}_M$ corresponding to the letters of I (resp. of the complement of I).

Example 8.3. As pointed out in [PP12], type A subword complexes can be used to provide a combinatorial model for many relevant families of geometric graphs (see Figure 8.2 for illustrations):

- triangulations of a convex polygon, see [Woo04, PP12, Stu11] and Remark 2.3.
- k-triangulations of a convex polygon, see [PS09, PP12, Stu11] and Remark 2.3.
- pseudotriangulations of a point set P in general position (no line contains three points). *Pseudotriangulations* of P are maximal pointed crossing-free sets of edges between points of P [PV96, RSS08]. They correspond to the vertices of the *pseudotriangulation polytope* of [RSS03].
- pseudotriangulations of a set of disjoint convex bodies in general position (no line is tangent to three convex bodies).

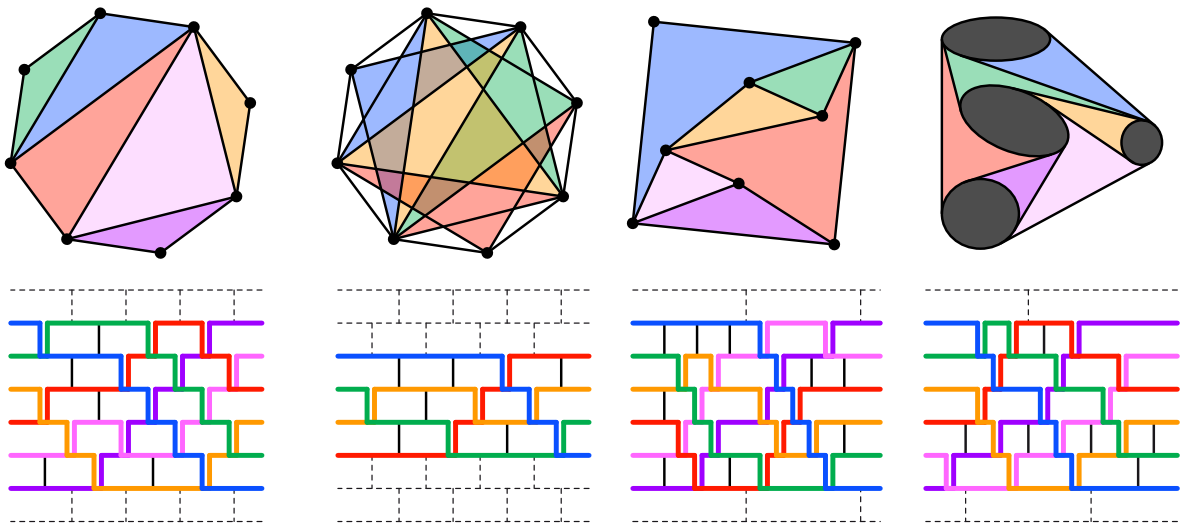

Figure 8.2: Sorting networks interpretations of certain geometric graphs: a triangulation of the convex octagon, a 2-triangulation of the convex octagon, a pseudotriangulation of a point set, and a pseudotriangulation of a set of disjoint convex bodies.

8.1.2 Root function and flips

Root function. The combinatorial and geometric properties of subword complexes are encoded in the root functions of their facets, defined in [CLS14]. For $X \subseteq [\ell]$, we denote by ΠM_X the product of the reflections $m_x \in M$, for $x \in X$, in the order given by M.

Definition 8.4 ([CLS14])**.** *For a facet I of $\mathcal{C}_{\mathrm{sub}}(M)$,*
- *the root function $\boldsymbol{r}(I,\cdot)$ associates to each position $k \in [\ell]$ a root $\boldsymbol{r}(I,k) := \Pi M_{[k-1]\smallsetminus I}(\alpha_{m_k})$,*
- *the root configuration $\boldsymbol{R}(I)$ is the multiset $\boldsymbol{R}(I) := \{\!\{\boldsymbol{r}(I,i) \mid i \in I\}\!\}$.*

For instance, for $M = \tau_2\tau_3\tau_1\tau_3\tau_2\tau_1\tau_2\tau_3\tau_1$, we have $\boldsymbol{r}(\{2,3,9\},2) = \tau_2(\boldsymbol{e}_4 - \boldsymbol{e}_3) = \boldsymbol{e}_4 - \boldsymbol{e}_2$ and $\boldsymbol{r}(\{2,3,9\},7) = \tau_2\tau_3\tau_2\tau_1(\boldsymbol{e}_3 - \boldsymbol{e}_2) = \boldsymbol{e}_3 - \boldsymbol{e}_1$. Moreover, the root configuration of the facet $\{2,3,9\}$ is $\boldsymbol{R}(\{2,3,9\}) = \{\!\{\boldsymbol{e}_4 - \boldsymbol{e}_2, \boldsymbol{e}_3 - \boldsymbol{e}_1, \boldsymbol{e}_3 - \boldsymbol{e}_4\}\!\}$.

Example 8.5. Keep the notations of Example 8.2. For any $k \in [\ell]$, we have $\boldsymbol{r}(I,k) = \boldsymbol{e}_t - \boldsymbol{e}_b$, where t and b are such that the tth and bth pseudolines of Λ_I arrive respectively on top and bottom of the kth commutator of $\mathcal{N}_M$. For example, for $M = \tau_2\tau_3\tau_1\tau_3\tau_2\tau_1\tau_2\tau_3\tau_1$, the root $\boldsymbol{r}(\{2,3,9\},7) = \boldsymbol{e}_3 - \boldsymbol{e}_1$ can be read in the 7th commutator of Figure 8.1 (right). In [PS12], the root configuration $\boldsymbol{R}(I)$ is studied as the incidence configuration of the contact graph $\Lambda_I^{\#}$ of the pseudoline arrangement Λ_I, see Definition 2.2.

Flips. As the subword complex is a simplicial sphere, there is a flip operation between its facets. For a given facet I of $\mathcal{C}_{\mathrm{sub}}(M)$, the map $\boldsymbol{r}(I,\cdot) : [\ell] \to \Phi$ can be used to understand the flips in I.

Lemma 8.6. *Let I be any facet of the subword complex $\mathcal{C}_{\mathrm{sub}}(M)$.*
(1) The map $\boldsymbol{r}(I,\cdot) : k \mapsto \boldsymbol{r}(I,k)$ is a bijection between the complement of I and Φ^+.
(2) If I and J are two adjacent facets of $\mathcal{C}_{\mathrm{sub}}(M)$ with $I \smallsetminus i = J \smallsetminus j$, the position j is the unique position in the complement of I for which $\boldsymbol{r}(I,j) \in \{\pm\boldsymbol{r}(I,i)\}$. Moreover, $\boldsymbol{r}(I,j) = \boldsymbol{r}(I,i) \in \Phi^+$ if $i < j$, while $\boldsymbol{r}(I,j) = -\boldsymbol{r}(I,i) \in \Phi^-$ if $j < i$.
(3) In the situation of (2), the map $\boldsymbol{r}(J,\cdot)$ is obtained from the map $\boldsymbol{r}(I,\cdot)$ by:

$$\boldsymbol{r}(J,k) = \begin{cases} s_{\boldsymbol{r}(I,i)}(\boldsymbol{r}(I,k)) & \text{if } \min(i,j) < k \leq \max(i,j), \\ \boldsymbol{r}(I,k) & \text{otherwise.} \end{cases}$$

Example 8.7. Keep the notations of Example 8.2. Let I and J be two adjacent facets of $\mathcal{C}_{\mathrm{sub}}(M)$, with $I \smallsetminus i = J \smallsetminus j$. Then j is the position of the crossing between the two pseudolines of Λ_I which are in contact at position i, and the pseudoline arrangement Λ_J is obtained from the pseudoline arrangement Λ_I by exchanging the contact at i with the crossing at j. See Figure 8.1 (middle and right).

Root independent subword complexes. The geometry of the root configuration $\boldsymbol{R}(I)$ encodes many combinatorial properties of I. In fact, the facet I is relevant for the brick polytope only when its root configuration is pointed. This is in particular the case when $\boldsymbol{R}(I)$ forms an independent set of V. The following property shows that this property is independent of the facet.

Lemma 8.8. *Either all the root configurations $\boldsymbol{R}(I)$ for facets I of $\mathcal{C}_{\mathrm{sub}}(M)$ are simultaneously linearly independent in V, or none of them is.*

Definition 8.9. *We say that $\mathcal{C}_{\mathrm{sub}}(M)$ is root independent when all the root configurations of its facets are linearly independent.*

Example 8.10. In type A, the root configuration $\boldsymbol{R}(I)$ is linearly independent if and only if the contact graph of Λ_I is a forest. For example, the subword complex $\mathcal{C}_{\mathrm{sub}}(M)$ of Figure 8.1 is root independent.

8.2 BRICK POLYTOPES OF SUBWORD COMPLEXES

8.2.1 Weight function and brick polytope

Weight function. Recall that, for $X \subseteq [\ell]$, we denote by ΠM_X the product of the reflections $m_x \in M$, for $x \in X$, in the order given by M.

Definition 8.11. *For a facet I of $\mathcal{C}_{\mathrm{sub}}(M)$, the weight function $\boldsymbol{w}(I,\cdot)$ associates to each position $k \in [\ell]$ a weight $\boldsymbol{w}(I,k) := \Pi M_{[k-1]\smallsetminus I}(\omega_{m_k})$.*

The root function $\boldsymbol{r}(\cdot,\cdot)$ and the weight function $\boldsymbol{w}(\cdot,\cdot)$ have similar definitions and are indeed closely related, as illustrated by the following statement.

Lemma 8.12. *Let I be a facet of the subword complex $\mathcal{C}_{\mathrm{sub}}(M)$.*

(1) If $m_k = m_{k+1}$, we have $\boldsymbol{w}(I,k+1) = \begin{cases} \boldsymbol{w}(I,k) & \text{if } k \in I, \\ \boldsymbol{w}(I,k) - \boldsymbol{r}(I,k) & \text{if } k \notin I. \end{cases}$

(2) If I and J are two adjacent facets of $\mathcal{C}_{\mathrm{sub}}(M)$ with $I \smallsetminus i = J \smallsetminus j$, then the map $\boldsymbol{w}(J,\cdot)$ is obtained from the map $\boldsymbol{w}(I,\cdot)$ by:

$$\boldsymbol{w}(J,k) = \begin{cases} s_{\boldsymbol{r}(I,i)}(\boldsymbol{w}(I,k)) & \text{if } \min(i,j) < k \le \max(i,j), \\ \boldsymbol{w}(I,k) & \text{otherwise.} \end{cases}$$

(3) For $j \notin I$, we have $\langle \boldsymbol{r}(I,j) \mid \boldsymbol{w}(I,k) \rangle$ is non-negative if $j \ge k$, and non-positive if $j < k$.

Brick polytope. We are now ready to define the brick polytope of a subword complex.

Definition 8.13. *The brick vector of the facet I is $\boldsymbol{b}(I) := \sum_{k\in[\ell]} \boldsymbol{w}(I,k)$. The brick polytope $\mathbb{BP}(M)$ of the word M is the convex hull $\mathbb{BP}(M) := \operatorname{conv}\{\boldsymbol{b}(I) \mid I \text{ facet of } \mathcal{C}_{\mathrm{sub}}(M)\}$ of all the brick vectors.*

For instance, for the word $M = \tau_2\tau_3\tau_1\tau_3\tau_2\tau_1\tau_2\tau_3\tau_1$, we have $\boldsymbol{w}(\{2,3,9\},2) = \tau_2(\boldsymbol{e}_4) = \boldsymbol{e}_4$ and $\boldsymbol{w}(\{2,3,9\},7) = \tau_2\tau_3\tau_2\tau_1(\boldsymbol{e}_3+\boldsymbol{e}_4) = \boldsymbol{e}_2+\boldsymbol{e}_3$. Moreover, the brick vector of the facet $\{2,3,4\}$ is $\boldsymbol{b}(\{2,3,9\}) = \boldsymbol{e}_1 + 6\boldsymbol{e}_2 + 5\boldsymbol{e}_3 + 6\boldsymbol{e}_4 = (1,6,5,6)$. The brick polytope $\mathbb{BP}(M)$ is a pentagonal prism, represented in Figure 8.3.

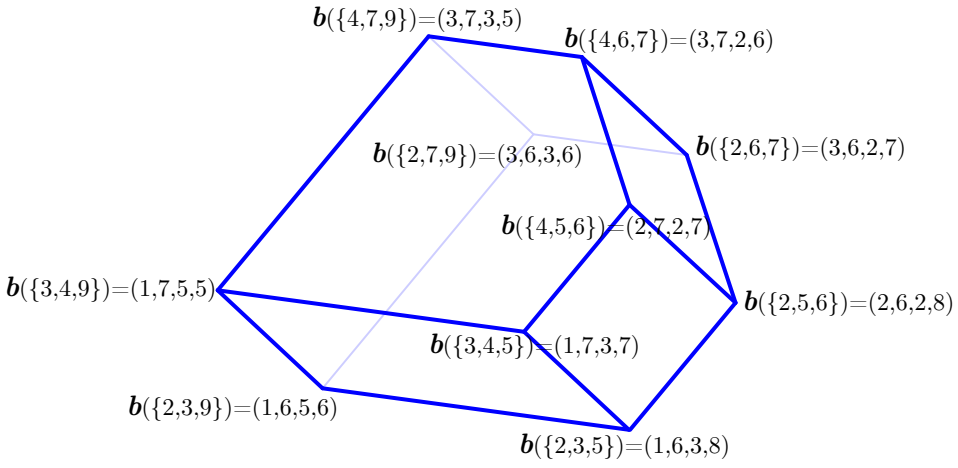

Figure 8.3: The brick polytope $\mathbb{BP}(M)$ of the word $M = \tau_2\tau_3\tau_1\tau_3\tau_2\tau_1\tau_2\tau_3\tau_1$.

Example 8.14. In type A, we can read this definition on the sorting network interpretation of Example 8.2. Define the *bricks* of $\mathcal{N}_M$ as the connected components of its complement, bounded on the right by a commutator of $\mathcal{N}_M$. For a facet I of $\mathcal{C}_{\mathrm{sub}}(M)$ and a position $k \in [\ell]$, the weight $\boldsymbol{w}(I,k)$ is the characteristic vector of the pseudolines of Λ_I which pass above the kth brick of $\mathcal{N}_M$. For any $p \in [n+1]$, the pth coordinate of the brick vector $\boldsymbol{b}(I)$ is the number of bricks of $\mathcal{N}_M$ below the pth pseudoline of Λ_I. See Figure 8.1 for an illustration. This was the original definition used in type A in [PS12], which explains the name *brick polytope*.

8.2.2 Properties of brick polytopes

Although we defined brick polytopes for any word M, we only present their geometric and combinatorial properties when $\mathcal{C}_{\mathrm{sub}}(M)$ is root independent. The general case, discussed in Conjecture 8.18, is understood in type A in [PS12] but not for subword complexes on arbitrary finite Coxeter groups. Note that further properties of brick polytopes, in particular their Minkowski sum decompositions as Coxeter matroid polytopes, are discussed in [PS15a].

8.2.2.1 Geometry of brick polytopes.

The main tool to understand the geometry of the brick polytope is the following statement, which follows from the connection between the root and weight functions observed in Lemma 8.12.

Lemma 8.15. *If I and J are two adjacent facets of $\mathcal{C}_{\mathrm{sub}}(M)$, with $I \smallsetminus i = J \smallsetminus j$, then the difference of the brick vectors $\boldsymbol{b}(I) - \boldsymbol{b}(J)$ is a positive multiple of $\boldsymbol{r}(I,i)$.*

Proposition 8.16. *When the subword complex $\mathcal{C}_{\mathrm{sub}}(M)$ is root independent, then for any facet I of $\mathcal{C}_{\mathrm{sub}}(M)$, the cone $\boldsymbol{C}(I) := \mathbb{R}_{\geq 0}\{\boldsymbol{b}(J) - \boldsymbol{b}(I) \mid J \text{ facet of } \mathcal{C}_{\mathrm{sub}}(M)\}$ of the brick polytope $\mathbb{BP}(M)$ at the brick vector $\boldsymbol{b}(I)$ coincides with the cone $\mathbb{R}_{\leq 0}\boldsymbol{R}(I) = \mathbb{R}_{\geq 0}\{-\boldsymbol{r}(I,i) \mid i \in I\}$.*

Proposition 8.16 is the main step to show the central result of [PS15a].

Theorem 8.17. *When the subword complex $\mathcal{C}_{\mathrm{sub}}(M)$ is root independent, it is realized by the polar of the brick polytope $\mathbb{BP}(M)$.*

The following conjecture extends this result to subword complexes that are not root independent. It is known in type A and has several consequences presented in [PS12].

Conjecture 8.18. *For any facet I of $\mathcal{C}_{\mathrm{sub}}(M)$, the cone of the brick polytope $\mathbb{BP}(M)$ at the brick vector $\boldsymbol{b}(I)$ coincides with the cone $\mathbb{R}_{\leq 0}\boldsymbol{R}(I)$. In particular, the brick vector $\boldsymbol{b}(I)$ for a facet I of $\mathcal{C}_{\mathrm{sub}}(M)$ is a vertex of the brick polytope $\mathbb{BP}(M)$ if and only if the cone $\mathbb{R}_{\leq 0}\boldsymbol{R}(I)$ is pointed.*

8.2.2.2 Surjection and increasing flip graphs.

The geometry of the cones of the brick polytope defines a surjection κ from W to the facets of $\mathcal{C}_{\mathrm{sub}}(M)$, where the facet $\kappa(w)$ is defined equivalently by:

- the root configuration $\boldsymbol{R}(\kappa(w))$ of the facet $\kappa(w)$ is contained in $w(\Phi^+)$,
- the cone $\boldsymbol{C}(\kappa(w))$ of the vertex $\boldsymbol{b}(\kappa(w))$ in $\mathbb{BP}(M)$ is contained in the cone $\boldsymbol{C}(w)$,
- the normal cone $\boldsymbol{C}^\diamond(\kappa(w))$ of the vertex $\boldsymbol{b}(\kappa(w))$ in $\mathbb{BP}(M)$ contains the chamber $\boldsymbol{C}^\diamond(w)$.

The following statement is a geometric reformulation of this map.

Corollary 8.19. *The Coxeter fan refines the normal fan of the brick polytope. Namely, for any facet I of $\mathcal{C}_{\mathrm{sub}}(M)$, the normal cone $\boldsymbol{C}^\diamond(I)$ of the vertex $\boldsymbol{b}(I)$ in $\mathbb{BP}(M)$ is the union of the chambers $\boldsymbol{C}^\diamond(w)$ of the Coxeter fan of W given by the elements $w \in W$ with $\kappa(w) = I$.*

Example 8.20. In type A, the cones $\boldsymbol{C}(I)$ and $\boldsymbol{C}^\diamond(I)$ are given by the contact graph $\Lambda_I^\#$ of Λ_I [PS12]:
- the cone $\boldsymbol{C}(I)$ is the incidence cone $\boldsymbol{C}(\Lambda_I^\#) \coloneqq \mathbb{R}_{\geq 0}\{\boldsymbol{e}_j - \boldsymbol{e}_i \mid (i,j) \in \Lambda_I^\#\}$,
- the normal cone $\boldsymbol{C}^\diamond(I)$ is the braid cone $\boldsymbol{C}^\diamond(\Lambda_I^\#) \coloneqq \{\boldsymbol{x} \in \mathbb{R}^n \mid \boldsymbol{x}_i \leq \boldsymbol{x}_j \text{ for all } (i,j) \in \Lambda_I^\#\}$.

Therefore, an element $w \in W$ lies in the fiber $\kappa^{-1}(I)$ if and only if it is a linear extension of the transitive closure of $\Lambda_I^\#$. See also Section 1.2.

Generalizing the Tamari lattice [Tam51] and the Cambrian lattices [Rea06], we now consider the increasing flip order, introduced in [KM04]. Many order theoretic properties of this increasing flip order are developed in [PS13].

Definition 8.21. *For two adjacent facets I and J of $\mathcal{C}_{\mathrm{sub}}(M)$ with $I \smallsetminus i = J \smallsetminus j$, the flip from I to J is* increasing *if $i < j$, or equivalently (by Lemma 8.6 (2)) if $\boldsymbol{r}(I,i) = -\boldsymbol{r}(J,j) \in \Phi^+$. The* increasing flip order *is the transitive closure $\prec$ of the increasing flip graph.*

For a root independent subword complex, this increasing flip order is an orientation of the graph of the brick polytope.

Proposition 8.22. *When the subword complex $\mathcal{C}_{\mathrm{sub}}(M)$ is root independent, the graph of the brick polytope $\mathbb{BP}(M)$, oriented in the direction $\boldsymbol{\omega} \coloneqq -\sum_{s \in S} \omega_s$, is the Hasse diagram of the increasing flip order.*

As in the classical case, the map κ provides a surjection from the weak order $\leq_{\mathsf{W}}$ on W to the increasing flip order on $\mathcal{C}_{\mathrm{sub}}(M)$. The combinatorial behavior of this surjection is somewhat similar to that of a lattice quotient as illustrated by the following statement.

Proposition 8.23. *The map κ from the elements of the Coxeter group W to the facets of the subword complex $\mathcal{C}_{\mathrm{sub}}(M)$ satisfies the following properties:*
- *its fibers are closed by intervals: if two elements $\underline{w} \leq_{\mathsf{W}} \overline{w}$ of W lie in the same fiber of κ, then the weak order interval $[\underline{w}, \overline{w}]_{\mathsf{W}} \coloneqq \{w \in W \mid \underline{w} \leq_{\mathsf{W}} w \leq_{\mathsf{W}} \overline{w}\}$ lies in the same fiber of κ.*
- *the increasing flip graph on $\mathcal{C}_{\mathrm{sub}}(M)$ is the quotient of the Hasse diagram of the weak order by the fibers of the map κ: a facet I is covered by a facet J in increasing flip order if and only if there exist $w_I \in \kappa^{-1}(I)$ and $w_J \in \kappa^{-1}(J)$ such that w_I is covered by w_J in weak order.*

However, it turns out that increasing flip orders on subword complexes are not lattice quotients in general. Surprizingly, the increasing flip order is not even always a lattice. For instance, consider the word $M = \tau_1\tau_2\tau_3\tau_2\tau_1\tau_2\tau_3\tau_2\tau_1$ in $\mathfrak{S}_4$, and the four facets $I_1 = \{1,2,9\}$, $I_2 = \{1,3,4\}$, $J_1 = \{1,8,9\}$ and $J_2 = \{6,7,9\}$ of $\mathcal{C}_{\mathrm{sub}}(M)$. For $i,j \in \{1,2\}$, we then have that $I_i < J_j$ in the increasing flip poset, but J_1 and J_2 are not comparable. Thus, I_1 and I_2 do not have a unique join and the increasing flip graph on $\mathcal{C}_{\mathrm{sub}}(M)$ is not a lattice.

8.2.3 Duplicated words

We conclude this section with a first family of words that yield an interesting family of brick polytopes.

Definition 8.24. *Let $w_\circ \coloneqq w_1 \cdots w_N$ be a reduced expression of the longest element $w_\circ$ of W. For $P \subseteq [N]$, we obtain a new word $w_\circ^P \in S^*$ by duplicating the letters of $w_\circ$ at positions in P.*

The following statement describes the subword complex $\mathcal{C}_{\mathrm{sub}}(w_\circ^P)$ and brick polytope $\mathbb{BP}(w_\circ^P)$. For a position $k \in [N]$, we define
- $\alpha_k \coloneqq w_1 \cdots w_{k-1}(\alpha_{w_k})$ the root at position k in $w_\circ$,
- $k^* \coloneqq k + |P \cap [k-1]|$ the new position in $w_\circ^P$ of the kth letter of $w_\circ$.

Proposition 8.25. *Consider the duplicated word $w_\circ^P$.*

1. *The facets of the subword complex $\mathcal{C}_{\mathrm{sub}}(w_\circ^P)$ are precisely the sets $I_\varepsilon := \{p^* + \varepsilon_p \,|\, p \in P\}$ where $\varepsilon := (\varepsilon_1, \dots, \varepsilon_n) \in \{0,1\}^P$.*
2. *The roots of a facet I_ε of $\mathcal{C}_{\mathrm{sub}}(w_\circ^P)$ are given by $\boldsymbol{r}(I_\varepsilon, p^* + 1) = (-1)^{\varepsilon_p}\alpha_p$ for $p \in P$ and $\boldsymbol{r}(I_\varepsilon, k^*) = \alpha_k$ for $k \in [N]$. The root configuration of I_ε is thus $\boldsymbol{R}(I_\varepsilon) = \{\!\{(-1)^{\varepsilon_p}\alpha_p \mid p \in P\}\!\}$. The subword complex $\mathcal{C}_{\mathrm{sub}}(w_\circ^P)$ is root independent if and only if $\{\!\{\alpha_p \mid p \in P\}\!\}$ is a basis.*
3. *The weights of a facet I_ε of $\mathcal{C}_{\mathrm{sub}}(w_\circ^P)$ are given by $\boldsymbol{w}(I_\varepsilon, p^* + 1) = \omega_p + \varepsilon_p\alpha_p$ for $p \in P$ and $\boldsymbol{w}(I_\varepsilon, k^*) = \omega_k$ for $k \in [N]$. The brick vector of I_ε is thus $\boldsymbol{b}(I_\varepsilon) = \Theta + \sum_{p\in P} \varepsilon_p\alpha_p$, where $\Theta := \sum_{k\in[N]} \omega_k + \sum_{p\in P} \omega_p$. The brick polytope $\mathbb{BP}(w_\circ^P)$ is a zonotope, whose edges are directed by $\{\alpha_p \,|\, p \in P\}$. In particular, it is a parallelepiped when $\{\alpha_p \,|\, p \in P\}$ is a basis.*
4. *The normal fan of its brick polytope $\mathbb{BP}(w_\circ^P)$ is the fan formed by the hyperplanes orthogonal to the roots $\{\alpha_p \,|\, p \in P\}$.*
5. *The increasing flip order is the boolean lattice. In particular, it is the graph of the brick polytope $\mathbb{BP}(w_\circ^P)$ if and only if $\{\alpha_p \,|\, p \in P\}$ is a basis.*

8.3 GENERALIZED ASSOCIAHEDRA REVISITED

In this section, we show that brick polytopes provide a powerful approach to the generalized associahedra constructed by C. Hohlweg, C. Lange and H. Thomas [HLT11]. In fact, it gives a vertex description of these polytopes and thus provides a simple proof that their vertex barycenter is at the origin (an alternative proof based on universal associahedra was already mentioned in Section 7.2.3.2).

8.3.1 Generalized associahedra from brick polytopes

Consider a finite Coxeter system (W, S), let c be a *Coxeter element* (*i.e.* the product of all simple reflections of S in a given order), and let $B_\circ$ be the corresponding acyclic initial exchange matrix. Following [Rea07b], we choose an arbitrary reduced expression for c and let $w(c)$ denote the *c-sorting word* of w, *i.e.* the lexicographically first (as a sequence of positions) reduced subword of c^∞ for w. In particular, $w_\circ(c)$ denotes the c-sorting word of the longest element $w_\circ \in W$. Let $N := \ell(w_\circ) = |\Phi^+|$, and let $m := n + N$ be the length of $cw_\circ(c)$. The following statement was proven in [CLS14].

Theorem 8.26 ([CLS14])**.** *For any Coxeter element c of W, the subword complex $\mathcal{C}_{\mathrm{sub}}(cw_\circ(c))$ is isomorphic to the cluster complex $\mathcal{C}_{\mathrm{clu}}(B_\circ)$.*

Since the subword complex $\mathcal{C}_{\mathrm{sub}}(cw_\circ(c))$ is root independent, we can apply our brick polytope construction to obtain polytopal realizations of the cluster complex.

Theorem 8.27. *For any Coxeter element c of W, the polar of the brick polytope $\mathbb{BP}(cw_\circ(c))$ realizes the subword complex $\mathcal{C}_{\mathrm{sub}}(cw_\circ(c))$, thus the cluster complex $\mathcal{C}_{\mathrm{clu}}(B_\circ)$.*

In fact, these brick polytopes are translates of the known realizations of the generalized associahedra studied in [HLT11, Ste13].

Proposition 8.28. *Up to the translation by the vector τ, the brick polytope $\mathbb{BP}(cw_\circ(c))$ coincides with the c-associahedron $\mathbb{Asso}(c)$ in [HLT11].*

This brick polytope interpretation provides a new perspective on the c-associahedra of [HLT11]. In particular, we obtain independent elementary proofs of the following two results, which are the heart of the construction of [HLT11]. We say that an element $w \in W$ is a *singleton* if $\kappa^{-1}(\kappa(w)) = \{w\}$. We denote here by $q := \sum_s \omega_s$ the sum of all weights of ∇.

Proposition 8.29. *Up to translation by τ, the brick polytope $\mathbb{BP}(cw_\circ(c))$ is obtained from the W-permutahedron $\mathbb{P}\mathrm{erm}(W)$ removing all facets which do not intersect the set $\{w(q) \mid w \in W \text{ singleton}\}$.*

Proposition 8.30. *The following properties are equivalent for an element $w \in W$:*
(i) The element w is a singleton, i.e. $\kappa^{-1}(\kappa(w)) = \{w\}$.
(ii) The root configuration $\boldsymbol{R}(\kappa(w)) := \{\boldsymbol{r}(\kappa(w), i) \mid i \in \kappa(w)\}$ equals $w(\Delta)$.
(iii) The weight configuration $\boldsymbol{W}(\kappa(w)) := \{\boldsymbol{w}(\kappa(w), i) \mid i \in \kappa(w)\}$ equals $w(\nabla)$.
(iv) The vertex $\boldsymbol{b}(\kappa(w))$ of the brick polytope $\mathbb{BP}(cw_\circ(c))$ and the vertex $w(q)$ of the W-permutahedron $\mathbb{P}\mathrm{erm}(W)$ coincide up to the translation τ, i.e. $\boldsymbol{b}(\kappa(w)) = \tau + w(q)$.
(v) There exist reduced expressions for w and c such that w is a prefix of $cw_\circ(c)$.
(vi) The complement of $\kappa(w)$ in $cw_\circ(c)$ is $w_\circ(c)$.

8.3.2 Word operations and vertex barycenter

The brick polytope interpretation of Section 8.3.1 provides a vertex description of the generalized associahedra of [HLT11], and thus a first approach to the intriguing question of the vertex barycenter of these polytopes. The approach of [PS15b], is based on the following four operations on words, which translate into geometric operations on the corresponding brick polytopes. We denote by φ the conjugation map defined by $\varphi(s) := w_\circ s w_\circ$. Moreover, in order to distinguish between the different subword complexes in the following statements, we denote by $\boldsymbol{b}_M(I)$ the brick vector of a facet I in the subword complex $\mathcal{C}_{\mathrm{sub}}(M)$.

Lemma 8.31. *If $\pi(M) := m_{\pi(1)} \cdots m_{\pi(p)}$ is obtained from M by a sequence of transpositions of consecutive commuting letters, then π induces an isomorphism between the subword complexes $\mathcal{C}_{\mathrm{sub}}(M)$ and $\mathcal{C}_{\mathrm{sub}}(\pi(M))$. Moreover, $\boldsymbol{b}_{\pi(M)}(\pi(I)) = \boldsymbol{b}_M(I)$ for any facet I of $\mathcal{C}_{\mathrm{sub}}(M)$.*

Lemma 8.32. *If $M^{\circlearrowleft} := m_2 \cdots m_p \varphi(m_1)$, then the rotation $\rho : i \mapsto (i-1)$ induces an isomorphism between the subword complexes $\mathcal{C}_{\mathrm{sub}}(M)$ and $\mathcal{C}_{\mathrm{sub}}(M^{\circlearrowleft})$. Moreover, $\boldsymbol{b}_{M^{\circlearrowleft}}(\rho(I)) - \boldsymbol{b}_M(I)$ belongs to $-2\omega_{m_1} + \mathbb{R}\alpha_{m_1}$ for any facet I of $\mathcal{C}_{\mathrm{sub}}(M)$.*

Lemma 8.33. *If $M^{\updownarrow} := \varphi(m_1) \ldots \varphi(m_p)$, then the subword complexes $\mathcal{C}_{\mathrm{sub}}(M)$ and $\mathcal{C}_{\mathrm{sub}}(M^{\updownarrow})$ coincide. Moreover, $\boldsymbol{b}_{M^{\updownarrow}}(I) = -w_\circ(\boldsymbol{b}_M(I))$ for any facet I of $\mathcal{C}_{\mathrm{sub}}(M)$.*

Lemma 8.34. *If $M^{\leftrightarrow} := m_p \cdots m_1$, then the mirror $\mu : i \mapsto m - i + 1$ induces an isomorphism between the subword complexes $\mathcal{C}_{\mathrm{sub}}(M)$ and $\mathcal{C}_{\mathrm{sub}}(M^{\leftrightarrow})$. Moreover, $\boldsymbol{b}_{M^{\leftrightarrow}}(\mu(I)) = w_\circ(\boldsymbol{b}_M(I)) + \sum_{\beta \in \Phi^+} \beta$ for any facet I of $\mathcal{C}_{\mathrm{sub}}(M)$.*

Let us now denote by $\mathbf{bary}(c)$ the barycenter of the associahedron $\mathbb{A}\mathrm{sso}(c)$. Combining Lemmas 8.31 and 8.32, we obtain that all c-associahedra $\mathbb{A}\mathrm{sso}(c)$ have the same vertex barycenter.

Proposition 8.35. *We have $\mathbf{bary}(c) = \mathbf{bary}(c')$ for any Coxeter elements c, c' of W.*

Combining Lemmas 8.33 and 8.34, we obtain that the barycenter of the superposition of the vertices of the two associahedra $\mathbb{A}\mathrm{sso}(c)$ and $\mathbb{A}\mathrm{sso}(c^{-1})$ is the origin.

Proposition 8.36. *We have $\mathbf{bary}(c) + \mathbf{bary}(c^{-1}) = 0$ for any Coxeter element c.*

Finally, Propositions 8.35 and 8.36 provide a simple proof of the following statement conjectured in [HLT11] (an alternative proof based on universal associahedra was already mentioned in Section 7.2.3.2). A more general statement, valid for all fairly balanced permutahedra and associahedra, and an orbit refinement of this statement can be found in [PS15b].

Theorem 8.37. *For any Coxeter element c of W, the vertex barycenters of the c-associahedron $\mathbb{A}\mathrm{sso}(c)$ and the permutahedron $\mathbb{P}\mathrm{erm}(W)$ coincide.*

IV

Part Four

NON-KISSING AND NON-CROSSING COMPLEXES

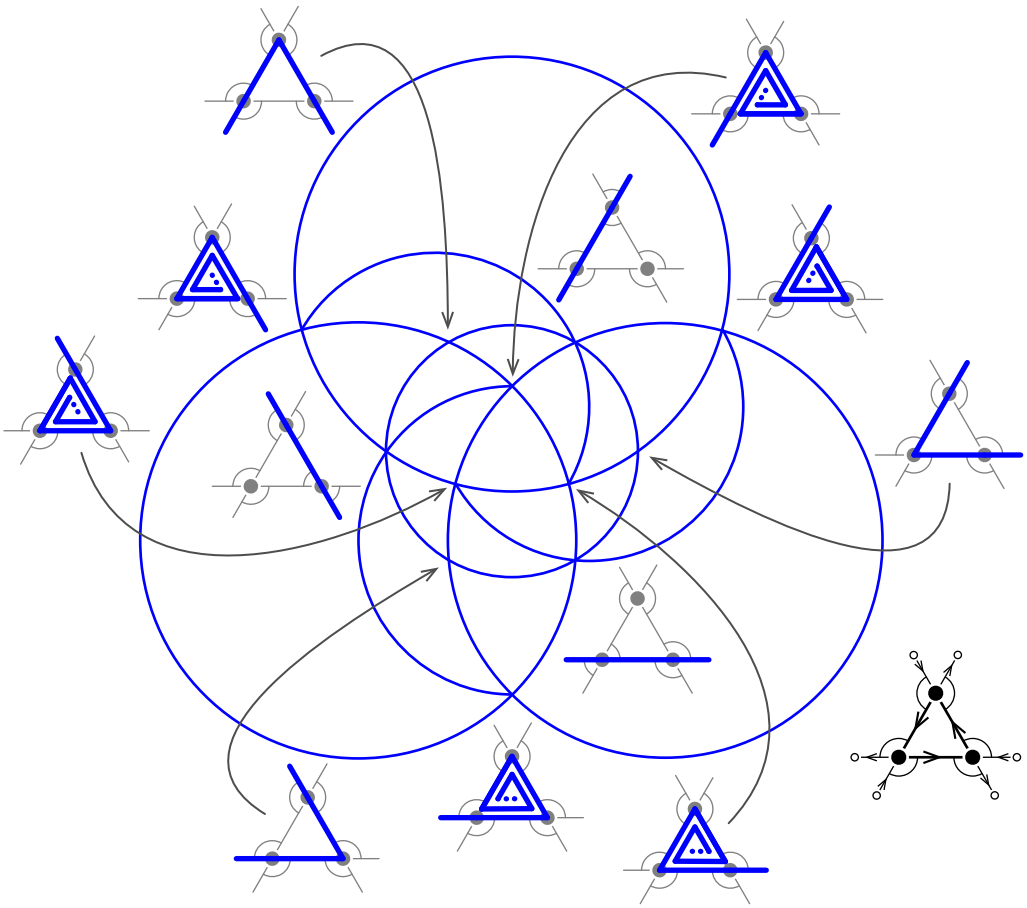

Grid associahedra and accordiohedra. The motivation of this part of the document arises from two recent generalizations of the classical associahedron, illustrated in Figure 8.4:

1. **Grid associahedra.** The non-kissing complex is the simplicial complex of sets of mutually non-kissing paths in a fixed shape of a grid. Introduced by T. K. Petersen, P. Pylyavskyy and D. Speyer in [PPS10] for a staircase shape, and studied by F. Santos, C. Stump and V. Welker [SSW17] for rectangular shapes, it was extended by T. McConville in [McC17] for arbitrary shapes. This complex is known to be a simplicial sphere, and it was actually realized as a polytope using successive edge stellations and suspensions in [McC17, Sect. 4]. Moreover, the dual graph of the non-kissing complex has a natural orientation which equips its facets with a lattice structure [McC17, Thm. 1.1, Sect. 5–8]. Further lattice theoretic and geometric aspects of this complex were developed by A. Garver and T. McConville in [GM17a].
2. **Accordiohedra.** The accordion complex is the simplicial complex of sets of mutually non-crossing accordion diagonals of a fixed dissection of a convex polygon. It was initially defined and studied by Y. Baryshnikov [Bar01] and F. Chapoton [Cha16] when the dissection is a quadrangulation. Later, A. Garver and T. McConville [GM18] defined the complex on the dual tree of the dissection, and showed in particular that the dual graph of the accordion complex is equipped with a lattice structure. More recently, this complex was realized as a polytope in [MP19], using tools inspired from cluster algebras and generalized associahedra.

Note that the classical associahedra of J.-L. Loday [Lod04] and C. Hohlweg and C. Lange [HL07] are instances of both families: they are grid associahedra of ribbons and accordiohedra of triangulations.

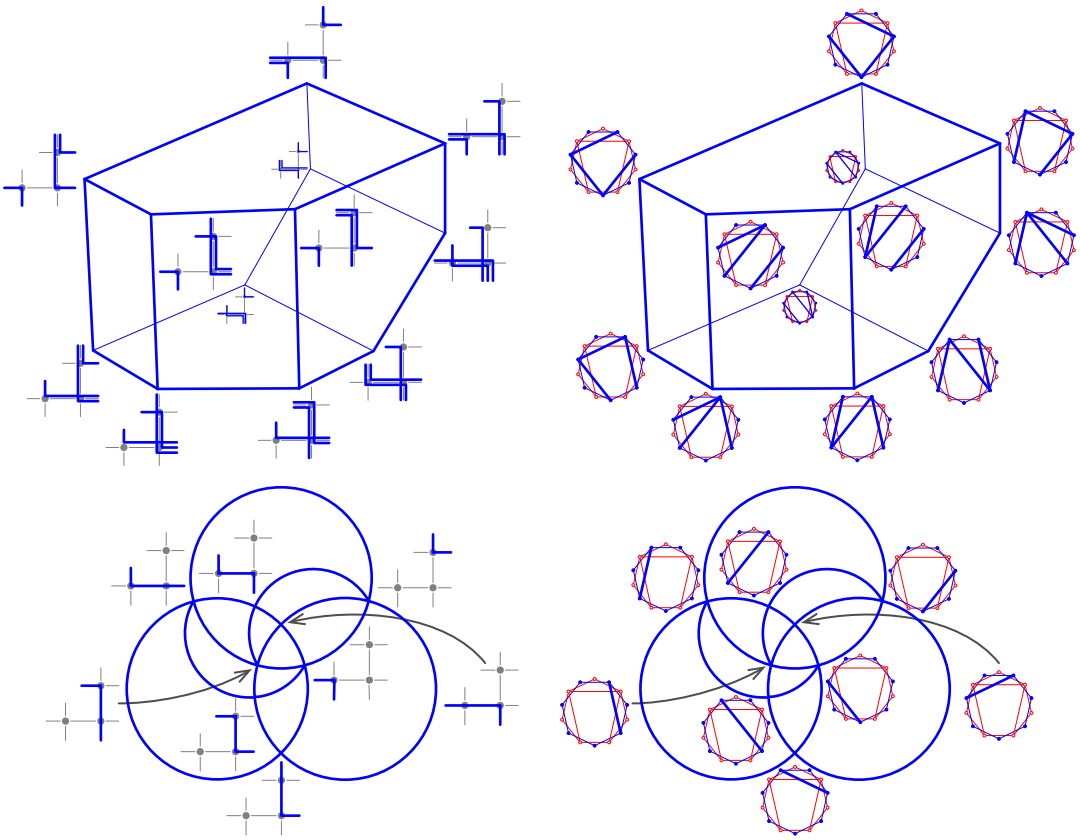

Figure 8.4: A grid associahedron and an accordiohedron (top) and their normal fans (bottom).

Non-kissing versus non-crossing. It was already observed in [PPP17] that non-kissing complexes of grids and accordion complexes of dissections are special cases of a more general simplicial complex, defined for any gentle quiver (see also [BDM+17]).

Reporting on a recent joint work with Y. Palu and P.-G. Plamondon [PPP19], we actually show in Chapter 9 that these two families of simplicial complexes can be unified once we generalize both. On the algebraic side, we consider in Section 9.1 the non-kissing complex of a locally gentle quiver (*i.e.* a quiver with a very strong local condition around each vertex, see Definition 9.1). On the geometric side, we consider in Section 9.2 the non-crossing complex of an arbitrary oriented punctured marked surface with boundary endowed with a pair of dual cellular dissections.

We then present in Section 9.3 an explicit bijection between (isomorphism classes of) locally gentle quivers and (homeomorphism classes of) oriented punctured marked surfaces with boundary endowed with a pair of dual cellular dissections. Namely, from a cellular dissection D on a surface, one gets a locally gentle quiver in the usual way (*i.e.* vertices on the arcs of D, arrows joining consecutive arcs around the cells of D, and relations for triples of consecutive arcs around the cells of D). Conversely, from a locally gentle quiver $\bar{Q}$, we construct a surface equipped with a pair of dual dissections by a simple procedure, starting with lozenges corresponding to the arrows of $\bar{Q}$, and glueing them side by side according to the relations and the non-relations of $\bar{Q}$. Moreover, this bijection sends walks on the quiver to accordions on the surface, kissing walks to crossing accordions, and thus the non-kissing complex of the quiver to the non-crossing complex of the surface.

Support τ-tilting theory. Similar instances of simplicial complexes arise naturally from the representation theory of associative algebras. To each bound quiver $\bar{Q} = (Q, I)$ is associated a path algebra $\boldsymbol{k}Q/I$: its underlying vector space is generated by paths on Q avoiding any relation in I, and the product of two paths p, q is their concatenation when it is a path, and 0 otherwise. The representation theory of these algebras is extremely rich and interesting. In particular, T. Adachi, O. Iyama and I. Reiten introduced in [AIR14] a simplicial complex over certain indecomposable τ-rigid modules, called support τ-tilting complex. For instance, in the case of the path algebra of a quiver which is a straight line, the support τ-tilting complex is an associahedron.

It turns out that the representation theory of gentle algebras is particularly well-understood [BR87]. Using this understanding, we proved in a joint work with Y. Palu and P.-G. Plamondon [PPP17] that the non-kissing complex of any gentle quiver $\bar{Q}$ is isomorphic to the support τ-tilting complex of the corresponding gentle algebra $\boldsymbol{k}Q/I$. In short, to any walk in $\bar{Q}$ corresponds a representation of $\bar{Q}$, and this correspondence takes non-kissing walks to τ-compatible representations.

It turns out that an important part of the material presented in this part of the document extends to support τ-tilting complexes of finite dimensional algebras. For instance, the lattice theory of torsion classes is developed in [DIR+17] and polytopal realizations of τ-tilting finite algebras are constructed in [PPP17].

I have chosen not to present the representation theoretic aspects of this story as it is quite different from the combinatorial and geometric flavor of the rest of this document. Details can be found in [PPP17, Sect. 1].

Non-kissing combinatorics and geometry. In Chapter 10, we present combinatorial and geometric properties of non-kissing complexes (and thus of non-crossing complexes) developed in a joint work with Y. Palu and P.-G. Plamondon [PPP17], extending those of the associahedron studied in the rest of this document.

We first show in Section 10.1 that the non-kissing complex of a locally gentle quiver $\bar{Q}$ is a pseudomanifold: the number of walks in each facet is the number of vertices of $\bar{Q}$, and each walk in a facet can be exchanged with an other walk to get a new facet of the non-kissing complex. The understanding of this flip is based on properties of the combinatorial notions of distinguished walks and distinguished arrows, inspired from the work of T. McConville [McC17] in the grid situation.

The flip graph on non-kissing facets actually comes with a natural orientation. In Section 10.2, we show that this oriented flip graph defines a lattice structure on non-kissing facets. The approach, originally due to T. McConville on grid quivers [McC17], echoes the first part of this document: we interpret the non-kissing lattice as a lattice quotient of a lattice of biclosed sets of strings which plays the role of the weak order.

Finally, we study geometric realizations of finite non-kissing complexes in Section 10.3. We construct the non-kissing fan based on $\boldsymbol{g}$-vectors of walks, and show that this fan is the normal fan of the non-kissing associahedron obtained from a suitable choice of right hand sides based on kissing numbers. In fact, we can prove for a certain class of gentle quivers that the type cone of the non-kissing fan is a simplex, which enables to apply the realization method discussed in Section 7.3. Finally, we observe that all the geometry of the non-kissing associahedron is in fact hidden in well-chosen projections of the classical associahedra, thus opening the question to project further cluster algebra structures, in particular scattering diagrams.

Chapter Nine

9 NON-KISSING VERSUS NON-CROSSING

This chapter, adapted from a joint work with Y. Palu and P.-G. Plamondon [PPP19], introduces two simplicial complexes: the non-kissing complex of a locally gentle quiver (Section 9.1) and the non-crossing complex of an oriented punctured surface with boundary endowed with a pair of dual celullar dissections (Section 9.2). Both complexes appeared earlier in specific cases: the non-kissing complex of a grid appeared in [McC17], while the non-crossing complex of a disk appeared in [GM18, MP19]. This chapter presents an explicit bijection between (isomorphism classes of) locally gentle quivers and (homeomorphism classes of) oriented punctured marked surfaces with boundary endowed with a pair of dual cellular dissections, which sends the non-kissing complex of the quiver to the non-crossing complex of the surface (Section 9.3). Further properties of the non-kissing complexes (and thus of the non-crossing complexes) are developed in Chapter 10.

9.1 NON-KISSING COMPLEX

9.1.1 Locally gentle quivers and their blossoming quivers

We consider a (bound) *quiver* $\bar{Q} := (Q, I)$, formed by a finite quiver $Q := (Q_0, Q_1, s, t)$ and an ideal I of the path algebra $\boldsymbol{k}Q$ (the k-vector space generated by all paths in Q, including vertices as paths of length zero, with multiplication induced by concatenation of paths) such that I is generated by linear combinations of paths of length at least two. Note that we **do not require** that the quotient algebra $\boldsymbol{k}Q/I$ be finite dimensional. The following definition is adapted from [BR87]. See Figure 9.1.

Definition 9.1 ([BR87])**.** *A locally gentle quiver $\bar{Q} := (Q, I)$ is a (finite) quiver where:*

(i) each vertex $a \in Q_0$ has at most two incoming and two outgoing arrows,
(ii) the ideal I is generated by paths of length exactly two,
(iii) for any arrow $\beta \in Q_1$, there is at most one arrow $\alpha \in Q_1$ such that $t(\alpha) = s(\beta)$ and $\alpha\beta \notin I$ (resp. $\alpha\beta \in I$) and at most one arrow $\gamma \in Q_1$ such that $t(\beta) = s(\gamma)$ and $\beta\gamma \notin I$ (resp. $\beta\gamma \in I$).

The algebra $\boldsymbol{k}Q/I$ is called a locally gentle algebra. A gentle quiver is a locally gentle quiver $\bar{Q}$ such that the algebra $\boldsymbol{k}Q/I$ is finite-dimensional, then called gentle algebra.

Definition 9.2. *A locally gentle quiver $\bar{Q}$ is complete if any vertex $a \in Q_0$ is incident to either one (a is a leaf) or four arrows (a is an internal vertex). The pruned subquiver of a quiver $\bar{Q}$ is the locally gentle quiver obtained by deleting all leaves of $\bar{Q}$ (degree one vertices) and their incident arrows. The blossoming quiver of a locally gentle quiver $\bar{Q}$ is the complete locally gentle quiver $\bar{Q}^{\text{❀}}$ whose pruned subquiver is $\bar{Q}$. The vertices of $Q_0^{\text{❀}} \smallsetminus Q_0$ are called blossom vertices, and the arrows in $Q_1^{\text{❀}} \smallsetminus Q_1$ are called blossom arrows. See Figure 9.1*

Remark 9.3. Note that $\bar{Q}^{\text{❀}}$ has $2|Q_0| - |Q_1|$ incoming blossom arrows and $2|Q_0| - |Q_1|$ outgoing blossom arrows. Therefore, it has $|Q_0^{\text{❀}}| = |Q_0| + 2(2|Q_0| - |Q_1|) = 5|Q_0| - 2|Q_1|$ vertices and $|Q_1^{\text{❀}}| = |Q_1| + 2(2|Q_0| - |Q_1|) = 4|Q_0| - |Q_1|$ arrows.

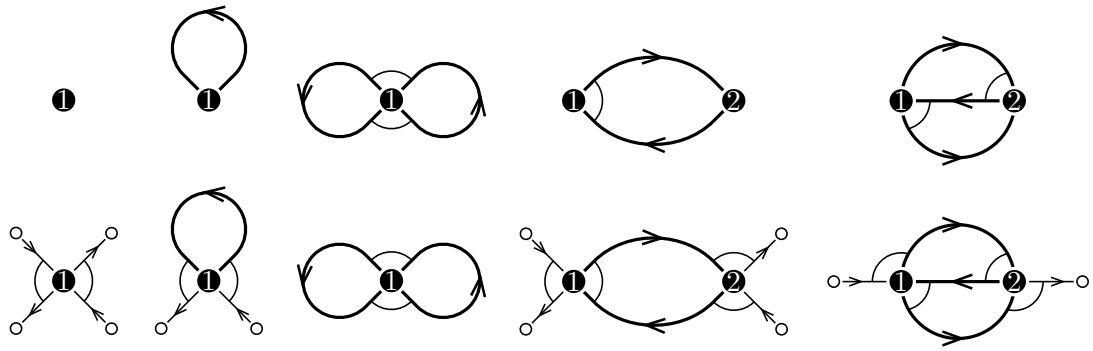

Figure 9.1: Some locally gentle quivers (top) and their blossoming quivers (bottom). Initial vertices are solid while blossom vertices are hollow, and initial arrows are bold while blossom arrows are thin.

9.1.2 Strings and walks

The non-kissing complex is constructed using the combinatorics of strings and walks in the quiver $\bar{Q}$, whose definitions are now briefly recalled. The terminology and notations in the following definitions are borrowed from [BR87, CB18].

For any arrow α of Q, define a formal inverse α^{-1} with the properties that $s(\alpha^{-1}) = t(\alpha)$, $t(\alpha^{-1}) = s(\alpha)$, $\alpha^{-1}\alpha = \varepsilon_{t(\alpha)}$ and $\alpha\alpha^{-1} = \varepsilon_{s(\alpha)}$, where ε_v is the path of length zero starting and ending at the vertex $v \in Q_0$.

Definition 9.4. *Let $\bar{Q} := (Q, I)$ be a locally gentle quiver. A finite string in $\bar{Q}$ is a word of the form $\rho = \alpha_1^{\varepsilon_1}\alpha_2^{\varepsilon_2}\cdots\alpha_\ell^{\varepsilon_\ell}$, where:*
(i) $\alpha_i \in Q_1$ and $\varepsilon_i \in \{-1, 1\}$ for all $i \in [\ell]$,
(ii) $t(\alpha_i^{\varepsilon_i}) = s(\alpha_{i+1}^{\varepsilon_{i+1}})$ for all $i \in [\ell - 1]$,
(iii) there is no path $\pi \in I$ such that π or π^{-1} appears as a factor of ρ, and
(iv) ρ is reduced, in the sense that no factor $\alpha\alpha^{-1}$ or $\alpha^{-1}\alpha$ appears in ρ, for $\alpha \in Q_1$.
The integer ℓ is called the length of the string ρ. We let $s(\rho) := s(\alpha_1^{\varepsilon_1})$ and $t(\rho) := t(\alpha_\ell^{\varepsilon_\ell})$ denote the source and target of ρ. For each vertex $a \in Q_0$, there is also a string of length zero, denoted by ε_a, that starts and ends at a.

Definition 9.5. *An oriented cycle c in Q such that $c, c^2 \notin I$ is called primitive if it cannot be written as an n-th power ($n > 1$) of a cycle.*

If c is an oriented cycle in Q such that $c, c^2 \notin I$, we write c^∞ for the infinite word $ccc\cdots$, and ${}^\infty c$ for the infinite word $\cdots ccc$, and ${}^\infty c^\infty$ for the bi-infinite word ${}^\infty cc^\infty$. We let ${}^{-\infty}c := {}^\infty(c^{-1}) = (c^\infty)^{-1}$ and $c^{-\infty} := (c^{-1})^\infty = ({}^\infty c)^{-1}$.

Definition 9.6. *An eventually cyclic string for $\bar{Q}$ is a word ρ of the form ${}^\infty(c_1^{\varepsilon_1})\sigma(c_2^{\varepsilon_2})^\infty$, where c_1, c_2 are oriented cycles in $\bar{Q}$ (with at most one of them of length zero) and $\varepsilon_1, \varepsilon_2$ are signs in $\{\pm 1\}$ such that $c_1^{2\varepsilon_1}\sigma c_2^{2\varepsilon_2}$ is a finite string in $\bar{Q}$.*

Definition 9.7. *A string for $\bar{Q}$ is a word which is either a finite string or an eventually cyclic infinite string. We often implicitly identify the two inverse strings ρ and ρ^{-1}, and call it an undirected string.*

To avoid distinguishing between finite and (bi-)infinite words, we denote strings as products $\rho = \prod_{i<\ell<j} \alpha_\ell^{\varepsilon_\ell}$ where $i < j \in \mathbb{Z} \cup \{\pm\infty\}$, $\varepsilon_\ell \in \{\pm 1\}$ and $\alpha_\ell \in Q_1$ for all $i < \ell < j$.

Definition 9.8. *A walk of a locally gentle quiver $\bar{Q}$ is a maximal string of its blossoming quiver $\bar{Q}^{\text{❀}}$ (meaning that at each end it either reaches a blossom vertex of $\bar{Q}^{\text{❀}}$ or enters an infinite oriented cycle). As for strings, we implicitly identify the two inverse walks ω and ω^{-1}, and call it an undirected walk.*

Definition 9.9. *A substring of a walk $\omega = \prod_{i<\ell<j} \alpha_\ell^{\varepsilon_\ell}$ of $\bar{Q}$ is a string $\sigma = \prod_{i'<\ell<j'} \alpha_\ell^{\varepsilon_\ell}$ of $\bar{Q}$ for some $i \leq i' < j' \leq j$, where the inequality $i \leq i'$ (resp. $j' \leq j$) is strict when $i \neq -\infty$ (resp. $j \neq \infty$). In other words, σ is a factor of ω such that*

- *the endpoints of σ are not allowed to be the possible blossom endpoints of ω,*
- *the position of σ as a factor of ω matters (the same string at a different position is considered a different substring).*

Note that the string ε_a is a substring of ω for each occurence of a as a vertex of ω. We denote by $\Sigma(\omega)$ the set of substrings of ω. We use the same notation for undirected walks.

Definition 9.10. *We say that the substring $\sigma = \prod_{i'<\ell<j'} \alpha_\ell^{\varepsilon_\ell}$ is at the bottom (resp. on top) of the walk $\omega = \prod_{i<\ell<j} \alpha_\ell^{\varepsilon_\ell}$ if $i' = -\infty$ or $\varepsilon_{i'} = 1$, and $j' = +\infty$ or $\varepsilon_{j'} = -1$ (resp. if $i' = -\infty$ or $\varepsilon_{i'} = -1$, and $j' = \infty$ or $\varepsilon_{j'} = 1$). In other words the (at most) two arrows of ω incident to the endpoints of σ point towards σ (resp. outwards from σ). We denote by $\Sigma_{\text{bot}}(\omega)$ and $\Sigma_{\text{top}}(\omega)$ the sets of bottom and top substrings of ω respectively. We use the same notations for undirected walks.*

Definition 9.11. *A peak (resp. deep) of a walk ω is a substring of ω of length zero which is on top (resp. at the bottom of ω). A corner is either a peak or a deep (in other words, it is a vertex of ω where the arrows change direction). A walk ω is straight if it has no corner (i.e. if ω or ω^{-1} is a path in $\bar{Q}^{\text{❀}}$), and bending otherwise. A peak walk (resp. deep walk) is a walk with a unique corner (in other words, it switches orientation only once), which is a peak (resp. deep). For $a \in Q_0$, we denote by a_{peak} the peak walk with peak at a and by a_{deep} the deep walk with deep at a (note that those are indeed unique by local gentleness of $\bar{Q}$).*

9.1.3 Non-kissing complex

We can now define the non-kissing complex of a locally gentle quiver following [McC17, PPP17, BDM+17]. We start with the kissing relation for walks.

Definition 9.12. *Let ω and ω' be two undirected walks on $\bar{Q}$. We say that ω kisses ω' if $\Sigma_{\text{top}}(\omega) \cap \Sigma_{\text{bot}}(\omega')$ contains a* finite *substring. In other words, there exist a finite common substring σ of ω and ω' such that the arrows of ω incident to σ are both outgoing while the arrows of ω' incident to σ are both incoming. We say that ω and ω' are kissing if ω kisses ω' or the opposite (or both).*

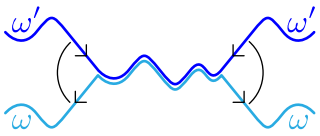

Note that we authorize the situation where the common finite substring is reduced to a vertex a, meaning that a is a peak of ω and a deep of ω'. Observe also that ω can kiss ω' several times, that ω and ω' can mutually kiss, and that ω can kiss itself.

Definition 9.13. *The non-kissing complex of $\bar{Q}$ is the simplicial complex $\mathcal{K}_{\text{nk}}(\bar{Q})$ whose faces are the collections of pairwise non-kissing walks of $\bar{Q}$. Note that self-kissing walks never appear in $\mathcal{K}_{\text{nk}}(\bar{Q})$ by definition. In contrast, no straight walk can kiss another walk by definition, so that they appear in all facets of $\mathcal{K}_{\text{nk}}(\bar{Q})$. The reduced non-kissing complex $\mathcal{C}_{\text{nk}}(\bar{Q})$ is the simplicial complex whose faces are the collections of pairwise non-kissing bending walks of $\bar{Q}$.*

9.2 ACCORDION COMPLEX, SLALOM COMPLEX, AND NON-CROSSING COMPLEX

We now temporarily switch topic and present the accordion complex and the slalom complex of a pair of dual dissections of an orientable surface. The latter is directly inspired from the case of a disk treated in [GM18], while the former is obtained by duality as was already observed in the case of a disk in [MP19]. In the general case of arbitrary orientable surfaces, the correspondence between accordions and slaloms requires a little more attention and is treated in Section 9.2.3.

9.2.1 Dual dissections of a surface

Before defining accordions and slaloms, we need a strong notion of pairs of dual dissections of an orientable surface. We first review classical definitions of curves, arcs and dissections of a surface adapting it to our setting.

Definition 9.14. *A marked surface $\bar{\mathcal{S}} := (\mathcal{S}, M)$ is an orientable surface $\mathcal{S}$ with boundaries, together with a set M of marked points which can be on the boundary of $\mathcal{S}$ or not. For $V \subset \mathcal{S}$,*

(i) a V-arc on $\bar{\mathcal{S}}$ is a curve on $\mathcal{S}$ connecting two points of V and whose interior is disjoint from M and the boundary of $\mathcal{S}$.

(ii) a V-curve on $\bar{\mathcal{S}}$ is a curve on $\mathcal{S}$ which at each end either reaches a point of V or infinitely circles around and finally reaches a puncture of M, and whose interior is disjoint from M and the boundary of $\mathcal{S}$.

As usual, curves and arcs are considered up to homotopy relative to their endpoints in $\mathcal{S} \setminus M$, and curves homotopic to a boundary are not allowed.

Definition 9.15. *Two curves or arcs cross when they intersect in their interior. We will always assume that collections of arcs on a surface are in minimal position, in the sense that they cross each other transversaly, and the number of crossings is minimal.*

Definition 9.16. *A dissection of $\bar{\mathcal{S}}$ is a collection D of pairwise non-crossing arcs on $\bar{\mathcal{S}}$. The edges of D are its arcs together with the boundary arcs of $\bar{\mathcal{S}}$. The faces of D are the connected components of the complement of the union of the edges of D in the surface $\mathcal{S}$. We denote by $\mathcal{V}(D)$, $\mathcal{E}(D)$ and $\mathcal{F}(D)$ the sets of vertices, edges and faces of D respectively. The dissection D is cellular if all its faces are topological disks. For $V \subseteq M$, a V-dissection is a dissection with only V-arcs.*

All throughout the chapter, all dissections are considered cellular.

Definition 9.17. *Consider a marked surface $\bar{\mathcal{S}} := (\mathcal{S}, V \sqcup V^\star)$, where V and $V^\star$ are two disjoint sets of marked points so that the points of V and $V^\star$ that are on the boundary of $\mathcal{S}$ alternate. A cellular V-dissection D of $\bar{\mathcal{S}}$ and a cellular $V^\star$-dissection $D^\star$ of $\bar{\mathcal{S}}$ are dual cellular dissections if there are bijections $V^\star \leftrightarrow \mathcal{F}(D)$, $V \leftrightarrow \mathcal{F}(D^\star)$, and $\mathcal{E}(D) \leftrightarrow \mathcal{E}(D^\star)$, all denoted by * in both directions, such that*

1. *for each vertex $v \in V$, the closure of the face $v^\star$ of $D^\star$ contains v;*
2. *for each vertex $w \in V^\star$, the closure of the face $w^\star$ of D contains w;*
3. *for each edge $e \in \mathcal{E}(D)$, the edges e and $e^\star$ intersect exactly once in their interior; moreover, e intersects (in their interior) no other edge of $D^\star$, and $e^\star$ intersects (in their interior) no other edge of D.*

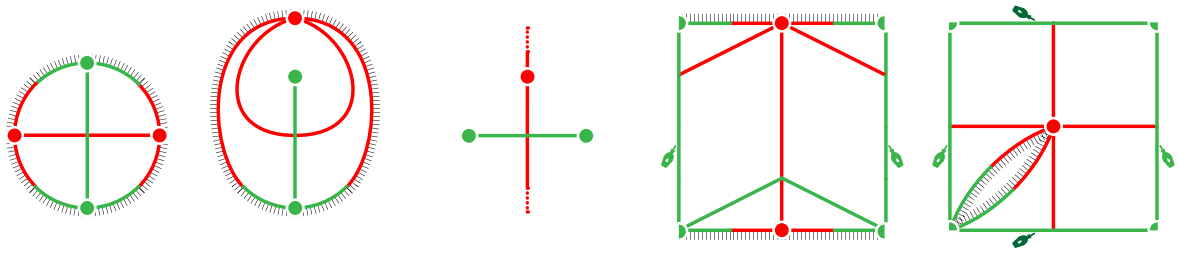

Figure 9.2: Some pairs $(D, D^\star)$ of dual cellular dissections on different surfaces. The dissection D is in green while its dual dissection $D^\star$ is in red. The boundaries of the surfaces are shaded, and the glue symbols indicate how to identify some edges to get the desired surfaces. The first two surfaces are disks, the third is a sphere without boundary, the fourth is a cylinder, and the fifth is a torus with one boundary component.

Some examples of dual cellular dissections on different surfaces are represented in Figure 9.2. Note that contrarily to the usual conventions, the dual vertex $f^\star$ of a face f of D is not always in the interior of the face f. More precisely, each face f has either no or exactly one edge on the boundary of $\mathcal{S}$. Its dual vertex $f^\star$ then lies in the interior of f and is a puncture of $\bar{\mathcal{S}}$ in the former case, and on the boundary edge of f in the latter case. In fact, this forces the following characterization of the cellular dissections that admit a dual cellular dissection.

Proposition 9.18. *The following assertions are equivalent for a cellular V-dissection D of a marked surface $\bar{\mathcal{S}} := (\mathcal{S}, V \sqcup V^\star)$ such that the points of V and $V^\star$ along the boundary of $\mathcal{S}$ alternate:*
(i) there exists a cellular $V^\star$-dissection $D^\star$ of $\bar{\mathcal{S}}$ such that D and $D^\star$ are dual cellular dissections,
(ii) each face of D contains exactly one point of $V^\star$ (in particular, at most one boundary edge).
Moreover, the cellular dissection $D^\star$ is uniquely determined.

Definition 9.19. *We consider a set B of points on the boundary of the surface $\mathcal{S}$ such that B and $V \cup V^\star$ alternate along the boundary of $\mathcal{S}$. The points of B are called the* blossom points*. See e.g. Figures 9.3 and 9.4 where the blossom points appear as white hollow vertices.*

9.2.2 Accordion complex and slalom complex

Let $\bar{\mathcal{S}} := (\mathcal{S}, V \sqcup V^\star)$ be a surface with two disjoint sets V and $V^\star$ of marked points, and let B be the corresponding blossom points on the boundary of $\mathcal{S}$. We say that a B-curve is *external* if it is homotopic to a boundary arc of $\mathcal{S} \setminus B$, and *internal* otherwise. Note that no B-curve can cross an external B-curve. Consider two dual cellular dissections D and $D^\star$ of $\bar{\mathcal{S}}$.

The following definition generalises the one of [MP19] for the case where $\bar{\mathcal{S}}$ is a disk. A very similar definition appears in [BCSo18] in a slightly different context under the name "permissible arc".

Definition 9.20. *A D-accordion is a B-curve α of $\bar{\mathcal{S}}$ such that whenever α meets a face f of D,*
(i) it enters crossing an edge a of f and leaves crossing an edge b of f (in other words, α is not allowed to circle around $f^\star$ when $f^\star$ is a puncture),
(ii) the two edges a and b of f crossed by α are consecutive along the boundary of f,
(iii) α, a and b bound a disk inside f that does not contain $f^\star$.
By convention, we also consider that the punctures of V are D-accordions that are considered external. If we were working on the universal cover of the surface, the D-accordion associated to a puncture would be the infinite line crossing all (infinitely many) arcs attached to the puncture.

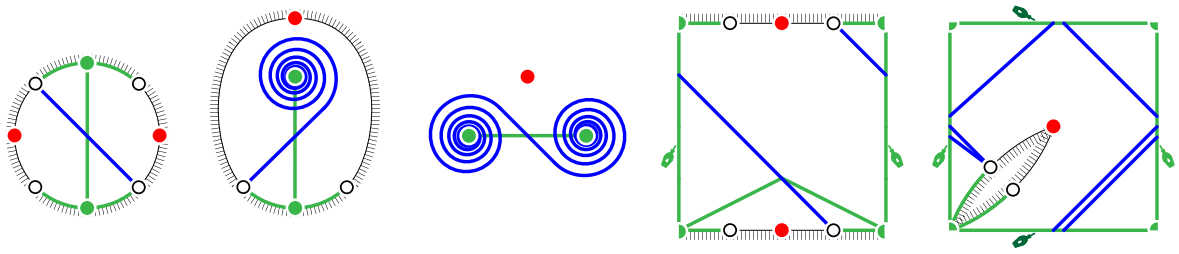

Figure 9.3: Some D-accordions (in blue) for the dissections D of Figure 9.2 (in green).

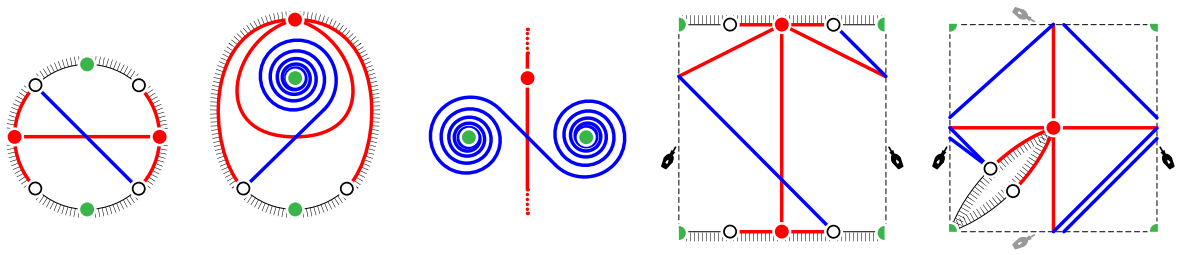

Figure 9.4: Some $D^\star$-slaloms (in blue) for the dual dissections $D^\star$ of Figure 9.2 (in red).

Figure 9.3 illustrates some D-accordions for the dissections D of Figure 9.2.

Remark 9.21. In Definition 9.20, observe that:

- the edges of a and b of f crossed by α might coincide, see the second example in Figure 9.3.
- the first condition is automatically satisfied if $f^\star$ is not a puncture, *i.e.* when it lies on the boundary of $\mathcal{S}$.

Definition 9.22. *The D-accordion complex $\mathcal{K}_{\mathrm{acc}}(D)$ is the simplicial complex whose faces are the collections of pairwise non-crossing D-accordions. Note that self-crossing accordions never appear in $\mathcal{K}_{\mathrm{acc}}(D)$ by definition. In contrast, no external accordion can cross another accordion, so that they appear in all facets of $\mathcal{K}_{\mathrm{acc}}(D)$. The reduced D-accordion complex $\mathcal{C}_{\mathrm{acc}}(D)$ is the simplicial complex whose faces are the collections of pairwise non-crossing internal D-accordions.*

The following definition generalizes the one from [GM18] for the case where $\bar{\mathcal{S}}$ is a disk.

Definition 9.23. *A $D^\star$-slalom is a B-curve α of $\bar{\mathcal{S}}$ such that, whenever α crosses an edge $a^\star$ of $D^\star$ contained in two faces $f^\star, g^\star$ of $D^\star$, the marked points f and g lie on opposite sides of α in the union of $f^\star$ and $g^\star$ glued along $a^\star$. Here, we consider that f lies on the right (resp. left) of α when α circles clockwise (resp. counterclockwise) around f. By convention, we also consider that the punctures of V are $D^\star$-slaloms that are considered external. If we were working on the universal cover of the surface, the $D^\star$-slalom associated to a puncture would be an infinite line never crossing any arc of $D^\star$.*

Figure 9.4 illustrates some $D^\star$-slaloms for the dual dissections $D^\star$ of Figure 9.2.

Definition 9.24. *The $D^\star$-slalom complex $\mathcal{K}_{\mathrm{sla}}(D^\star)$ is the simplicial complex whose faces are the collections of pairwise non-crossing $D^\star$-slaloms. Note that self-crossing slaloms never appear in $\mathcal{K}_{\mathrm{sla}}(D^\star)$ by definition. In contrast, no external slalom can cross another slalom, so that they appear in all facets of $\mathcal{K}_{\mathrm{sla}}(D^\star)$. The reduced $D^\star$-slalom complex $\mathcal{C}_{\mathrm{sla}}(D^\star)$ is the simplicial complex whose faces are the collections of pairwise non-crossing internal $D^\star$-slaloms.*

9.2.3 Accordions versus slaloms and the non-crossing complex

The following statement is illustrated by Figures 9.3 and 9.4.

Proposition 9.25. *For two dual cellular dissections D and $D^\star$, the D-accordions are precisely the $D^\star$-slaloms and the (reduced) D-accordion complex coincides with the (reduced) $D^\star$-slalom complex.*

Definition 9.26. *We call* non-crossing complex *of the pair of dual cellular dissections $(D, D^\star)$ the simplicial complex $\mathcal{K}_{\mathrm{nc}}(D, D^\star) := \mathcal{K}_{\mathrm{acc}}(D) = \mathcal{K}_{\mathrm{sla}}(D^\star)$. Similarly, the* reduced non-crossing complex *of $(D, D^\star)$ is $\mathcal{C}_{\mathrm{nc}}(D, D^\star) := \mathcal{C}_{\mathrm{acc}}(D) = \mathcal{C}_{\mathrm{sla}}(D^\star)$.*

Remark 9.27. The D-slaloms and the $D^\star$-accordions are defined dually and also coincide.

Example 9.28. When the dissection D is a classical dissection of a polygon (with no punctures) where each cell has at most one boundary edge, the dual dissection $D^\star$ is a tree. The non-crossing complex in this situation was treated in detail in [GM18, MP19]. Note that even when the surface $\mathcal{S}$ is a disk, we authorize in the present chapter both D and $D^\star$ to have interior faces and punctures.

Remark 9.29. A quick disclaimer about accordion complexes and slalom complexes of arbitrary cellular dissections. As stated in Proposition 9.18, a cellular dissection D with a face containing more than one boundary edge does not admit a dual cellular dissection $D^\star$. This prevents the use of the definitions given in this section. Although the accordion complex (resp. slalom complex) could still be defined as in [MP19] (resp. [GM18]) for the disk, the resulting complexes would be joins of smaller accordion complexes (resp. slalom complexes) defined in this chapter. See [MP19, Prop. 2.4] for a detailed statement in the case of the disk.

9.3 Non-kissing versus non-crossing

In this section, we show that non-kissing and non-crossing complexes actually coincide. Namely, any pair of dual cellular dissections $(D, D^\star)$ defines a locally gentle quiver $\bar{Q}_D$ (see Section 9.3.1) such that the non-crossing complex $\mathcal{K}_{\mathrm{nc}}(D, D^\star)$ is isomorphic to the non-kissing complex $\mathcal{K}_{\mathrm{nk}}(\bar{Q}_D)$. Conversely, any locally gentle quiver $\bar{Q}$ gives rise to a surface $\mathcal{S}_{\bar{Q}}$ equipped with a pair of dual cellular dissections $D_{\bar{Q}}$ and $D^\star_{\bar{Q}}$ (see Section 9.3.2) such that the non-kissing complex $\mathcal{K}_{\mathrm{nk}}(\bar{Q})$ is isomorphic to the non-crossing complex $\mathcal{K}_{\mathrm{nc}}(D_{\bar{Q}}, D^\star_{\bar{Q}})$.

9.3.1 The quiver of a dissection

Let D and $D^\star$ be two dual cellular dissections of a marked surface $\bar{\mathcal{S}} := (\mathcal{S}, V \sqcup V^\star)$.

Definition 9.30. *The quiver $\bar{Q}_D = (Q_D, I_D)$ of the dissection D is defined as follows:*

(i) the set of vertices of Q_D is the set of edges of D,

(ii) there is an arrow from a to b for each common endpoint v of a and b such that b comes immediately after a in the counterclockwise order around v,

(iii) the ideal I_D is generated by the paths of length two in Q_D obtained by composing arrows which correspond to triples of consecutive edges in a face of D.

The quiver of the dissection $D^\star$ is the quiver $\bar{Q}_{D^\star} = (Q_{D^\star}, I_{D^\star})$ defined by replacing D by $D^\star$ in the above.

Figure 9.5 illustrates this construction for the dissections of Figure 9.2.

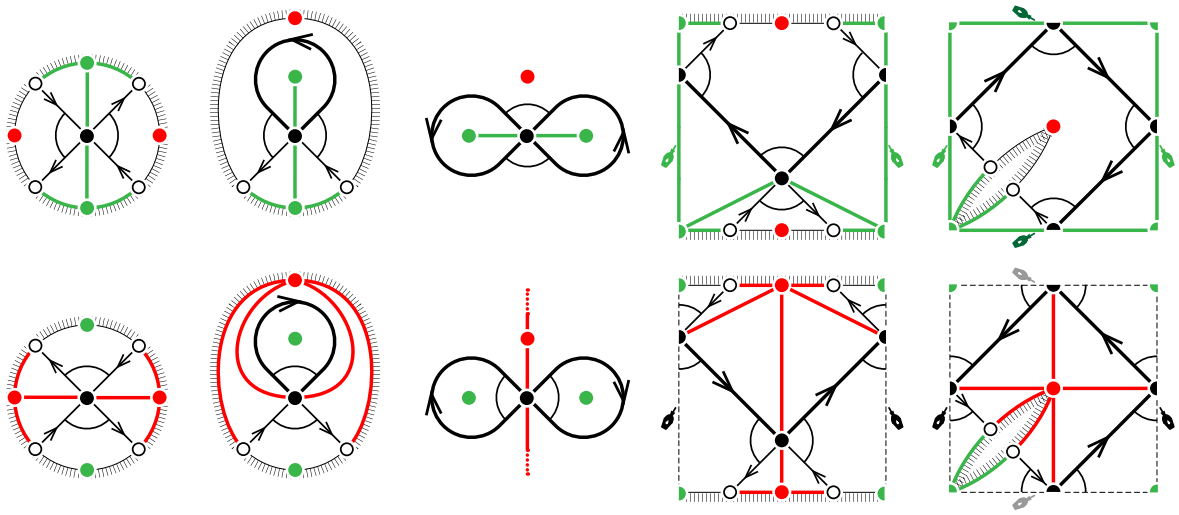

Figure 9.5: The quivers associated to the dissections of Figure 9.2. As stated in Proposition 9.34, dual dissections give rise to Koszul dual quivers.

Remark 9.31. The blossoming quiver $\bar{Q}_D^{\text{❀}}$ of the quiver $\bar{Q}_D$ is obtained with the same procedure by considering additional blossom vertices along the boundary of the surface. See Figure 9.5.

Lemma 9.32. *The quiver $\bar{Q}_D = (Q_D, I_D)$ is a locally gentle quiver.*

Definition 9.33. *The Koszul dual of a locally gentle quiver $\bar{Q} := (Q, I)$ is the quiver $\bar{Q}^! := (Q^!, I^!)$ defined as follows:*

(i) the quiver $Q^!$ is equal to the opposite quiver of Q, that is, the quiver obtained from Q by reversing all arrows,

(ii) the ideal $I^!$ is generated by the opposites of the paths of length two in Q that do not appear in I.

It is seen in [BH08] that the Koszul dual of a locally gentle algebra $\boldsymbol{k}Q/I$ is isomorphic to $\boldsymbol{k}Q^!/I^!$. Note that $\bar{Q}^!$ is locally gentle, and that Koszul duality is an involution and commutes with blossoming: $(\bar{Q}^!)^! = \bar{Q}$ and $(\bar{Q}^!)^{\text{❀}} = (\bar{Q}^{\text{❀}})^!$. Examples are represented on Figure 9.6.

The following proposition appears in [OPS18, Prop. 1.25].

Proposition 9.34. *Let D and $D^\star$ be two dual cellular dissections of a marked surface $(\mathcal{S}, V \sqcup V^\star)$. The quivers $\bar{Q}_D$ and $\bar{Q}_{D^\star}$ are Koszul dual to each other.*

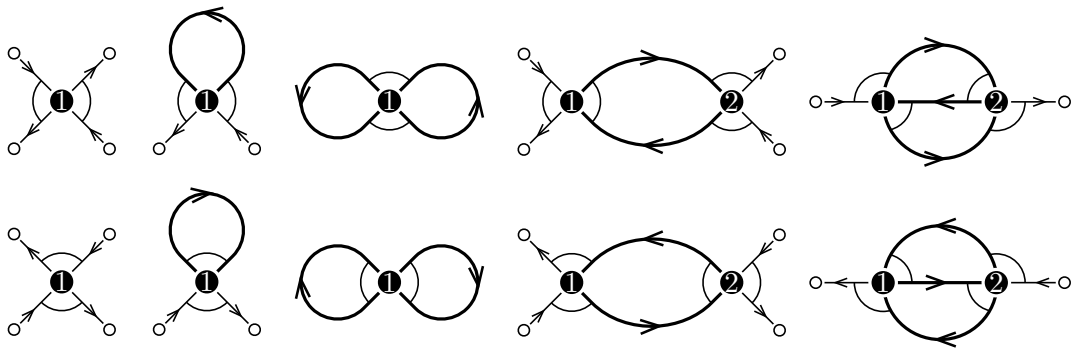

Figure 9.6: The Koszul duals (bottom) of the blossoming quivers (top) of Figure 9.1.

9.3.2 The surface of a locally gentle quiver

We now associate a surface to a locally gentle quiver. This construction yields the same surface as the one constructed in [OPS18] (see Remark 9.41 for a comparison of the two constructions).

Definition 9.35. *The surface $\mathcal{S}_{\bar{Q}}$ of a locally gentle quiver $\bar{Q} := (Q, I)$ is the surface obtained from the blossoming quiver $\bar{Q}^{\bullet}$ as follows:*

(i) for each arrow $\alpha \in Q_1^{\bullet}$, consider a lozenge $L(\alpha)$ with sides

$$E^s_{nr}(\alpha) = [v(\alpha), s(\alpha)] \quad E^t_{nr}(\alpha) = [v(\alpha), t(\alpha)] \quad \textit{(green)}$$
$$E^s_{r}(\alpha) = [f^\star(\alpha), s(\alpha)] \quad E^t_{r}(\alpha) = [f^\star(\alpha), t(\alpha)] \quad \textit{(red)}$$

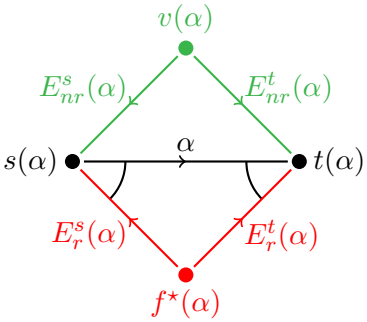

(ii) for any $\alpha, \beta \in Q_1^{\bullet}$ with $t(\alpha) = s(\beta)$, identify:
- *$E^t_r(\alpha)$ with $E^s_r(\beta)$ if $\alpha\beta \in I$,*
- *$E^t_{nr}(\alpha)$ with $E^s_{nr}(\beta)$ if $\alpha\beta \notin I$.*

Figure 9.7 illustrates this construction for the quivers of Figure 9.1. Definition 9.35 constructs an orientable surface $\mathcal{S}_{\bar{Q}}$ with boundaries, endowed with two disjoint sets $V_{\bar{Q}}$ and $V^\star_{\bar{Q}}$ of marked points and two dual cellular dissections $D_{\bar{Q}}$ and $D^\star_{\bar{Q}}$ defined as follows.

Definition 9.36. *The surface $\mathcal{S}_{\bar{Q}}$ is endowed with:*
- *the set $V_{\bar{Q}}$ of points $v(\alpha)$ for $\alpha \in Q_1^{\bullet}$ after the identifications given by (ii),*
- *the $V_{\bar{Q}}$-dissection $D_{\bar{Q}}$ given by all sides $E^s_{nr}(\alpha)$ and $E^t_{nr}(\alpha)$ for $\alpha \in Q_1^{\bullet}$ after the identifications given by (ii).*

The set $V^\star_{\bar{Q}}$ and the $V^\star_{\bar{Q}}$-dissection $D^\star_{\bar{Q}}$ are defined similarly by using $f^\star(\alpha)$, $E^s_r(\alpha)$ and $E^t_r(\alpha)$.

Proposition 9.37. *Let $\bar{Q}$ be a locally gentle quiver. Then the dissections $D_{\bar{Q}}$ and $D^\star_{\bar{Q}}$ are cellular and dual to each other.*

The following statement immediately follows from the definitions and was probably already observed by the reader on Figure 9.7.

Theorem 9.38. *Up to isomorphism, the constructions of Definitions 9.30 and 9.35 are inverse to each other. They induce a bijection between the set of isomorphism classes of locally gentle quivers and the set of homeomorphism classes of marked surfaces with a pair of dual cellular dissections.*

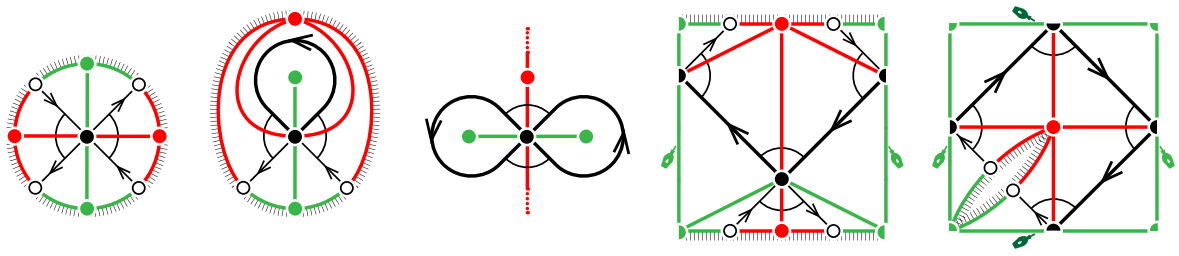

Figure 9.7: The surfaces $\mathcal{S}_{\bar{Q}}$ for the quivers $\bar{Q}$ of Figure 9.1.

Remark 9.39. The following observations are useful for the computation of examples.

(i) The set $V_{\bar{Q}}$ has one vertex for each straight walk in $\bar{Q}$ (equivalently, for each maximal path in $\bar{Q}$). Finite straight walks yield vertices on the boundary of $\mathcal{S}_{\bar{Q}}$, while infinite cyclic straight walks in $\bar{Q}$ yield punctures of $\mathcal{S}_{\bar{Q}}$ in $V_{\bar{Q}}$. We denote by p the number of infinite cyclic straight walks in $\bar{Q}$.

(ii) The dissection $D_{\bar{Q}}$ has one edge for each vertex $a \in \bar{Q}_0$, obtained by concatenation of the sides $E^t_{nr}(\alpha) = E^s_{nr}(\beta)$ and $E^t_{nr}(\alpha') = E^s_{nr}(\beta')$ where $a = t(\alpha) = s(\beta) = t(\alpha') = s(\beta')$, $\alpha\beta \notin I$ and $\alpha'\beta' \notin I$. We denote by $\varepsilon(a)$ the edge of $D_{\bar{Q}}$ corresponding to a.

(iii) The dissection $D_{\bar{Q}}$ has one ℓ-cell for each straight walk of length ℓ in $\bar{Q}^!$.

(iv) Similar statements hold dually for $V^\star_{\bar{Q}}$ and $D^\star_{\bar{Q}}$, and we define $p^\star$ and $\varepsilon^\star(a)$ similarly.

(v) The number of punctures of $\mathcal{S}_{\bar{Q}}$ is the number $p + p^\star$ of infinite straight walks in $\bar{Q}$ and $\bar{Q}^!$.

(vi) The number b of boundary components of $\mathcal{S}_{\bar{Q}}$ can be computed as follows. There are two natural perfect matchings whose vertices are the blossom vertices of $\bar{Q}$: one is obtained by joining the endpoints of each finite straight walk of $\bar{Q}$, and the other is obtained similarly from $\bar{Q}^!$. Let G be the superposition of these two perfect matchings. Then the number b of boundary components of $\mathcal{S}_{\bar{Q}}$ is the number of connected components of G.

(vii) The genus of the surface $\mathcal{S}_{\bar{Q}}$ is $g = (|Q_1| - |Q_0| - b - p - p^\star + 2)/2$, where b is the number of boundary components (see above for a way to compute b) and $p + p^\star$ the number of punctures (*i.e.* infinite straight walks in $\bar{Q}$ and in $\bar{Q}^!$).

Proposition 9.40. *For any gentle quiver $\bar{Q}$ with Koszul dual $\bar{Q}^!$, the surfaces $\mathcal{S}_{\bar{Q}}$ and $\mathcal{S}_{\bar{Q}^!}$ coincide, but $D_{\bar{Q}^!} = D^\star_{\bar{Q}}$ and $D^\star_{\bar{Q}^!} = D_{\bar{Q}}$.*

Remark 9.41. The construction of the surface given in Definition 9.35 yields the same surface as the one constructed in [OPS18]. A notable difference is that in [OPS18], only $D_{\bar{Q}}$ is given, and $D^\star_{\bar{Q}}$ is deduced (it is called the dual lamination). Another minor difference is that the construction in [OPS18] is written only for gentle algebras, while here it is generalized to locally gentle algebras.

Example 9.42. Consider a *Cambrian quiver* (*a.k.a.* type A quiver), that is any orientation of a line with no relations. Two such quivers are represented in Figure 9.8. Note that we can choose to position the blossom vertices in such a way that for any arrow β, the arrows α and γ such that $\alpha\beta \in I$ and $\beta\gamma \in I$ are on the right of β. We apply Remark 9.39 to understand the corresponding surfaces. The corresponding perfect matchings (see Remark 9.39 (vi)) form a cycle with green and red arrows alternating. Moreover, $\bar{Q}$ and $\bar{Q}^!$ have no infinite straight walks. Since $|Q_1| = |Q_0| - 1$, the corresponding surfaces are disks (1 boundary component, no puncture and genus 0). The dissection $D_{\bar{Q}}$ is a triangulation with no internal triangles, and the orientation of $\bar{Q}$ indicates how to glue these triangles. For instance, the Cambrian quiver completely oriented in one direction yields a fan triangulation, with all internal edges incident to the same vertex, as in Figure 9.8 (left).

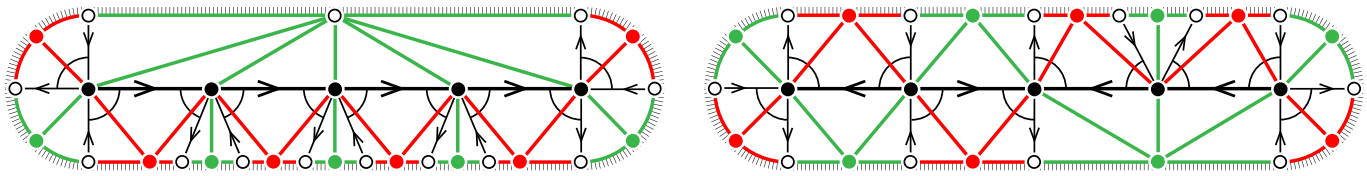

Figure 9.8: The surface $\mathcal{S}_{\bar{Q}}$ for two Cambrian paths on 5 vertices.

Example 9.43. Consider the family of *cycle quivers* indicated in Figure 9.9. We apply Remark 9.39 to understand the corresponding surfaces. The corresponding perfect matchings (see Remark 9.39 (vi)) form a cycle with green and red arrows alternating. Moreover, $\bar{Q}$ has 1 infinite straight walk, while $\bar{Q}^!$ has none. Since $|Q_1| = |Q_0|$, the corresponding surfaces are punctured disks (1 boundary component, 1 puncture and genus 0). See Figure 9.9.

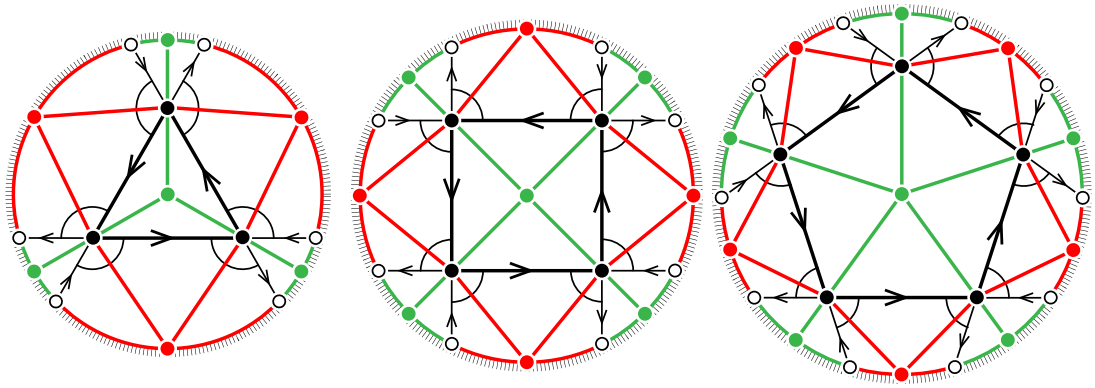

Figure 9.9: The surface $\mathcal{S}_{\bar{Q}}$ for the cycle quivers with $3, 4, 5$ vertices.

Example 9.44. Consider the family of *reversed path quivers* indicated in Figure 9.10. We apply Remark 9.39 to understand the corresponding surfaces. The corresponding perfect matchings (see Remark 9.39 (vi)) look like  . Moreover, $\bar{Q}$ has no infinite straight walk, while $\bar{Q}^!$ has $|Q_0| - 1$ infinite straight walks. Since $|Q_1| = 2|Q_0| - 2$, the corresponding surfaces have 1 boundary component and genus 0.

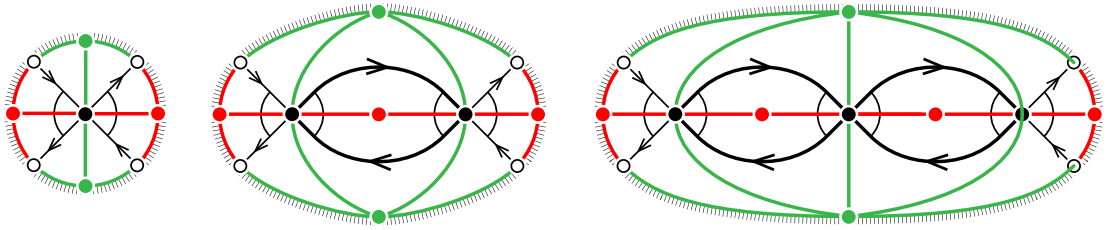

Figure 9.10: The surface $\mathcal{S}_{\bar{Q}}$ for the reversed path quivers with $1, 2, 3$ vertices.

9.3.3 Non-crossing and non-kissing complexes coincide

Let $\bar{Q}$ be a locally gentle quiver. For each edge of the dissection $D_{\bar{Q}}$ on $\mathcal{S}_{\bar{Q}}$, we fix a point on the interior of this edge, which we call its "middle point" (this is the black vertex on the pictures). To each walk on $\bar{Q}$, we will now associate a $D_{\bar{Q}}$-accordion.

Definition 9.45. *For any arrow α on $\bar{Q}^{\circledast}$, let $\gamma(\alpha)$ be the curve on $\mathcal{S}_{\bar{Q}}$ which goes from the middle point of the edge of D corresponding to $s(\alpha)$ to the middle point of the edge of D corresponding to $t(\alpha)$ by following the angle corresponding to α. Define $\gamma(\alpha^{-1})$ to be $\gamma(\alpha)^{-1}$.*

Definition 9.46. *Let $\omega = \prod_{i<\ell<j} \alpha_\ell^{\varepsilon_\ell}$ be a (possibly infinite) walk on $\bar{Q}$. Define the curve $\gamma(\omega)$ to be the concatenation of the curves $\gamma(\alpha_\ell^{\varepsilon_\ell})$ of Definition 9.45.*

In practice, we represent $\gamma(\omega)$ by a curve which intersects itself only transversaly, and such that if it circles infinitely around a puncture, then it spirals towards it.

Lemma 9.47. *Let ω be a walk on $\bar{Q}$. Then $\gamma(\omega)$ is a $D_{\bar{Q}}$-accordion.*

Lemma 9.48. *Let γ be a $D_{\bar{Q}}$-accordion. There exists a unique undirected walk $\omega(\gamma)$ such that we have $\gamma\big(\omega(\gamma)\big) = \gamma$.*

Proposition 9.49. *The maps $\gamma(-)$ and $\omega(-)$ induce mutually inverse bijections between the set of undirected walks on $\bar{Q}$ and the set of $D_{\bar{Q}}$-accordions on $\mathcal{S}_{\bar{Q}}$.*

Lemma 9.50. *Two undirected walks ω_1 and ω_2 on $\bar{Q}$ are non-kissing if and only if the corresponding $D_{\bar{Q}}$-accordions $\gamma(\omega_1)$ and $\gamma(\omega_2)$ are non-crossing on $\mathcal{S}_{\bar{Q}}$.*

Theorem 9.51. *The non-kissing and non-crossing complexes are isomorphic:*
- *for any locally gentle quiver $\bar{Q}$, the non-kissing complex $\mathcal{K}_{\mathrm{nk}}(\bar{Q})$ is isomorphic to the non-crossing complex $\mathcal{K}_{\mathrm{nc}}(D_{\bar{Q}}, D^\star_{\bar{Q}})$,*
- *for any pair of dual cellular dissections $D, D^\star$ of an oriented surface, the non-crossing complex $\mathcal{K}_{\mathrm{nc}}(D, D^\star)$ is isomorphic to the non-kissing complex $\mathcal{K}_{\mathrm{nk}}(\bar{Q}_{D,D^\star})$.*

Remark 9.52. Note that our construction of the surface $\mathcal{S}_{\bar{Q}}$ implies that the quiver $\bar{Q}$ is naturally embedded on $\mathcal{S}_{\bar{Q}}$. If we force all D-accordions (or $D^\star$-slaloms) to follow the arrows of $\bar{Q}$, then a D-accordion (or $D^\star$-slalom) is really seen as a walk on $\bar{Q}$.

We conclude with an important example of facets of the non-kissing and non-crossing complexes.

Example 9.53. We have seen in Definition 9.11 that each vertex a of Q gives rise to a *peak walk* a_{peak} (resp. *deep walk* a_{deep}) with a single peak (resp. deep) at a and no other corner. The set of all such walks forms the *peak facet* $F_{\mathrm{peak}} := \{a_{\mathrm{peak}} \,|\, a \in Q_0\}$ (resp. the *deep facet* $F_{\mathrm{deep}} := \{a_{\mathrm{deep}} \,|\, a \in Q_0\}$) of the non-kissing complex $\mathcal{C}_{\mathrm{nk}}(\bar{Q})$. As an example of Theorem 9.51, let us now describe the corresponding non-crossing facets of $\mathcal{C}_{\mathrm{nc}}(D_{\bar{Q}}, D^\star_{\bar{Q}})$.

For an edge a of D, we denote by a_{prev} (resp. a_{next}) the curve obtained by moving each endpoint v of a as follows:
- if v is on the boundary of $\mathcal{S}$, then move (continuously) v until it reaches the following blossom vertex along the boundary of $\mathcal{S}$ while keeping the boundary of $\mathcal{S}$ on the right,
- if v is a puncture, then rotate around v in counterclockwise (resp. clockwise) direction.

Examples are illustrated in Figure 9.11.

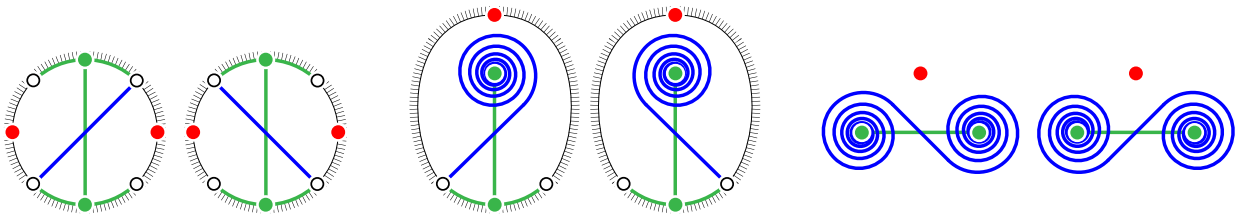

Figure 9.11: The curves a_{prev} (left) and a_{next} (right) associated to an edge a of D for three different dissections.

We invite the reader to check that $\gamma(a_{\mathrm{peak}}) = \varepsilon(a)_{\mathrm{prev}}$ (resp. $\gamma(a_{\mathrm{deep}}) = \varepsilon(a)_{\mathrm{next}}$), where $\varepsilon(a)$ denotes the edge of $D_{\bar{Q}}$ corresponding to $a \in Q_0$ (see Remark 9.39 (ii)). Therefore, the peak facet (resp. the deep facet) can be thought of as the dissection $D_{\bar{Q}}$ slightly rotated clockwise (resp. counterclockwise) on the surface $\mathcal{S}_{\bar{Q}}$.

Chapter Ten

10 NON-KISSING LATTICES AND NON-KISSING ASSOCIAHEDRA

This chapter investigates further the structure of finite non-kissing complexes (or equivalently of finite non-crossing complexes) defined in Chapter 9. We first show that these simplicial complexes are pseudomanifolds: all their facets have the same cardinality and any ridge is contained in precisely two facets. In other words, there is a flip operation that replaces a single walk in a non-kissing facet (Section 10.1). We then show that the increasing flip graph defines a lattice structure on non-kissing facets that we call non-kissing lattice (Section 10.2). The approach, originally due to T. McConville on grid quivers [McC17], echoes the first part of this document: we interpret the non-kissing lattice as a lattice quotient of a lattice of biclosed sets of strings which plays the role of the weak order. Finally, we construct a non-kissing fan and a non-kissing associahedron that realize the non-kissing complex (Section 10.3). We conclude by the observation that all the geometry of the non-kissing associahedron is in fact hidden in well-chosen projections of the classical associahedra, thus opening the question to project further cluster algebra structures. The results of this chapter are based on a joint work with Y. Palu and P.-G. Plamondon [PPP17], although the extension to locally gentle algebras was only discussed later in [PPP19], and the type cone approach of Section 10.3.4 is borrowed from [PPPP19].

10.1 FLIPS IN NON-KISSING COMPLEXES

We consider the non-kissing complex $\mathcal{K}_{\mathrm{nk}}(\bar{Q})$ of a locally gentle quiver $\bar{Q}$ defined in Section 9.1 and illustrated in Figure 10.1. We now show that the non-kissing complex is a *pseudomanifold*, *i.e.* that it is *pure* (all facets have the same dimension) and *thin* (there is a well-defined notion of flips).

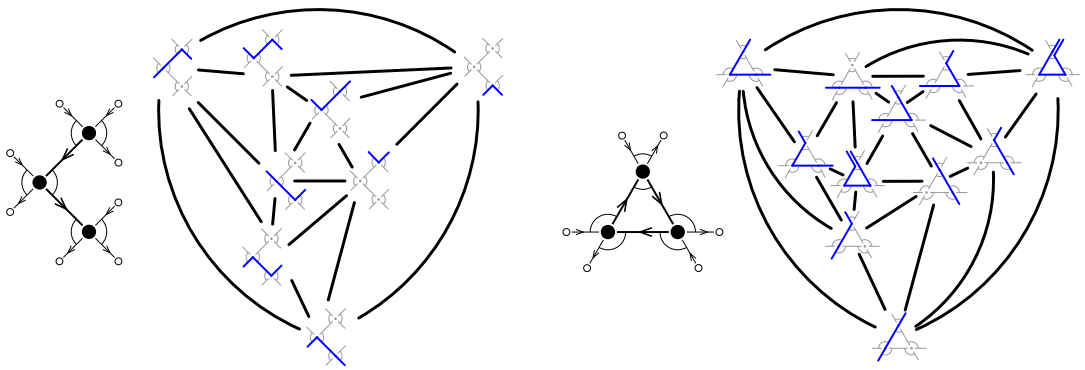

Figure 10.1: The reduced non-kissing complex $\mathcal{C}_{\mathrm{nk}}(\bar{Q})$ for two specific quivers.

10.1.1 Distinguished walks, arrows and strings

An essential tool to understand the combinatorics of the non-kissing complex is the notion of distinguished walks, arrow and strings, originating from [McC17] in the grid situation.

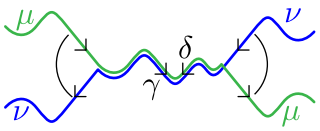

A *marked walk* $\omega_\star$ is a walk $\omega = \alpha_1^{\varepsilon_1} \cdots \alpha_\ell^{\varepsilon_\ell}$ with a marked arrow $\alpha_i^{\varepsilon_i}$. Note that if ω contains several occurrences of $\alpha_i^{\pm}$, only one occurrence is marked. Consider two distinct non-kissing walks $\mu_\star, \nu_\star$ marked at an arrow $\gamma^\varepsilon \in Q_1^{\circledast}$. Let σ denote their maximal common substring containing that occurrence of γ. Since $\mu_\star \neq \nu_\star$, their common substring σ is strict, so that $\mu_\star$ and $\nu_\star$ split at least at one endpoint of σ. Define the *countercurrent order at* γ by $\mu_\star \prec_\gamma \nu_\star$ when $\mu_\star$ enters and/or exits σ in the direction of γ, while $\nu_\star$ enters and/or exits σ in the opposite direction.

Remark 10.1. Note that the countercurrent order $\prec_\gamma$ is:
- well-defined: if both endpoints of σ are in Q_0, then $\mu_\star$ (resp. $\nu_\star$) enters and exits σ in the same direction since $\mu_\star$ and $\nu_\star$ are non-kissing;
- independent of the orientation of $\mu_\star$ and $\nu_\star$: $\mu_\star \prec_\gamma \nu_\star \iff (\mu_\star)^{-1} \prec_\gamma \nu_\star \iff \mu_\star \prec_\gamma (\nu_\star)^{-1}$; we thus also consider $\prec_\gamma$ as a relation on undirected marked walks;
- dependent of which occurrence of γ is marked on μ and ν.

Remark 10.2. The countercurrent order might be more natural in the non-crossing complex as it corresponds to the distance of the accordions from a vertex, see [GM18, MP19] and [PPP19, Rem. 5.4].

Lemma 10.3. *For any face F of $\mathcal{K}_{\mathrm{nk}}(\bar{Q})$, the countercurrent order $\prec_\gamma$ defines a total order on the walks of F marked at an occurrence of γ.*

In all pictures, we represent the walks passing through γ in increasing order of $\prec_\gamma$ from the left side to the right side of γ. See *e.g.* Figure 10.2 (right). Observe that the straight walk containing γ is always $\prec_\gamma$-minimal. The $\prec_\gamma$-maximal walk enables us to define distinguished walks and arrows.

Definition 10.4. *For a face F of $\mathcal{K}_{\mathrm{nk}}(\bar{Q})$, define:*
- *the* distinguished walk *of F at an arrow γ as the $\prec_\gamma$-maximal walk* $\mathbf{dw}(\gamma, F)$,
- *the* distinguished arrows *of a walk $\omega \in F$ as the arrows* $\mathbf{da}(\omega, F) := \{\gamma \in \omega \,|\, \mathbf{dw}(\gamma, F) = \omega\}$.

The following statement is inspired from [McC17, Thm. 3.2] and illustrated in Figure 10.2.

Proposition 10.5. *Each bending (resp. straight) walk of a facet $F \in \mathcal{K}_{\mathrm{nk}}(\bar{Q})$ contains precisely 2 (resp. 1) distinguished arrows pointing in opposite directions (resp. in the direction of the walk).*

It enables to count the number of walks in each facet of $\mathcal{K}_{\mathrm{nk}}(\bar{Q})$ by double counting (each arrow has a distinguished walk, while each bended / straight walk has two / one distinguished arrows).

Corollary 10.6. *The non-kissing complex $\mathcal{K}_{\mathrm{nk}}(\bar{Q})$ is pure of dimension $3|Q_0| - |Q_1|$. The reduced non-kissing complex $\mathcal{C}_{\mathrm{nk}}(\bar{Q})$ is pure of dimension $|Q_0|$.*

We conclude by the notion of distinguished string that will be useful in Sections 10.2.4 and 10.3.1.

Definition 10.7. *The* distinguished string *of a bending walk ω in a facet $F \in \mathcal{K}_{\mathrm{nk}}(\bar{Q})$ is the substring $\mathbf{ds}(\omega, F)$ of ω located between the two distinguished arrows of ω. A string σ of $\bar{Q}$ is* distinguishable *if there exists a walk ω in a non-kissing facet $F \in \mathcal{K}_{\mathrm{nk}}(\bar{Q})$ such that $\sigma = \mathbf{ds}(\omega, F)$ is the distinguished string of $\omega \in F$.*

Proposition 10.8. *A string σ on $\bar{Q}$ is distinguishable if and only if $\Sigma_{\mathrm{bot}}(\sigma) \cap \Sigma_{\mathrm{top}}(\sigma) = \{\sigma\}$.*

Example 10.9. In the peak facet $F_{\mathrm{peak}} := \{a_{\mathrm{peak}} \,|\, a \in Q_0\}$ and deep facet $F_{\mathrm{deep}} := \{a_{\mathrm{deep}} \,|\, a \in Q_0\}$ of Example 9.53, we have $\mathbf{ds}(a_{\mathrm{peak}}, F_{\mathrm{peak}}) = \mathbf{ds}(a_{\mathrm{deep}}, F_{\mathrm{deep}}) = \varepsilon_a$ for any vertex $a \in Q_1$.

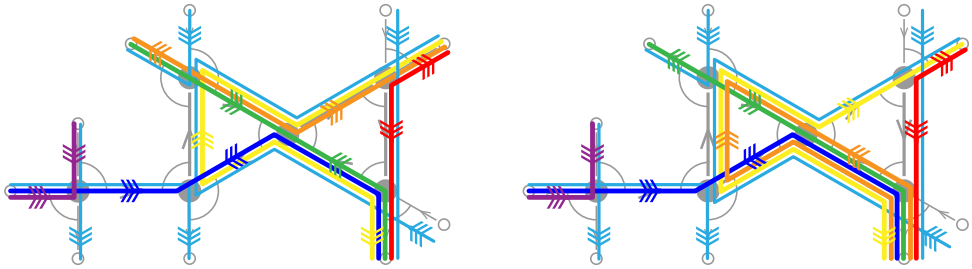

Figure 10.2: Flipping the red walk ω to the orange walk ω'. The walks μ, ν involved in the flip are the blue and green walks. Distinguished arrows are marked with triple arrows.

10.1.2 Flips

We now show that the non-kissing complex $\mathcal{C}_{\mathrm{nk}}(\bar{Q})$ is thin, *i.e.* that any codimension 1 non-kissing face of $\mathcal{C}_{\mathrm{nk}}(\bar{Q})$ is contained in exactly two non-kissing facets of $\mathcal{C}_{\mathrm{nk}}(\bar{Q})$, or in other words that there is a flip operation on non-kissing facets. Here again, it is more convenient to work with the unreduced non-kissing complex $\mathcal{K}_{\mathrm{nk}}(\bar{Q})$. The following statement is illustrated in Figure 10.2.

Proposition 10.10. *Consider a non-kissing facet $F \in \mathcal{K}_{\mathrm{nk}}(\bar{Q})$ and a bending walk $\omega \in F$. The distinguished substring $\sigma = \mathbf{ds}(\omega, F)$ splits ω into $\omega = \rho\sigma\tau$. Let $\{\alpha, \beta\} := \mathbf{da}(\omega, F)$ be the distinguished arrows of ω in F, and α' and β' be the other two arrows of $Q_1^{\circledcirc}$ incident to the endpoints of σ and such that $\alpha'\alpha \in I$ or $\alpha\alpha' \in I$, and $\beta'\beta \in I$ or $\beta\beta' \in I$. Let $\mu := \mathbf{dw}(\alpha', F \smallsetminus \{\omega\})$ and $\nu := \mathbf{dw}(\beta', F \smallsetminus \{\omega\})$. Then*

(i) The string σ splits the walks μ into $\mu = \rho'\sigma\tau$ and ν into $\nu = \rho\sigma\tau'$.

(ii) The walk $\omega' := \rho'\sigma\tau'$ is kissing ω but no other walk of F. Moreover, ω' is the only other walk besides ω which is not kissing any other walk of $F \smallsetminus \{\omega\}$.

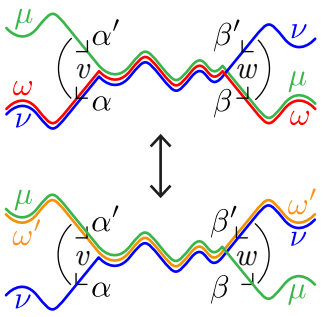

We say that $F \triangle \{\omega, \omega'\}$ is obtained from F by flipping ω, and that the flip is supported by σ.

Corollary 10.11. *The reduced non-kissing complex $\mathcal{C}_{\mathrm{nk}}(\bar{Q})$ is a pseudomanifold without boundary.*

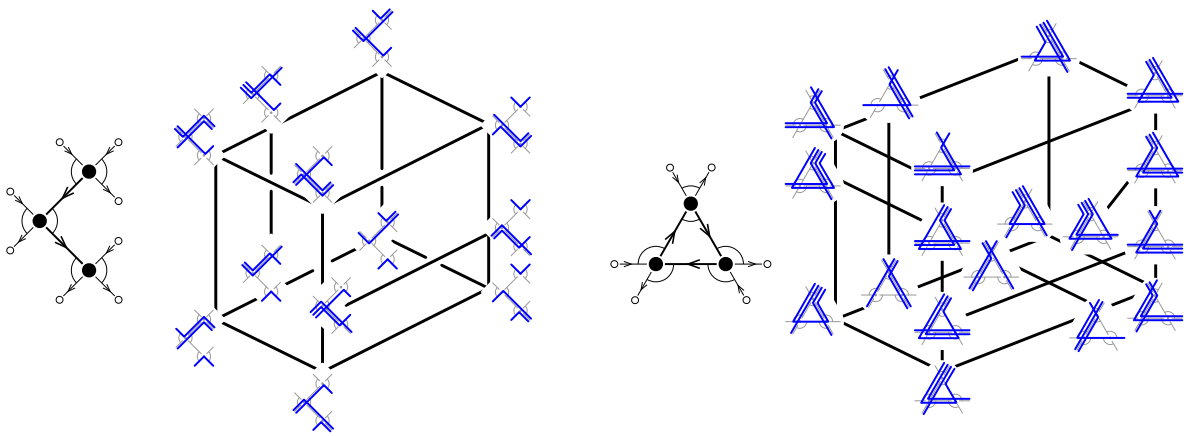

Figure 10.3: The non-kissing oriented flip graph $\mathcal{G}_{\mathrm{nk}}(\bar{Q})$ for two specific quivers. The graph is oriented from bottom to top, with the peak facet F_{peak} at the bottom and the deep facet F_{deep} on top.

10.2 NON-KISSING LATTICES

The flip operation of Proposition 10.10 and Figure 10.2 exchanges two kissing walks ω, ω'. The flip is *increasing* when their common substring is on top of ω and on the bottom of ω'. This yields the *increasing flip graph*, whose vertices are non-kissing facets and arcs are increasing flips. Note that the *peak facet* $\{v_{\text{peak}} \,|\, v \in Q_0\}$ is a source and the *deep facet* $\{v_{\text{deep}} \,|\, v \in Q_0\}$ is a sink of the increasing flip graph. See Figure 10.3. The main result of this section is the following statement.

Theorem 10.12. *If $\mathcal{C}_{\text{nk}}(\bar{Q})$ is finite, the increasing flip graph is the Hasse diagram of a congruence-uniform lattice, that we call* non-kissing lattice *and denote by $\mathcal{L}_{\text{nk}}(\bar{Q})$.*

We have briefly presented lattice quotients and canonical join representations in Sections 1.1.1, 4.1.1 and 4.1.2, see [Rea16b, Sect. 9.5] for a detailed survey. A lattice L is *congruence-uniform* if its join-irreducible elements are in bijection with the join-irreducibles of its lattice of congruences, and similarly for meet-irreducibles. Congruence-uniform lattices behave nicely with join representations and congruence lattices. To achieve Theorem 10.12, we use a technique developed by T. McConville for grid quivers [McC17]: we identify the non-kissing lattice with a quotient of a lattice of biclosed sets of strings.

10.2.1 Biclosed sets of strings

A *closure operator* on a finite set $\mathcal{S}$ is a map $S \mapsto S^{\text{cl}}$ on subsets of $\mathcal{S}$ such that:

$$\varnothing^{\text{cl}} = \varnothing, \qquad S \subseteq S^{\text{cl}}, \qquad (S^{\text{cl}})^{\text{cl}} = S^{\text{cl}}, \qquad \text{and} \qquad S \subseteq T \Longrightarrow S^{\text{cl}} \subseteq T^{\text{cl}},$$

for any $S, T \subseteq \mathcal{S}$. A subset $S \subseteq \mathcal{S}$ is *closed* if $S^{\text{cl}} = S$, *coclosed* if $\mathcal{S} \smallsetminus S$ is closed, and *biclosed* if it is both closed and coclosed. We denote by $\mathsf{Bic}(\mathcal{S})$ the inclusion poset of biclosed subsets of $\mathcal{S}$. The following criterion, adapted from [McC17, Thm. 5.5], provides simple sufficient conditions for $\mathsf{Bic}(\mathcal{S})$ to be a congruence uniform lattice.

Theorem 10.13 (Adapted from [McC17, Thms. 5.2 & 5.5])**.** *If $(\mathcal{S}, \lhd)$ is a poset with a closure operator $S \mapsto S^{\text{cl}}$ such that:*
(i) for each cover relation $S \subset T$ in $\mathsf{Bic}(\mathcal{S})$, there is a unique $\tau \in (T \smallsetminus S)$ such that $S \cup \{\tau\}^{\text{cl}} = T$,
(ii) $R \cup \big((S \cup T) \smallsetminus R\big)^{\text{cl}} \in \mathsf{Bic}(\mathcal{S})$ for $R, S, T \in \mathsf{Bic}(\mathcal{S})$ with $R \subseteq S \cap T$, and
(iii) if $\rho, \sigma, \tau \in \mathcal{S}$ with $\rho \in \{\sigma, \tau\}^{\text{cl}} \smallsetminus \{\sigma, \tau\}$, then $\sigma \lhd \rho$ and $\tau \lhd \rho$,
then the inclusion poset $\mathsf{Bic}(\mathcal{S})$ of biclosed sets of $\mathcal{S}$ is a congruence-uniform lattice.

In a locally gentle quiver $\bar{Q}$, we define the *closure* S^{cl} of a set S of strings of $\bar{Q}$ as the set of all strings of the form $\sigma_1 \alpha_1^{\varepsilon_1} \sigma_2 \alpha_2^{\varepsilon_2} \dots \alpha_{\ell-1}^{\varepsilon_{\ell-1}} \sigma_\ell$ where $\sigma_i \in S, \alpha_i \in Q_1$ and $\varepsilon_i \in \{-1, 1\}$. Let $\mathsf{Bic}(\bar{Q})$ be the inclusion poset on biclosed sets of strings of $\bar{Q}$. Figure 10.4 illustrates the notions of closed, coclosed and biclosed sets of strings. Figure 10.6 (left) shows the poset $\mathsf{Bic}(\bar{Q})$ for the quiver of Figure 10.1 (left), with the empty set in the bottom and the set of all strings of $\bar{Q}$ on top.

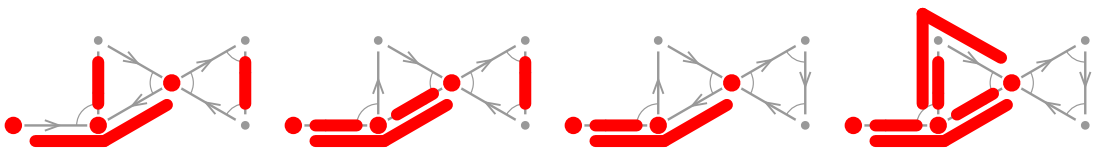

Figure 10.4: Four sets of strings on the quiver of Figure 10.2. The first is neither closed nor coclosed, the second is closed but not coclosed, the third is coclosed but not closed, and the fourth is biclosed.

Example 10.14. Before going further, we want to observe that the poset of biclosed sets of strings plays here the same role as the weak order in Part I of this document. Namely, in the case when the quiver $\bar{Q}$ is an oriented path on n vertices with no relation, observe that:

- the strings are in bijection with pairs $(i, j) \in \binom{n+1}{2}$,
- the closure on strings translates to the concatenation $(i, j) \circ (k, \ell) = \delta_{j=k}(i, \ell)$,
- biclosed sets of strings are in bijection with inversion sets of permutations of $[n + 1]$, and
- the poset of biclosed sets $\mathsf{Bic}(\bar{Q})$ is isomorphic to the weak order on $\mathfrak{S}_{n+1}$.

See Figure 10.8 (top left) for an example.

The criterion of Theorem 10.13 yields the following result.

Theorem 10.15. *When $\bar{Q}$ has finitely many strings, the inclusion poset of biclosed sets $\mathsf{Bic}(\bar{Q})$ is a congruence-uniform lattice.*

10.2.2 Non-kissing congruence

Recall from Section 1.1.1 that a lattice congruence $\equiv$ on a finite lattice L can be defined by its projection maps $\pi_\downarrow$ and $\pi^\uparrow$, sending an element $x \in L$ to the minimum and maximum of its equivalence class respectively. We now define a lattice congruence on the lattice of biclosed sets, adapting the definition of [McC17, Sect. 7] for grid quivers.

Definition 10.16. *For a biclosed set $S \in \mathsf{Bic}(\bar{Q})$, define*

$$\pi_\downarrow(S) := \{\sigma \text{ string on } Q \mid \Sigma_{\mathrm{bot}}(\sigma) \subseteq S\} \quad \text{and} \quad \pi^\uparrow(S) := \{\sigma \text{ string on } Q \mid \Sigma_{\mathrm{top}}(\sigma) \cap S \neq \varnothing\}.$$

where we still denote by $\Sigma_{\mathrm{bot}}(\sigma)$ and $\Sigma_{\mathrm{top}}(\sigma)$ the sets of bottom and top substrings of a string σ.

These sets, illustrated in Figure 10.5, satisfy the following properties.

Proposition 10.17. *For any $S \in \mathsf{Bic}(\bar{Q})$, the sets $\pi_\downarrow(S)$ and $\pi^\uparrow(S)$ are biclosed. Moreover:*
(i) $\pi_\downarrow(S) \subseteq S \subseteq \pi^\uparrow(S)$ for any element $S \in \mathsf{Bic}(\bar{Q})$,
(ii) $\pi_\downarrow \circ \pi_\downarrow = \pi_\downarrow \circ \pi^\uparrow = \pi_\downarrow$ and $\pi^\uparrow \circ \pi^\uparrow = \pi^\uparrow \circ \pi_\downarrow = \pi^\uparrow$,
(iii) $\pi_\downarrow$ and $\pi^\uparrow$ are order preserving.
Therefore, the fibers of $\pi^\uparrow$ and $\pi_\downarrow$ coincide and are the classes of a lattice congruence $\equiv$ on $\mathsf{Bic}(\bar{Q})$, called non-kissing congruence.

Example 10.18. If $\bar{Q}$ is an oriented path with no relation, $\equiv$ is a Cambrian congruence of the weak order [Rea06]. The congruence classes of $\equiv$ appear as blue rectangles in Figure 10.6.

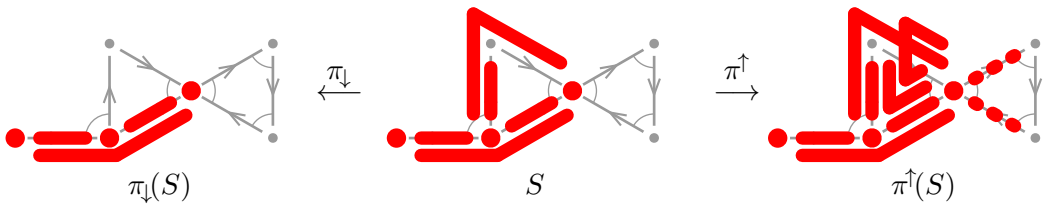

Figure 10.5: A biclosed set of strings S (middle) with $\pi_\downarrow(S)$ (left) and $\pi^\uparrow(S)$ (right). For readibility, $\pi^\uparrow(S)$ is only partially drawn: the remaining strings are obtained by adding independently the two dotted arrows to all strings containing their left endpoint.

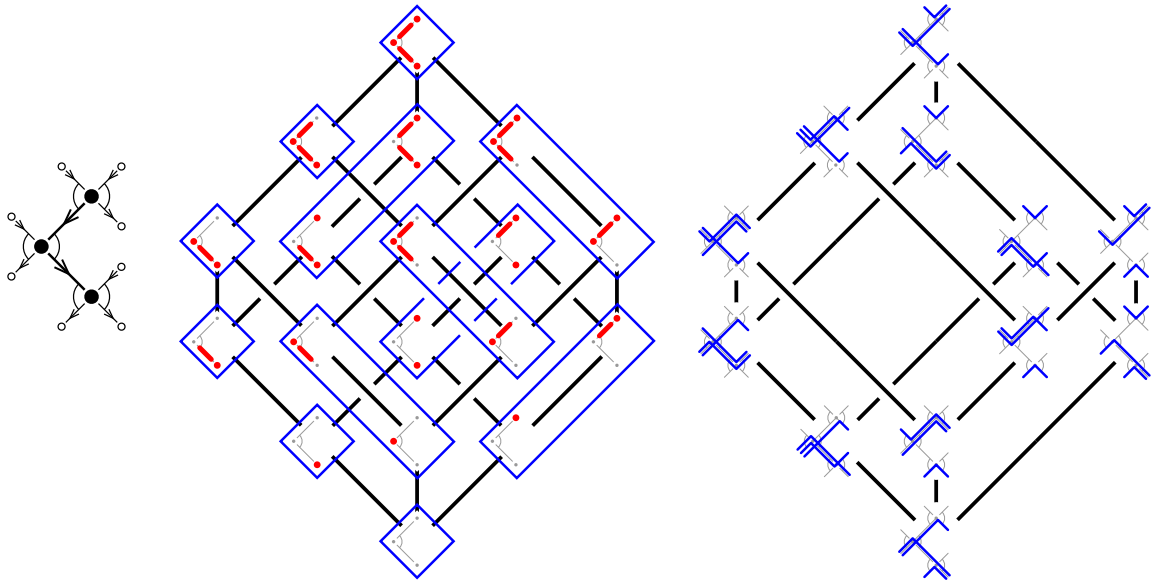

Figure 10.6: The inclusion lattice of biclosed sets $\mathsf{Bic}(\bar{Q})$ with congruence classes of $\equiv$ in blue (left), and the corresponding non-kissing lattice $\mathcal{L}_{\mathrm{nk}}(\bar{Q})$ (right).

10.2.3 Non-kissing lattice

Coming back to our original problem, we now aim to show that the increasing flip graph on non-kissing facets is isomorphic to the Hasse diagram of the quotient of the lattice of biclosed set $\mathsf{Bic}(\bar{Q})$ of Section 10.2.1 by the non-kissing congruence of Section 10.2.2. The next two propositions provide explicit maps between biclosed sets of strings and non-kissing facets illustrated in Figure 10.7. These maps extend previous definitions of [McC17] for grid quivers.

Proposition 10.19. *For $S \in \mathsf{Bic}(\bar{Q})$ and $\alpha \in Q_1^{\circledcirc}$, let $\omega(\alpha, S) := \alpha_{-\ell}^{\varepsilon_{-\ell}} \cdots \alpha_{-1}^{\varepsilon_{-1}} \cdot \alpha \cdot \alpha_1^{\varepsilon_1} \cdots \alpha_r^{\varepsilon_r}$ be the directed walk containing α defined by*

- *$\varepsilon_i = -1$ if the string $\alpha_1^{\varepsilon_1} \cdots \alpha_{i-1}^{\varepsilon_{i-1}}$ belongs to S, and $\varepsilon_i = 1$ otherwise, for all $i \in [r]$,*
- *$\varepsilon_{-i} = 1$ if the string $\alpha_{-i+1}^{\varepsilon_{-i+1}} \cdots \alpha_{-1}^{\varepsilon_{-1}}$ belongs to S, and $\varepsilon_i = -1$ otherwise, for all $i \in [\ell]$.*

Then the set $\{\omega(\alpha, S) \mid \alpha \in Q_1^{\circledcirc}\}$ contains $2|Q_0| - |Q_1|$ straight walks and $|Q_0|$ pairs of inverse directed bending walks, which are all pairwise non-kissing. We thus obtain a facet $\eta(S)$ of $\mathcal{K}_{\mathrm{nk}}(\bar{Q})$ by identifying these pairs of inverse directed bending walks.

Proposition 10.20. *For any facet $F \in \mathcal{K}_{\mathrm{nk}}(\bar{Q})$, the set of strings $\zeta(F) := \Big(\bigcup_{\omega \in F} \Sigma_{\mathrm{bot}}(\omega)\Big)^{\mathrm{cl}}$ is biclosed.*

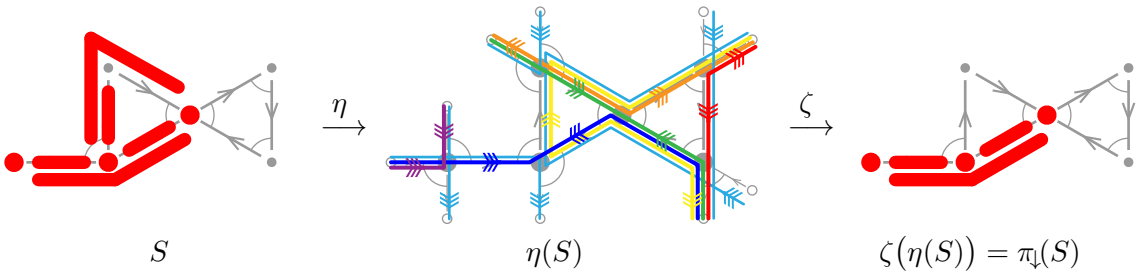

Figure 10.7: The maps η (left) and ζ (right) between non-kissing facets and biclosed sets.

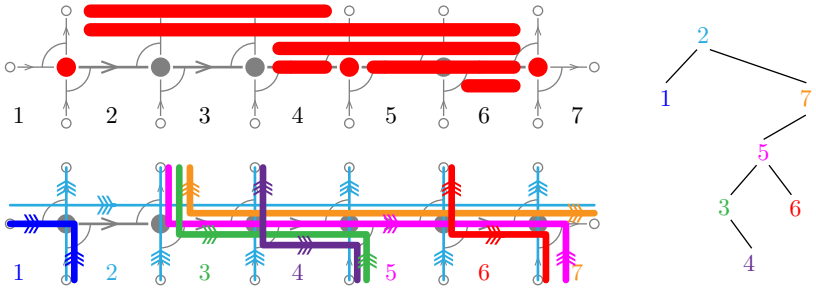

Figure 10.8: The biclosed set of strings S of the straight quiver corresponding to the inversion set of the permutation 2751346 (top left), the corresponding non-kissing facet $\eta(S)$ (bottom left), and the standard binary search tree obtained by insertion of 2751346 (right), see also Figure 1.2.

Example 10.21. When the quiver is an oriented path with no relation, the map η should be thought of as the map from permutations to triangulations defined in [Rea06]. Conversely, ζ maps a triangulation to the minimal permutation in its fiber under η. For the straight quiver, η plays the role of the binary search tree insertion while ζ selects the minimal linear extension of a binary tree. See Figure 10.8.

Using these maps, we show that the increasing flip graph on non-kissing facets is isomorphic to the Hasse diagram of the lattice quotient $\mathsf{Bic}(\bar{Q})/\equiv$.

Theorem 10.22. *The maps $\eta : \mathsf{Bic}(\bar{Q}) \to \mathcal{K}_{\mathrm{nk}}(\bar{Q})$ and $\zeta : \mathcal{K}_{\mathrm{nk}}(\bar{Q}) \to \mathsf{Bic}(\bar{Q})$ satisfy:*

- *$\eta\big(\zeta(F)\big) = F$ for any facet $F \in \mathcal{K}_{\mathrm{nk}}(\bar{Q})$,*
- *$\zeta\big(\eta(S)\big) = \pi_{\downarrow}(S)$ for any biclosed set $S \in \mathsf{Bic}(\bar{Q})$,*
- *for any facet $F' \in \mathcal{C}_{\mathrm{nk}}(\bar{Q})$ and $\sigma \in \zeta(F')$, there exists an increasing flip $F \to F'$ supported by σ if and only if $\zeta(F') \smallsetminus \{\sigma\}$ is biclosed.*

Therefore, the facets of $\mathcal{K}_{\mathrm{nk}}(\bar{Q})$ are in bijection with the congruence classes of $\equiv$ and the increasing flip graph is the Hasse diagram of the lattice quotient $\mathsf{Bic}(\bar{Q})/\equiv$.

10.2.4 Canonical join complex

Congruence-uniform lattices behave nicely with join representations and congruence lattices. In particular, congruence-uniform lattices are semi-distributive, so that any element admits a canonical join representation. The collection of sets J which define canonical join representations in L is the *canonical join complex* of L.

To conclude our study of the non-kissing lattice $\mathcal{L}_{\mathrm{nk}}(\bar{Q})$, we describe its canonical join complex. Recall that a string σ of $\bar{Q}$ is *distinguishable* if there is a facet $F \in \mathcal{K}_{\mathrm{nk}}(\bar{Q})$ and a walk $\omega \in F$ such that $\sigma = \mathbf{ds}(\omega, F)$. One checks that $\Sigma_{\mathrm{bot}}(\sigma)^{\mathrm{cl}}$ is biclosed so that we can define $\mathbf{ji}(\sigma) := \eta\big(\Sigma_{\mathrm{bot}}(\sigma)^{\mathrm{cl}}\big)$.

Proposition 10.23. *The map $\mathbf{ji} : \sigma \mapsto \mathbf{ji}(\sigma) := \eta\big(\Sigma_{\mathrm{bot}}(\sigma)^{\mathrm{cl}}\big)$ defines a bijection between the distinguishable strings of $\bar{Q}$ and the join-irreducible elements of the non-kissing lattice $\mathcal{L}_{\mathrm{nk}}(\bar{Q})$.*

Therefore, distinguishable strings are building blocks for canonical join representations in $\mathcal{L}_{\mathrm{nk}}(\bar{Q})$. A *descent* of a facet $F \in \mathcal{K}_{\mathrm{nk}}(\bar{Q})$ is a string σ which is the distinguished string of a walk ω of F and is a bottom substring of ω (so that the flip of ω in F is a descent in the non-kissing lattice). We denote by $\mathrm{des}(F)$ the set of descents of F.

Proposition 10.24. *The canonical join representation of $F \in \mathcal{L}_{\mathrm{nk}}(\bar{Q})$ is given by $F = \bigvee_{\sigma \in \mathrm{des}(F)} \mathbf{ji}(\sigma)$.*

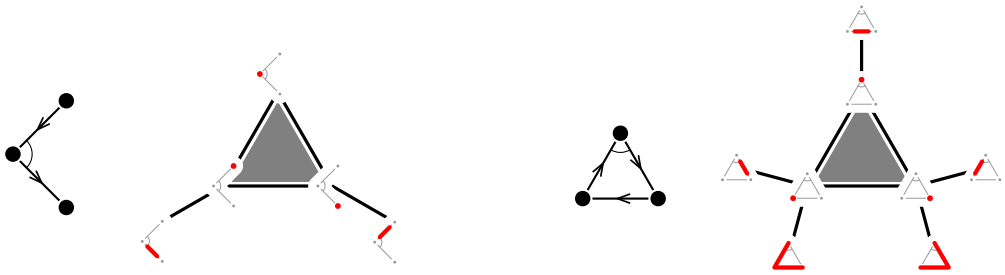

Figure 10.9: The non-friendly complex $\mathcal{C}_{\mathrm{nf}}(\bar{Q})$ for two specific quivers.

To conclude, we characterize which subsets of strings correspond to canonical join representations in the non-kissing lattice $\mathcal{L}_{\mathrm{nk}}(\bar{Q})$. Following [GM17a], we say that two strings are *non-friendly* if $\Sigma_{\mathrm{top}}(\sigma) \cap \Sigma_{\mathrm{bot}}(\tau) = \varnothing = \Sigma_{\mathrm{bot}}(\sigma) \cap \Sigma_{\mathrm{top}}(\tau)$. We call *non-friendly complex* the simplicial complex of sets of pairwise non-friendly distinguishable strings.

Theorem 10.25. *The following assertions are equivalent for a set Σ of distinguishable strings of $\bar{Q}$:*
- *any two strings of Σ are non-friendly,*
- *$\{\mathbf{ji}(\sigma) \,|\, \sigma \in \Sigma\}$ is the canonical join-representation of a facet of $\mathcal{K}_{\mathrm{nk}}(\bar{Q})$,*
- *Σ is the descent set of a non-kissing facet $F \in \mathcal{K}_{\mathrm{nk}}(\bar{Q})$.*

In other words, the canonical join complex of $\mathcal{L}_{\mathrm{nk}}(\bar{Q})$ is isomorphic to the non-friendly complex.

Example 10.26. When the quiver is a straight path with no relation, the non-friendly complex is isomorphic to the non-crossing partition complex. For dissection quivers, one can interpret the non-friendly condition directly on the dissection, thus providing a simple bijection between the facets of the non-kissing complex and the serpent nests of the dissection [Cha16].

10.3 Non-kissing associahedra

In this section, we provide geometric realizations of the non-kissing complex $\mathcal{C}_{\mathrm{nk}}(\bar{Q})$ when it is finite, inspired by similar constructions of [MP19] for dissection quivers and [GM18] for grid quivers.

10.3.1 g- and c-vectors

Let $(\boldsymbol{e}_a)_{a\in Q_0}$ be the standard basis of $\mathbb{R}^{Q_0}$. We first define an analog of the characteristic vector for multisets.

Definition 10.27. *For a multiset $A \coloneqq \{\!\{a_1, \dots, a_m\}\!\}$ of vertices of Q_0, we denote by $\boldsymbol{m}_A \in \mathbb{R}^{Q_0}$ the multiplicity vector of A defined by $\boldsymbol{m}_A \coloneqq \sum_{i\in[m]} \boldsymbol{e}_{a_i} = \sum_{a\in Q_0} |\{i \in [m] \,|\, a_i = a\}|\, \boldsymbol{e}_a$. For a string σ of $\bar{Q}$, we define $\boldsymbol{m}_\sigma \coloneqq \boldsymbol{m}_{A(\sigma)}$ where $A(\sigma)$ is the multiset of vertices of σ.*

We now define two families of vectors that will play a crucial role in the geometric construction. These vectors are illustrated in Figure 10.10.

Definition 10.28. *For a walk ω on $\bar{Q}$, we denote by $\mathbf{peaks}(\omega)$ (resp. by $\mathbf{deeps}(\omega)$) the multiset of vertices of Q_0 corresponding to the peaks (resp. deeps) of ω. The $\boldsymbol{g}$-vector of a walk ω is the vector $\boldsymbol{g}(\omega) \in \mathbb{R}^{Q_0}$ defined by $\boldsymbol{g}(\omega) \coloneqq \boldsymbol{m}_{\mathbf{peaks}(\omega)} - \boldsymbol{m}_{\mathbf{deeps}(\omega)}$. Observe that $\boldsymbol{g}(\omega) = 0$ for a straight walk ω. For a set Ω of walks, we let $\boldsymbol{g}(\Omega) \coloneqq \{\boldsymbol{g}(\omega) \,|\, \omega \in \Omega\}$.*

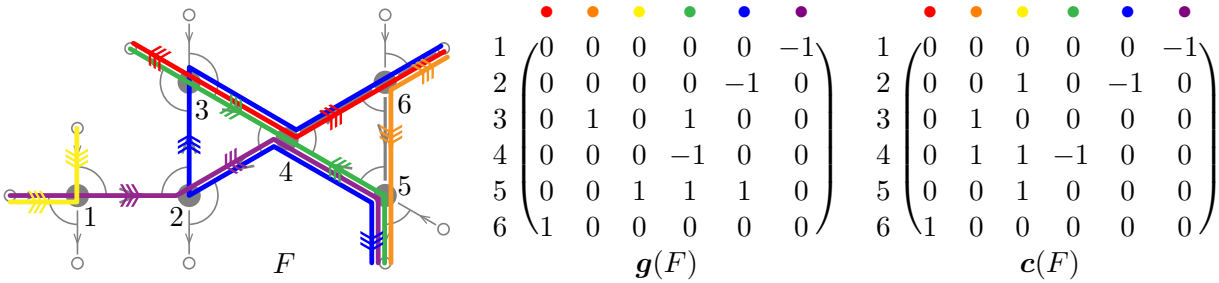

Figure 10.10: The $\boldsymbol{g}$- and $\boldsymbol{c}$-matrices of a non-kissing facet F. Their columns correspond to the $\boldsymbol{g}$- and $\boldsymbol{c}$-vectors of the different walks of F. Note that $\boldsymbol{g}(F) \cdot \boldsymbol{c}(F)^T = \mathbb{1}$.

Definition 10.29. *Consider a bending walk ω in a non-kissing facet $F \in \mathcal{C}_{\mathrm{nk}}(\bar{Q})$. Recall from Proposition 10.5 that the walk ω carries two distinguished arrows $\mathbf{da}(\omega, F)$ surrounding its distinguished string $\mathbf{ds}(\omega, F)$ (see Figure 10.10). Define*

$$\varepsilon(\omega, F) := \begin{cases} 1 & \text{if } \mathbf{ds}(\omega, F) \text{ is a top substring of } \omega \text{ (i.e. the arrows } \mathbf{da}(\omega, F) \text{ point outside),} \\ -1 & \text{if } \mathbf{ds}(\omega, F) \text{ is a bottom substring of } \omega \text{ (i.e. if the arrows } \mathbf{da}(\omega, F) \text{ point inside).} \end{cases}$$

The $\boldsymbol{c}$-vector of a walk ω of F is the vector $\boldsymbol{c}(\omega \in F) \in \mathbb{R}^{Q_0}$ defined by $\boldsymbol{c}(\omega \in F) := \varepsilon(\omega, F)\, \boldsymbol{m}_{\mathbf{ds}(\omega, F)}$. We let $\boldsymbol{c}(F) := \{\boldsymbol{c}(\omega \in F) \,|\, \omega \in F\}$ be the set of $\boldsymbol{c}$-vectors of a non-kissing facet $F \in \mathcal{C}_{\mathrm{nk}}(\bar{Q})$, and $\boldsymbol{C}(\bar{Q}) := \bigcup_F \boldsymbol{c}(F)$ be the set of all $\boldsymbol{c}$-vectors of all non-kissing facets $F \in \mathcal{C}_{\mathrm{nk}}(\bar{Q})$.

Remark 10.30. These definitions can as well be translated to the non-crossing complex, using analogues of shear coordinates for cluster algebras arising from triangulations and laminations on surfaces defined by S. Fomin and D. Thurston [FST08, FT18]. See [MP19] and [PPP19, Prop. 6.7 & 6.8].

Example 10.31. The $\boldsymbol{g}$- and $\boldsymbol{c}$-vectors in the peak and deep facets F_{peak} and F_{deep} are given by

$$\boldsymbol{g}(a_{\mathrm{peak}}) = \boldsymbol{e}_a, \quad \boldsymbol{g}(a_{\mathrm{deep}}) = -\boldsymbol{e}_a, \quad \boldsymbol{c}(a_{\mathrm{peak}} \in F_{\mathrm{peak}}) = \boldsymbol{e}_a, \quad \text{and} \quad \boldsymbol{c}(a_{\mathrm{deep}} \in F_{\mathrm{deep}}) = -\boldsymbol{e}_a.$$

Remark 10.32. The definitions of $\boldsymbol{g}$- and $\boldsymbol{c}$-vectors immediately imply the *sign-coherence property*, stating that for any non-kissing facet $F \in \mathcal{C}_{\mathrm{nk}}(\bar{Q})$:

- for any $\omega \in F$, all coordinates of the $\boldsymbol{c}$-vector $\boldsymbol{c}(\omega \in F)$ have the same sign,
- for $a \in Q_0$, the ath coordinates of all $\boldsymbol{g}$-vectors $\boldsymbol{g}(\omega)$ for $\omega \in F$ have the same sign (otherwise, the corresponding walks would kiss at v).

In particular, a $\boldsymbol{c}$-vector is called *positive* when all its coordinates are non-negative and *negative* when all its coordinates are non-positive.

Remark 10.33. There is a subtle relation between $\boldsymbol{c}$-vectors and strings. Indeed, $\boldsymbol{c}$-vectors are multiplicity vectors of the vertex multisets of some strings of $\bar{Q}$, but:

- not all strings are distinguishable (see Definition 10.7 and Proposition 10.8), and
- distinct distinguishable strings may have identical vertex multisets.

The $\boldsymbol{g}$- and $\boldsymbol{c}$-vectors have been designed so that the following statement holds, see Figure 10.10.

Proposition 10.34. *For any non-kissing facet $F \in \mathcal{C}_{\mathrm{nk}}(\bar{Q})$, the set of $\boldsymbol{g}$-vectors $\boldsymbol{g}(F)$ and the set of $\boldsymbol{c}$-vectors $\boldsymbol{c}(F)$ form dual bases.*

Finally, the $\boldsymbol{g}$-vectors of the walks involved in a flip satisfy the following linear dependence.

Lemma 10.35. *The $\boldsymbol{g}$-vectors of the walks $\omega, \omega', \mu, \nu$ involved in the flip of Proposition 10.10 satisfy the linear dependence $\boldsymbol{g}(\omega) + \boldsymbol{g}(\omega') = \boldsymbol{g}(\mu) + \boldsymbol{g}(\nu)$.*

10.3.2 Non-kissing fans

We now present a fan realization of $\mathcal{C}_{\mathrm{nk}}(\bar{Q})$. Note that it was constructed in [MP19] for dissection quivers and in [GM17a] for grid quivers. Both constructions extend the type A Cambrian fans of N. Reading and D. Speyer [RS09] obtained for path quivers with no relations.

Theorem 10.36. *For a locally gentle quiver $\bar{Q}$ with finite non-kissing complex $\mathcal{C}_{\mathrm{nk}}(\bar{Q})$, the collection of cones $\mathcal{F}^{\boldsymbol{g}}(\bar{Q}) := \{\mathbb{R}_{\geq 0}\, \boldsymbol{g}(F) \mid F \text{ non-kissing face of } \mathcal{C}_{\mathrm{nk}}(\bar{Q})\}$ forms a complete simplicial fan, that we call the non-kissing fan of $\bar{Q}$, or $\boldsymbol{g}$-vector fan of $\bar{Q}$.*

Remark 10.37. Call *$\boldsymbol{c}$-vector fan* the fan $\mathcal{F}^{\boldsymbol{c}}(\bar{Q})$ defined by the arrangement of the hyperplanes orthogonal to the $\boldsymbol{c}$-vectors of $\boldsymbol{C}(\bar{Q})$. Be aware that contrarily to the $\boldsymbol{g}$-vector fan whose rays are the $\boldsymbol{g}$-vectors, the $\boldsymbol{c}$-vectors are not the rays but the normal vectors of the hyperplanes of the $\boldsymbol{c}$-vector fan. By Proposition 10.34, any non-maximal cone of $\mathcal{F}^{\boldsymbol{g}}(\bar{Q})$ is supported by an hyperplane orthogonal to a $\boldsymbol{c}$-vector of $\boldsymbol{C}(\bar{Q})$. The $\boldsymbol{g}$-vector fan $\mathcal{F}^{\boldsymbol{g}}(\bar{Q})$ thus coarsens the $\boldsymbol{c}$-vector fan $\mathcal{F}^{\boldsymbol{c}}(\bar{Q})$. Observe however that the $\boldsymbol{c}$-vector fan $\mathcal{F}^{\boldsymbol{c}}(\bar{Q})$ is not necessarily a Coxeter arrangement of finite type, it is not even always simplicial.

To illustrate Theorem 10.36 and Remark 10.37, we have represented in Figure 10.11 the $\boldsymbol{c}$-vector fan $\mathcal{F}^{\boldsymbol{c}}(\bar{Q})$ and the $\boldsymbol{g}$-vector fan $\mathcal{F}^{\boldsymbol{g}}(\bar{Q})$ for two specific quivers. We use the classical projection to represent 3-dimensional fans: the fan is intersected with the unit sphere and stereographically projected to the plane from the pole in direction $(1, 1, 1)$.

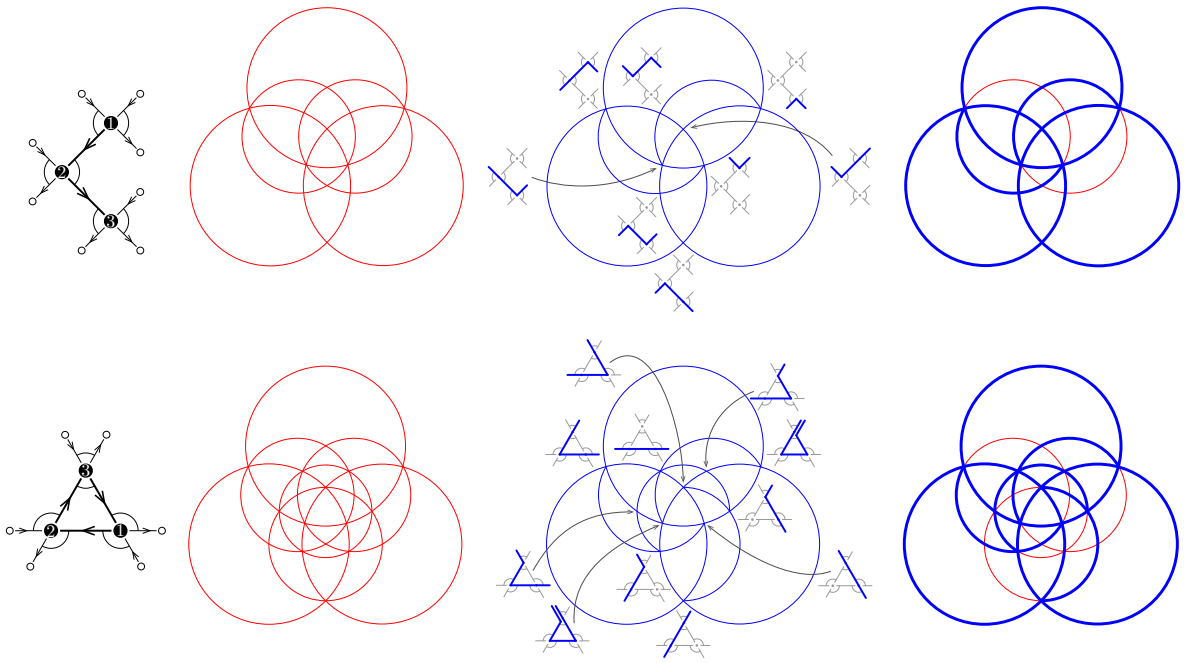

Figure 10.11: Stereographic projections of the $\boldsymbol{c}$-vector fans $\mathcal{F}^{\boldsymbol{c}}(\bar{Q})$ (red, left) and the $\boldsymbol{g}$-vector fans $\mathcal{F}^{\boldsymbol{g}}(\bar{Q})$ (blue, middle) for two specific quivers. The 3-dimensional fan is intersected with the unit sphere and stereographically projected to the plane from the pole in direction $(1, 1, 1)$. Note that the $\boldsymbol{g}$-vector fan is supported by the $\boldsymbol{c}$-vector fan (right).

10.3.3 Non-kissing associahedra

We now construct a polytopal realization of the $\boldsymbol{g}$-vector fan $\mathcal{F}^{\boldsymbol{g}}(\bar{Q})$. This construction is inspired from classical associahedra, constructed by J.-L. Loday [Lod04] and C. Hohlweg and C. Lange [HL07] and the previously constructed accordiohedra of [MP19]. In contrast, it closes the question of the polytopality of the $\boldsymbol{g}$-vector fan of a grid quiver remained open in [GM17a] (although alternative polytopal realizations for the grid-associahedra were constructed in [SSW17] using the dual of a nice triangulation of an order polytope and in [McC17, Sect. 4] by a sequence of suspensions and edge subdivisions). We start with the following notion of kissing number.

Definition 10.38. *For two walks ω, ω' on $\bar{Q}$, let $\kappa(\omega, \omega')$ be the number of kisses of ω to ω'. Note that kisses are counted with multiplicities if ω or ω' pass twice through the same substring. The* kissing number *of ω and ω' is $\mathrm{KN}(\omega, \omega') := \kappa(\omega, \omega') + \kappa(\omega', \omega)$. Since $\mathcal{C}_{\mathrm{nk}}(\bar{Q})$ is finite, we can define the* kissing number *of a walk ω on $\bar{Q}$ as $\mathrm{KN}(\omega) := \sum_{\omega'} \mathrm{KN}(\omega, \omega')$, where the sum runs over all walks ω' on $\bar{Q}$.*

The fundamental property of these kissing numbers are their behavior under the flip operation.

Lemma 10.39. *The kissing number KN of the walks $\omega, \omega', \mu, \nu$ involved in the flip of Proposition 10.10 satisfy the inequality $\mathrm{KN}(\omega) + \mathrm{KN}(\omega') > \mathrm{KN}(\mu) + \mathrm{KN}(\nu)$.*

The following statement thus follows from the combination of Lemmas 10.35 and 10.39 with the characterization of polytopal realizations of a simplicial fan of Proposition 7.28.

Theorem 10.40. *For a locally gentle quiver $\bar{Q}$ with finite non-kissing complex $\mathcal{C}_{\mathrm{nk}}(\bar{Q})$, the $\boldsymbol{g}$-vector fan $\mathcal{F}^{\boldsymbol{g}}(\bar{Q})$ is the normal fan of the* non-kissing associahedron *$\mathbb{A}\mathrm{sso}(\bar{Q})$ defined equivalently as:*

(i) the convex hull of the points $\sum_{\omega \in F} \mathrm{KN}(\omega)\, \boldsymbol{c}(\omega \in F)$ for all facets $F \in \mathcal{C}_{\mathrm{nk}}(\bar{Q})$, or

(ii) the intersection of the halfspaces $\big\{\boldsymbol{x} \in \mathbb{R}^{Q_0} \mid \langle \boldsymbol{g}(\omega) \,|\, \boldsymbol{x} \rangle \le \mathrm{KN}(\omega)\big\}$ for all walks ω on $\bar{Q}$.

Remark 10.41. For path quivers with no relation, we recover the associahedra of C. Hohlweg and C. Lange [HL07]. The latter are obtained by deleting inequalities in the facet description of the classical permutahedron. For an arbitrary locally gentle quiver $\bar{Q}$, the natural generalization of the permutahedron is the *zonotope* $\mathbb{Z}\mathrm{ono}(\bar{Q}) := \sum_\sigma [-\boldsymbol{m}_\sigma, \boldsymbol{m}_\sigma]$ obtained as the Minkowski sum of the multiplicity vectors of all distinguishable strings (or equivalently of all $\boldsymbol{c}$-vectors, with multiplicity). In contrast to the case of path quivers with no relations, observe that:

- The oriented graph of $\mathbb{Z}\mathrm{ono}(\bar{Q})$ is not always the Hasse diagram of a lattice, as observed in [McC17, Rem. 6.2]. The lattice of biclosed sets $\mathrm{Bic}(\bar{Q})$ was designed in [McC17] to play the role of this missing lattice structure on $\mathbb{Z}\mathrm{ono}(\bar{Q})$.
- The non-kissing associahedron $\mathbb{A}\mathrm{sso}(\bar{Q})$ is not always obtained by deleting inequalities in the facet description of the zonotope $\mathbb{Z}\mathrm{ono}(\bar{Q})$. The question to characterize the quivers for which it happens remains open. As shown in [PPP17], a sufficient (but not necessary) condition is that there is no two mutually kissing walks (*i.e.* such that $\kappa(\omega, \omega')\, \kappa(\omega', \omega) > 0$). This includes the situation of the accordion complex of a disk, treated in [MP19].

To illustrate Theorem 10.40 and Remark 10.41, we have represented in Figure 10.12 the non-kissing associahedron $\mathbb{A}\mathrm{sso}(\bar{Q})$ and the zonotope $\mathbb{Z}\mathrm{ono}(\bar{Q})$ for two specific quivers.

To conclude, we observe that our realization of the non-kissing complex has the following relevant property regarding the non-kissing lattice studied in Section 10.2.

Proposition 10.42. *When oriented in the linear direction $\boldsymbol{\omega} := (-1, \dots, -1) \in \mathbb{R}^{Q_0}$, the graph of the non-kissing associahedron $\mathbb{A}\mathrm{sso}(\bar{Q})$ is (isomorphic to) the increasing flip graph of $\bar{Q}$.*

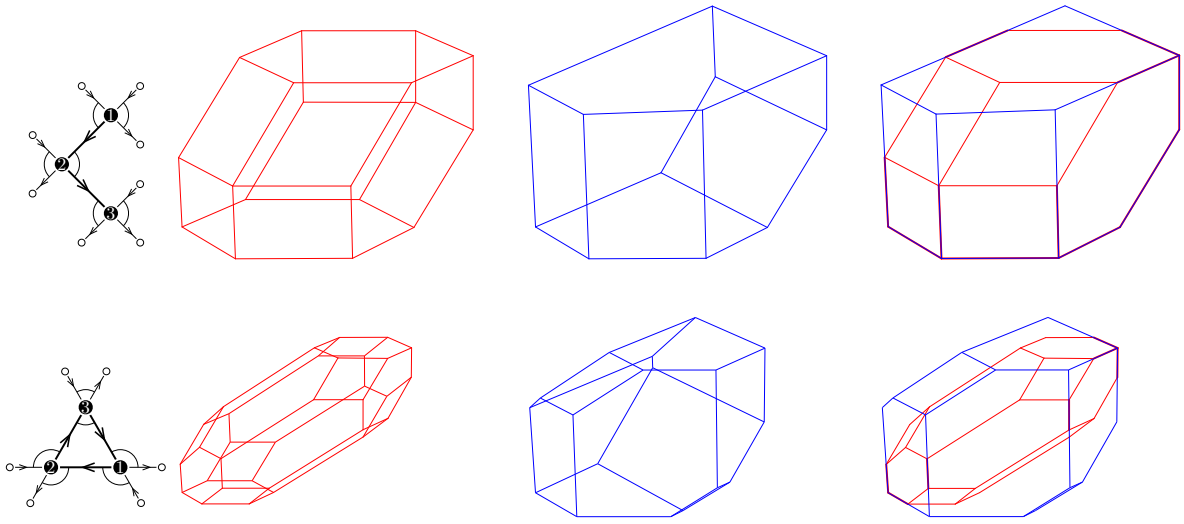

Figure 10.12: The zonotope $\mathbb{Z}\mathrm{ono}(\bar{Q})$ (red, left) and the non-kissing associahedron $\mathbb{A}\mathrm{sso}(\bar{Q})$ (blue, middle) for two specific quivers. Observe that the facet defining inequalities of $\mathbb{A}\mathrm{sso}(\bar{Q})$ are not necessarily facet defining inequalities of $\mathbb{Z}\mathrm{ono}(\bar{Q})$ (right).

10.3.4 Type cones of non-kissing fans

We now briefly discuss how the type cone approach presented in Section 7.3 for the $\boldsymbol{g}$-vector fans of finite type cluster algebras can be partially adapted to the $\boldsymbol{g}$-vector fans of non-kissing complexes. More details can be found in [PPPP19].

First, applying Definition 7.29 and Lemma 10.35, we obtain the following description of the type cone of the $\boldsymbol{g}$-vector fan $\mathcal{F}^{\boldsymbol{g}}(\bar{Q})$ for any gentle quiver $\bar{Q}$. It lives in the vector space $\mathbb{R}^{\mathcal{W}(\bar{Q})}$ indexed by the set $\mathcal{W}(\bar{Q})$ of all walks on $\bar{Q}$.

Corollary 10.43. *For any non-kissing finite gentle quiver $\bar{Q}$, the type cone of $\mathcal{F}^{\boldsymbol{g}}(\bar{Q})$ is given by*

$$\mathbb{TC}\big(\mathcal{F}^{\boldsymbol{g}}(\bar{Q})\big) = \left\{ \boldsymbol{h} \in \mathbb{R}^{\mathcal{W}(\bar{Q})} \;\middle|\; \begin{array}{l} \boldsymbol{h}_\omega = 0 \text{ for any improper walk } \omega \\ \boldsymbol{h}_\omega + \boldsymbol{h}_{\omega'} > \boldsymbol{h}_\mu + \boldsymbol{h}_\nu \text{ for any exchangeable walks } \omega, \omega' \end{array} \right\},$$

where the walks μ and ν for two exchangeable walks ω, ω' are defined in Proposition 10.10.

For instance, the type cone of the fan of Figure 10.11 (top) lives in $\mathbb{R}^8$ and has a linearity space of dimension 3. It has 5 facet-defining inequalities (given below), which correspond to the flips described in Proposition 10.45 and Theorem 10.46 and illustrated in Figure 10.13 (left).

	walks	$\boldsymbol{g}$-vectors								
		$\begin{bmatrix}1\\0\\0\end{bmatrix}$	$\begin{bmatrix}0\\1\\0\end{bmatrix}$	$\begin{bmatrix}0\\0\\1\end{bmatrix}$	$\begin{bmatrix}1\\-1\\0\end{bmatrix}$	$\begin{bmatrix}0\\1\\-1\end{bmatrix}$	$\begin{bmatrix}-1\\0\\0\end{bmatrix}$	$\begin{bmatrix}0\\-1\\0\end{bmatrix}$	$\begin{bmatrix}0\\0\\-1\end{bmatrix}$	
facet		0	−1	1	0	1	0	0	0	Ⓐ
defining		0	1	0	0	−1	0	0	1	Ⓑ
inequalities		−1	0	0	1	1	0	0	−1	Ⓒ
		1	0	0	−1	0	0	1	0	Ⓓ
		0	0	0	1	0	1	−1	0	Ⓔ

The type cone of the fan of Figure 10.11 (bottom) lives in $\mathbb{R}^{11}$ and has a linearity space of dimension 3. It has 9 facet-defining inequalities (given below), which correspond to the flips illustrated in Figure 10.13 (right). In particular, it is not simplicial.

	walks	$\boldsymbol{g}$-vectors	facet defining inequalities	
	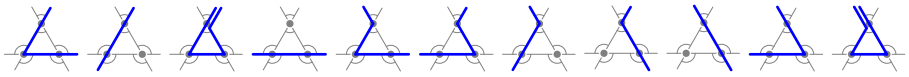	$\begin{bmatrix}1\\0\\0\end{bmatrix}$ $\begin{bmatrix}0\\1\\0\end{bmatrix}$ $\begin{bmatrix}0\\0\\1\end{bmatrix}$ $\begin{bmatrix}1\\-1\\0\end{bmatrix}$ $\begin{bmatrix}1\\0\\-1\end{bmatrix}$ $\begin{bmatrix}0\\-1\\1\end{bmatrix}$ $\begin{bmatrix}0\\1\\-1\end{bmatrix}$ $\begin{bmatrix}-1\\0\\1\end{bmatrix}$ $\begin{bmatrix}-1\\0\\0\end{bmatrix}$ $\begin{bmatrix}0\\-1\\0\end{bmatrix}$ $\begin{bmatrix}0\\0\\-1\end{bmatrix}$		
		-1 1 0 0 1 0 -1 0 0 0 0		Ⓐ
		1 0 0 0 -1 0 0 0 0 0 1		Ⓑ
		0 0 0 1 -1 0 1 0 0 0 0		Ⓒ
		1 0 -1 -1 0 1 0 0 0 0 0		Ⓓ
		0 0 0 -1 1 0 0 0 0 1 -1		Ⓔ
		0 0 1 0 0 -1 0 0 0 1 0		Ⓕ
		0 0 0 1 0 -1 0 1 0 0 0		Ⓖ
		0 0 0 0 0 1 0 -1 1 -1 0		Ⓗ
		0 -1 0 0 0 0 1 1 -1 0 0		Ⓚ

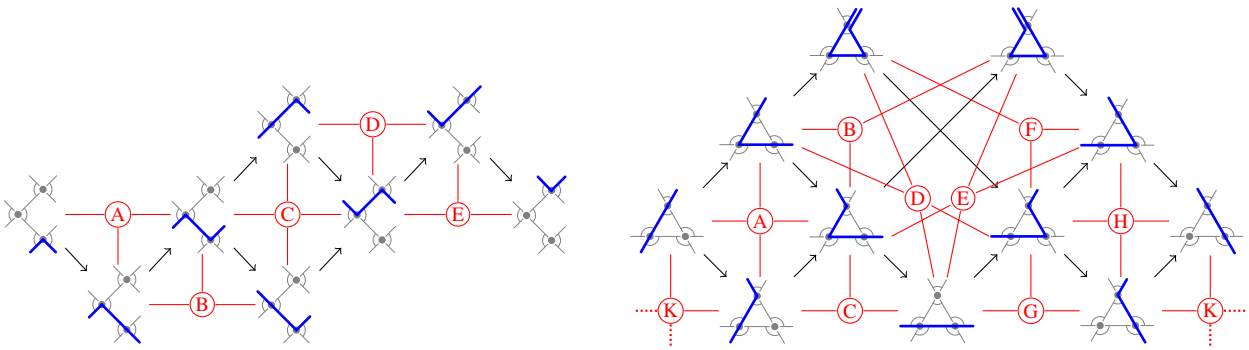

Figure 10.13: The facet-defining inequalities of the type cone $\mathbb{TC}\big(\mathcal{F}^{\boldsymbol{g}}(\bar{Q})\big)$ of the non-kissing fan, represented on the Auslander Reiten quiver of the gentle algebra of $\bar{Q}$. While they correspond to meshes on the left, they are not as clear in the general case as on the right.

As illustrated in this last example, the type cone of the non-kissing fan is not always simplicial and we do not always understand its extremal adjacent pairs. However, the situation is simpler for the following special family of gentle quivers, that contains in particular the grid and dissection quivers of [McC17, GM18], thus the classical associahedron.

Definition 10.44. *A gentle quiver $\bar{Q}$ is called:*

(i) 2-acyclic *if it contains no cycle of length 2,*

(ii) brick *if it satisfies the following three equivalent conditions:*

- *any (non necessarily oriented) cycle of $\bar{Q}$ contains at least two relations in I,*
- *any string of $\bar{Q}$ is distinguishable,*
- *no walk on $\bar{Q}$ is self-kissing.*

For a string σ of $\bar{Q}$, we denote by $\sigma\nwarrow$ (resp. $\sigma\swarrow$) the unique string of the blossoming quiver $\bar{Q}^{\blacktriangle}$ of the form $\sigma\nwarrow = \sigma\alpha_1^{-1}\alpha_2\dots\alpha_\ell$ (resp. $\sigma\swarrow = \sigma\alpha_1\alpha_2^{-1}\dots\alpha_\ell^{-1}$) with $\ell \geq 1$ and $\alpha_1, \dots, \alpha_\ell \in Q_1$ and such that $t(\alpha_\ell)$ (resp. $s(\alpha_\ell)$) is a blossom of $\bar{Q}^{\blacktriangle}$. These notations are motivated by the representation of strings used in [BR87, PPP17], and the terminology usually says that $\sigma\nwarrow$ (resp. $\sigma\swarrow$) is obtained by adding a *hook* (resp. a *cohook*) to σ. We define similarly $\nearrow\sigma$ (resp. $\searrow\sigma$). The walk $\nearrow(\sigma\nwarrow) = (\nearrow\sigma)\nwarrow$ of $\bar{Q}$ is simply denoted by $\nearrow\sigma\nwarrow$, and we define similarly $\searrow\sigma\swarrow$, $\nearrow\sigma\swarrow$ and $\searrow\sigma\nwarrow$.

Proposition 10.45. *For any brick and 2-acyclic gentle quiver $\bar{Q}$ and any string σ on $\bar{Q}$, the walks $\searrow\sigma\swarrow$ and $\nearrow\sigma\nwarrow$ are exchangeable with distinguished substring σ.*

We use these particular exchangeable pairs to describe the type cone of the $\boldsymbol{g}$-vector fan $\mathcal{F}^{\boldsymbol{g}}(\bar{Q})$.

Theorem 10.46. *For any brick and 2-acyclic gentle quiver $\bar{Q}$, the type cone $\mathbb{TC}\big(\mathcal{F}^{\boldsymbol{g}}(\bar{Q})\big)$ is simplicial and the exchanges of Proposition 10.45 precisely correspond to the extremal adjacent pairs of the $\boldsymbol{g}$-vector fan $\mathcal{F}^{\boldsymbol{g}}(\bar{Q})$.*

Combining Corollary 7.33 and Theorem 10.46, we derive the following description of all polytopal realizations of the $\boldsymbol{g}$-vector fan $\mathcal{F}^{\boldsymbol{g}}(\bar{Q})$ for brick 2-acyclic gentle quivers. They are parametrized by the positive orthant $\mathbb{R}_{>0}^{\mathcal{S}(\bar{Q})}$ indexed by the set $\mathcal{S}(\bar{Q})$ of strings of $\bar{Q}$.

Theorem 10.47. *For any brick and 2-acyclic gentle quiver $\bar{Q}$ and any $\boldsymbol{\ell} \in \mathbb{R}_{>0}^{\mathcal{S}(\bar{Q})}$, the polytope*

$$R_{\boldsymbol{\ell}}(\bar{Q}) := \left\{ \boldsymbol{z} \in \mathbb{R}^{\mathcal{W}(\bar{Q})} \;\middle|\; \begin{array}{l} \boldsymbol{z} \geq 0 \quad \text{and} \quad \boldsymbol{z}_\omega = 0 \text{ for any staight walk } \omega \\ \boldsymbol{z}_{\searrow\sigma\swarrow} + \boldsymbol{z}_{\nearrow\sigma\nwarrow} - \boldsymbol{z}_{\nearrow\sigma\swarrow} - \boldsymbol{z}_{\searrow\sigma\nwarrow} = \boldsymbol{\ell}_\sigma \text{ for all } \sigma \in \mathcal{S}(\bar{Q}) \end{array} \right\}$$

is a realization of the non-kissing fan $\mathcal{F}^{\boldsymbol{g}}(\bar{Q})$. Moreover, the polytopes $R_{\boldsymbol{\ell}}(\bar{Q})$ for $\boldsymbol{\ell} \in \mathbb{R}_{>0}^{\mathcal{S}(\bar{Q})}$ describe all polytopal realizations of $\mathcal{F}^{\boldsymbol{g}}(\bar{Q})$.

The question to describe the type cone of the $\boldsymbol{g}$-vector fan $\mathcal{F}^{\boldsymbol{g}}(\bar{Q})$ for arbitrary gentle quivers remains open. See Figure 10.13 (right) for a surprising example.

10.3.5 Coordinate sections and projections

We conclude the chapter with a natural operation on quivers that illustrates a result of [PPS18]. Intuitively, we blind a strict subset of the vertices of a quiver, meaning that we forbid peaks and deeps at these blinded vertices. More formally, this corresponds to the following operation.

Definition 10.48. *Consider a locally gentle quiver $\bar{Q} = (Q, I)$ and a vertex $a \in Q_0$. Denote by $K_a := \{\alpha\beta \,|\, \alpha, \beta \in Q_1 \text{ with } t(\alpha) = s(\beta) = a\}$ the set of paths of length 2 with middle vertex a and let $I_a := K_a \cap I$ and $J_a := K_a \smallsetminus I$. We denote by $\bar{Q}_{\blacktriangleleft v \blacktriangleright} = (Q_{\blacktriangleleft a \blacktriangleright}, I_{\blacktriangleleft a \blacktriangleright})$ the quiver where*

$$(Q_{\blacktriangleleft a \blacktriangleright})_0 = Q_0 \smallsetminus \{a\}, \qquad (Q_{\blacktriangleleft a \blacktriangleright})_1 = \{\alpha \in Q_1 \,|\, s(\alpha) \neq a \neq t(\alpha)\} \cup J_a,$$
$$I_{\blacktriangleleft a \blacktriangleright} = \{\sigma \in I \smallsetminus I_a \,|\, s(\sigma) \neq a \neq t(\sigma)\} \cup \{\alpha\beta\gamma \,|\, \alpha\beta \in I \text{ and } \beta\gamma \in J_a \text{ or } \alpha\beta \in J_a \text{ and } \beta\gamma \in I\}.$$

We say that $\bar{Q}_{\blacktriangleleft a \blacktriangleright}$ is obtained by blinding a in $\bar{Q}$. Finally, for a subset $A = \{a_1, \dots, a_\ell\}$ of Q_0, we let $\bar{Q}_{\blacktriangleleft A \blacktriangleright} := ((\bar{Q}_{\blacktriangleleft a_1 \blacktriangleright})_{\blacktriangleleft a_2 \blacktriangleright} \dots)_{\blacktriangleleft a_\ell \blacktriangleright}$.

The reader is invited to check that the blinded quiver $Q_{\blacktriangleleft a \blacktriangleright}$ is still a locally gentle quiver, that $(Q_{\blacktriangleleft a \blacktriangleright})^{\blacktriangle} = (Q^{\blacktriangle})_{\blacktriangleleft a \blacktriangleright}$, and that $\bar{Q}_{\blacktriangleleft A \blacktriangleright}$ is independent of the ordering of A.

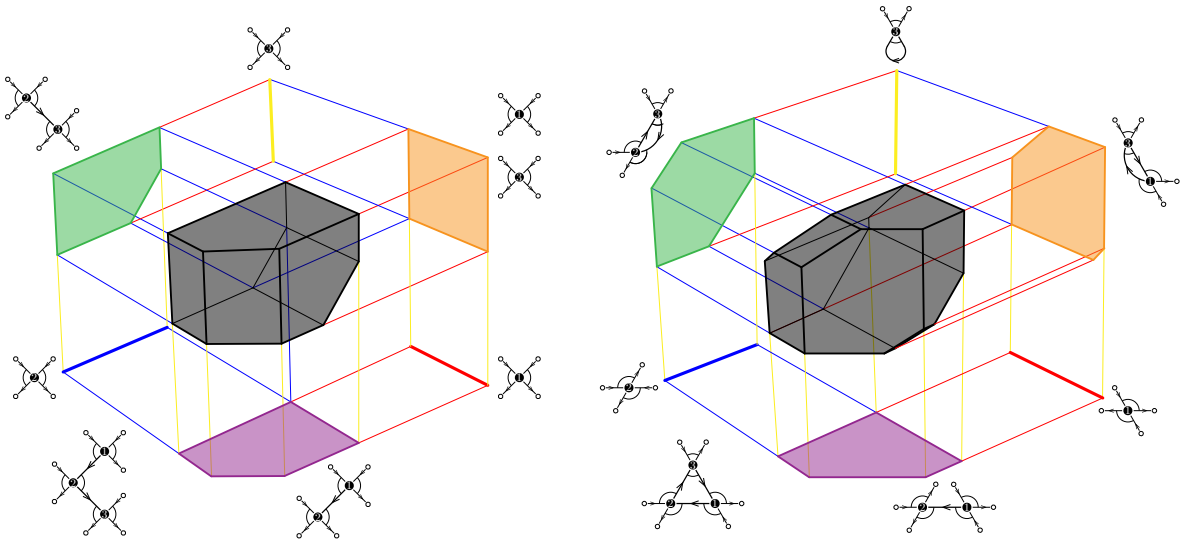

Figure 10.14: All possible coordinate projections of the non-kissing associahedra $\mathbb{A}\mathrm{sso}(\bar{Q})$ for two specific quivers.

Proposition 10.49. *Consider a locally gentle quiver $\bar{Q}$, a subset $A \subsetneq Q_0$, and the quiver $\bar{Q}_{\langle A \rangle}$.*

(i) The non-kissing complex $\mathcal{K}_{\mathrm{nk}}(\bar{Q}_{\langle A \rangle})$ is isomorphic to the subcomplex of the non-kissing complex $\mathcal{K}_{\mathrm{nk}}(\bar{Q})$ induced by walks with no corner at a vertex of A.

(ii) The $\boldsymbol{g}$-vector fan $\mathcal{F}^{\boldsymbol{g}}(\bar{Q}_{\langle A \rangle})$ is the section $\{C \in \mathcal{F}^{\boldsymbol{g}}(\bar{Q}) \,|\, C \subseteq A^\perp\}$ of the $\boldsymbol{g}$-vector fan $\mathcal{F}^{\boldsymbol{g}}(\bar{Q})$ by the coordinate plane $A^\perp := \{\boldsymbol{x} \in \mathbb{R}^{Q_0} \,|\, \langle \boldsymbol{e}_a \,|\, \boldsymbol{x} \rangle = 0 \text{ for all } a \in A\}$.

(iii) When $\mathcal{K}_{\mathrm{nk}}(\bar{Q})$ is finite, the normal fan of the projection of the non-kissing associahedron $\mathbb{A}\mathrm{sso}(\bar{Q})$ to the coordinate plane $A^\perp$ is the $\boldsymbol{g}$-vector fan $\mathcal{F}^{\boldsymbol{g}}(\bar{Q}_{\langle A \rangle})$.

To illustrate Proposition 10.49, we have represented in Figure 10.14 all possible coordinate projections of the non-kissing associahedra $\mathbb{A}\mathrm{sso}(\bar{Q})$ for two specific quivers.

Example 10.50. Consider a triangulation T of a convex polygon and a dissection D whose edges are included in T. Then the dissection quiver $\bar{Q}(D)$ coincides with the blinded quiver $\bar{Q}(T)_{\langle A \rangle}$ where A are the vertices of $\bar{Q}(T)$ corresponding to the diagonals of T not in D. In particular, the $\boldsymbol{g}$-vector fan of any dissection quiver $\bar{Q}(D)$ is a section of the $\boldsymbol{g}$-vector fan of a type A quiver, and is realized by a projection of the associahedron of [HPS18]. See [PPS18].

OPEN PROBLEMS AND PERSPECTIVES

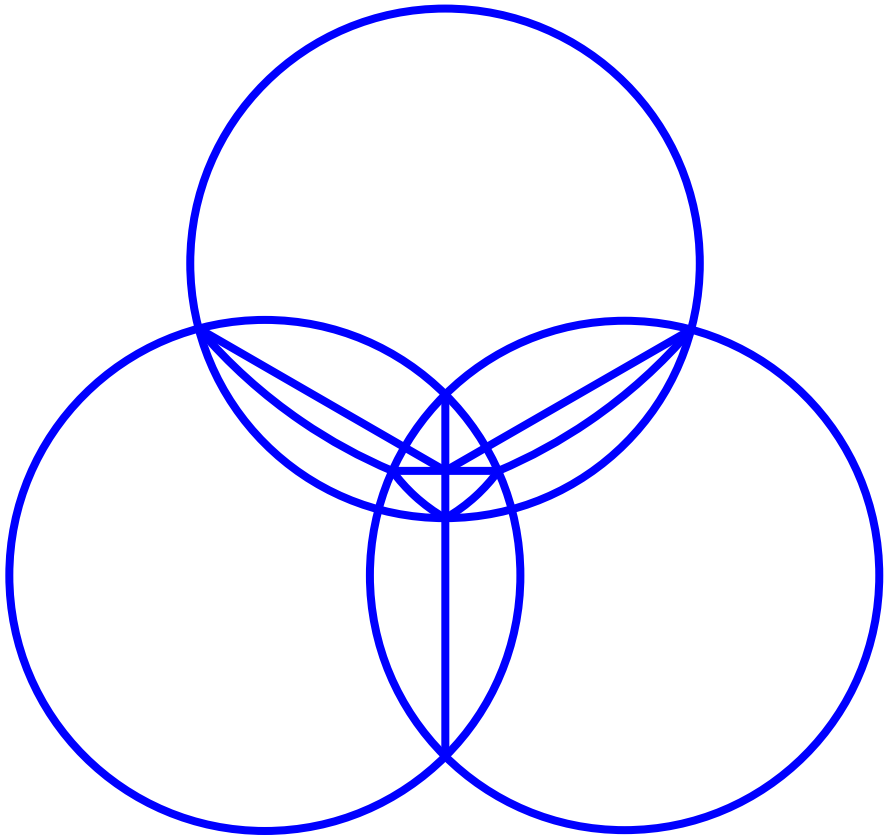

To conclude, we gather some research directions motivated by the material presented in this document. Our presentation is brief and sketchy, as there is still quite some work to make these ideas precise. We believe that some of the problems presented here are good entry points to the topic and provide research projects suitable for Master and PhD students.

A PERMUTREEHEDRA AND QUOTIENTOPES

A.1 Permutreehedra, quotientopes and removahedra

All permutreehedra of Chapter 3 and all quotientopes of Chapter 4 belong to the following family of polytopes introduced by A. Postnikov in [Pos09].

Definition A.1 ([Pos09, PRW08]). *A generalized permutahedron is a polytope whose normal fan coarsens the braid fan* $\mathcal{F}(n)$.

This implies in particular that they are all obtained by gliding inequalities of the permutahedron $\mathbb{P}\mathrm{erm}(n)$ orthogonally to their normal vectors. However, there is an apparent contrast between our constructions of the permutreehedra in Section 3.2.2 and of the quotientopes in Sections 4.2.2 and 4.2.3. Namely, the permutreehedra are constructed in Section 3.2.2 by gliding the inequalities *outside* the permutahedron $\mathbb{P}\mathrm{erm}(n)$, while the quotientopes are constructed in Sections 4.2.2 and 4.2.3 by gliding the inequalities *inside* the permutahedron $\mathbb{P}\mathrm{erm}(n)$. In particular, the fan refinements translates to the following polytope inclusions:

1. for permutahedra, if $\mathcal{F}(\delta)$ refines $\mathcal{F}(\delta')$, then $\mathbb{PT}(\delta)$ is contained in $\mathbb{PT}(\delta')$. For example, the permutahedron $\mathbb{P}\mathrm{erm}(n) = \mathbb{PT}(\bigoplus^n)$ is contained in the associahedron $\mathbb{A}\mathrm{sso}(n) = \mathbb{PT}(\bigotimes^n)$ which is contained in the cube $\mathbb{PT}(\bigotimes^n)$. See Proposition 3.19 and Figure 3.6.
2. for quotientopes, if $\mathcal{F}(\equiv)$ refines $\mathcal{F}(\equiv')$, then $\mathbb{QT}^f(\equiv)$ contains $\mathbb{QT}^f(\equiv')$. For example, the permutahedron (quotientope of the finest congruence) contains all quotientopes, while the cube (quotientope of the coarsest congruence) is contained in all quotientopes (as usual, we only consider the congruences $\equiv$ such that $\mathcal{F}(\equiv)$ is essential). See Remark 4.9 and Figure 4.5.

In fact, as the classical construction of the associahedron [Lod04] and its generalizations [HL07, LP18, Pil13], the permutreehedra are obtained by just forgetting some facets of the permutahedron $\mathbb{P}\mathrm{erm}(n)$, and thus belong to the following special family of polytopes studied in [Pil17].

Definition A.2 ([Pil17]). *A removahedron is a polytope obtained by deleting inequalities from the facet description of the permutahedron* $\mathbb{P}\mathrm{erm}(n)$.

The similar construction fails for arbitrary quotientopes: already when $n = 4$, there exists a lattice congruence $\equiv$ of the weak order on $\mathfrak{S}_n$ for which the quotient fan $\mathcal{F}(\equiv)$ is not the normal fan of the corresponding removahedron (defined by all inequalities of the permutahedron $\mathbb{P}\mathrm{erm}(n)$ normal to the rays of $\mathcal{F}(\equiv)$). In fact, we believe that this gives one more characterization of the permutree congruences (the equivalence between the points (i), (ii) and (iii) below is known and was already mentioned in Example 4.5).

Conjecture A.3. *Consider a lattice congruence $\equiv$ of the weak order on $\mathfrak{S}_n$ whose arcs include the basic arcs $(i, i+1, n, \varnothing)$ so that $\mathcal{F}(\equiv)$ is essential. Then the following conditions are equivalent:*

(i) *$\equiv$ is the δ-permutree congruence $\equiv_\delta$ for some decoration $\delta \in \{\bigoplus, \bigotimes, \bigotimes, \bigotimes\}^n$,*
(ii) *the arcs of $\mathcal{I}_\equiv$ are all arcs that do not cross some fixed vertical walls above and/or below the points of $[n]$,*
(iii) *the forcing maximal arcs not in $\mathcal{I}_\equiv$ are all of the form $(i-1, i+1, n, \varnothing)$ and $(i-1, i+1, n, \{i\})$,*
(iv) *the quotient fan $\mathcal{F}(\equiv)$ is the normal fan of its removahedron, defined by all inequalities of the permutahedron $\mathbb{P}\mathrm{erm}(n)$ normal to the rays of $\mathcal{F}(\equiv)$.*

A.2 Permutreehedra for finite Coxeter groups

As illustrated by Chapter 3 and Conjecture A.3, the permutree congruences are very relevant and well-behaved lattice congruences of the weak order on $\mathfrak{S}_n$. It is tempting to explore similar congruences of the weak order on any arbitrary finite Coxeter group, in the same spirit as the Cambrian congruences defined by N. Reading in [Rea06]. For this, recall that for any finite Coxeter group W, the Cambrian congruences can be characterized as the minimal lattice congruences of the weak order on W (in the congruence lattice of the weak order on W) that contract exactly one boundary of each polygon of the W-permutahedron containing the fundamental point. This motivates the following definition, which fits to the type A situation [PP18, Rem. 2.16].

Definition A.4. *For any finite Coxeter group W, the permutree congruences are the minimal lattice congruences of the weak order on W that contract some (either none, one, or both) of the boundaries of each polygon of the W-permutahedron containing the fundamental point.*

Note that the non-trivial (*i.e.* non-square) polygons of the W-permutahedron containing the fundamental point correspond to the non-trivial rank 2 standard parabolic subgroups of W, or equivalently to the edges of the Dynkin diagram of W. Therefore, the permutree congruences of the weak order on W can be encoded by a decoration δ on the edges of the Dynkin diagram of W.

As any lattice congruence of the weak order on W, such a permutree congruence $\equiv_\delta$ defines a quotient fan $\mathcal{F}(\delta)$ obtained by glueing together the chambers of the Coxeter arrangement corresponding to elements in the same congruence class for $\equiv_\delta$. One of the natural questions is to realize the quotient fan $\mathcal{F}(\delta)$ using the same method as in Section 3.2.2.

Conjecture A.5. *For any permutree congruence $\equiv_\delta$ of any finite Coxeter group W, the quotient fan $\mathcal{F}(\delta)$ is the normal fan of the corresponding removahedron.*

Note that this conjecture holds in three particular situations:

- in type A for any permutree congruence by the construction of Section 3.2.2,
- in type B for any permutree congruence by recent work on type B lattice congruences [PPR20],
- in any type for the Cambrian congruences of [Rea06] by the construction of the generalized associahedra of [HLT11].

Another promising direction of research is to explore the corresponding Coxeter combinatorics. The minimal and maximal elements of W in their congruence classes should be interpreted in terms of specific properties of their inversion sets and of their reduced expressions, exactly as aligned and sortable elements for the Cambrian congruences. Bijections with other objects (in particular generalizations of non-crossing partitions of W) should also appear using canonical join representations as in Section 4.1.

Finally, one can even imagine to extend permutree congruences beyond Coxeter groups, in at least two relevant situations:

- On the one hand, Definition A.4 extends to an arbitrary hyperplane arrangement $\mathcal{H}$ whose poset of region is a lattice, and Conjecture A.5 could still hold replacing permutahedra by any zonotope realizing $\mathcal{H}$, or even any polytopal realization of $\mathcal{H}$. Indeed, it turns out that the type A (and even type B) permutreehedra can be obtained as removahedra starting not only from the classical permutahedron $\mathbb{P}\mathrm{erm}(n)$, but from any polytopal realization of the braid arrangement.
- On the other hand, following the work of [Pil13] on signed tree associahedra, it is certainly possible to define a relevant notion of graph permutreehedra which would provide a common generalization of the graph associahedra of [CD06] and of the permutrees of [PP18]. Given

a graph whose vertices are decorated by $\{\textcircled{\scriptsize |}, \textcircled{\scriptsize Y}, \textcircled{\scriptsize \&}, \textcircled{\scriptsize *}\}$, the G-permutreehedron would have vertices corresponding to trees with nodes labeled by the vertices of G and local rules around each node given by the decoration of the corresponding vertex in G. The classical graph associahedra would correspond to the case when each vertex is decorated by $\textcircled{\scriptsize Y}$, and the classical permutrees would correspond to the case when the graph is a path. While we already have a natural definition for chordful graphs (*a.k.a.* block graphs, *i.e.* containing all chords of their cycles), the situation of general graphs is still mysterious.

A.3 Quotientopes for hyperplane arrangements

Consider a central hyperplane arrangement $\mathcal{H}$ defining a fan $\mathcal{F}$, and a distinguished base region B of $\mathcal{F}$. Recall from Section 5.3.1 that the poset of regions $\mathsf{R}(\mathcal{H}, B)$ is the poset whose elements are the regions of $\mathcal{F}$ ordered by inclusion of separating sets (the set of hyperplanes of $\mathcal{H}$ that separate the given region form the base region B). By the work of A. Björner, P. Edelman and G. Ziegler [BEZ90], we know that $\mathsf{R}(\mathcal{H}, B)$ is always a lattice when the fan $\mathcal{F}$ is simplicial, and that the chamber B must be simplicial for $\mathsf{R}(\mathcal{H}, B)$ to be a lattice. See also the survey of N. Reading [Rea16b] for further conditions, in particular a discussion on tight arrangements. We assume here that $\mathsf{R}(\mathcal{H}, B)$ is a lattice.

Consider now a lattice congruence $\equiv$ of the poset of regions $\mathsf{R}(\mathcal{H}, B)$. In the same spirit as Theorem 4.6, N. Reading proved in [Rea05] that the lattice congruence $\equiv$ defines a complete fan $\mathcal{F}(\equiv)$ obtained by glueing together the cones of the fan $\mathcal{F}$ that belong to the same congruence class of $\equiv$. Even if it is certainly a bit adventurous at this point, we conjecture that the polytopality of this quotient fan holds at this level of generality.

Conjecture A.6. *For any central hyperplane arrangement $\mathcal{H}$ defining a fan $\mathcal{F}$ and any base region B of $\mathcal{F}$ such that the poset of regions $\mathsf{R}(\mathcal{H}, B)$ is a lattice, and for any lattice congruence $\equiv$ of the poset of regions $\mathsf{R}(\mathcal{H}, B)$, the quotient fan $\mathcal{F}(\equiv)$ is the normal fan of a polytope.*

In the construction of Section 4.2.2 and its proof presented in [PS19], we benefited from three specific features of the type A Coxeter arrangement:

- we used the simpliciality of the arrangement,
- we used the action of $\mathfrak{S}_n$ to transport our understanding of the linear dependencies from the initial chamber to any other chamber,
- these linear dependencies are very simple in type A (only 3 or 4 terms and $0/1$ coefficients).

These properties hold for any finite Coxeter group (for the last property though, the linear dependencies can get up to 5 terms, and some coefficients equal to 2 appear in non-simply-laced types). This suggests to focus the search for a construction for Conjecture A.6 to Coxeter arrangements.

The next case beyond type A is the type B_n arrangement. The combinatorics of the congruences of the type B_n weak order can be described in terms of centrally symmetric configurations of arcs of type A_{2n-1}. In particular, some type B_n lattice quotients can be understood as centrally symmetric type A_{2n-1} quotients, and the corresponding type B_n quotient fans can be obtained as normal fans of the intersection of type A_{2n-1} quotientopes with the centrally symmetric plane $\left\{\boldsymbol{x} \in \mathbb{R}^{2n-1} \,\middle|\, x_i = x_{2n-i} \text{ for } i \in [n-1]\right\}$. However, the forcing relations among type B_n shards are more subtle than just the centrally symmetric forcing relations of type A_{2n-1}, so that most type B_n quotients have no type A_{2n-1} counterparts (type B_2 already provides interesting examples). Nevertheless, adapting the approach of Section 4.2.3, we have recently managed to realize all type B_n quotient fans [PPR20] (the proof requires some polishment, but the construction has at least been computationally confirmed for the 4, 20, 72 and 232 type B_n principal congruences for $n = 2$, 3, 4 and 5, and thus for all type B_n lattice congruences up to $n = 5$).

Note that the tool of shards is still available in the general context of hyperplane arrangements. Shards are defined geometrically as pieces of the hyperplanes of $\mathcal{H}$, obtained after certain cuts. Namely, for each codimension 2 face F of the arrangement, consider the subarrangement $\mathcal{H}_F$ of all hyperplanes of $\mathcal{H}$ containing F, and cut all non-basic hyperplanes of $\mathcal{H}_F$ by the basic hyperplanes of $\mathcal{H}_F$ (*i.e.* the hyperplanes bounding the region of $\mathcal{H}_F$ containing the base region B). The shards are the pieces that remain once the cuts corresponding to all codimensioin 2 faces of $\mathcal{H}$ have been performed. Moreover, these cuts define a forcing graph on shards (which might have cycles), and the congruences of the poset of regions $\mathsf{R}(\mathcal{H}, B)$ are closely related to the subsets of shards that are closed in this graph (we skip here the precise statements, see [Rea16b, Sect. 9-7.3] for details).

The first tempting direction to prove Conjecture A.6 in full generality is to follow the approach of Section 4.2.2. The starting observation is that the fan $\mathcal{F}$ of any hyperplane arrangement $\mathcal{H}$ is the normal fan of a zonotope described:

- either as the Minkowski sum of arbitrary normal vectors of the hyperplanes of $\mathcal{H}$,
- or by the inequalities of the form $\langle \boldsymbol{r} \,|\, \boldsymbol{x} \rangle \leq h_{\boldsymbol{r}}$ for each ray $\boldsymbol{r}$ of $\mathcal{F}$, where $h_{\boldsymbol{r}}$ is the sum of the distances of $\boldsymbol{r}$ to all hyperplanes of $\mathcal{H}$.

Indeed, this holds for a single hyperplane H and therefore for a hyperplane arrangement since the normal fan of a Minkowski sum is the common refinement of the normal fans of the summands. The idea hidden behind the construction of Section 4.2.2 is to split the contribution of each hyperplane $H \in \mathcal{H}$ to the height $h_{\boldsymbol{r}}$ (*i.e.* the distance of $\boldsymbol{r}$ to H) into the shards contained in H. To mimic this for arbitrary hyperplane arrangements, we initially thought that we could use the subarrangement of $\mathcal{H}$ formed by the hyperplanes that cut the hyperplane H. Namely, a shard Σ should contribute to a ray $\boldsymbol{r}$ only if $\boldsymbol{r}$ lies in the region containing Σ in the subarrangement formed by the hyperplanes of $\mathcal{H}$ cutting Σ. This precisely corresponds to the description of Section 4.2.2 when $\mathcal{H}$ is the braid arrangement. However, already in type B_3, it might happen that a ray that is not in a hyperplane H lies outside the regions of all the shards contained in H. The precise repartition of the contributions thus remains unclear.

Another tempting direction to Conjecture A.6 is to follow the approach of Section 4.2.3. The difficulty here is to create the shard polytope of a given shard Σ, *i.e.* a polytope whose normal fan would contain the shard Σ and would be contained in the union of the shards forced by Σ. In the construction of Section 4.2.3 in type A, we use the very convenient combinatorial model of alternating matchings, and one of the key hidden points was that all differences between the characteristic vectors of two alternating matchings connected by an edge were roots. In the general situation of hyperplane arrangements, we will have to play with the geometry of the normal vectors of the hyperplanes.

A.4 Type cones of quotient fans

We have seen in Section 7.3 that it is sometimes possible to understand the type cone of a fan (*i.e.* the space of all its polytopal realizations), and that this approach is particularly interesting when this type cone is simplicial as in Sections 7.3.2 and 10.3.4.

The type cones of quotient fans are particularly tempting to study since:

- coarsenings of fans translate to faces of type cones: if $\mathcal{F}$ refines $\mathcal{G}$, then $\mathbb{TC}(\mathcal{G})$ is a face of $\mathbb{TC}(\mathcal{F})$.
- the type cone of the braid arrangement is well understood: it is given by the space of submodular functions on $[n]$, *i.e.* functions $h : 2^{[n]} \to \mathbb{R}$ such that $h(A) + h(B) > h(A \cap B) + h(A \cup B)$ for any distinct $A, B \subseteq [n]$.

Unfortunately, we have no description of the type cone of quotient fans at the moment. We do not even know which quotient fans have a simplicial type cone. Another intriguing question is the relation between the shard polytopes of Section 4.2.3 and the rays of the type cone of the quotient fans.

A first step to approach these type cones is to understand them for subfamilies of quotient fans. For instance, the permutree fans of Chapter 3 is already interesting. In this case, one can show that the wall-crossing inequalities are just some submodular inequalities.

Proposition A.7. *Consider a decoration $\delta \in \{\textcircled{\scriptsize I}, \textcircled{\scriptsize Y}, \textcircled{\scriptsize X}, \otimes\}^n$ and two proper subsets R and R' of $[n]$. If the two rays $\mathbf{r}(R)$ and $\mathbf{r}(R')$ are exchanged in two adjacent maximal cones C and C' of the δ-permutree fan, then both $\mathbf{r}(R \cap R')$ and $\mathbf{r}(R \cup R')$ are also rays of both C and C'. Therefore the facet defining inequalities of the type cone of the δ-permutree fan are some submodular inequalities.*

Understanding precisely which pairs of subsets R, R' of $[n]$ correspond to a facet of the type cone of the δ-permutree fan is more challenging. The first step is to understand the pairs of exchangeable rays of the δ-permutree fan.

Lemma A.8. *A proper subset R of $[n]$ corresponds to a ray of the δ-permutree fan if and only if for all $i < j < k$, if $i, k \in R$ and $j \notin R$ then $\delta_j \in \{\textcircled{\scriptsize I}, \textcircled{\scriptsize X}\}$, and if $i, k \notin R$ and $j \in R$ then $\delta_j \in \{\textcircled{\scriptsize I}, \textcircled{\scriptsize Y}\}$.*

Lemma A.9. *Two proper subsets R and R' of $[n]$ satisfying the conditions of Lemma A.8 correspond to two exchangeable rays of the δ-permutree fan if and only if (up to exchanging R and R'):*

- *$i := \max(R \smallsetminus R') < \min(R' \smallsetminus R) =: j$,*
- *$\delta_i \neq \textcircled{\scriptsize I}$ or $|R \smallsetminus R'| = 1$, and $\delta_j \neq \textcircled{\scriptsize I}$ or $|R' \smallsetminus R| = 1$,*
- *for all $i < k < j$, if $k \in R \cap R'$ then $\delta_k \in \{\textcircled{\scriptsize I}, \textcircled{\scriptsize Y}\}$ and if $k \notin R \cap R'$ then $\delta_k \in \{\textcircled{\scriptsize I}, \textcircled{\scriptsize X}\}$.*

We now arrive to the following conjectural description of the type cone of the δ-permutree fan.

Conjecture A.10. *The submodular inequality given by two proper subsets R and R' of $[n]$ defines a facet of the type cone of the δ-permutree fan if and only if R and R' satisfy:*

- *the conditions of Lemma A.8 to be rays of the δ-permutree fan,*
- *the conditions of Lemma A.9 to be exchangeable rays of the δ-permutree fan,*
- *the additional condition $\delta_i = \otimes$ or $|R \smallsetminus R'| = 1$, and $\delta_j = \otimes$ or $|R' \smallsetminus R| = 1$.*

This conjecture (checked computationally) would imply in particular the following one.

Conjecture A.11. *The type cone of the δ-permutree fan is simplicial if and only if $\delta \in \{\textcircled{\scriptsize Y}, \textcircled{\scriptsize X}, \otimes\}^n$.*

A.5 Schröderization for quotientopes

We finally briefly mention a direction of research related to the faces of the quotientopes in relation to the construction of Hopf algebras on faces of all quotientopes.

As already mentioned, it is well known that the faces of the permutahedron $\mathbb{P}\mathrm{erm}(n)$ are in bijection with ordered partitions of $[n]$ and admit a lattice structure, called pseudopermutahedron [KLN+01] or facial weak order [DHP18], extending the classical weak order on permutations. See Chapter 5. Moreover, any lattice congruence $\equiv_{\mathsf{W}}$ of the classical weak order gives rise to a lattice congruence $\equiv_{\mathsf{F}}$ of the facial weak order, whose classes correspond to the faces of the quotientope $\mathbb{QT}(\equiv_{\mathsf{W}})$. The lattice structure of the faces of the quotientope are therefore clearly understood via lattice quotients of the facial weak order.

In contrast, the construction of Hopf algebra structures on all faces of all quotientopes still requires some work. In [Cha00], F. Chapoton constructed Hopf algebras on all faces of the permutahedra, of the associahedra and of the cubes generalizing the Hopf algebras presented in Section 1.3. This construction was extended to Hopf algebras on faces of all permutreehedra (simultaneously) in [PP18]. It would be interesting to develop combinatorial models similar to non-crossing arc diagrams and to construct Hopf structures similar to that of Section 4.3 for all faces of all quotientopes.

B PIPE DREAMS AND SUBWORD COMPLEXES

B.1 Lattices of acyclic pipe dreams

We have seen in Chapter 2 that the increasing flip graphs on acyclic k-twists is the Hasse diagram of the quotient of the weak order by the k-twist congruence (defined by the fibers of the k-twist correspondence). This is a specific example of a more general statement on pipe dreams. Recall that a *pipe dream* P is a filling of a triangular shape with crosses $+$ and elbows $\curvearrowright$ so that all pipes entering on the left side exit on the top side. We only consider *reduced* pipe dreams, where two pipes cross at most once. We label the pipes of P by $[m]$ from bottom to top, and denote $\omega(P)$ the order of the pipes on the top of the triangle, from left to right. For instance, a (k, n)-twist can be seen as a pipe dream with $n+2k$ pipes and $\omega(P) = (2k+n)\dots(k+n+1)(k+1)\dots(k+n)k\dots 1$. The *contact graph* of a pipe dream is the directed multigraph whose vertices are the pipes and with an arc from the SE-pipe to the WN-pipe of each elbow. A pipe dream is *acyclic* if its contact graph is. Pipe dreams are connected via *flips*, exchanging an elbow between two pipes with the unique cross between these two pipes. We observed the following statement in joint work with N. Bergeron and C. Ceballos (unpublished).

Theorem B.1. *For any permutation $\omega \in \mathfrak{S}_m$, the increasing flip graph on the acyclic pipe dreams P with $\omega(P) = \omega$ is a lattice quotient of the interval $[e, \omega]$ of the weak order.*

The idea is that a pipe dream corresponds to an interval of the weak order given by the linear extensions of its contact graph, which all belong to the interval $[e, \omega]$. This can also be phrased using an insertion algorithm, similar to that of Section 2.1.2. This statement can be extended to subword complexes in arbitrary finite Coxeter groups as follows.

Conjecture B.2. *For any finite Coxeter group W, any Coxeter element c of W and any element $w \in W$, the increasing flip poset on the acyclic facets of the subword complex $\mathcal{C}_{\mathrm{sub}}(w_\circ(c), w)$ is a lattice quotient of the interval $[e, w]$ of the weak order on W.*

Here, a facet F of the subword complex $\mathcal{C}_{\mathrm{sub}}(w_\circ(c), w)$ is called *acyclic* if its root configuration $\boldsymbol{R}(F)$ is pointed. The hope is that for any facet F of $\mathcal{C}_{\mathrm{sub}}(w_\circ(c), w)$, the set of elements $w \in W$ such that the root cone $\mathbb{R}_{\leq 0}\boldsymbol{R}(F)$ contains the chamber $\mathbb{R}_{\geq 0}w(\Delta)$ forms an interval of the weak order, and that these intervals define a lattice congruence of the weak order on the interval $[e, w]$. This conjecture is confirmed by computational experiments. A first combinatorial objective is to study Conjecture B.2 in type A, *i.e.* for all Cambrian shapes described in the preprint version of [Pil18].

Note that Conjecture B.2 is a particular instance of several tempting statements on lattice properties of subword complexes. Indeed, one can vary several parameters:

- consider only pipe dreams in type A or all subword complexes for any finite Coxeter groups,
- consider only the acyclic facets or all facets of the subword complex,
- consider only the specific words $w_0(c)$ or all possible words,
- consider all increasing flips or only chute moves (certain very specific flips).

The general situation where we consider the increasing flip order on all facets of the subword complex $\mathcal{C}_{\mathrm{sub}}(M)$ is not necessarily a lattice quotient as discussed in Section 8.2.2.2. In Conjecture B.2, we use both that the specificity of the word $w_\circ$ defining the subword complex $\mathcal{C}_{\mathrm{sub}}(w_\circ(c), w)$ and the acyclicity of the facets. Another situation where we might obtain a lattice is the situation when we consider all facets but only the chute moves.

B.2 Compatibility degrees for subword complexes

Compatibility degrees and denominator vectors in finite type cluster algebras. As already mentioned in Theorem 7.2, for any initial seed $(B_\circ, P_\circ, X_\circ)$, any cluster variable x of $\mathcal{A}(B_\circ, P_\circ)$ can be written as a Laurent polynomial $x = F(X_\circ)/\prod_{y\in X_\circ} y^{d_{yx}}$, where $d_{yx} \in \mathbb{N}$ and F is a polynomial not divisible by any variable of $X_\circ$. This enables to define the following denominator vector associated to each cluster variable.

Definition B.3 ([FZ02])**.** *The* $\boldsymbol{d}$*-vector* $\boldsymbol{d}(B_\circ, x)$ *of a cluster variable* $x \in \mathcal{A}(B_\circ, P_\circ)$ *is the vector* $\boldsymbol{d}(B_\circ, x) := \sum_{y\in X_\circ} d_{yx}\alpha_y$ *of exponents of the denominator of* x *written as a Laurent polynomial in the variables of* $X_\circ$*. Note that the* $\boldsymbol{d}$*-vector of an initial cluster variable* $x \in X_\circ$ *is the corresponding negative root* $\boldsymbol{d}(B_\circ, x) = -\alpha_x$*. Finally, we denote by* $\boldsymbol{d}(B_\circ, \Sigma) := \{\boldsymbol{d}(B_\circ, x) \,|\, x \in \Sigma\}$ *the set of* $\boldsymbol{d}$*-vectors of a seed* Σ *of* $\mathcal{A}(B_\circ, P_\circ)$*.*

For finite type cluster algebras, the denominator vectors are extremely useful. Namely, it was proved in [FZ03a] that if we start from a finite type bipartite initial seed:

- the $\boldsymbol{d}$-vectors define a bijection from cluster variables to almost positive roots, and
- the coefficient d_{yx} coincides with the *compatibility degree* $(\alpha_y \parallel \boldsymbol{d}(B_\circ, x))$ of [FZ03b, Sect. 3.1].

These results were extended to any initial acyclic seed (see *e.g.* [Kel11, Thm. 3.1 & Sect. 3.3]), and the connection between denominator vectors and compatibility degrees even hold for any initial seed (acyclic or not), as shown in [CP15b]. We thus prefer the notation $(x \parallel y)$ instead of d_{xy}. We think of the compatibility degree $(x \parallel y)$ as a sort of measure of the incompatibility of the variables x and y in the cluster complex. Namely, it enables to characterize compatible and exchangeable cluster variables.

Proposition B.4. *For any distinct cluster variables* x, y *in a finite type cluster algebra:*
(i) $(x \parallel y) \geq 0$*,*
(ii) $(x \parallel y) = 0 \iff (y \parallel x) = 0 \iff$ *x and y are compatible (i.e. in a common cluster),*
(iii) $(x \parallel y) = 1 = (y \parallel x) \iff$ *x and y are exchangeable (i.e. in two adjacent clusters).*

Moreover, the compatibility degree has the following symmetry property.

Proposition B.5. *If* $D := [(x \parallel y)]_{x,y\in\mathcal{X}(B_\circ)}$ *is the compatibility matrix of* $\mathcal{C}_{\mathrm{clu}}(B_\circ)$*, and* $D^\vee$ *is the compatibility matrix of the dual cluster complex* $\mathcal{C}_{\mathrm{clu}}(B_\circ^\vee)$*, then* $D^\vee = D^T$*.*

We conclude this short recollections on $\boldsymbol{d}$-vectors with the following geometric conjecture, already mentioned in [CSZ15, Qu. 5.13], and illustrated in Figure B.15. This conjecture is proved in [FZ03a] for the bipartite initial cluster, in [Ste13] for all acyclic initial clusters, in [CSZ15, Sect. 5] for any initial cluster in type A, and in [MP17] for any initial cluster in type B and C.

Conjecture B.6. *For any finite type exchange matrix* $B_\circ$*, the cones* $\{\mathbb{R}_{\geq 0}\,\boldsymbol{d}(B_\circ, \Sigma) \,|\, \Sigma$ *seed of* $\mathcal{A}(B_\circ)\}$*, together with all their faces, form a polytopal complete simplicial fan* $\mathcal{F}^{\boldsymbol{d}}(\bar{Q})$*, called the* $\boldsymbol{d}$*-vector fan.*

Compatibility degree in root independent subword complexes. Consider now a root independent subword complex $\mathcal{C}_{\mathrm{sub}}(M)$. For any position $j \in [m]$, we can thus decompose the root $\boldsymbol{r}(I, j)$ on the basis $\boldsymbol{R}(I)$ as $\boldsymbol{r}(I, j) := \sum_{i\in I} \lambda(I, i, j)\boldsymbol{r}(I, i)$. We are interested in the coefficients $\lambda(I, i, j)$.

Proposition B.7. *The coefficients* $\lambda(I, i, j)$ *are independent of the choice of the reference facet* I*.*

Definition B.8. *The compatibility degree of two vertices* i, j *of* $\mathcal{C}_{\mathrm{sub}}(M)$ *is* $(i \parallel j) := (-1)^{i\geq j}\lambda(I, i, j)$*. The compatibility vector* $\boldsymbol{d}(I, j)$ *of a position* $j \in [m]$ *with respect to the facet* I *of* $\mathcal{C}_{\mathrm{sub}}(M)$ *is the vector* $\boldsymbol{d}(I, j) := \sum_{i\in I}(i \parallel j)\boldsymbol{r}(I, i)$*. We denote by* $\boldsymbol{d}(I, J) := \{\boldsymbol{d}(I, j) \,|\, j \in J\}$ *the set of compatibility vectors of a face* J *of* $\mathcal{C}_{\mathrm{sub}}(M)$*.*

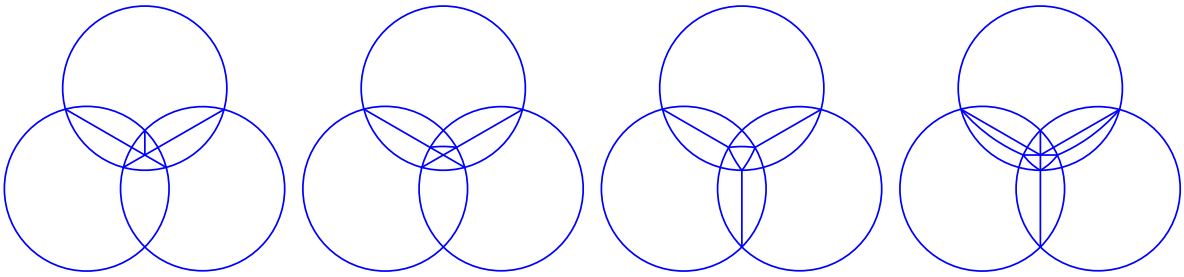

Figure B.15: The $\boldsymbol{d}$-vector fan $\mathcal{F}^{\boldsymbol{d}}(B_\circ)$ for all type A_3 and the cyclic type C_3 initial exchange matrices of Figure 7.1. Each 3-dimensional fan is intersected with the unit sphere and stereographically projected to the plane from the pole $(-1,-1,-1)$.

Conjecture B.9. *For any distinct vertices i, j of the subword complex $\mathcal{C}_{\mathrm{sub}}(M)$:*
(i) $(i \parallel j) \geq 0$,
(ii) $(i \parallel j) = 0 \iff (j \parallel i) = 0 \iff$ *i and j are compatible (i.e. in a common facet of $\mathcal{C}_{\mathrm{sub}}(M)$),*
(iii) $(i \parallel j) = 1 = (j \parallel i) \iff$ *i and j are exchangeable (i.e. in two adjacent facets of $\mathcal{C}_{\mathrm{sub}}(M)$).*

Conjecture B.10. *For any vertices i, j of $\mathcal{C}_{\mathrm{sub}}(M)$, we have $(i \parallel j)\, a_{q_j q_i} = (j \parallel i)\, a_{q_i q_j}$, where $[a_{st}]_{s,t\in S}$ is the Cartan matrix. In other words, if $M^\vee$ is the same word as M but on the dual root system, then the compatibility matrices $D := [(i \parallel j)]_{i,j}$ of $\mathcal{C}_{\mathrm{sub}}(M)$ and $D^\vee$ of $\mathcal{C}_{\mathrm{sub}}(M^\vee)$ satisfy $D^\vee = D^T$.*

Example B.11. In type A, a reference facet I of $\mathcal{C}_{\mathrm{sub}}(M)$ gives a spanning tree of $[n+1]$. For any position $j \notin I$, there is a unique cycle in $I \cup j$. The coefficient $\lambda(I, i, j)$ is ± 1 if i appears in this cycle, and 0 otherwise. T. Manneville proved (personal notes) using braid relations on M that in a root independent subword complex of type A, any two distinct positions are either compatible or exchangeable. This is equivalent to Conjecture B.9 and implies Conjecture B.10.

Example B.12. For any Coxeter element c, the isomorphism of Theorem 8.26 sends the compatibility degree in the subword complex $\mathcal{C}_{\mathrm{sub}}(cw_\circ(c))$ to the compatibility degree in the cluster complex $\mathcal{C}_{\mathrm{clu}}(B_\circ)$. Therefore, Conjectures B.9 and B.10 hold by Propositions B.4 and B.5.

An important property to manipulate the compatibility degrees of Definition B.8 is their behavior with respect to the flips, meaning the relation between the compatibility degrees of two exchangeable positions. Note that we can here perform a flip on both sides of the compatibility degree.

Proposition B.13. *Consider two adjacent facets I_1, I_2 of $\mathcal{C}_{\mathrm{sub}}(M)$, with $I_1 \smallsetminus i_1 = I_2 \smallsetminus i_2$ for $i_1 < i_2$, and a vertex j of $\mathcal{C}_{\mathrm{sub}}(M)$. Then $(i_1 \parallel j) + (i_2 \parallel j) = \sum_{i \in X_j} (-1)^{i<i_1} (i \parallel j)\, \langle \boldsymbol{r}(I_2, i_1)^\vee \,|\, \boldsymbol{r}(I_2, i)\rangle$, where $X_j := I_1 \cap\,]i_1, i_2[$ if $j \notin\,]i_1, i_2]$ and $X_j := I_1 \smallsetminus [i_1, i_2]$ if $j \in\,]i_1, i_2]$.*

Conjecture B.14. *Consider two adjacent facets J_1, J_2 of $\mathcal{C}_{\mathrm{sub}}(M)$, with $J_1 \smallsetminus j_1 = J_2 \smallsetminus j_2$ for $j_1 < j_2$, and a vertex i of $\mathcal{C}_{\mathrm{sub}}(M)$. Then $(i \parallel j_1) + (i \parallel j_2) = \sum_{j \in Y_i} (-1)^{j<j_1} (i \parallel j)\, \langle \boldsymbol{r}(J_2, j)^\vee \,|\, \boldsymbol{r}(J_2, j_1)\rangle$, where $Y_i := J_1 \cap\,]j_1, j_2[$ if $i \notin\,]j_1, j_2]$ and $Y_i := J_1 \smallsetminus [j_1, j_2]$ if $i \in\,]j_1, j_2]$.*

We conclude with the following extension of Conjecture B.6.

Conjecture B.15. *For any facet I of a root independent subword complex $\mathcal{C}_{\mathrm{sub}}(M)$, the collection of cones $\mathcal{F}^{\boldsymbol{d}}(I) := \{\mathbb{R}_{\geq 0}\, \boldsymbol{d}(I, J) \mid J \text{ face of } \mathcal{C}_{\mathrm{sub}}(M)\}$ forms a polytopal complete simplicial fan.*

B.3 Algebraic connections of pipe dreams

To conclude on pipe dreams, let us just briefly mention two recent algebraic connections that open many questions beyond the scope of this document.

Signaletic operads. Motivated by the natural decomposition of the product in the $\boldsymbol{k}\mathfrak{AT}^k$ algebra into 2^k operations observed in [Pil18], we introduced signaletic operads and their Koszul dual citelangis operads in [HP19], which generalize the dendriform operad (see Remark 2.33). These operads are defined in terms of circulations of cars in a tree according to traffic signals placed at its nodes. This simple perspective enables to define combinatorial actions of these operads on certain permutations and posets, and to understand the corresponding free algebras on one generator. This opens several open problems described in [HP19]. For instance, it would be interesting to extend these constructions to the case where the cars can stop or fork at a given node, generalizing the tridendriform operad.

Pipe dreams and diagonal harmonics. In our recent joint work [BCP18] with N. Bergeron and C. Ceballos, we made an unexpected connection between the combinatorics of the ν-Tamari lattice on pipe dreams [PRV17] and enumerative properties of multivariate diagonal harmonics [Ber13, BPR12]. This connection uses combinatorial data on pipe dreams to interpret certain algebraic expressions in multivariate diagonal harmonics. A lot of combinatorial properties of pipe dreams remain to be understood to develop this promising connection.

C Non-kissing associahedra

C.1 Sections of scattering diagrams

We conclude with a general research direction motivated by Proposition 10.49. First, as observed in [MP19], the operation of Proposition 10.49 also makes sense for cluster algebras.

Proposition C.1. *Fix an initial seed $(B_\circ, P_\circ, X_\circ)$ and a subset $Y_\circ \subseteq X_\circ$ of initial cluster variables. Consider the coordinate plane $Y_\circ^\perp := \mathbb{R}\{\omega_x \,|\, x \in X_\circ \smallsetminus Y_\circ\} = \{\boldsymbol{v} \in V \,|\, \langle \boldsymbol{v} \,|\, \alpha_{y_\circ}\rangle = 0 \text{ for all } y_\circ \in Y_\circ\}$ and the subcomplex $\mathcal{C}_{\mathrm{clu}}(B_\circ)_{\text{◖}Y_\circ\text{◗}}$ of the cluster complex $\mathcal{C}_{\mathrm{clu}}(B_\circ)$ induced by the cluster variables x whose $\boldsymbol{g}$-vector $\boldsymbol{g}(B_\circ, x)$ lies in $Y_\circ^\perp$. Then:*

- *the complex $\mathcal{C}_{\mathrm{clu}}(B_\circ)_{\text{◖}Y_\circ\text{◗}}$ is a pseudomanifold,*
- *the subset $\mathcal{F}^{\boldsymbol{g}}(\bar{Q})_{\text{◖}Y_\circ\text{◗}} := \big\{C \in \mathcal{F}^{\boldsymbol{g}}(\bar{Q}) \,\big|\, C \subseteq Y_\circ^\perp\big\}$ of the $\boldsymbol{g}$-vector fan $\mathcal{F}^{\boldsymbol{g}}(\bar{Q})$ coincides with its section by $Y_\circ^\perp$, and is a realization of the restricted complex $\mathcal{C}_{\mathrm{clu}}(B_\circ)_{\text{◖}Y_\circ\text{◗}}$,*
- *in finite type, $\mathcal{F}^{\boldsymbol{g}}(\bar{Q})_{\text{◖}Y_\circ\text{◗}}$ is the normal fan of the projection of the $B_\circ$-associahedron $\mathbb{A}\mathrm{sso}(B_\circ)$ on the coordinate plane $Y_\circ^\perp$.*

Note that this restriction operation is in fact purely geometric, and would actually make sense for any fan which refines the coordinate fan.

We now want to discuss possible extensions of this operation to scattering diagrams, which lie at the interface between mathematical physics, algebra, and discrete geometry. Motivated by physics, they have received a particular attention in the cluster algebra community due to the seminal paper of M. Gross, P. Hacking, S. Keel and M. Kontsevich [GHKK18].

We only need here a very informal and unprecise definition. A *scattering diagram* $\mathcal{D}$ is a set of walls (codimension 1 cones) where each wall $\mathfrak{d}$ is endowed with a scattering function $f_\mathfrak{d}$. This function $f_\mathfrak{d}$ should be thought of as the result of scattering a ray reaching the wall $\mathfrak{d}$. These functions can be composed along paths in the scattering diagram. The main requirement of scattering diagrams

is a coherence condition that ensures that the compositions of the scattering functions along two paths with the same endpoints coincide.

To each rank d cluster algebra, one can associate a scattering diagram whose walls contain the walls of the g-vector fan. In fact, there are no other wall for finite type cluster algebras and the scattering function at each wall is a simple rational function constructed from the normal vector of the wall (*i.e.* the corresponding c-vector). The following conjecture should extend Proposition C.1.

Conjecture C.2. *Fix an initial seed $(B_\circ, P_\circ, X_\circ)$ and any subset $Y_\circ \subseteq X_\circ$ of initial cluster variables. Consider the scattering diagram $\mathcal{D}$ given by the cluster algebra $\mathcal{A}_{\mathrm{pr}}(B_\circ)$ and denote by $\mathcal{D}_{\blacklozenge Y_\circ \blacklozenge}$ the walls of $\mathcal{D}$ contained in the coordinate plane $Y_\circ^\perp$ defined in Proposition C.1. Then there is an evaluation of the scattering functions $f_{\mathfrak{d}}$ for the walls $\mathfrak{d} \in \mathcal{D}_{\blacklozenge Y_\circ \blacklozenge}$ that defines a scattering structure on $\mathcal{D}_{\blacklozenge Y_\circ \blacklozenge}$.*

Note that this procedure will in particular produce scattering diagrams for all non-kissing complexes. Indeed, applying the results of Chapter 9, the non-kissing complex $\mathcal{K}_{\mathrm{nk}}(\bar{Q})$ of a gentle quiver $\bar{Q}$ can be seen as the non-crossing complex $\mathcal{K}_{\mathrm{nc}}(D, D^\star)$ of the corresponding pair $(D_{\bar{Q}}, D^\star_{\bar{Q}})$ of dual cellular dissections on the surface $\mathcal{S}_{\bar{Q}}$. Complete the dissection $D_{\bar{Q}}$ into a triangulation T of $\mathcal{S}_{\bar{Q}}$, and consider its quiver $\bar{Q}_T$. Again by Chapter 9, the non-kissing complex $\mathcal{K}_{\mathrm{nk}}(\bar{Q}_T)$ can be seen as the non-crossing complex $\mathcal{K}_{\mathrm{nc}}(T, T^\star)$, which is the cluster complex $\mathcal{C}_{\mathrm{clu}}(T)$ of the cluster algebra associated to the triangulation T of $\mathcal{S}_{\bar{Q}}$ as defined in [FST08, FT18]. Moreover, since $D_{\bar{Q}} \subseteq T$, the vertices Q_0 of $\bar{Q}$ are vertices of $\bar{Q}_T$, and the non-kissing complex $\mathcal{K}_{\mathrm{nk}}(\bar{Q})$ coincides with the non-kissing complex $\mathcal{K}_{\mathrm{nk}}((\bar{Q}_T)_{\blacklozenge Q_0 \blacklozenge})$. It follows that $\mathcal{K}_{\mathrm{nk}}(\bar{Q})$ can be seen as the subcomplex of the cluster complex $\mathcal{C}_{\mathrm{clu}}(T)$ induced by the variables whose $\boldsymbol{g}$-vectors are contained in the coordinate plane corresponding to $Q_\circ$. Conjecture C.2 would therefore produce a relevant scattering diagram for $\mathcal{K}_{\mathrm{nk}}(\bar{Q})$.

C.2 Rays of the type cones of non-kissing fans

In Sections 7.3.2 and 10.3.4, we have seen the type cone approach to describe all polytopal realizations of the $\boldsymbol{g}$-vector fans of cluster algebras and non-kissing complexes. The main message is that the facets defining inequalities of the type cone correspond to certain specific flips (meshes) that can be identified and understood.

It is also interesting to consider the rays of the type cone. Indeed, convex combinations in the type cone correspond to Minkowski decompositions of polytopal realizations. In other words, any polytopal realization of a fan $\mathcal{F}$ is a Minkowski combination of the polytopes defined by the rays of the type cone of $\mathcal{F}$. For cluster complexes, the rays of the type cone of the $\boldsymbol{g}$-vector fan correspond to the Newton polytopes of the F-polynomials of the cluster algebra. Although quite vague, we believe that the following question is worth investigating.

Conjecture C.3. *For any gentle quiver $\bar{Q}$, the rays of the type cone of the non-kissing fan $\mathcal{F}^{\boldsymbol{g}}(\bar{Q})$ are Newton polytopes of polynomials associated to the gentle algebra $\mathbb{K}Q/I$.*

C.3 Graph properties of non-kissing associahedra

The following relevant properties of the graphs of the permutahedron and the associahedron have been particularly considered in the literature:

1. **Hamiltonicity.** Both the permutahedron [Ste64, Joh63, Tro62] and the associahedron [Luc87, HN99] admit an Hamiltonian cycle. In fact, all graph associahedra admit an Hamiltonian cycle [MP15], and all (type A) quotientopes admit an Hamiltonian path [HM19].

2. **Diameter.** The diameter of the permutahedron $\mathbb{P}\mathrm{erm}(n)$ is $n(n-1)/2$ and that of the associahedron $\mathbb{A}\mathrm{sso}(n)$ is $2n-6$ for $n > 10$. The later motivated intensive research and relevant approaches, involving volumetric arguments in hyperbolic geometry [STT88] and combinatorial properties of Thompson's groups [Deh10], until a purely combinatorial proof was finally found [Pou14]. This result was extended to all generalized associahedra in [Pou17, CP16] and studied for graph associahedra in [MP15].
3. **Non-leaving face property.** Both the permutahedron and the associahedron have the property that all geodesics between two given vertices v and w always remain in the smallest face containing v and w. This property was observed for the associahedron in [STT88], extended to all generalized associahedra in [CP16, Wil17] and studied for graph associahedra in [MP15].

We believe that these properties are worth investigating for all generalizations of the associahedron introduced in this document, in particular for quotientopes and for non-kissing associahedra.

BIBLIOGRAPHY

[AHBHY18] Nima Arkani-Hamed, Yuntao Bai, Song He, and Gongwang Yan. Scattering forms and the positive geometry of kinematics, color and the worldsheet. *J. High Energy Phys.*, (5):096, front matter+75, 2018.

[AIR14] Takahide Adachi, Osamu Iyama, and Idun Reiten. τ-tilting theory. *Compos. Math.*, 150(3):415–452, 2014.

[AS05] Marcelo Aguiar and Frank Sottile. Structure of the Malvenuto-Reutenauer Hopf algebra of permutations. *Adv. Math.*, 191(2):225–275, 2005.

[AS06] Marcelo Aguiar and Frank Sottile. Structure of the Loday-Ronco Hopf algebra of trees. *J. Algebra*, 295(2):473–511, 2006.

[Bar01] Yuliy Baryshnikov. On Stokes sets. In *New developments in singularity theory (Cambridge, 2000)*, volume 21 of *NATO Sci. Ser. II Math. Phys. Chem.*, pages 65–86. Kluwer Acad. Publ., Dordrecht, 2001.

[BB93] Nantel Bergeron and Sara Billey. RC-graphs and Schubert polynomials. *Experiment. Math.*, 2(4):257–269, 1993.

[BB05] Anders Björner and Francesco Brenti. *Combinatorics of Coxeter groups*, volume 231 of *Graduate Texts in Mathematics*. Springer, New York, 2005.

[BCP18] Nantel Bergeron, Cesar Ceballos, and Vincent Pilaud. Hopf dreams. Preprint, arXiv:1807.03044, 2018.

[BCSo18] Karin Baur and Raquel Coelho Simões. A geometric model for the module category of a gentle algebra. Preprint, arXiv:1803.05802, 2018.

[BDM+17] Thomas Brüstle, Guillaume Douville, Kaveh Mousavand, Hugh Thomas, and Emine Yıldırım. On the combinatorics of gentle algebras. Preprint, arXiv:1707.07665. To appear in *Canad. J. Math.*, 2017.

[Ber13] François Bergeron. Multivariate diagonal coinvariant spaces for complex reflection groups. *Adv. Math.*, 239:97–108, 2013.

[BEZ90] Anders Björner, Paul H. Edelman, and Günter M. Ziegler. Hyperplane arrangements with a lattice of regions. *Discrete Comput. Geom.*, 5(3):263–288, 1990.

[BFS90] Louis J. Billera, Paul Filliman, and Bernd Sturmfels. Constructions and complexity of secondary polytopes. *Adv. Math.*, 83(2):155–179, 1990.

[BH08] Christine Bessenrodt and Thorsten Holm. Weighted locally gentle quivers and Cartan matrices. *J. Pure and Appl. Algebra*, 212:204–221, 2008.

[BHKN01] François Boulier, Florent Hivert, Daniel Krob, and Jean-Christophe Novelli. Pseudo-permutations. II. Geometry and representation theory. In *Discrete models: combinatorics, computation, and geometry (Paris, 2001)*, Discrete Math. Theor. Comput. Sci. Proc., AA, pages 123–132 (electronic). Maison Inform. Math. Discrèt. (MIMD), Paris, 2001.

[Bjö84] Anders Björner. Orderings of Coxeter groups. In *Combinatorics and algebra (Boulder, Colo., 1983)*, volume 34 of *Contemp. Math.*, pages 175–195. Amer. Math. Soc., Providence, RI, 1984.

[BLS+99] Anders Björner, Michel Las Vergnas, Bernd Sturmfels, Neil White, and Günter M. Ziegler. *Oriented matroids*, volume 46 of *Encyclopedia of Mathematics and its Applications*. Cambridge University Press, Cambridge, second edition, 1999.

[BMDM+18] Véronique Bazier-Matte, Guillaume Douville, Kaveh Mousavand, Hugh Thomas, and Emine Yıldırım. ABHY Associahedra and Newton polytopes of F-polynomials for finite type cluster algebras. Preprint, arXiv:1808.09986, 2018.

[Bok06] Jürgen Bokowski. *Computational oriented matroids*. Cambridge University Press, Cambridge, 2006.

[Bou68] Nicolas Bourbaki. *Groupes et algèbres de Lie, Chapitres IV–VI*. Actualités Scientifiques et Industrielles, No. 1337. Hermann, Paris, 1968.

[BP14] Jürgen Bokowski and Vincent Pilaud. Enumerating topological (n_k)-configurations. *Comput. Geom.*, 47(2, part A):175–186, 2014.

[BP15] Jürgen Bokowski and Vincent Pilaud. On topological and geometric (19_4) configurations. *European J. Combin.*, 50:4–17, 2015.

[BP16] Jürgen Bokowski and Vincent Pilaud. Quasi-configurations: building blocks for point-line configurations. *Ars Math. Contemp.*, 10(1):99–112, 2016.

[BPR12] François Bergeron and Louis-François Préville-Ratelle. Higher trivariate diagonal harmonics via generalized Tamari posets. *Journal of Combinatorics*, 3(3):317–341, 2012.

[BR87] M. C. R. Butler and Claus Michael Ringel. Auslander-Reiten sequences with few middle terms and applications to string algebras. *Comm. Algebra*, 15(1-2):145–179, 1987.

[BW91] Anders Björner and Michelle L. Wachs. Permutation statistics and linear extensions of posets. *J. Combin. Theory Ser. A*, 58(1):85–114, 1991.

[BZ09] Nantel Bergeron and Mike Zabrocki. The Hopf algebras of symmetric functions and quasi-symmetric functions in non-commutative variables are free and co-free. *J. Algebra Appl.*, 8(4):581–600, 2009.

[CB18] William Crawley-Boevey. Classification of modules for infinite-dimensional string algebras. *Trans. Amer. Math. Soc.*, 370(5):3289–3313, 2018.

[CD06] Michael P. Carr and Satyan L. Devadoss. Coxeter complexes and graph-associahedra. *Topology Appl.*, 153(12):2155–2168, 2006.

[CFZ02] Frédéric Chapoton, Sergey Fomin, and Andrei Zelevinsky. Polytopal realizations of generalized associahedra. *Canad. Math. Bull.*, 45(4):537–566, 2002.

[Cha00] Frédéric Chapoton. Algèbres de Hopf des permutahèdres, associahèdres et hypercubes. *Adv. Math.*, 150(2):264–275, 2000.

[Cha16] Frédéric Chapoton. Stokes posets and serpent nests. *Discrete Math. Theor. Comput. Sci.*, 18(3), 2016.

[CLS14] Cesar Ceballos, Jean-Philippe Labbé, and Christian Stump. Subword complexes, cluster complexes, and generalized multi-associahedra. *J. Algebraic Combin.*, 39(1):17–51, 2014.

[CP15a] Cesar Ceballos and Vincent Pilaud. Cluster algebras of type D: pseudotriangulations approach. *Electron. J. Combin.*, 22(4):Paper 4.44, 27, 2015.

[CP15b] Cesar Ceballos and Vincent Pilaud. Denominator vectors and compatibility degrees in cluster algebras of finite types. *Trans. Amer. Math. Soc.*, 367:1421–1439, 2015.

[CP16] Cesar Ceballos and Vincent Pilaud. The diameter of type D associahedra and the non-leaving-face property. *European J. Combin.*, 51:109–124, 2016.

[CP17] Grégory Chatel and Vincent Pilaud. Cambrian Hopf Algebras. *Adv. Math.*, 311:598–633, 2017.

[CPP19] Grégory Chatel, Vincent Pilaud, and Viviane Pons. The weak order on integer posets. *Algebraic Combinatorics*, 2(1):1–48, 2019.

[CSZ15] Cesar Ceballos, Francisco Santos, and Günter M. Ziegler. Many non-equivalent realizations of the associahedron. *Combinatorica*, 35(5):513–551, 2015.

[Deh10] Patrick Dehornoy. On the rotation distance between binary trees. *Adv. Math.*, 223(4):1316–1355, 2010.

[DHMP19] Aram Dermenjian, Christophe Hohlweg, Thomas McConville, and Vincent Pilaud. The facial weak order on hyperplane arrangements. Preprint, arXiv:1910.03511, 2019.

[DHP18] Aram Dermenjian, Christophe Hohlweg, and Vincent Pilaud. The facial weak order and its lattice quotients. *Trans. Amer. Math. Soc.*, 370(2):1469–1507, 2018.

[DIR+17] Laurent Demonet, Osamu Iyama, Nathan Reading, Idun Reiten, and Hugh Thomas. Lattice theory of torsion classes. Preprint, arXiv:1711.01785, 2017.

[DRS10] Jesus A. De Loera, Jörg Rambau, and Francisco Santos. *Triangulations: Structures for Algorithms and Applications*, volume 25 of *Algorithms and Computation in Mathematics*. Springer Verlag, 2010.

[Ede84] Paul H. Edelman. A partial order on the regions of $\mathbb{R}^n$ dissected by hyperplanes. *Trans. Amer. Math. Soc.*, 283:617–631, 1984.

[Fom] Sergey Fomin. Cluster algebras portal. http://www.math.lsa.umich.edu/~fomin/cluster.html.

[FPP11] Julien Ferté, Vincent Pilaud, and Michel Pocchiola. On the number of simple arrangements of five double pseudolines. *Discrete Comput. Geom.*, 45(2):279–302, 2011.

[FST08] Sergey Fomin, Michael Shapiro, and Dylan Thurston. Cluster algebras and triangulated surfaces I. Cluster complexes. *Acta Math.*, 201(1):83–146, 2008.

[FT18] Sergey Fomin and Dylan Thurston. Cluster algebras and triangulated surfaces. Part II: Lambda lengths. *Mem. Amer. Math. Soc.*, 255(1223):v+97, 2018.

[FZ02] Sergey Fomin and Andrei Zelevinsky. Cluster algebras. I. Foundations. *J. Amer. Math. Soc.*, 15(2):497–529, 2002.

[FZ03a] Sergey Fomin and Andrei Zelevinsky. Cluster algebras. II. Finite type classification. *Invent. Math.*, 154(1):63–121, 2003.

[FZ03b] Sergey Fomin and Andrei Zelevinsky. Y-systems and generalized associahedra. *Ann. of Math. (2)*, 158(3):977–1018, 2003.

[FZ05] Sergey Fomin and Andrei Zelevinsky. Cluster algebras. III. Upper bounds and double Bruhat cells. *Duke Math. J.*, 126(1):1–52, 2005.

[FZ07] Sergey Fomin and Andrei Zelevinsky. Cluster algebras. IV. Coefficients. *Compos. Math.*, 143(1):112–164, 2007.

[GHKK18] Mark Gross, Paul Hacking, Sean Keel, and Maxim Kontsevich. Canonical bases for cluster algebras. *J. Amer. Math. Soc.*, 31(2):497–608, 2018.

[Gir12] Samuele Giraudo. Algebraic and combinatorial structures on pairs of twin binary trees. *J. Algebra*, 360:115–157, 2012.

[GKL+95] Israel M. Gelfand, Daniel Krob, Alain Lascoux, Bernard Leclerc, Vladimir S. Retakh, and Jean-Yves Thibon. Noncommutative symmetric functions. *Adv. Math.*, 112(2):218–348, 1995.

[GKZ08] Israel Gelfand, Mikhail Kapranov, and Andrei Zelevinsky. *Discriminants, resultants and multidimensional determinants*. Modern Birkhäuser Classics. Birkhäuser Boston Inc., Boston, MA, 2008. Reprint of the 1994 edition.

[GM17a] Alexander Garver and Thomas McConville. Enumerative properties of Grid-Associahedra. Preprint, arXiv:1705.04901, 2017.

[GM17b] Alexander Garver and Thomas McConville. Lattice properties of oriented exchange graphs and torsion classes. *Algebr. Represent. Theory*, 2017.

[GM18] Alexander Garver and Thomas McConville. Oriented flip graphs of polygonal subdivisions and noncrossing tree partitions. *J. Combin. Theory Ser. A*, 158:126–175, 2018.

[GP18] Joël Gay and Vincent Pilaud. The weak order on weyl posets. Preprint, arXiv:1804.06572. To appear in *Canad. J. Math.*, 2018.

[Hai84] Mark Haiman. Constructing the associahedron. Unpublished manuscript, 11 pages, available at http://www.math.berkeley.edu/~mhaiman/ftp/assoc/manuscript.pdf, 1984.

[HL07] Christophe Hohlweg and Carsten Lange. Realizations of the associahedron and cyclohedron. *Discrete Comput. Geom.*, 37(4):517–543, 2007.

[HLR10] Christophe Hohlweg, Jonathan Lortie, and Annie Raymond. The centers of gravity of the associahedron and of the permutahedron are the same. *Electron. J. Combin.*, 17(1):Research Paper 72, 14, 2010.

[HLT11] Christophe Hohlweg, Carsten Lange, and Hugh Thomas. Permutahedra and generalized associahedra. *Adv. Math.*, 226(1):608–640, 2011.

[HM19] Hung P. Hoang and Torsten Mütze. Combinatorial generation via permutation languages. II. Lattice congruences. Preprint, arXiv:1911.12078, 2019.

[HN99] Ferran Hurtado and Marc Noy. Graph of triangulations of a convex polygon and tree of triangulations. *Comput. Geom.*, 13(3):179–188, 1999.

[HNT05] Florent Hivert, Jean-Christophe Novelli, and Jean-Yves Thibon. The algebra of binary search trees. *Theoret. Comput. Sci.*, 339(1):129–165, 2005.

[Hoh12] Christophe Hohlweg. Permutahedra and associahedra: generalized associahedra from the geometry of finite reflection groups. In *Associahedra, Tamari lattices and related structures*, volume 299 of *Prog. Math. Phys.*, pages 129–159. Birkhäuser/Springer, Basel, 2012.

[HP19] Florent Hivert and Vincent Pilaud. Signaletic operads. Preprint, arXiv:1906.02228, 2019.

[HPS18] Christophe Hohlweg, Vincent Pilaud, and Salvatore Stella. Polytopal realizations of finite type $\mathbf{g}$-vector fans. *Adv. Math.*, 328:713–749, 2018.

[Hum90] James E. Humphreys. *Reflection groups and Coxeter groups*, volume 29 of *Cambridge Studies in Advanced Mathematics*. Cambridge University Press, Cambridge, 1990.

[Joh63] Selmer M. Johnson. Generation of permutations by adjacent transposition. *Math. Comp.*, 17:282–285, 1963.

[Kel01] Bernhard Keller. Introduction to a-infinity algebras and modules. *Homology Homotopy Appl.*, 3(1):1–35., 2001.

[Kel11] Bernhard Keller. On cluster theory and quantum dilogarithm identities. In *Representations of algebras and related topics*, EMS Ser. Congr. Rep., pages 85–116. Eur. Math. Soc., Zürich, 2011.

[KLN+01] Daniel Krob, Matthieu Latapy, Jean-Christophe Novelli, Ha-Duong Phan, and Sylviane Schwer. Pseudo-Permutations I: First Combinatorial and Lattice Properties. 13th International Conference on Formal Power Series and Algebraic Combinatorics (FPSAC 2001), 2001.

[KLR03] Christian Kassel, Alain Lascoux, and Christophe Reutenauer. The singular locus of a Schubert variety. *J. Algebra*, 269(1):74–108, 2003.

[KM04] Allen Knutson and Ezra Miller. Subword complexes in Coxeter groups. *Adv. Math.*, 184(1):161–176, 2004.

[KM05] Allen Knutson and Ezra Miller. Gröbner geometry of Schubert polynomials. *Ann. of Math. (2)*, 161(3):1245–1318, 2005.

[KT97] Daniel Krob and Jean-Yves Thibon. Noncommutative symmetric functions. IV. Quantum linear groups and Hecke algebras at $q = 0$. *J. Algebraic Combin.*, 6(4):339–376, 1997.

[Law14] Shirley Law. Combinatorial realization of the Hopf algebra of sashes. Preprint, arXiv:1407.4073, 2014.

[Lee89] Carl W. Lee. The associahedron and triangulations of the n-gon. *European J. Combin.*, 10(6):551–560, 1989.

[Lod04] Jean-Louis Loday. Realization of the Stasheff polytope. *Arch. Math. (Basel)*, 83(3):267–278, 2004.

[LP18] Carsten Lange and Vincent Pilaud. Associahedra via spines. *Combinatorica*, 38(2):443–486, 2018.

[LR98] Jean-Louis Loday and María O. Ronco. Hopf algebra of the planar binary trees. *Adv. Math.*, 139(2):293–309, 1998.

[LR12] Shirley Law and Nathan Reading. The Hopf algebra of diagonal rectangulations. *J. Combin. Theory Ser. A*, 119(3):788–824, 2012.

[Luc87] Joan M. Lucas. The rotation graph of binary trees is Hamiltonian. *J. Algorithms*, 8(4):503–535, 1987.

[McC17] Thomas McConville. Lattice structure of Grid-Tamari orders. *J. Combin. Theory Ser. A*, 148:27–56, 2017.

[McM71] Peter McMullen. On zonotopes. *Trans. Amer. Math. Soc.*, 159:91–109, 1971.

[McM73] Peter McMullen. Representations of polytopes and polyhedral sets. *Geometriae Dedicata*, 2:83–99, 1973.

[MP15] Thibault Manneville and Vincent Pilaud. Graph properties of graph associahedra. *Sém. Lothar. Combin.*, pages Art. B73d, 31 pp, 2015.

[MP17] Thibault Manneville and Vincent Pilaud. Compatibility fans for graphical nested complexes. *J. Combin. Theory Ser. A*, 150:36–107, 2017.

[MP19] Thibault Manneville and Vincent Pilaud. Geometric realizations of the accordion complex of a dissection. *Discrete Comput. Geom.*, 61(3):507–540, 2019.

[MPP11] Benjamin Matschke, Julian Pfeifle, and Vincent Pilaud. Prodsimplicial neighborly polytopes. *Discrete Comput. Geom.*, 46(1):100–131, 2011.

[MR95] Claudia Malvenuto and Christophe Reutenauer. Duality between quasi-symmetric functions and the Solomon descent algebra. *J. Algebra*, 177(3):967–982, 1995.

[MTTV19] Naruki Masuda, Hugh Thomas, Andy Tonks, and Bruno Vallette. The diagonal of the associahedra. Preprint, arXiv:1902.08059, 2019.

[Nov00] Jean-Christophe Novelli. On the hypoplactic monoid. *Discrete Math.*, 217(1-3):315–336, 2000. Formal power series and algebraic combinatorics (Vienna, 1997).

[NRT11] Jean-Christophe Novelli, Christophe Reutenauer, and Jean-Yves Thibon. Generalized descent patterns in permutations and associated Hopf algebras. *European J. Combin.*, 32(4):618–627, 2011.

[NS14] Tomoki Nakanishi and Salvatore Stella. Diagrammatic description of c-vectors and d-vectors of cluster algebras of finite type. *Electron. J. Combin.*, 21(1):Paper 1.3, 107, 2014.

[NT06] Jean-Christophe Novelli and Jean-Yves Thibon. Polynomial realizations of some trialgebras. 18th International Conference on Formal Power Series and Algebraic Combinatorics (FPSAC 2006), 2006.

[NT10a] Jean-Christophe Novelli and Jean-Yves Thibon. Free quasi-symmetric functions and descent algebras for wreath products, and noncommutative multi-symmetric functions. *Discrete Math.*, 310(24):3584–3606, 2010.

[NT10b] Jean-Christophe Novelli and Jean-Yves Thibon. Free quasi-symmetric functions and descent algebras for wreath products, and noncommutative multi-symmetric functions. *Discrete Math.*, 310(24):3584–3606, 2010.

[NZ12] Tomoki Nakanishi and Andrei Zelevinsky. On tropical dualities in cluster algebras. In *Algebraic groups and quantum groups*, volume 565 of *Contemp. Math.*, pages 217–226. Amer. Math. Soc., Providence, RI, 2012.

[OPS18] Sebastian Opper, Pierre-Guy Plamondon, and Sibylle Schroll. A geometric model for the derived category of gentle algebras. Preprint, arXiv:1801.09659, 2018.

[Pil06] Annette Pilkington. Convex geometries on root systems. *Comm. Algebra*, 34(9):3183–3202, 2006.

[Pil13] Vincent Pilaud. Signed tree associahedra. Preprint, arXiv:1309.5222, 2013.

[Pil17] Vincent Pilaud. Which nestohedra are removahedra? *Rev. Colombiana Mat.*, 51(1):21–42, 2017.

[Pil18] Vincent Pilaud. Brick polytopes, lattice quotients, and Hopf algebras. *J. Combin. Theory Ser. A*, 155:418–457, 2018.

[Pil19] Vincent Pilaud. Hopf algebras on decorated noncrossing arc diagrams. *J. Combin. Theory Ser. A*, 161:486–507, 2019.

[Pos09] Alexander Postnikov. Permutohedra, associahedra, and beyond. *Int. Math. Res. Not. IMRN*, (6):1026–1106, 2009.

[Pou14] Lionel Pournin. The diameter of associahedra. *Adv. Math.*, 259:13–42, 2014.

[Pou17] Lionel Pournin. The asymptotic diameter of cyclohedra. *Israel J. Math.*, 219(2):609–635, 2017.

[PP12] Vincent Pilaud and Michel Pocchiola. Multitriangulations, pseudotriangulations and primitive sorting networks. *Discrete Comput. Geom.*, 48(1):142–191, 2012.

[PP18] Vincent Pilaud and Viviane Pons. Permutrees. *Algebraic Combinatorics*, 1(2):173–224, 2018.

[PP20] Vincent Pilaud and Viviane Pons. The Hopf algebra of integer binary relations. In *Algebraic Combinatorics, Resurgence, Moulds and Applications (CARMA)*, volume 31 of *IRMA Lectures in Mathematics and Theoretical Physics*, pages 299–344. Europ. Math. Soc., 2020.

[PPP17] Yann Palu, Vincent Pilaud, and Pierre-Guy Plamondon. Non-kissing complexes and tau-tilting for gentle algebras. Preprint, arXiv:1707.07574. To appear in *Mem. Amer. Math. Soc.*, 2017.

[PPP19] Yann Palu, Vincent Pilaud, and Pierre-Guy Plamondon. Non-kissing and non-crossing complexes for locally gentle algebras. *J. Comb. Algebra*, 3(4):401–438, 2019.

[PPPP19] Arnau Padrol, Yann Palu, Vincent Pilaud, and Pierre-Guy Plamondon. Associahedra for finite type cluster algebras and minimal relations between $\boldsymbol{g}$-vectors. Preprint, arXiv:1906.06861, 2019.

[PPR20] Arnau Padrol, Vincent Pilaud, and Julian Ritter. Quotientopes via minkowski sums of shard polytopes. In preparation, 2020.

[PPS10] T. Kyle Petersen, Pavlo Pylyavskyy, and David E. Speyer. A non-crossing standard monomial theory. *J. Algebra*, 324(5):951–969, 2010.

[PPS12] Julian Pfeifle, Vincent Pilaud, and Francisco Santos. Polytopality and cartesian products of graphs. *Israel J. Math.*, 192(1):121–141, 2012.

[PPS18] Vincent Pilaud, Pierre-Guy Plamondon, and Salvatore Stella. A τ-tilting approach to dissections of polygons. *SIGMA Symmetry Integrability Geom. Methods Appl.*, 14:Paper No. 045, 8, 2018.

[PR06] Patricia Palacios and María O. Ronco. Weak Bruhat order on the set of faces of the permutohedron and the associahedron. *J. Algebra*, 299(2):648–678, 2006.

[PRV17] Louis-François Préville-Ratelle and Xavier Viennot. The enumeration of generalized Tamari intervals. *Trans. Amer. Math. Soc.*, 369(7):5219–5239, 2017.

[PRW08] Alexander Postnikov, Victor Reiner, and Lauren K. Williams. Faces of generalized permutohedra. *Doc. Math.*, 13:207–273, 2008.

[PS09] Vincent Pilaud and Francisco Santos. Multitriangulations as complexes of star polygons. *Discrete Comput. Geom.*, 41(2):284–317, 2009.

[PS12] Vincent Pilaud and Francisco Santos. The brick polytope of a sorting network. *European J. Combin.*, 33(4):632–662, 2012.

[PS13] Vincent Pilaud and Christian Stump. EL-labelings and canonical spanning trees for subword complexes. In *Discrete Geometry and Optimization*, Fields Institute Communications Series, pages 213–248. Springer, 2013.

[PS15a] Vincent Pilaud and Christian Stump. Brick polytopes of spherical subword complexes and generalized associahedra. *Adv. Math.*, 276:1–61, 2015.

[PS15b] Vincent Pilaud and Christian Stump. Vertex barycenter of generalized associahedra. *Proc. Amer. Math. Soc.*, 143(6):2623–2636, 2015.

[PS19] Vincent Pilaud and Francisco Santos. Quotientopes. *Bull. Lond. Math. Soc.*, 51(3):406–420, 2019.

[PV96] Michel Pocchiola and Gert Vegter. Topologically sweeping visibility complexes via pseudotriangulations. *Discrete Comput. Geom.*, 16(4):419–453, 1996.

[Rea03] Nathan Reading. Lattice and order properties of the poset of regions in a hyperplane arrangement. *Algebra Universalis*, 50(2):179–205, 2003.

[Rea04] Nathan Reading. Lattice congruences of the weak order. *Order*, 21(4):315–344, 2004.

[Rea05] Nathan Reading. Lattice congruences, fans and Hopf algebras. *J. Combin. Theory Ser. A*, 110(2):237–273, 2005.

[Rea06] Nathan Reading. Cambrian lattices. *Adv. Math.*, 205(2):313–353, 2006.

[Rea07a] Nathan Reading. Clusters, Coxeter-sortable elements and noncrossing partitions. *Trans. Amer. Math. Soc.*, 359(12):5931–5958, 2007.

[Rea07b] Nathan Reading. Sortable elements and Cambrian lattices. *Algebra Universalis*, 56(3-4):411–437, 2007.

[Rea14] Nathan Reading. Universal geometric cluster algebras. *Math. Z.*, 277(1-2):499–547, 2014.

[Rea15] Nathan Reading. Noncrossing arc diagrams and canonical join representations. *SIAM J. Discrete Math.*, 29(2):736–750, 2015.

[Rea16a] Nathan Reading. Finite Coxeter groups and the weak order. In *Lattice theory: special topics and applications. Vol. 2*, pages 489–561. Birkhäuser/Springer, Cham, 2016.

[Rea16b] Nathan Reading. Lattice theory of the poset of regions. In *Lattice theory: special topics and applications. Vol. 2*, pages 399–487. Birkhäuser/Springer, Cham, 2016.

[RS09] Nathan Reading and David E. Speyer. Cambrian fans. *J. Eur. Math. Soc.*, 11(2):407–447, 2009.

[RSS03] Günter Rote, Francisco Santos, and Ileana Streinu. Expansive motions and the polytope of pointed pseudo-triangulations. In *Discrete and computational geometry*, volume 25 of *Algorithms Combin.*, pages 699–736. Springer, Berlin, 2003.

[RSS08] Günter Rote, Francisco Santos, and Ileana Streinu. Pseudo-triangulations—a survey. In *Surveys on discrete and computational geometry*, volume 453 of *Contemp. Math.*, pages 343–410. Amer. Math. Soc., Providence, RI, 2008.

[SS93] Steve Shnider and Shlomo Sternberg. *Quantum groups: From coalgebras to Drinfeld algebras*. Series in Mathematical Physics. International Press, Cambridge, MA, 1993.

[SS12] Luis Serrano and Christian Stump. Maximal fillings of moon polyominoes, simplicial complexes, and Schubert polynomials. *Electron. J. Combin.*, 19, 2012.

[SSW17] Francisco Santos, Christian Stump, and Volkmar Welker. Noncrossing sets and a Grassmann associahedron. *Forum Math. Sigma*, 5:e5, 49, 2017.

[Sta63] Jim Stasheff. Homotopy associativity of H-spaces I, II. *Trans. Amer. Math. Soc.*, 108(2):293–312, 1963.

[Sta99] Richard P. Stanley. *Enumerative combinatorics. Vol. 2*, volume 62 of *Cambridge Studies in Advanced Mathematics*. Cambridge University Press, Cambridge, 1999. With a foreword by Gian-Carlo Rota and appendix 1 by Sergey Fomin.

[Ste64] Hugo Steinhaus. *One hundred problems in elementary mathematics*. Basic Books Inc. Publishers, New York, 1964.

[Ste13] Salvatore Stella. Polyhedral models for generalized associahedra via Coxeter elements. *J. Algebraic Combin.*, 38(1):121–158, 2013.

[Str12] Ross Street. Parenthetic remarks. In *Associahedra, Tamari lattices and related structures*, volume 299 of *Prog. Math. Phys.*, pages 251–268. Birkhäuser/Springer, Basel, 2012.

[STT88] Daniel D. Sleator, Robert E. Tarjan, and William P. Thurston. Rotation distance, triangulations, and hyperbolic geometry. *J. Amer. Math. Soc.*, 1(3):647–681, 1988.

[Stu11] Christian Stump. A new perspective on k-triangulations. *J. Combin. Theory Ser. A*, 118(6):1794–1800, 2011.

[Tam51] Dov Tamari. *Monoides préordonnés et chaînes de Malcev*. PhD thesis, Université Paris Sorbonne, 1951.

[Tro62] H. F. Trotter. Algorithm 115: Perm. *Commun. ACM*, 5(8):434–435, 1962.

[Vie07] Xavier Viennot. Catalan tableaux and the asymmetric exclusion process. In *19th International Conference on Formal Power Series and Algebraic Combinatorics (FPSAC 2007)*. 2007.

[Wil17] Nathan Williams. W-associahedra have the non-leaving-face property. *European J. Combin.*, 62:272–285, 2017.

[Woo04] A. Woo. Catalan numbers and Schubert polynomials for $w = 1(n+1)...2$. Preprint, arXiv:math/0407160, 2004.

[YZ08] Shih-Wei Yang and Andrei Zelevinsky. Cluster algebras of finite type via Coxeter elements and principal minors. *Transform. Groups*, 13(3-4):855–895, 2008.

ABSTRACT

Permutahedra and **associahedra** are classical polytopes whose face structures are described by the combinatorics of permutations and binary trees. We present a combinatorial, geometric and algebraic study of generalizations of these polytopes around four main topics:

1. **Lattice quotients of the weak order:** We study the lattice congruences of the weak order on permutations, construct polytopal realizations called quotientopes, and define corresponding combinatorial Hopf algebra. We develop in particular several families of examples, including k-twists and permutrees generalizing binary trees in two different directions.
2. **Beyond the weak order:** We study some generalizations of the weak order on the one hand to all faces of the permutahedra of finite Coxeter groups, and on the other hand to integer posets or to specific subsets of crystallographic root systems.
3. **Cluster algebras and generalized associahedra:** We construct polytopal realizations for the g-vector fans of the finite type cluster algebras, first via the construction of a universal associahedron, then via the description of the type cones of these fans, and finally via the construction of brick polytopes of subword complexes.
4. **Non-kissing and non-crossing complexes:** We study simplicial complexes associated to gentle quivers or equivalently to certain dissections of surfaces. In the situation when these complexes are finite, we show that they admit lattice structures generalizing the Tamari lattice and polytopal realizations generalizing the associahedra.

RÉSUMÉ

Les **permutaèdres** et les **associaèdres** sont des polytopes classiques dont les structures de faces sont données par la combinatoire des permutations et des arbres binaires. Nous présentons une étude combinatoire, géométrique et algébrique de généralisations de ces polytopes autour de quatre thèmes principaux :

1. **Treillis quotients de l'ordre faible :** Nous étudions les congruences de treillis de l'ordre faible sur les permutations, construisons des réalisations polytopales appelées quotientopes, et définissons des algèbres de Hopf combinatoires associées. Nous développons en particulier plusieurs familles d'exemples, dont les k-twists et les permutarbres qui généralisent les arbres binaires dans deux directions différentes.
2. **Au delà de l'ordre faible :** Nous étudions des généralisations de l'ordre faible d'une part à toutes les faces des permutaèdres des groupes de Coxeter finis, et d'autre part aux posets sur des entiers ou sur certains sous-ensembles de systèmes de racines cristallographiques.
3. **Algèbres amassées et associaèdres généralisés :** Nous construisons des réalisations polytopales des éventails de g-vecteurs des algèbres amassées de type fini, d'abord via la construction d'un associaèdre universel, ensuite via la description des cônes de type de ces éventails, et enfin via la construction des polytopes de briques de complexes de sous-mots.
4. **Complexes platoniques et parallèles :** Nous étudions des complexes simpliciaux associés aux carquois aimables ou de manière équivalente à certaines dissections de surfaces. Dans le cas où ces complexes sont finis, nous montrons qu'ils admettent des structures de treillis généralisant le treillis de Tamari et des réalisations polytopales généralisant les associaèdres.